

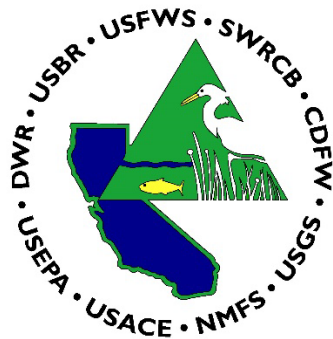
Ecological Impacts of Drought on the Sacramento-San Joaquin Delta

with special attention to the extreme drought of 2020-2021

PRELIMINARY REPORT

February 1, 2022

Prepared By the Interagency Ecological Program Drought Management, Analysis, and Synthesis Team (Drought MAST)



Interagency Ecological Program

COOPERATIVE ECOLOGICAL
INVESTIGATIONS SINCE 1970

Drought MAST team members:

- Rosemary Hartman¹
- Arthur Barros²
- Samuel Bashevkin⁴
- Christina Burdi²
- David Bosworth¹
- Leela Dixit¹
- Ted Flynn¹
- Jereme Gaeta²
- Elizabeth Keller³
- Peggy Lehman¹
- Peter Nelson¹
- Sarah Perry¹
- Nicholas Rasmussen¹
- Jenna Rinde²
- Evan Sawyer³
- Tyler Salman¹
- Laura Twardochleb¹

With technical assistance from:

- Keith Bouma-Gregson⁵
- Elizabeth Stumpner⁵

1. California Department of Water Resources
2. California Department of Fish and Wildlife
3. NOAA Fisheries, West Coast Region
4. Delta Science Program, Delta Stewardship Council
5. U.S. Geological Survey, California Water Sciences Center

Suggested Citation: Drought MAST. 2022. Ecological Impacts of Drought on the Sacramento-San Joaquin Delta. Preliminary report. Interagency Ecological Program for the San Francisco Estuary. Technical Report #XX. Sacramento, CA. 230 p.

Disclaimer

The views presented here are those of the authors and do not necessarily represent the views of their respective agencies or the Interagency Ecological Program. Any use of trade, firm, or product names is for descriptive purposes only and does not imply endorsement by the U.S. Government or the State of California. This is a preliminary report. Some of the data from 2021 has not been processed or fully analyzed. A more comprehensive report will follow, and may reach different conclusions from this preliminary report.

Executive Summary

The record-breaking drought of 2020-2021 highlighted the need for increased understanding of the impact of droughts on the Delta ecosystem and how management actions undertaken during droughts impact ecosystem processes. Therefore, the Interagency Ecological Program (IEP) Management Analysis and Synthesis Team began an analysis to investigate changes to major ecosystem parameters that occur during multi-year droughts. The team analyzed flow, water quality, nutrients, phytoplankton, zooplankton, aquatic vegetation, clams, jellyfish, and finfish to see which parameters increased and which decreased during multi-year droughts versus multi-year wet periods or neutral periods. The team also compared these parameters as measured during the 2020-2021 drought versus previous droughts to see whether this drought stands out against the historical record, and to see whether management actions taken during 2021 impacted ecosystem responses to the drought.

Some parameters responded strongly to multi-year droughts, while others responded primarily to conditions within the year, rather than multiple years. The overall effect of drought in the Delta typically includes (Figure 1):

- Reduced flow
- Increased temperature
- Increased water clarity
- Some increased nutrient concentrations
- Local increases in phytoplankton and zooplankton in the South Delta, but decreases in Suisun Bay, and highest abundances of both phytoplankton and zooplankton at intermediate flows.
- Most pelagic fish decline, with particularly large effects seen in Longfin Smelt and age-0 Striped Bass.
- Salmon change their migration patterns, and juvenile salmon that out-migrate during droughts have lower return rates.

To respond to droughts, water resource managers decrease exports from the Delta, shift outflow patterns, and attempt to balance human and environmental needs for an increasingly scarce water supply.

2021 was hotter and drier than almost any previous year, with the limited precipitation failing to result in predicted streamflow. The Temporary Urgency Change Petition (TUCP) that was in effect during summer 2021 and the West False River Emergency Drought Salinity Barrier (Barrier) had a few apparent impacts on the Delta; however, the effects of the drought were so large that they masked the effects of these actions on the ecosystem-wide

scale. Most ecosystem components were similar to other dry years, however (see Figure 2):

- Summer outflow and exports were unusually low.
- Salinity was unusually high.
- Secchi depth was high, continuing the general increasing trend.
- Temperatures were unusually high.
- Dissolved ammonia and nitrate+nitrite were low.
- Harmful algal blooms were similar to 2020, but more intense than during the 2012-2016 drought. A large bloom in Franks Tract during July and August may have been exacerbated by the Barrier.
- Pelagic fishes had some of the lowest abundances on record, lower than previous droughts, though Longfin Smelt experienced a surprising population increase.

There are many aspects to these ecosystem responses that are still poorly understood. We do not understand many of the mechanisms behind fishes' responses to drought. We have not uncovered many of the drivers behind the increase in aquatic vegetation or harmful algal blooms. While we found some changes to migration timing for salmon, we need further investigation to clarify the patterns. Many ecosystem components were not evaluated in this report, such as other migratory fishes (including sturgeon and lamprey), birds, mammals, upstream impacts, and many aspects of human responses to drought. All of these avenues may become important for future management of drought in the Delta.

This is a preliminary report. Some of the data from 2021 has not been processed or fully analyzed. A more comprehensive report will be completed later in 2022. If the drought extends through water year 2022, an additional year of data will be collected and integrated in a comprehensive report in 2023.

Ecosystem Responses to Drought

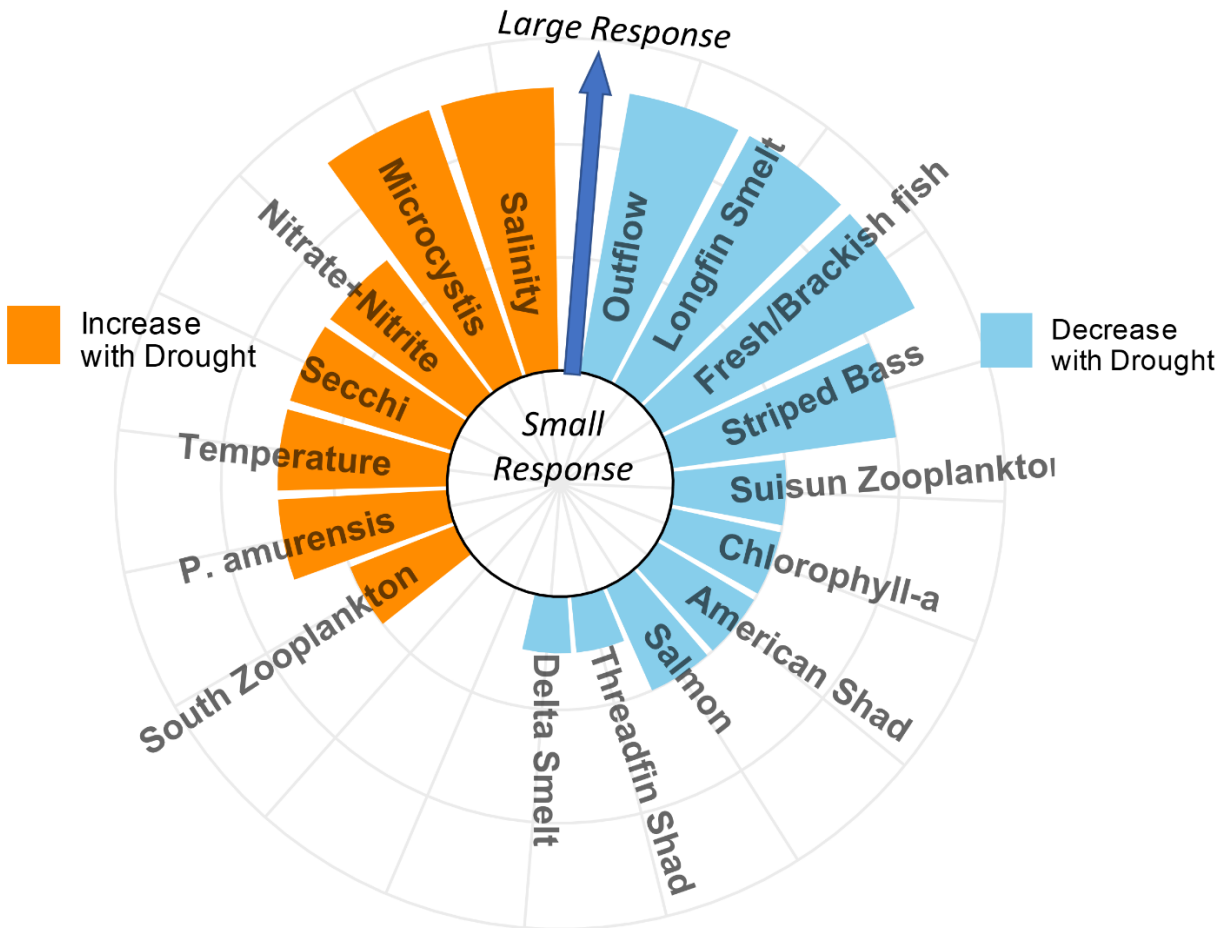


Figure 1. Plot of major ecological parameters and their relationship with Drought. Relationships were ranked on a qualitative scale of zero (no relationship) to 5 (large relationship) to multi-year droughts. Blue bars on the right side of the circle represent parameters with decreases during droughts. Orange bars on the left side of the circle represent parameters that increase during droughts.

Conditions in 2021 compared to previous droughts

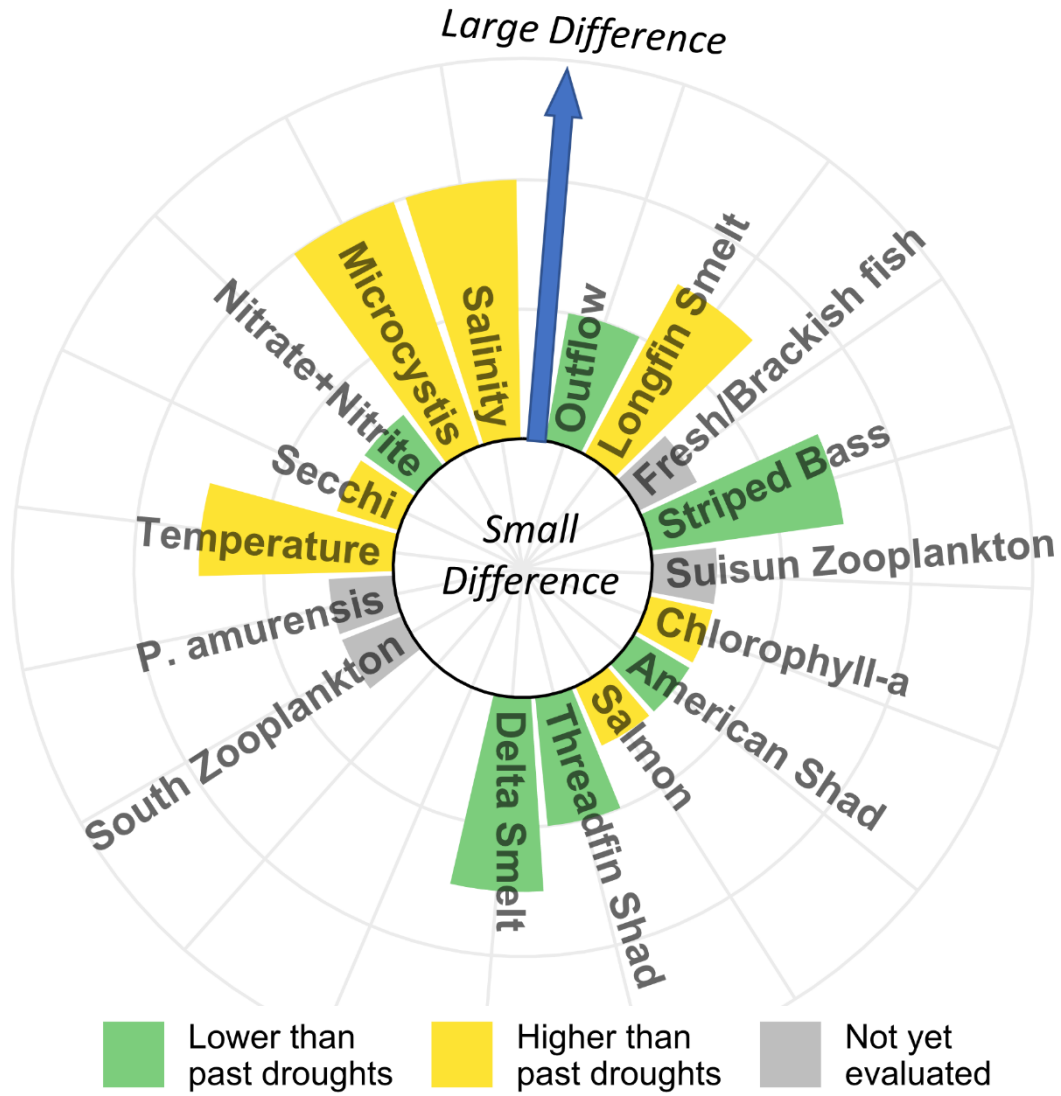


Figure 2. Plot of major ecological parameters in 2021 and their magnitude in comparison to previous droughts. Some of these differences may be due to the 2021 TUCP and/or Emergency Drought Barrier. Relationships were ranked on a qualitative scale of zero (similar to previous droughts) to 5 (very different from previous droughts). Green bars represent parameters that decreased relative to past droughts. Yellow bars represent parameters that increased relative to past droughts. Grey bars are parameters for which we have not completed data processing and analysis. Some parameters are

only available through September of 2021, so this plot should be considered preliminary.

Contents

Ecological Impacts of Drought on the Sacramento-San Joaquin Delta	1
Disclaimer	3
Executive Summary	4
Contents	9
Abbreviations and Acronyms	24
Introduction/Background	26
Research Questions	26
Regulatory Background	26
Drought actions of 2021	32
Scientific Background	34
Predictions	42
Materials and Methods	44
Study Site	44
Study Design	45
Water Quality and Hydrology	47
Chlorophyll-a and Microcystis	51
Aquatic Vegetation	57
Invertebrates	58
Fish	62
Results	74
Hydrology	74
Water quality	89
Chlorophyll-a	127
<i>Microcystis</i> index	138
Aquatic Vegetation	142
Zooplankton	145
Jellyfish	153

Clams..... 155

Fish..... 160

Summary Plot..... 187

Discussion..... 190

 Drought in the Delta..... 190

 Hydrology 190

 Water Quality 192

 Chlorophyll-a..... 195

Microcystis index..... 196

 Aquatic Vegetation 198

 Zooplankton 199

 Jellyfish 200

 Clams..... 201

 Fish..... 202

 Effect of Drought Management Actions 208

 The Future 210

Acknowledgements 212

Works Cited 213

Appendix A. Supplemental Information **Error! Bookmark not defined.**

 Sacramento Water Year Index definition **Error! Bookmark not defined.**

 Statistical Inference in a Bayesian Framework **Error! Bookmark not defined.**

 Supplemental Results **Error! Bookmark not defined.**

 Catch accumulation curves..... **Error! Bookmark not defined.**

Table of Figures

Figure 1. Plot of major ecological parameters and their relationship with Drought. Relationships were ranked on a qualitative scale of zero (no relationship) to 5 (large relationship) to multi-year droughts. Blue bars on the right side of the circle represent parameters with decreases during droughts. Orange bars on the left side of the circle represent parameters that increase during droughts.6

Figure 2. Plot of major ecological parameters in 2021 and their magnitude in comparison to previous droughts. Some of these differences may be due to the 2021 TUCP and/or Emergency Drought Barrier. Relationships were ranked on a qualitative scale of zero (similar to previous droughts) to 5 (very different from previous droughts). Green bars represent parameters that decreased relative to past droughts. Yellow bars represent parameters that increased relative to past droughts. Grey bars are parameters for which we have not completed data processing and analysis. Some parameters are only available through September of 2021, so this plot should be considered preliminary.7

Figure 3. Plot of water year indexes for the Sacramento Valleys from 1905 to 2021. Data is from the California Department of Water Resources (<https://cdec.water.ca.gov/reportapp/javareports?name=WSIHIST>) . Periods classified as “Droughts” (multiple dry, critically dry, and below normal years in a row) are highlighted by yellow bars below the x-axis. Periods classified as “Wet Periods” (multiple wet years in a row) are highlighted with blue bars below the x axis. “Neutral” periods (neither drought nor wet period) are highlighted in green below the x-axis..... 27

Figure 4. Timeline of drought actions and important environmental regulations. Row 1 -Major droughts. Row 2 – Major changes to Delta Water Quality/flow standards in response to drought. Row 3 – Drought emergency declarations. Row 4 – Emergency drought barriers. Row 5 – Federal Endangered Species Act biological opinions. Row 6 – California Endangered Species Act Incidental Take Permits. Row 7 – Water Rights decisions..... 31

Figure 5. Map of regions used for drought analyses..... 45

Figure 6. Map of station locations in the upper San Francisco Estuary used for the short-term (2011-2021) analysis of chlorophyll-a concentration..... 53

Figure 7. Map of sampling stations used for the long-term analysis of chlorophyll-a concentration measured between 1975 and 2021. 54

Figure 8. The *Microcystis* visual surface colony rating index used by IEP surveys ranges from 1 for no colonies observed to 5 for a dense mat of colonies on the surface of the water..... 56

Figure 9. Map of stations in the upper San Francisco Estuary used in the *Microcystis* visual index analysis. 57

Figure 10. Map of the Delta with regions denoted by thick bordered and colored polygons, sub-regions denoted by thin bordered polygons, and Fall Midwater Trawl Study stations included in the analysis denoted by red bordered yellow points. Only sub-regions with Fall Midwater Trawl Study stations are labeled. Inset map illustrates the study region relative to the state of California. 67

Figure 11 Median annual catch (points) for (top) Threadfin Shad and (bottom) Longfin Smelt, the selected sub-community assemblage representatives, across sub-regions. Colored backgrounds indicate annual water year category of Droughts (red), Wet Periods (blue), and other (i.e., Neutral; tan) year types. No data were collected in 1979. Gray line (right-axis) indicates annual Sacramento Valley Index. The vertical dashed line denotes the separation of Pre-POD era from the Post-POD era as defined by Thomson et al. (2010)). NOTE: Longfin Smelt catch (b) is log₁₀-scaled..... 70

Figure 12. Boxplots of Delta Outflow from the Dayflow model for each value of the Drought year classification (Drought period [D], Neutral [N], and Wet period [W]), with 2020 and 2021 shown separately. Note that the y-axis is scaled to log₁₀ units (19 negative values are not displayed). 74

Figure 13 Observed (boxplots) and model-predicted (red points ±95% confidence intervals) log-transformed Delta outflow (Dayflow) for the seasonal-drought model by A) season and B) Drought year classification (Drought period [D], Neutral [N], and Wet period [W]). Different letters above the box plots identify statistically significant (p < 0.05) differences from a Tukey post-hoc test. 76

Figure 14. Boxplots of Delta Outflow from the Dayflow model of the Drought year classification (Drought period [D], Neutral [N], and Wet period [W]), with 2020 and 2021 shown separately grouped by season. Note that the y-axis is scaled to log₁₀ units (19 negative values are not displayed). 77

Figure 15. Comparison of Dayflow outflow and combined USGS outflow computed from four continuous monitoring stations between 2011 – 2021 during (A) all flow conditions and (B) low flow conditions (<10,000 cfs; inset). Purple bounding box in top panel represents low-flow conditions in bottom panel. Dayflow outflow <10,000 cfs represents ~59% of short-term record. Adopted from Monismith (2016). Inset map of USGS continuous

monitoring station in the Western Delta (red circles) Image from Google Earth. 78

Figure 16. Observed (boxplots) and model-predicted (red points $\pm 95\%$ confidence intervals) log-transformed combined net outflow for the seasonal-year model across the short-term record. Different letters above the box plots identify statistically significant ($p < 0.05$) differences from a Tukey post-hoc test. 80

Figure 17. Observed (boxplots) and model-predicted (red points $\pm 95\%$ confidence intervals) log-transformed Cache Slough net flow for the seasonal-year model. Different letters above the box plots identify statistically significant ($p < 0.05$) differences from a Tukey post-hoc test. . 81

Figure 18. Boxplots of export by Drought year classification (Drought [D], Neutral [N] and Wet Periods [W]), with 2021 and 2020 shown separately. 83

Figure 19. Observed (boxplots) and model-predicted (red points $\pm 95\%$ confidence intervals) exports for the seasonal-year model. Different letters above the box plots identify statistically significant ($p < 0.05$) differences from a Tukey post-hoc test. 84

Figure 20. Observed (boxplots) and model-predicted (red points $\pm 95\%$ confidence intervals) exports for the seasonal-drought model by A) season and B) Drought year classification (Drought period [D], Neutral [N], and Wet period [W]) Different letters above the box plots identify statistically significant ($p < 0.05$) differences from a Tukey post-hoc test. 85

Figure 21. Boxplots of X2 (km) for each value of the Drought year classification (Drought period [D], Neutral [N], and Wet period [W]), with 2021 and 2020 shown separately. 86

Figure 22. Boxplots of X2 of the Drought year classification (Drought period [D], Neutral [N], and Wet period [W]), with 2020 and 2021 shown separately grouped by season. 87

Figure 23. Observed (boxplots) and model-predicted (red points $\pm 95\%$ confidence intervals) X2 for the seasonal-year model. Different letters above the box plots identify statistically significant ($p < 0.05$) differences from a Tukey post-hoc test. 88

Figure 24. Boxplots of temperature for each value of the Drought year classification (Drought period [D], Neutral [N], and Wet period [W]), with 2020 and 2021 shown separately. 90

Figure 25. Observed (boxplots) and model-predicted (red points $\pm 95\%$ confidence intervals) temperatures for the regional-drought model by A) Region and B) Drought year classification (Drought period [D], Neutral [N],

and Wet period [W]). Different letters above boxplots identify statistically significant ($p < 0.05$) differences from a Tukey post-hoc test. 92

Figure 26. Observed (boxplots) and model-predicted (red points $\pm 95\%$ confidence intervals) temperatures for the regional-year model. Different letters above boxplots identify statistically significant ($p < 0.05$) differences from a Tukey post-hoc test. 93

Figure 27. Observed (boxplots) and model-predicted (red points $\pm 95\%$ confidence intervals) temperatures for the seasonal-drought model by A) season and B) Drought year classification (Drought period [D], Neutral [N], and Wet period [W]). Different letters above boxplots identify statistically significant ($p < 0.05$) differences from a Tukey post-hoc test. 94

Figure 28. Observed (boxplots) and model-predicted (red points $\pm 95\%$ confidence intervals) temperatures for the seasonal-year model. Different letters above boxplots identify statistically significant ($p < 0.05$) differences from a Tukey post-hoc test. 95

Figure 29. Boxplots of salinity for each Drought year classification (Drought period [D], Neutral [N], and Wet period [W]) alongside 2020 and 2021. ... 96

Figure 30. Observed (boxplots) and model-predicted (red points $\pm 95\%$ confidence intervals) salinities for the regional by Drought year classification model. Different letters above the box plots identify statistically significant ($p < 0.05$) differences from a Tukey post-hoc test. 99

Figure 31. Observed (boxplots) and model-predicted (red points $\pm 95\%$ confidence intervals) salinities for the regional by year model. Different letters above the box plots identify statistically significant ($p < 0.05$) differences from a Tukey post-hoc test. 100

Figure 32. Observed (boxplots) and model-predicted (red points $\pm 95\%$ confidence intervals) salinities for the seasonal by Drought year classification model. Different letters above the box plots identify statistically significant ($p < 0.05$) differences from a Tukey post-hoc test. 101

Figure 33. Observed (boxplots) and model-predicted (red points $\pm 95\%$ confidence intervals) salinities for the seasonal by year model. Different letters above the box plots identify statistically significant ($p < 0.05$) differences from a Tukey post-hoc test. 102

Figure 34. Boxplots of secchi depth for each Drought year classification type alongside 2020 and 2021 103

Figure 35. Observed (boxplots) and model-predicted (red points $\pm 95\%$ confidence intervals) log-transformed secchi depth for the regional by Drought year classification model. Different letters above the box plots

identify statistically significant ($p < 0.05$) differences from a Tukey post-hoc test..... 106

Figure 36. Observed (boxplots) and model-predicted (red points $\pm 95\%$ confidence intervals) log-transformed secchi depth for the regional by year model. Different letters above the box plots identify statistically significant ($p < 0.05$) differences from a Tukey post-hoc test. 107

Figure 37. Observed (boxplots) and model-predicted (red points $\pm 95\%$ confidence intervals) log-transformed secchi depth for the seasonal by Drought year classification model. Different letters above the box plots identify statistically significant ($p < 0.05$) differences from a Tukey post-hoc test..... 108

Figure 38. Observed (boxplots) and model-predicted (red points $\pm 95\%$ confidence intervals) secchi depth for the seasonal by year model. Different letters above the box plots identify statistically significant ($p < 0.05$) differences from a Tukey post-hoc test..... 109

Figure 39. Boxplots of dissolved ammonia for each Drought year classification (Drought period [D], Neutral [N], and Wet period [W]) value with 2020 and 2021 shown separately from other Dry values. Data plotted prior to simulations. Red lines represent the highest reporting limit of censored data. Y-axis was cut off at 0.5 so boxplots were more visible; no outliers for 2020 and 2021 were above this value. 110

Figure 40. Boxplots of dissolved ammonia for each Year Type value with 2020 and 2021 shown separately from other Dry values. Red lines represent the highest reporting limit of censored data. Y-axis was cut off at 0.5 so boxplots were more visible; no outliers for 2020 and 2021 were above this value. 111

Figure 41. Boxplots of observed log-transformed dissolved ammonia (mg/L as N) values by (a) drought year classification (Drought period [D], Neutral [N], and Wet period [W]) (b) year type (c) season (long-term dataset) and (d) season (short-term dataset). Model-predicted values using seasonal averages with 95% confidence intervals are displayed as red points. Values below reporting limits were estimated via simulation. Letters represent different groups based on pairwise comparisons. 113

Figure 42. Boxplots of observed log-transformed dissolved ammonia (mg/L as N) values by (a) drought year classification (Drought period [D], Neutral [N], and Wet period [W]) (b) year type (c) region (long-term dataset) and (d) region (short-term dataset). Model-predicted values using regional averages with 95% confidence intervals are displayed as red points. Values

below reporting limits were estimated via simulation. Letters represent different groups based on pairwise comparisons. 114

Figure 43. Boxplots of dissolved nitrate nitrite for each Drought year classification (Drought period [D], Neutral [N], and Wet period [W]) value with 2020 and 2021 shown separately from other Dry values. Red lines represent the highest reporting limit of censored data. Y-axis was cut off at 3.5 so boxplots were more visible; no outliers for 2020 and 2021 were above this value. 115

Figure 44. Boxplots of dissolved nitrate nitrite for each Year Type value with 2020 and 2021 shown separately from other Dry values. Red lines represent the highest reporting limit of censored data. Y-axis was cut off at 3.5 so boxplots were more visible; no outliers for 2020 and 2021 were above this value. 116

Figure 45. Boxplots of observed log-transformed dissolved nitrate nitrite (mg/L as N) values by (a) drought year classification (b) year type (c) season (long-term dataset) and (d) season (short-term dataset). Model-predicted values using seasonal averages with 95% confidence intervals are displayed as red points. Letters represent different groups based on pairwise comparisons. 118

Figure 46. Boxplots of observed log-transformed dissolved nitrate nitrite (mg/L as N) values by (a) drought year classification (b) year type (c) region (long-term dataset) and (d) region (short-term dataset). Model-predicted values using regional averages with 95% confidence intervals are displayed as red points. Values below reporting limits were estimated via simulation. Letters represent different groups based on pairwise comparisons. 119

Figure 47. Boxplots of dissolved orthophosphate for each Drought year classification value with 2020 and 2021 shown separately from other Dry values. Red lines represent the highest reporting limit of censored data. Y-axis was cut off at 0.4 so boxplots were more visible; no outliers for 2020 and 2021 were above this value. 120

Figure 48. Boxplots of dissolved orthophosphate for each Year Type value with 2020 and 2021 shown separately from other Dry values. Red lines represent the highest reporting limit of censored data. Y-axis was cut off at 0.4 so boxplots were more visible; no outliers for 2020 and 2021 were above this value. 121

Figure 49. Boxplots of observed log-transformed dissolved orthophosphate values (mg/L as P) by (a) drought year classification (b) year type (c) season (long-term dataset) and (d) season (short-term dataset). Model-predicted values using seasonal averages with 95% confidence intervals are

displayed as red points. Letters represent different groups based on pairwise comparisons. 123

Figure 50. Boxplots of observed log-transformed dissolved orthophosphate (mg/L as P) values by (a) drought year classification (b) year type (c) region (long-term dataset) and (d) region (short-term dataset). Model-predicted values using regional averages with 95% confidence intervals are displayed as red points. Letters represent different groups based on pairwise comparisons. 124

Figure 51. Dissolved Oxygen timeseries at stations representing the lower Sacramento River (DEC; USGS stations 11455478 and 11455485, teal) and the Toe Drain (TOE; USGS stations 11455139 and 11455140, orange). Inset map of station locations. 125

Figure 52. Toe Drain dissolved oxygen timeseries across water years (2014 – present). 126

Figure 53. Lower Sacramento River timeseries across water years (2014 – present) 127

Figure 54. Boxplots showing the log-average (white diamond), median (bar), interquartile range between the 25th and 75th percentile (box), 1.5 times the interquartile range (whiskers), and outliers (points) of chlorophyll-a concentration for each year between 2011 – 2021. Y-axis scaled by log₁₀. 128

Figure 55 Boxplots showing the log-average (white diamond), median (bar), interquartile range between the 25th and 75th percentile (box), 1.5 times the interquartile range (whiskers), and outliers (points) of chlorophyll-a concentration for wet, neutral, and drought year classifications during 2011 – 2021. Different letters above boxplots represents significant differences in marginal means at the 0.05 significance level. Y-axis scaled by log₁₀ 129

Figure 56 Boxplots showing the log-average (white diamond), median (bar), interquartile range between the 25th and 75th percentile (box), 1.5 times the interquartile range (whiskers), and outliers (points) of chlorophyll-a concentration for three water year types by region and season. Y-axis scaled by log₁₀. 131

Figure 57. Pairwise comparisons for differences in water year type within and between seasons. Estimated marginal means (black dot) and estimated error around differences between the means (red arrow) for chlorophyll-a concentration measured for wet, below average and drought years during 2011-2021. Red arrows that do not overlap indicate that the means differ at the 0.05 level of significance. 133

Figure 58 Yearly log-average (white diamond), median (bar), inter-quartile range between 25th and 75th percentiles (box), 1.5 times the interquartile range (whiskers), and outliers (circles) for chlorophyll- <i>a</i> concentration measured during 1975 - 2021 for four regions of the upper San Francisco Estuary. Colors show water year types for each water year. Y-axis scaled by \log_{10}	134
Figure 59. Log-average (white diamond), median (bar), inter-quartile range between 25th and 75th percentiles (box), 1.5 times the interquartile range (whiskers), and outliers (circles) for chlorophyll- <i>a</i> concentration measured during 1975-2021 in the upper San Francisco Estuary. Different letters above boxplots represents significant differences in marginal means at the 0.05 significance level. Y-axis scaled by \log_{10}	136
Figure 60. Log-average (white diamond), median (bar), inter-quartile range between 25th and 75th percentiles (box), 1.5 times the interquartile range (whiskers), and outliers (circles) for chlorophyll- <i>a</i> concentration among water years by region and season for data collected between 1975 and 2021. Y-axis scaled by \log_{10}	138
Figure 61 Number of <i>Microcystis</i> index scores observed for none, low and high biomass among regions for wet, below average and drought water year types during 2011-2021.	139
Figure 62. Probability of obtaining a low or high <i>Microcystis</i> index score for wet, below average and drought water year types during 2011-2021 among regions based on an ordinal model. The probability of scores in each combination of year type and season sum to 1. Error bars indicate the 95% credible interval for the probability estimate. Non-overlapping credible intervals are considered different at the 5% level of significance.	141
Figure 63. Time series of aquatic vegetation coverage in a region that includes the North and Central Delta and is based on annual remote sensing surveys. FAV = floating aquatic vegetation (includes <i>Eichhornia crassipes</i> and <i>Ludwigia</i> spp.). SAV = submersed aquatic vegetation (includes many species not distinguishable from remote sensing). Years without bars indicate those without data.	143
Figure 64. Comparison of aquatic vegetation coverage among water year types based on annual remote sensing surveys conducted over the North and Central Delta in 11 years during 2004-2020. FAV = floating aquatic vegetation (includes <i>Eichhornia crassipes</i> and <i>Ludwigia</i> spp.). SAV = submersed aquatic vegetation (includes many species not distinguishable from remote sensing).....	144

Figure 65. Time series of aquatic vegetation coverage in Franks Tract based on annual remote sensing surveys. FAV = floating aquatic vegetation (includes <i>Eichhornia crassipes</i> and <i>Ludwigia</i> spp.). SAV = submersed aquatic vegetation (includes many species not distinguishable from remote sensing). Years without bars indicate those without data.....	145
Figure 66. Biomass per unit effort of major zooplankton species versus Sacramento Valley Index, 1994-2020.	148
Figure 67. Non-metric multi-dimensional scaling plot of zooplankton community composition by drought year classification (Drought period [D], Neutral [N], and Wet period [W]).	149
Figure 68. Average total zooplankton biomass per unit effort biomass by drought year classification (Drought period [D], Neutral [N], and Wet period [W]). Drought year classification on its own was not significantly different (ANVOA $f = 3.006$, $p = 0.06$)	150
Figure 69. Average zooplankton biomass by biomass by drought year classification (Drought period [D], Neutral [N], and Wet period [W]) and season. Letters indicate groups not significantly different at the $p < 0.05$ level.	151
Figure 70. Average zooplankton biomass by drought year classification (Drought period [D], Neutral [N], and Wet period [W]) and region. Letters indicate groups not significantly different at the $p < 0.05$ level.....	152
Figure 71. Average zooplankton biomass by region and year for 2011-2020	153
Figure 72. Annual mean monthly jellyfish CPUE by region.....	154
Figure 73. Mean monthly Jellyfish CPUE for June-October, 2000-2021, separated by region and Drought year classification. The North Delta and South-Central regions were omitted due to extremely low jellyfish catch.	155
Figure 74. Monthly average density (clams/m ²) of invasive clams measured by GRTS and EMP by year. Letters denote groups with significantly different abundance (results of zero-inflated negative binomial model, (Table 21)). 2013 and 2016 were omitted due to small sample size.....	157
Figure 75. Monthly grazing rate of invasive clams as measured by GRTS and EMP by year for 2011-2019. Letters denote groups that are not significantly different at the $p < 0.05$ level. (Table 21).....	158
Figure 76. Average annual grazing rates for two species of invasive clams, 1976-present (<i>C. fluminea</i>) and 1987-present (<i>P. amurensis</i>) across the estuary by year type. Letters indicate groups without statistically significant	

differences. *C. fluminea* ANOVA F-value 1.028 on 2 and 37 Df. $p = 0.367$. *P. Amurensis* ANOVA F-value 6.81 on 2 and 28 Df, $p = 0.0039$ 159

Figure 77. Center of distribution (km from the Golden Gate) for *P. amurensis* versus the previous year’s Sacramento Valley Water Year index. Linear model of annual average distance versus the previous year’s Sacramento Valley index (coefficient -962, Adjusted R-squared: 0.2921 F-statistic: 14.21 on 1 and 31 DF, p -value: 0.000691) 160

Figure 78. Sacramento River winter-run Chinook Cohort Replacement Rate (1973-2020) by juvenile migration condition (Drought period, Neutral, or Wet period). 162

Figure 79. Central Valley spring-run Chinook Cohort Replacement Rate (1973-2020) by juvenile migration condition (Drought period [D], Neutral [N], or Wet period[W])...... 163

Figure 80. Central Valley fall-run Chinook Cohort Replacement Rate (1973-2020) by juvenile migration condition (Drought period [D], Neutral [N], or Wet period [W]). 164

Figure 81. Probability distribution of Juvenile Chinook salmon migration timing at Sherwood Harbor trawls from 1988-2021 by drought period type (Drought [D], Neutral [N], or Wet period [W]). 165

Figure 82. Probability distribution of Juvenile Chinook salmon migration timing at Chipps Island trawls from 1988-2021 by drought year classification (Drought [D], Neutral [N], or Wet period [W]). 166

Figure 83. Distribution of lengths of juvenile winter-run-sized Chinook salmon caught at Sherwood Harbor and Chipps Island trawls from 1988 to 2021 by Drought year classification (Drought [D], Neutral [N], or Wet period [W]). 167

Figure 84. Annual abundance indices for Longfin Smelt, Delta Smelt, Striped Bass, and American Shad as calculated by CDFW for their Spring Kodiak Trawl survey, 20mm survey, Summer Towntnet survey, and Fall Midwater Trawl survey for 2011-2021..... 169

Figure 85. Fall Midwater Trawl indices grouped by drought year classification (Drought period [D], Neutral [N], and Wet period [W]) for five pelagic fish species..... 171

Figure 86. Dendrogram of the species included in this analysis with colored boxes denoting significantly distinct species clusters. 174

Figure 87. Species specific silhouette widths with sub-community assemblages denoted via background color. Green colored bars denote the selected representative species. 175

Figure 88. Linear model predicted temporally dominant tensor across drought year classification for (left) the Threadfin Shad/White Catfish cluster, (middle) the marine cluster, and (right) the freshwater/brackish cluster. Letters above boxes indicate significantly different catch after accounting for species and sub-region. Note: the directionality of the anomaly can be positively or negatively related to catch; additional analyses are necessary to identify the trend. 176

Figure 89. Linear model predicted mean temporally dominant tensor across the observed range of the Sacramento Valley Index for (left) the Threadfin Shad/White Catfish cluster, (middle) the Marine cluster, and (right) the freshwater/brackish cluster. Shown with model confidence interval (polygon) and data (points). A significant p-value (i.e., ≤ 0.05) indicates the catch within the cluster changed significantly with the Sacramento Valley Index after accounting for species and sub-region. Note: the directionality of the anomaly can be positively or negatively related to catch; additional analyses are necessary to identify the trend. 177

Figure 90. Threadfin Shad model results. (a) Marginal mean Threadfin Shad catch highest probably densities Drought year classifications (Multiple Drought (Elsewhere "Drought"), "Neutral", and Multiple Wet (Elsewhere "Wet Period")). Letters above points indicate significant differences. (b) Bonferroni-corrected multiple comparisons of marginal means among water year type. Pairs with $\geq 95\%$ of posterior comparisons < 0 are considered significantly different water year types. 178

Figure 91. Longfin Smelt model results. (a) Marginal mean Longfin Smelt catch highest probably densities among Drought year classifications (Multiple Drought (Elsewhere "Drought"), "Neutral", and Multiple Wet (Elsewhere "Wet Period")). Letters above points indicate significant differences. (b) Bonferroni-corrected multiple comparisons of marginal means among water year type. Pairs with $\geq 95\%$ of posterior comparisons < 0 are considered significantly different water year types. 179

Figure 92. Threadfin Shad POD effect. (a) Threadfin Shad median catch Pre- and Post-POD (error bars represent 89% credible interval; categories labeled with different letters are significantly different). (b) Comparisons of catch between Pre- and Post-POD periods. A comparison with $\geq 95\%$ of posterior comparisons > 0 are considered significantly different. Model predictions are based on 2,000 posterior draws given the median of 20 sampling events per

sub-region per year, the median Sacramento Valley Index in Year_t of 7.08, and the median Sacramento Valley Index in Year_{t-1} of 6.89. 180

Figure 93 Threadfin Shad model prediction across (a) Sacramento Valley Index in Year_t given the Department of Water Quality water year hydrologic classification of threshold value between Below Normal and Above Normal (Sacramento Valley Index = 7.8) in Sacramento Valley Index in Year_{t-1} and (b) Sacramento Valley Index in Year_{t-1} given the hydrologic classification threshold value between Below Normal and Above Normal (Sacramento Valley Index = 7.8) in Sacramento Valley Index in Year_t. Lines represent median prediction and polygons represent 89% credible interval. Model predictions are based on 2,000 posterior draws given the median of 20 sampling events per sub-region per year. Data are constrained to the convex hull of observed values shown in Figure 94. 181

Figure 94 Threadfin Shad ZINB model (a, c, and e) pre- and (b, d, and f) post-POD (i.e., 2002) predicted (c and d) median catch, (a and b) upper 89% credible interval limit, and (e and f) lower 89% credible interval limit across Sacramento Valley Index in Year_t and Sacramento Valley Index in Year_{t-1} based on 2,000 posterior draws and given the median of 20 sampling events per sub-region per year. Open circles indicate observed values of Sacramento Valley Index in Year_t and Sacramento Valley Index in Year_{t-1}. The non-open circle points correspond to Sacramento Valley Index in Year_t and Sacramento Valley Index in Year_{t-1} scenarios predicted in Figure 95.. 182

Figure 95. Threadfin Shad ZINB model marginal mean catch given specific values of Sacramento Valley Index in Year_t (Sa_{Ct}) and Sacramento Valley Index in Year_{t-1} (Sa_{Ct-1}). The point type corresponds to the same point type in Figure 94. Error bars represent 89% credible interval. Posterior draws are based on the median of 20 sampling events per sub-region per year 183

Figure 96. Longfin Smelt POD effect. (a) Longfin Smelt median catch Pre- and Post-POD (error bars represent 89% credible interval; categories labeled with different letters are significantly different). (b) Comparisons of catch between Pre- and Post-POD periods. A comparison with $\geq 95\%$ of posterior comparisons > 0 are considered significantly different. Model predictions are based on 2,000 posterior draws given the median of 20 sampling events per sub-region per year, the median Sacramento Valley Index in Year_t of 7.08, and the median Sacramento Valley Index in Year_{t-1} of 6.89..... 184

Figure 97. Longfin Smelt model prediction across (a) Sacramento Valley Index in Year_t given the Sacramento Valley Index of 7.8 in Year_{t-1} and (b) Sacramento Valley Index in Year_{t-1} given Sacramento Valley Index of 7.8 in Year_t. Lines represent median prediction and polygons represent 89% credible interval. Model predictions are based on 2,000 posterior draws given

the median of 20 sampling events per sub-region per year. Data are constrained to the convex hull of observed values shown in Figure 98. 185

Figure 98 Longfin Smelt ZINB model (a, c, and e) pre- and (b, d, and f) post-POD (i.e., 2002) predicted (c and d) median catch, (a and b) upper 89% credible interval limit, and (e and f) lower 89% credible interval limit based on 2,000 posterior draws. Points indicate year-specific observed values of Sacramento Valley Index in Year_t and Sacramento Valley Index in Year_{t-1} based on 2,000 posterior draws and given the median of 20 sampling events per sub-region per year. Open circles indicate observed values of Sacramento Valley Index in Year_t and Sacramento Valley Index in Year_{t-1}. The non-open circle points correspond to Sacramento Valley Index in Year_t and Sacramento Valley Index in Year_{t-1} scenarios predicted in Figure 99.. 186

Figure 99. Longfin Smelt ZINB model marginal mean catch given specific values of Sacramento Valley Index in Year_t (Sac_t) and Sacramento Valley Index in Year_{t-1} (Sac_{t-1}). The point type corresponds to the same point type in Figure 98. Error bars represent 89% credible interval. Posterior draws are based on the median of 20 sampling events per sub-region per year. 187

Figure 100. Plot of major ecological parameters and their relationship with. Drought relationships were ranked on a qualitative scale of zero (no relationship) to 5 (large relationship) to multi-year droughts. Blue bars on the right side of the circle represent parameters with decreases during droughts. Orange bars on the left side of the circle represent parameters that increase during droughts. 188

Figure 101. Plot of major ecological parameters in 2021 and their magnitude in comparison to previous droughts. Some of these differences may be due to the 2021 TUCP and/or Emergency Drought Barrier. Relationships were ranked on a qualitative scale of zero (similar to previous droughts) to 5 (very different from previous droughts). Green bars represent parameters that decreased relative to past droughts. Yellow bars represent parameters that increased relative to past droughts. Grey bars are parameters for which we have not completed data processing and analysis. Some parameters are only available through September of 2021, so this plot should be considered preliminary. 189

Abbreviations and Acronyms

ANOVA – Analysis of Variance

Barrier – 2021-2022 West False River Emergency Drought Barrier

BPUE – Biomass per Unit Effort

CAWSC – California Water Science Center (USGS)

CDFW – California Department of Fish and Wildlife

CNRA – California Natural Resources Agency

CPUE – Catch/Count per Unit Effort

CRR – Cohort Replacement Rate

CSTARS – Center for Spatial Technology and Remote Sensing

CVFRC – Central Valley Fall Run Chinook

CVP – Central Valley Project

CVSRC – Central Valley Spring Run Chinook

DBW – California State Parks Division of Boating and Waterways

Df – Degrees of Freedom

DSP – Delta Science Program

DWR – Department of Water Resources

EDI – Environmental Data Initiative

EMP – Environmental Monitoring Program

Estuary – San Francisco Estuary

FAV – Floating Aquatic Vegetation

FMWT – Fall Midwater Trawl (CDFW)

F-value - ratio of two variances (F-value), and probability-value

GRTS – Generalized Random Tessellation Stratified sampling

IEP – Interagency Ecological Program

ITP – Incidental Take Permit

LSZ – Low Salinity Zone (0.5-6 PSU)

MAST – Management, Analysis and Synthesis Team

NCRO – North Central Region Office (DWR)

NMDS – Non-Metric Multi-Dimensional Scaling

NMFS – National Marine Fisheries Service

Pr(>F) –(also p-value) the probability of the assumed probability distribution will be greater than or equal to (or less than or equal to in some instances) observed results

PTA – Principal tensor analysis

Reclamation – US Bureau of Reclamation

SAV – Submerged Aquatic Vegetation

SRWRC – Sacramento River Winter Run Chinook

STN – Summer Townt Survey (CDFW)

Sum Sq - sum of squares

SWP – State Water Project

TAF – Thousand Acre Feet

TUCP (Temporary Urgency Change Petition

USFWS – US Fish and Wildlife Service

USGS – United States Geologic Survey

Water Board – California Water Resources Control Board

ZINB – Zero Inflated Negative Binomial

Introduction/Background

Research Questions

- How do ecosystem conditions in the Sacramento San-Joaquin Delta, Suisun Bay, and Suisun Marsh (the Delta) change during multi-year droughts?
- What are the ecosystem conditions in the Delta during the 2020-2021 drought, and how do they compare to previous droughts? Are any of the ecosystem conditions in the Delta during 2021 different because of the 2021 Temporary Urgency Change Petition (TUCP) or Emergency Drought Barrier (Barrier)?

Regulatory Background

California's Mediterranean climate is characterized by hot, dry summers, and cool, wet winters. There is typically little to no rainfall for six to nine months out of the year in the central and southern regions of the state. There is also high inter-annual variability, with average rainfall varying from a low of 23.8 cm in 1924 to a high of 105.8 cm in 2017, usually depending on just a few massive storms each year (Dettinger 2011). This high variability leads to frequent floods and multi-year droughts that result in massive year-to-year changes in both the aquatic community and the ability of managers to provide water for consumptive use.

Due to California's high inter-annual variation in precipitation and well-developed water storage and conveyance infrastructure, a single dry year does not necessarily constitute a drought. Droughts may be classified based on meteorology (a period of low precipitation), hydrology (period of low in-stream flows), or sociological (a shortage of water supply for human use). While there is no single agreed-upon definition for "drought", droughts in California generally occur when there are multiple years of low precipitation and a resulting water supply shortage (DWR 2020). For the purposes of this document, we are defining "drought" as two or more consecutive years with a Sacramento Valley Index of Below Normal, Dry, or Critically Dry (see Sacramento Valley Index in Appendix A, Supplemental Information for details on water year index). This is similar to, but slightly broader than the requirements of the California Department of Fish and Wildlife's (CDFW) Incidental Take Permit (ITP) for the State Water Project (SWP), which require drought contingency planning when there are consecutive Dry or Critically Dry years. We have chosen to include Below Normal years as well,

to be consistent with previous drought research (Mahardja et al. 2021), and to account for lack of reservoir recharge in below normal years.

Throughout this report, we will be comparing multi-year droughts to multi-year wet periods (defined as multiple Wet or Above Normal years in a row, as defined by the Sacramento Valley Index) and “Neutral” years, which are neither part of a drought nor wet period. We will be providing special attention to the drought of 2020-2021 and how it compares to previous droughts.

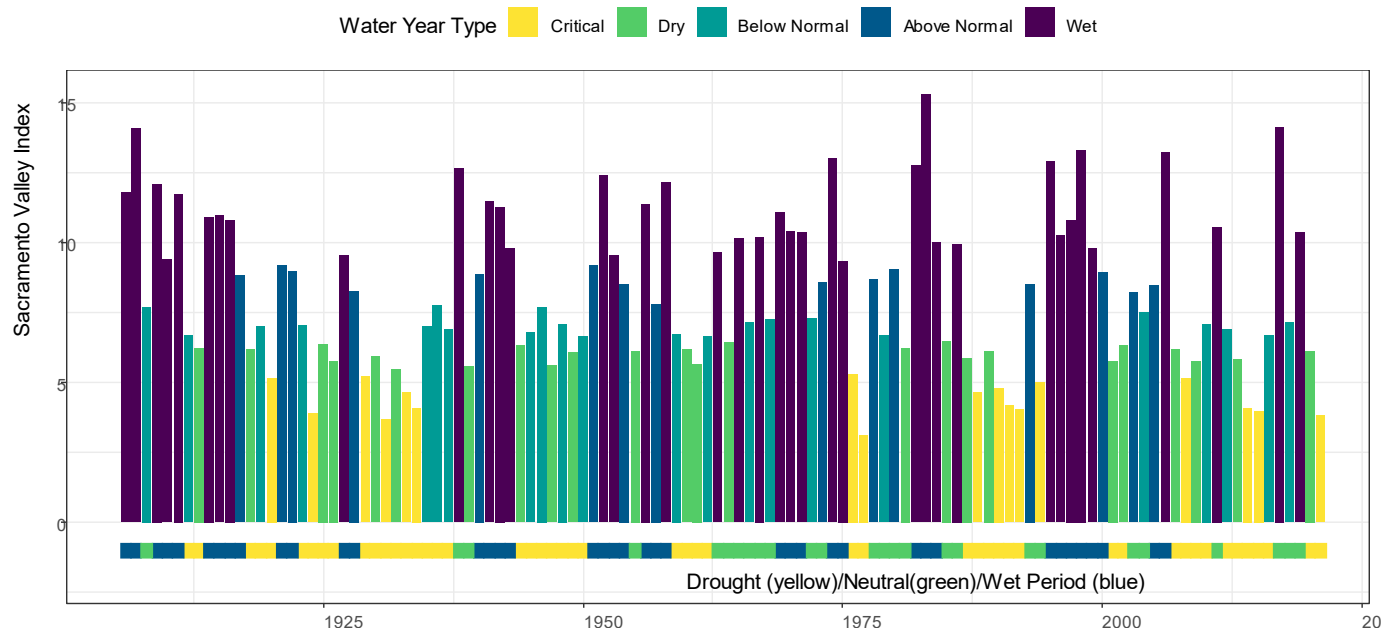


Figure 3. Plot of water year indexes for the Sacramento Valleys from 1905 to 2021. Data is from the California Department of Water Resources (<https://cdec.water.ca.gov/reportapp/javareports?name=WSIHIST>). Periods classified as “Droughts” (multiple dry, critically dry, and below normal years in a row) are highlighted by yellow bars below the x-axis. Periods classified as “Wet Periods” (multiple wet years in a row) are highlighted with blue bars below the x axis. “Neutral” periods (neither drought nor wet period) are highlighted in green below the x-axis.

Previous droughts in recent history include the dry periods of 1929-1937, 1944-1950, 1959-1962, 1976-1977, 1987-1992, 2001-2002, 2007-2010, and 2012-2016 (Figure 3). In pre-historical periods, tree ring analysis shows droughts lasting decades to hundreds of years (Stine 1994). Climate change could bring increased frequency of major floods and droughts, which will stress California’s environment and economy (Swain et al. 2018). The current drought (2020-2021, ongoing), has resulted in record low stream

flows, record low reservoir levels, extremely dry soils, low groundwater reserves, and problems providing enough water for wildlife and human uses.

History of drought actions

While California's dynamic and variable climate has caused frequent dry periods over the past 50 years, resource managers have responded to these periods of low precipitation with management actions, the interaction of which have produced the conditions seen in the Delta. Timing and magnitude of flows through the Delta are controlled by precipitation, rates of snowmelt, upstream dams, operable gates and weirs, and diversions. The amount of water released from upstream dams, the amount of water diverted at various points, and operation of gates within the Delta are controlled by a complex assortment of water quality standards and environmental protections which frequently change in response to new information and new infrastructure. While it is important to keep changes to these operations in mind when evaluating the impact of droughts, a full assessment of how regulations and drought management actions impact the hydrology of the Delta is beyond the scope of this report. Detailed patterns of water management in the historical record can be found in Reis et al. (2019), with a further discussion of flows for drought management in Durand et al. (2020) and the report "California's Most Significant Droughts: Comparing Historical and Recent Trends (DWR 2020). Notwithstanding, some context of water management is important in interpreting our results and is provided below.

Drought management actions directly impacting the Delta ecosystem may take several forms:

- Changes to Delta water quality and flow requirements, which may affect CVP/SWP export operations.
- Changes to operation of gates (e.g., the Suisun Marsh Salinity Control Gates and/or Delta Cross Channel Gates).
- Installation of temporary barriers.
- Changes to operation of fish hatcheries and other upstream actions (not covered in this report).
- Curtailment of diversions (not covered in this report).

Most drought management actions will be implemented faster if they occur during a declared state of emergency, since many environmental regulations are suspended. Drought emergencies have been declared three times in California's history, during the 2007-2009 drought, the 2012-2016 drought (DWR 2020), and the 2020-2021 drought (Newsom 2021). Bills allocating

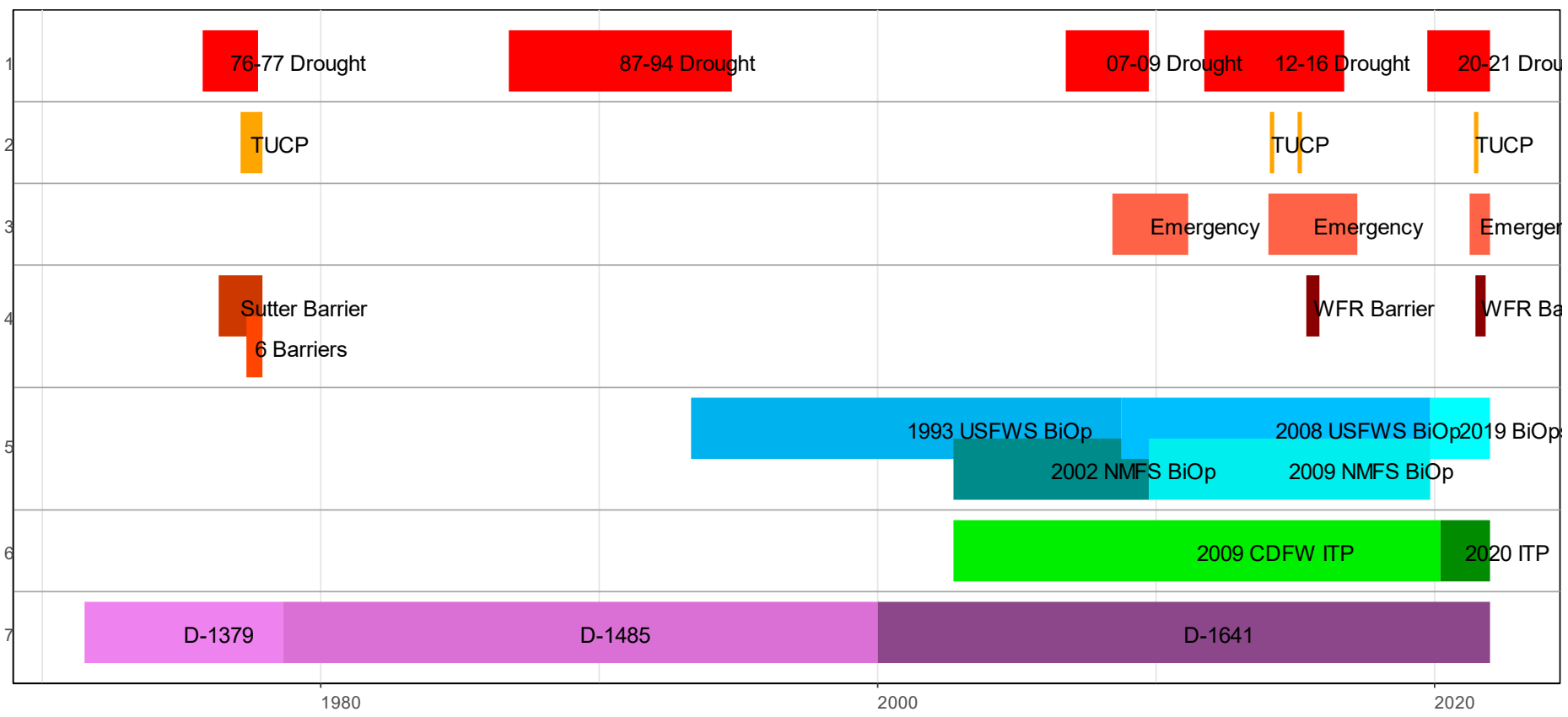
funding for drought actions, such as the 1977 Emergency Drought Act (Comptroller General of the United States 1977), two bills in 2014 including over \$700 million in emergency drought relief efforts, the 2014 water bond (Taylor 2016), and similar measures also increase the speed with which actions can take place.

Changes to Delta Outflow may be managed by reducing releases from upstream dams (often to preserve storage for cold-water pool management) or by reducing diversions. Within the Delta, the most impactful regulations controlling Delta outflow are biological opinions and incidental take permits for the State and Central Valley Water Projects, the Water Quality Control Plan for the San Francisco Bay/Sacramento San Joaquin Delta Estuary (i.e., the Bay-Delta Plan)(SWRCB 2018), the Water Quality Control plan for the Sacramento Basin and San Joaquin Basin (i.e., Basin Plan) (CVRWQCB 2009), water rights decisions (i.e., D-1641)(SWRCB 2000), and water rights contracts. During periods of extreme drought or governor-declared emergencies, these standards have been relaxed through Temporary Urgency Change Petitions (TUCPs). Most notably, changes to outflow standards were granted during the 1976-1977 drought, from February to March of 2014, February to March of 2015, and June to July of 2021 (see below for more on the 2021 TUCP, Figure 4). Likewise, the U.S. Bureau of Reclamation's (Reclamation) Sacramento River Settlement Contracts and the San Joaquin River Exchange Contracts both contain 'critical' year provisions to reduce the water delivery to 75% of the contractual amount.

Operation of gates and installation of temporary barriers have been used to combat salinity intrusion, maintain water quality for human uses, and benefit fishes. The Delta Cross Channel Gates are generally closed during the winter and salmon migration season and are open during the summer. During the 2012–2016 drought, operations to the gates were changed as part of the 2014 and 2015 TUCPs (DWR and USBR 2015) allowing the Delta Cross Channel gates to be opened during the spring, preventing salinity intrusion and preserving upstream storage. The Suisun Marsh Salinity Control gates are operated September–May to lower salinity in Suisun Marsh(USFWS et al. 2013). The gates begin operation earlier (September instead of October or November) when it is dry, and they continue operation later into the year. Up to four temporary barriers are installed annually in the South Delta for water quality (Wilson 2013). All these physical controls counteract some of the impacts of drought.

Emergency drought barriers have been installed three times in California history to combat salinity intrusion. In 1976 a barrier was installed in Sutter Slough, and in 1977 six more barriers were installed, including Old River east of Clifton Court, San Joaquin River near Mossdale, Rock Slough, Indian

Slough, Dutch Slough, and the head of Old River (Figure 4). In 2015 a barrier was installed in West False River from June to November (DWR 2019). In 2021, a barrier was installed in the same location in West False River in July (see Emergency Drought Barrier, below).



Drought actions of 2021

Water Year 2021 was the driest on record since 1977. Rainfall was well below average, but the snowpack in March, 2021 indicated that sufficient reservoir inflow was likely available to meet requirements. Conditions significantly changed at the end of April 2021 when it became clear that expected reservoir inflow from snowmelt failed to materialize. The May 90% exceedance forecast for the water year Sacramento Valley Four River Index identified a reduction of expected runoff of 685 TAF from the forecast generated only a month earlier in April. The combination of factors, including the May 2021 inflow forecast being far less than predicted, parched watershed soils and extremely low rainfall, continuing dry and warm conditions, and limited available water supplies in the Delta created an urgent need to act. As announced by the Governor in his May 10, 2021 Emergency Proclamation on drought conditions for the Bay-Delta and other watersheds, the continuation of extremely dry conditions in the Delta watershed meant there was not an adequate water supply to meet water right permit obligations for instream flows and water quality under Water Rights Decision 1641 (D-1641).

The 2020 Record of Decision on the Long-Term Operations of the Central Valley Project (CVP) and State Water Project (SWP) and the 2020 ITP for the SWP included a commitment to develop a "Drought Toolkit", containing voluntary actions which may help address the impact of drought and dry year conditions. The ITP also contains the requirement for a Drought Contingency Plan, containing specific actions to be undertaken in a drought year. These plans were developed by the California Department of Water Resources (DWR) and the US Bureau of Reclamation (Reclamation), in coordination with the US Fish and Wildlife Service (USFWS), National Marine Fisheries Service (NMFS), the California Department of Fish and Wildlife (CDFW), the State Water Resources Control Board (Water Board), and SWP and CVP Contractors. By February of each year following a critical year, DWR must report on the measures employed and assess their effectiveness. The 2021 Drought Contingency Plan includes a commitment to ecosystem monitoring to assess the impact of drought and drought actions. This report comprises the report on the effectiveness of ecosystem monitoring in the Delta and the ecosystem response to the drought and drought actions within the Delta. Several related reports are also in development. Specifically:

- A report on the impact of the TUCP and Emergency Drought Barrier on harmful algal blooms and aquatic weeds in the Delta¹. Submitted Dec. 15th 2021, with a supplemental report to be completed in June 2022.

¹ Available: https://www.waterboards.ca.gov/drought/tucp/docs/2021/20211215_cond8-report.pdf

- A report on all drought toolkit actions, to be submitted Feb 1st, 2022.
- A report on the effectiveness of the Emergency Drought Barrier, draft to be completed by March 2022.

2021 TUCP

Reclamation and DWR jointly submitted the TUCP to request the Water Board consider modifying requirements of Reclamation's and DWR's water right permits to enable changes in operations of CVP and SWP (collectively Projects) that will allow for delivery of water with conservation for later instream uses and water quality requirements. On June 1, 2021, the Water Board issued an order conditionally approving a petition and conditions requiring compliance with Delta water quality objectives in response to drought conditions (SWRCB 2021). The TUCP modification to some D-1641 requirements was intended to preserve Delta water quality while preserving some carryover storage in upstream reservoirs including Shasta and Oroville.

Substance of the Temporary, Urgency Change Petition

The Petitioners requested the following temporary changes to requirements that were imposed pursuant to D-1641 for the period June 1 through August 15:

- For June 1 – June 30, reduce the required minimum 14-day running average Delta outflow from 4,000 cfs to 3,000 cfs.
- For July 1 – July 31, reduce the required minimum monthly average Delta outflow from 4,000 cfs to 3,000 cfs, with a seven-day running average of no less than 2,000 cfs;
- For June 1 through July 31, limit the combined maximum export rate to no greater than 1,500 cfs when Delta outflow is below 4,000 cfs, and allow the 1,500 cfs limit to be exceeded when the Petitioners are meeting Delta outflow requirements pursuant to D-1641 or for moving transfer water; and
- From June 1 through August 15, move the compliance point for the Western Delta agricultural salinity requirement from Emmaton on the Sacramento River to Threemile Slough on the Sacramento River.

Emergency Drought Barrier

Along with the TUCP, DWR requested emergency authorization for installation of the 2021–2022 West False River Emergency Drought Salinity

Barrier (Barrier) in May of 2021. The Emergency Drought Barrier is a temporary physical rock fill barrier which reduces the intrusion of high-salinity water into the Central and South Delta, and such barriers have proven effective in the past Delta (DWR 2019). During drought conditions, water stored in upstream reservoirs may be insufficient to repel salinity moving upstream from San Francisco Bay. Without the protection of the Barrier, saltwater intrusions could render Delta water unusable for agricultural needs, reduce habitat value for aquatic species, and affect roughly 25 million Californians who rely on the export of this water for personal use. The 2021-2022 Barrier is very similar in terms of location, size, and design as the drought salinity barrier that was permitted and installed during the 2015 drought, though it will be kept in place through the winter of 2021/2022 instead of being removed in the fall. The barrier will be notched from Jan-April 2022 to allow fish passage.

Drought team and collaboration

The IEP Drought Management Analysis and Synthesis Team (MAST) was originally formed in 2014 to assess the impact of the major drought of 2012-2016. This team was reformed in spring of 2021 with several of the original members as well as many new members to assess the drought of 2020-2021 and future drought impacts. The team contains members from DWR, DSP, Reclamation, CDFW, USFWS, NMFS, and USGS who are all committed to synthesis and monitoring of ecosystem drought impacts. The team works closely with the Reclamation-led effort to develop a Drought Toolkit and the joint DWR/Reclamation team developing the annual Drought Contingency Plan.

Scientific Background

The influence of annual freshwater flow (or lack of flow) on water quality, productivity, and fishes of the Delta is relatively well-studied, though many responses are still difficult to predict. There are well-established relationships between freshwater flow and population levels of certain biota, most notably the Longfin Smelt (*Spirinchus thaleichthys*) which has much higher abundances and recruitment during high-flow conditions (Kimmerer et al. 2019). Other fishes, such as the Delta Smelt (*Hypomesus transpacificus*), have a more complicated relationship with flow. Temperature, rather than outflow has been indicated as the key driver of smelt population dynamics, particularly over the past ten years (FLOAT-MAST 2021; Schultz et al. 2019; Smith et al. 2021).

Multi-year droughts have received less study than seasonal or annual outflow. However, the 2012-2016 drought provided the impetus for a

number of studies and reports that give us a basis for predictions regarding major ecosystem changes we expect to see during a drought (Jabusch et al. 2018; Lehman et al. 2017; Mahardja et al. 2021; Singer et al. 2020)(Table 1). Based on similar information and experiences with previous drought operations (e.g. Kimmerer et al. 2019; Durand et al. 2020), we also provide a specific discussion of the expected influences of the TUCP and Emergency Drought Barrier (see text below and Table 1).

Hydrology and Water Quality

Reduced precipitation and the associated decrease in freshwater inputs to the estuary is the most obvious signal of a drought. In the Delta, hydrology is controlled through upstream dam releases, diversions, gates, and barriers (as discussed above). With lower annual precipitation, we can expect lower instream flows in all of the major rivers entering the Delta (Durand et al. 2020). Lower flows in the rivers will reduce the activation of off-channel habitat and limit floodplain inundation. The decreased inflow will have several direct impacts on water quality. Within the Delta, the salinity gradient will move inland due to greater oceanic and tidal influence under decreased outflow conditions. Water residence times in the Delta increases under low flows, allowing more time for biogeochemical processes to impact water quality, as well as more time for biota (e.g., phytoplankton and zooplankton) to grow. Lower freshwater flows, combined with an increase in aquatic weeds, will reduce sediment transport and turbidity (Conrad et al. Unpublished Manuscript; Hestir et al. 2016).

The 2021 TUCP and Barrier affect influential environmental drivers such as hydrology and salinity, though these effects are expected to be slight in comparison with the effect of the drought itself. Modeling completed for the 2015 Emergency Drought Barrier and TUCP showed a decrease in Sacramento River volume of approximately 200 TAF (DWR 2015) and a shift in the salinity field with slightly higher salinity in Suisun Bay and the Sacramento River, and lower salinity in the South Delta when compared to D-1641 conditions (Table 1). Forecasting for the summer of 2021 predicted increases in conductivity and increases in X2 similar to those seen in 2015. Models of the 2021 TUCP analyzed in the Biological Review currently predict an increase in conductivity of approximately 1000 $\mu\text{S}/\text{cm}$ at Chipps Island and an increase in X2 of 2 km June-August (see 2021 TUCP Biological Review).

Nutrients

We predicted that downstream transport of nutrients would decrease, but that concentrations may increase locally. Presence of nutrients in the system

is controlled by concentration and rate of input to the system (loading), as well as transport, transformation, and burial within the system.

Discharge from wastewater treatment plants provides the bulk of the nitrogen influx into the system, though nitrogen also enters the system from agricultural and urban runoff (Novick et al. 2015; Saleh and Domagalski 2015; Wankel et al. 2006). Based on predicted changes to hydrology, drought may not significantly impact loading from wastewater treatment plants, but it will reduce dilution and increase transport times, potentially leading to increases in observed concentrations in certain areas. During the 2012-2016 drought, an increase in ammonium concentrations was one of the responses noted (Conrad et al. draft manuscript). Upgrades to the Sacramento Regional's Wastewater Treatment Plant, which were completed in May of 2021, substantially reduced total nitrogen inputs to the Delta, and may change the response of nitrogen to the current drought (RegionalSan 2021).

We did not expect the 2021 TUCP or Emergency Drought Barrier to significantly impact loading or concentration of nutrients above any changes due to the drought itself.

Phytoplankton and Harmful Cyanobacteria Blooms

Phytoplankton (photosynthetic algae plus cyanobacteria) convert raw materials (sunlight and inorganic material in the water) into biomass that fuels the base of the aquatic food web (Durand 2015). However, exposure to some cyanobacteria, such as toxic strains of *Microcystis*, through dissolved toxins in the water, dietary intake, or impacts to dissolved oxygen can adversely affect the aquatic food web in the Delta by reducing the health and survival of phytoplankton, zooplankton and fish (Acuña et al. 2020; Acuna et al. 2012a; Acuna et al. 2012b; Ger et al. 2010a; Ger et al. 2010b; Sutula et al. 2017).

Phytoplankton occur throughout the water column in the Delta and their growth rate is directly related to water quality conditions. Research in the Delta has identified the influence of streamflow, light, water temperature, residence time, grazing by zooplankton and clams, salinity and nutrient concentration on both the biomass and community composition of the phytoplankton in the estuary (Cloern et al. 2020; Dugdale et al. 2007; Jassby and Cloern 2000; Lehman 1992a; Lehman and Smith 1991; Stumpner et al. 2020; Sutula et al. 2017). Because water quality conditions vary with drought, we also expect a direct link between drought conditions and both phytoplankton biomass and community composition.

We predicted the drought would increase the abundance of the potentially harmful cyanobacterium *Microcystis* and a decrease in chlorophyll-*a* concentration, an estimate of phytoplankton biomass, in most regions. Research has demonstrated that chlorophyll-*a* concentration was lower during critically dry years compared with wet years for the spring through fall across regions of the Delta between 1970 and 1993 (Lehman 1996). However, the highest chlorophyll-*a* concentration commonly occurred during years with intermediate streamflow (Lehman 1996). In Suisun Bay, high chlorophyll-*a* concentration also occurred when there was a decrease in upstream water diversion (Hammock et al. 2019).

Drought years in the past were characterized by a decrease in diatoms and an increase in cryptophytes and cyanobacteria (Lehman 2004; Lehman 1996; Lehman 2000). Although diatom abundance since 2000 has been low, relatively large diatom blooms in 2014 and 2016 were probably the result of long residence time coupled with a reduction of algal inhibitors (Glibert et al. 2014a; Jungbluth et al. 2021). The phytoplankton community in the Central and South Delta during the summer and fall has been characterized by blooms of the potentially toxic cyanobacterium *Microcystis* since 2000 (Lehman et al. 2005; Lehman et al. 2021). These harmful blooms are denser during drought years and vary positively with increased water temperature and residence time (Lehman et al. 2017; Lehman et al. 2020).

An important management concern is whether the placement of an Emergency Drought Barrier in West False River will promote harmful blooms in Franks Tract and the Central Delta by restricting tidal flow and increasing water residence time. A previous analysis of the impact of the 2015 West False River Drought Barrier determined there was no effect of the Barrier on phytoplankton biomass (Kimmerer et al. 2019). *Microcystis* biomass and total microcystins concentration in the Central Delta were greater in 2014 when the Barrier was not in place, compared with 2015 when the Barrier was in place, despite warmer seasonal water temperature (Lehman et al. 2018) and lower water flow rates east of the Barrier in 2015 (Kimmerer et al. 2019).

Zooplankton

We predicted a decline in zooplankton abundance during the drought, particularly in Suisun Bay and Suisun Marsh, decreasing the availability of this critical source of food for fishes. However, the drought likely impacted specific taxa differently and impacts varied by location. High outflow years transport freshwater zooplankton into Suisun Bay, increasing abundance of certain taxa (particularly the calanoid copepod *Pseudodiaptomus forbesi*) in this region (Kimmerer et al. 2018c). Such events are unlikely during a

drought, and we can therefore predict freshwater zooplankton like *P. forbesi* will likely decrease in the Suisun Bay and that many taxa will shift their center of distribution upstream. Analysis of the distribution of zooplankton communities during the previous drought found copepod density decreased during the driest summers, as did cladocerans (Conrad et al. Unpublished Manuscript). Other analyses, however, have not detected a trend between copepod densities and X2 over longer time frames (Hobbs et al. 2019).

The drought-induced change in phytoplankton communities discussed earlier may also have bottom-up effects on the zooplankton community, but these effects are difficult to predict. *Microcystis* and other toxigenic cyanobacteria may directly harm copepods in the estuary (Ger et al. 2009). Other cyanobacteria, usually considered “poor-quality” food for zooplankton, may comprise a larger proportion of zooplankton diet than previously thought (Kimmerer et al. 2018a). In contrast, diatoms are generally thought to be nutritious for zooplankton due to their high fatty acid content (Caramujo et al. 2008). Jungbluth et al. (2021), however, found that blooms of the diatom *Aulacoseira* seen during the 2012-2016 drought did not aid in zooplankton growth, potentially due to spikes on the filament ends that may deter grazing.

Floodplains may be highly productive sources of zooplankton with appropriate timing and duration of inundation. Flow pulses during the fall on the Yolo Bypass have been linked to several phytoplankton blooms and associated increases in zooplankton (Frantzich et al. 2018), though other pulses failed to provide the same magnitude of response (Twardochleb et al. 2021). Other studies of zooplankton have noted their abundance can be order of magnitude greater in flooded rice fields and managed floodplains compared to adjacent rivers (Corline et al. 2017; Grosholz and Gallo 2006; Jeffres et al. 2020; Sommer et al. 2001). Lack of floodplain inundation and low summer-fall flows, as predicted under drought may limit subsidies of this supply of zooplankton to downstream habitats.

We did not expect the TUCP or Barrier to significantly impact abundance of zooplankton above any changes due to the drought itself, though it may decrease transport of freshwater zooplankton from the Delta into Suisun Bay (As seen in Kimmerer et al. 2019).

Aquatic Weeds

Both submersed aquatic vegetation (SAV) and floating aquatic vegetation (FAV) establish more readily in slower-moving water, so low flow conditions that occur during droughts have been linked to increases in coverage of invasive vegetation. Changes to flow patterns caused by the 2015

Emergency Drought Barrier were implicated in the expansion of submerged vegetation in Franks Tract (Kimmerer et al. 2019). Increases to nutrients, such as seen during 2013-2014, may also facilitate expansion of aquatic vegetation, though this effect is less conclusive and more complicated since many, but not all SAV obtain nutrients through roots in bed sediment. (Boyer and Sutula 2015; Dahm et al. 2016).

The increase in aquatic vegetation may be mitigated by control methods. The Aquatic Invasive Plant Control Program of the CA State Parks Division of Boating and Waterways (DBW) is chiefly responsible for aquatic vegetation control in the Delta and primarily employs chemical control tools. DBW is permitted to treat up to 15,000 acres per year of aquatic vegetation, though typically they treat only about 40% of that limit (DBW 2020). For FAV control, DBW most commonly uses glyphosate but also uses some imazamox and 2,4-D. For SAV control, fluridone is by far the most commonly applied herbicide in the Delta. However, recent studies have shown use of fluridone on SAV in tidal environments, such as the Delta, are generally ineffective (Rasmussen et al. in review, Khanna et al. In review). Therefore, this treatment program may increase loading of herbicides into the system without significantly affecting weed abundance. Treatment of floating aquatic vegetation with herbicides is thought to be somewhat more effective, though there are noticeable changes in water quality post-treatment (Tobias et al. 2019).

It will be difficult to extract the response to the Barrier from the response to the drought. We predicted drought conditions would cause an increase in both FAV and SAV across the Delta. We predicted an increase in aquatic vegetation in Franks Tract after installation of the Barrier, due to the decrease in water velocity in the tract. While Durand et al. (2016) failed to detect a relationship between establishment of aquatic vegetation and velocity, in 2015, weeds increased in coverage within Franks Tract, and the area remained inundated with weeds even after high flows returned (Kimmerer et al. 2019). We expected a similar response to the 2021-2022 Barrier, though the high coverage of weeds within Franks Tract over the past several years will make it difficult to detect a response.

Fish

The native fish community of California evolved in response to regular cycles of floods and droughts, but recent droughts have resulted in major effects on the fish assemblage (Mahardja et al. 2021). We, therefore, predicted the general effects of the drought will be an increase in invasive fishes, particularly those associated with aquatic vegetation, and a decrease in floodplain spawners and pelagic fishes. The decline in pelagic fishes includes

a decline in abundance and recruitment of Delta Smelt and Longfin Smelt. We also predict a decrease in survival of out-migrating juvenile salmonids, and a shift toward later migration of juvenile salmonids.

Water management in today's system has, however, altered the frequency and magnitude of floods, as well as mitigated drought within the inherent capability of the system. The resulting hydrology, with lower spring outflow and higher summer base flows compared with historic conditions, is more like southeastern US rivers than historic California rivers. Introduced fishes from the Southeast thrive in these more stable conditions (Moyle et al. 2012). During droughts, stream flows are slower and water is warmer, making habitat more suitable for these invaders. Salinity intrusion during low flow periods would be predicted to reduce abundance of invasive freshwater centrarchids (such as Largemouth Bass, *Micropterus salmoides*), but there was no decline detected during the 2012-2016 drought (Conrad et al. Unpublished Manuscript).

The increase in submerged vegetation that occurred during the 2012-2016 drought may partially account for this surprising results. Increased vegetation may also contribute to the reduction in abundance of the pelagic fish community. Mahardja et al (2021) found that pelagic fish tended to decline during drought conditions. Pelagic fish often recovered quickly, but they did not always fully recover in wet years following a drought. In contrast, littoral fishes were more resistant to drought. For example, the invasive Mississippi Silverside (*Menidia audens*) experienced a marked increase in abundance during the drought (Mahardja et al. 2016).

Delta Smelt abundance is affected by habitat availability and quality, as defined by temperature, turbidity, and salinity. High-outflow years put the majority of fall low salinity zone habitat (0.5 to 6 PSU) in Suisun Marsh and Suisun Bay which results in greater habitat area (Sommer and Mejia 2013). However, this relationship only holds true during cool years. Warm, high-outflow years do not benefit smelt to the same degree (as seen during the hot, high-outflow year of 2017) (FLOAT MAST 2021). While dry years may be either warm or cool, droughts tend to be warmer, on average, than wet periods (Jeffries et al. 2016). Delta Smelt population numbers are critically low, with only two adult and eight larval smelt detected by the Enhanced Delta Smelt Monitoring Program in the first five months of 2021 ([USFWS data](#)). An extended drought, particularly if temperatures are warm, could push wild Delta Smelt to extirpation, leaving only a hatchery refuge population.

Longfin Smelt abundance is strongly tied to freshwater outflow, with large increases in population during high-outflow years (Kimmerer 2002a; Nobriga

and Rosenfield 2016). This may be tied to increased access to spawning/rearing habitat in San Pablo Bay and South San Francisco Bay during high-outflow periods (Grimaldo et al. 2017; Parker et al. 2017), but the specific mechanism remains elusive. Regardless of the mechanism, recruits per spawner decrease with lower outflow (Nobriga and Rosenfield 2016), and an extended drought may have major impacts on the population's ability to rebound after the drought. Longfin Smelt experienced record low population numbers during the 2012-2016 drought, and their population has yet to fully recover, so their population resilience may be substantially reduced (Mahardja et al. 2021).

The Bay-Delta, and its habitats, is also an important area for out-migrating salmon, serving as an area of transition where fish can acclimate to saltier conditions, and nursery areas where fish can forage and grow to improve their chance of ocean survival (Moyle et al. 2008). Juvenile Sacramento River winter-run Chinook (SRWRC) enter the Delta as early as September, when the majority have yet to undergo smoltification (Miller et al. 2010) and leave the Delta at Chipps Island between January and April (del Rosario et al. 2013). Likewise, Central Valley spring-run Chinook (*Oncorhynchus tshawytscha*, CVSRC) enter the Delta December through May, and will exit the Delta between March and May (McKenzie 2020). The effect of drought conditions on the Delta habitat, and in turn the effects on juvenile Chinook in the Delta, are connected to survival, migration timing and growth (Windell et al. 2017).

Salmonids may be impacted by drought at multiple life stages, not all of which are covered in this report. Higher water temperatures in the rivers may cause lower survival of adults returning to their spawning habitats, as well as lower egg survival. Once fry have left their spawning habitat to begin their outmigration, juvenile salmon are known to have low survival during low-outflow years (Michel et al. 2015). Salmon generally initiate migration during flow pulses, so their outmigration may be delayed in dry years (del Rosario et al. 2013; but see Morita 2019). Furthermore, low flow and high water temperatures in the Sacramento River may reduce survival before they reach the Delta.

Once in the Delta, higher temperatures and lower flow will result in higher predator activity (Hance et al. 2022; Henderson et al. 2019; Nobriga et al. 2021), and higher juvenile salmon metabolic stress (Del Rio et al. 2019; Farrell 2009), culminating in elevated salmon vulnerability to predation and pathogens (Marine and Cech Jr 2004). Lower flows may also result in shorter rearing time and smaller size of ocean entry, reducing ocean survival (Hassrick et al. 2016; Munsch et al. 2019). Reduced outflows also influence salmon migration routing (Melnychuk et al. 2010; Nobriga et al. 2021; Perry

et al. 2018), causing higher risk of salmon migration into the Central and South Delta where survival rates are known to be low relative to Steamboat Slough and the mainstem Sacramento River (Pope et al. 2021; Singer et al. 2020).

The TUCP and Barrier will cause a slight decrease in Delta outflow and a slight increase in X2, however this is not expected to have a significant impact on Delta-wide fish distribution or abundance beyond the impact of the drought itself. The increase in X2 will not cause a change in Delta Smelt habitat area since the Low Salinity Zone will already be restricted to the Sacramento River. There may be local increases in predatory fishes (Striped Bass and Black Bass) immediately around the Barrier since predatory fishes are known to congregate around artificial structures and eddies (Lehman et al. 2019; Sabal et al. 2016). Predation associated with the Barrier will be explored in more detail as part of the 2021-2022 Barrier Monitoring Plan.

The TUCP is unlikely to affect juvenile salmon in the Delta because the action was in effect during a time of year when few, if any, juvenile salmon were migrating through the Delta. Modeling conducted for the TUCP biological review showed salmonids to have a very small decrease in Delta survival and very small increase in south-Delta routing for any juvenile salmonids that do arrive in the Delta during TUCP conditions, but the 0-2% difference predicted by these models is unlikely to be detectable with monitoring. Juvenile salmonids may have come into contact with the Barrier before it was notched in Oct-Dec of 2021, but this may serve to prevent Sacramento migrants from entering the Central Delta.

Predictions

Table 1. Predictions for the effect droughts in the Delta overall and the impacts of the TUCP and Barrier seen in 2021.

Category	Drought Impacts	TUCP/Barrier Impacts
Hydrology and Water Quality	Lower flows Lower exports Decreased turbidity Increased temperature	Higher salinity in Sacramento River Lower salinity in Central and South Delta X2 shifts upstream up to ~2km

Nutrients	Increased ammonium Decreased loading from agriculture Increased residence time and concentration	Increased herbicides in Franks Tract
<i>Microcystis</i>	Bloom Increased abundance	Increase in Central/South Delta
Weeds	Distribution shifts upstream Increased total coverage Changed Species composition	Increased weeds in Franks Tract
Phytoplankton	Localized blooms	Localized blooms
Zooplankton	Changes in abundance More marine species in Suisun, center of distributions shift inland	Negligible impact
Delta Smelt	Decreased habitat quality Low Population Growth	Negligible impact
Longfin Smelt	Spawning habitat further inland Lower Population growth	Negligible impact
Salmonids	Decreased survival for outmigrating juveniles Decreased spawning success Longer upstream holding Reduced alternative life history strategies Increased predation	Small decrease in through-Delta survival for the small number of juvenile salmonids in the Delta.

Other Fish	Increased catch of marine species	Increased predators around Barrier (covered in effectiveness report of the Barrier)
	Decreased Splittail (floodplain spawners)	
	Decreased pelagic fish	

Materials and Methods

Study Site

This report chiefly covers the legal Sacramento-San Joaquin Delta, Suisun Bay, and Suisun Marsh. In some cases, it includes limited data collection outside these areas where necessary to describe habitat for anadromous species. We grouped our analyses into five regions: Suisun Bay, Suisun Marsh, the Sacramento-San Joaquin Confluence, the North Delta and the South/Central Delta (Figure 5).

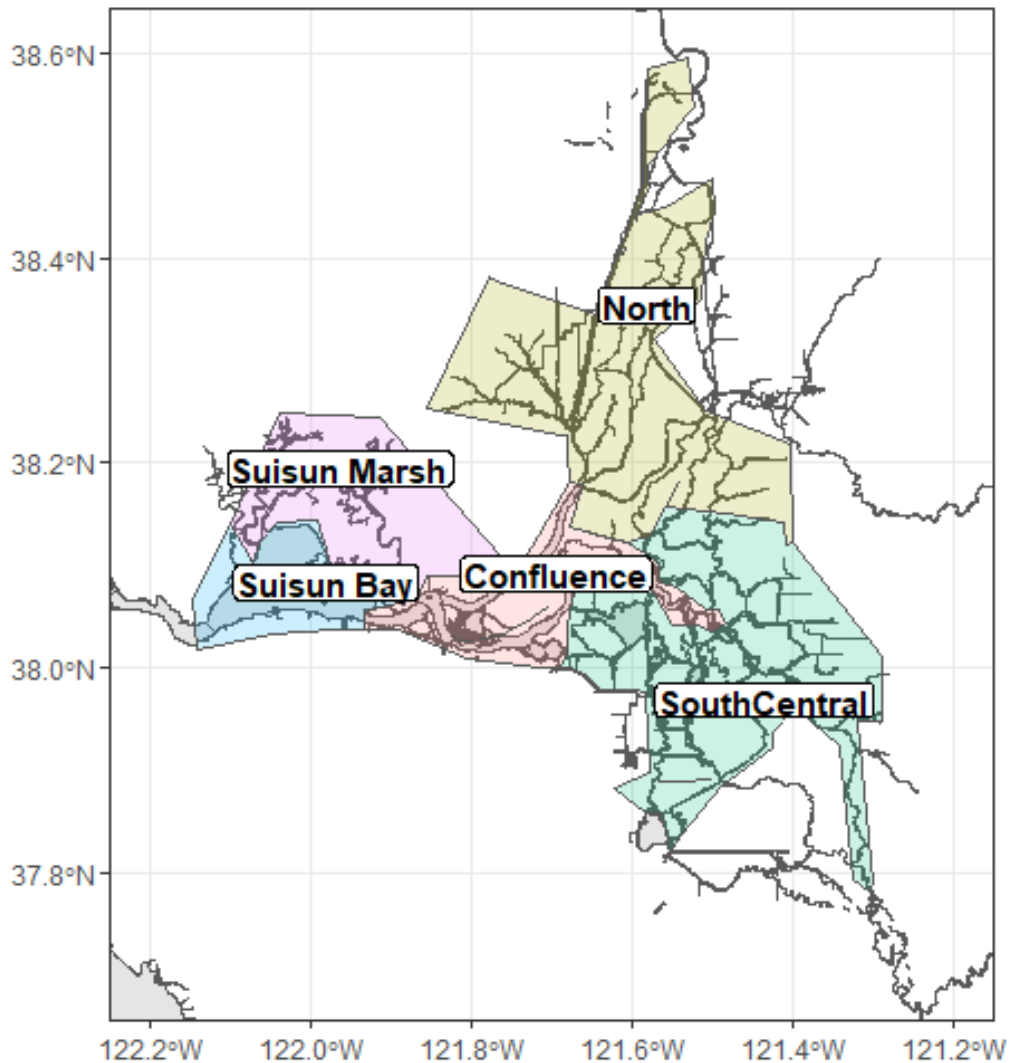


Figure 5. Map of regions used for drought analyses.

Study Design

For each of the ecosystem components analyzed, we assembled data from all available data sources. This often involved integrating data sets that were originally collected with very different study questions in mind, and may have occurred at different spatial and temporal scales. In order to standardize these data sets for comparisons, we stratified the data spatially and temporally. For most of the data sets, we conducted both long-term analyses over the entire length of data availability as well as short-term analyses over the past ten years. We used the long-term analysis to assess

the impact of multi-year drought in general, and the short-term analysis to assess the impact of the 2020-2021 drought and drought actions in particular. The general work flow is as follows, though not all metrics fit into this framework:

Short term analysis (2011-2021):

1. We assembled all relevant data, assessed their usefulness in answering our study questions, and reviewed the data for outliers and completeness.
2. We then calculated average values by month and region for each metric over the past ten years
3. We performed an ANOVA (or appropriate alternative model) with the following structure:
 - a. $\text{Metric} \sim \text{factor}(\text{year}) + \text{month} + \text{region}$
 - b. Station or subregion was used as a random effect, where appropriate
4. Years were analyzed as factors, then qualitatively discussed in the following classifications:
 - a. Wet years: 2011, 2017, 2019
 - b. Drought years, no Barrier: 2013, 2014, 2020
 - c. Drought years, w/Barrier: 2015, 2021
 - d. Below normal years: 2012, 2016, 2018
5. We then followed this up by a post-hoc analyses to see which years were different from one another and qualitatively discuss reasons for that difference.

Long-term analysis (1970-2021)

1. We assembled all relevant data, assessed their usefulness in answering our study questions, and reviewed the data for outliers and completeness.
2. We then calculated average values by season and region for each metric over the entire course of the data set.
3. Seasons were defined as Winter (December -February), Spring (March-May), Summer (June-August), and Fall (September-December). December was grouped with January and February of the following year
4. Years were categorized as "Drought" for multiple dry, below normal, or critically dry years in a row, "Wet Period" for multiple wet or above average years in a row, and "Neutral" for years not included in Wet Periods or Drought. Degree of drought was also assessed using the five Sacramento Valley Hydrologic Classification categories (Critically Dry, Dry, Below Normal, Above Normal, and Wet) as well as their

Sacramento Valley Index. (see:

<https://cdec.water.ca.gov/reportapp/javareports?name=WSIHIST>)

5. We performed an ANOVA (or appropriate alternative model) with the following structure:
 - a. Metric ~ Drought/Wet OR Metric ~ WaterYearType
 - b. Metric ~ Drought/Wet + Region
 - c. Metric ~ Drought/Wet + Season
 - d. Interaction terms were also included, when appropriate
6. We then followed this up by a post-hoc analyses to see which year categories were significantly different from one another.

Specific processes for analyzing the component data sets are described below:

Water Quality and Hydrology

Component Data Sets

Hydrology (Dayflow outputs of Delta Outflow, Delta Exports, X2, and USGS tidally-filtered discharge), water quality (water temperature, salinity, secchi depth, and dissolved oxygen), and nutrient (dissolved ammonia, dissolved nitrate + nitrite, and dissolved ortho-phosphate) data were downloaded from various sources. Data were primarily from the Dayflow model developed by DWR (<https://data.cnra.ca.gov/dataset/dayflow>), the discretewq R package (<https://github.com/sbashevkin/discretewq/>, (Bashevkin 2022)), the Water Quality Portal (<https://www.waterqualitydata.us/>), and the USGS National Water Information System (<http://waterdata.usgs.gov/nwis>, (USGS 2016)), with smaller contributions from the USBR Delta Outflow Computation reports (<https://www.usbr.gov/mp/cvo/pmdoc.html>) and personal data requests. We acquired all available data between December 1974 through at least September 2021, which we later included or excluded depending on the specific parameter and analysis. R code used for the compilation, cleaning, and aggregation of the data used in this report can be found in the DroughtData R package (<https://github.com/mountaindboz/DroughtData>).

At the time when we acquired data from Dayflow, it provided daily Delta outflow and total exports from before 1974 through water year (WY) 2020 (September 2020), and daily estimates of X2 from WY 1997 through WY 2020. To estimate the most recent Delta outflow and total exports data from October 2020 through November 2021, we used daily data from the USBR Delta Outflow Computation reports. For the daily X2 data not available from Dayflow, we used estimates from- (Hutton et al. 2017) for the December 1974 through WY 1996 period, and we calculated values using the equation from the Autoregressive Lag Model used by Dayflow (DWR 2002) and daily

outflow estimates from the USBR reports for October 2020 through November 2021 (<https://www.usbr.gov/mp/cvo/pmdoc.html>).

Tidally averaged discharge records from various USGS monitoring stations in the system were acquired from the USGS National Water Information System (NWIS) using the dataRetrieval package (De Cicco et al. 2018). The sum of tidally averaged (or net) discharge at four stations represents the USGS outflow; the four stations used to compute a USGS outflow are the Sacramento River at Rio Vista Bridge (11455420), Dutch Slough (11313433), Three Mile Slough (11337080), and San Joaquin at Jersey Point (11337190). Other USGS net discharge data were retrieved from Cache Slough at Ryer Island (11455350) and Cache Slough at Ryer Island Ferry (11455385).

The primary source of the water temperature, salinity, and secchi depth data was the discretewq R package. This package contains water quality data from many IEP surveys, but we used data from the Environmental Monitoring Program (EMP), Summer Towntet Trawl (STN), and Fall Midwater Trawl (FMWT) since these were the only long-term surveys with data available through 2021. At the time when we accessed data from the discretewq package, it contained STN data through 2021 and data from EMP and FMWT through 2020; however, we were able to acquire provisional data collected in 2021 from EMP and FMWT through direct data requests. Continuous dissolved oxygen data collected by USGS on the lower Sacramento River (stations 11455478 and 11455485) and the Toe Drain (11455139 and 11455140) were acquired from the USGS NWIS using the dataRetrieval package.

Most of the long-term (1975-2021) nutrient concentration data used in this report was also acquired from the discretewq package including data collected by the EMP and the USGS San Francisco Bay monitoring programs. In addition to this data, we added nutrient data collected by USGS at the Sacramento River at Freeport station (11447650) to the long-term data set. For the short-term (2013-2021) data set, we included the same monitoring programs and stations found in the long-term data set and added the more recent nutrient data collected at various locations by the USGS California Water Science Center (CAWSC). The Sacramento River at Freeport data and all the data collected by the CAWSC was downloaded from the Water Quality Portal hosted by the National Water Quality Monitoring Council. Some of the nutrient data collected by the CAWSC and used in this report is considered provisional.

Quality Assurance/Quality control

For the water quality (water temperature, salinity, and secchi depth) and nutrient parameters, we ensured that there was only one sample that represented a station and day in our data set to allow for each sample to have equal weight. We accomplished this by only including the sample collected closest to noon if multiple samples were collected on the same day at a station. In addition, for the water quality parameters, we removed anomalous values if they had a Z-score greater than 10 grouped by each Subregion as defined by the R_EDSM_Subregions_Mahardja_FLOAT shapefile from the deltamapr R package (Bashevkin 2021). We followed a similar approach for outlier removal for the nutrient data by removing values with modified Z-scores greater than 15 also grouped by each Subregion. Using the modified Z-score was more appropriate for the nutrient data set since it contains some values below the reporting limit (RL) for the laboratory method and the modified Z-score is more robust to this type of data since it is based on ranks or medians.

For all three nutrient parameters (dissolved ammonia, dissolved nitrate nitrite, and dissolved ortho-phosphate) the data set contained some values that were below the RL; however, the reporting limits were not always provided by the data sources. As a result, we had to make a few assumptions regarding the reporting limits for the nutrient data. For the EMP data, the most common historical RL was 0.01 for all three nutrient parameters, so we used this value for the records without reporting limits. For the data set provided by the USGS SF Bay monitoring program, values below the RL were not explicitly documented; however, through personal communication with USGS investigators we confirmed that if at least one of the three nutrient parameters had a value reported for a station and day, then we could assume that the other parameters were sampled but below the RL (Erica Nejad, USGS, Dec. 16, 2021). We used 0.0007 mg/L, 0.0007 mg/L, and 0.0015 mg/L as the reporting limits for dissolved ammonia, dissolved nitrate nitrite, and dissolved ortho-phosphate, respectively, for the USGS SF Bay data (Erica Nejad, USGS, personal comm.). And finally, for the USGS CAWSC nutrient data, we used the most common RL for each parameter and laboratory method for the records with missing RL values.

Data analysis methods

To prepare the data for a series of ANOVA models, we aggregated the long-term and short-term data sets in two ways: 1) seasonal averages for each year for all hydrology, water quality (water temperature, salinity, and secchi

depth), and nutrient parameters, and 2) regional (Figure 5) averages for each year for the water quality and nutrient parameters.

For the hydrology parameters, the seasonal averages were calculated as simple means of the daily values for each season year. The methods to aggregate the water quality and nutrient parameters were more involved and require further explanation. To do this, we first calculated monthly averages of the raw data for each region, which we then used to calculate seasonal averages for each region year. The seasonal averages that we used in the ANOVA models were then calculated by averaging these seasonal-regional averages by season and year. Similarly, we calculated the regional averages used in the ANOVA models by averaging the same seasonal-regional averages by region and year. Before calculating the seasonal and regional averages for the nutrient parameters, we substituted the values below the RL with simulated values based on a uniform distribution $U(0.001, RL)$. One simulation was run for each parameter. A seed was set prior to running the simulation to ensure reproducibility.

All analyses were conducted in R 4.1.1 (R Core Team 2021). To assess the relationship of each variable with year or drought year classification (Drought, Wet Period, or Neutral period, Figure 3) alongside its spatial or seasonal variability, we fit ANOVAs with type II sum of squares using the `aov` function from the `stats` package (R Core Team 2021) and the `Anova` function from the `car` package (Fox et al. 2021). We then conducted Tukey post-hoc tests for hydrology and water quality parameters and Sidak post-hoc tests for nutrient parameters using the `emmeans` package (Lenth et al. 2021) to determine which factor levels were significantly different from one another, using a significance threshold of $p < 0.05$.

We fit two model structures each on the regional and seasonal aggregated datasets (only seasonal for the hydrology parameters). The first model directly evaluated the impact of the drought year classification by including the drought year classification and region/season as fixed effects. The second model evaluated the year-to-year variability by including categorical year and region/season as fixed effects.

We used all years of data (1975-2021) in all models of the hydrology and water quality parameters; however, the input data varied between the model structures for the nutrient data. For the models that included the drought year classification as a fixed effect, we used the long-term (1975-2021) nutrient data set to look at long-term trends between Drought, Neutral, and Wet Periods. However, we used the short-term (2013-2021) data set for the models that used categorical year to assess nutrient differences between recent years. As mentioned above, the short-term

nutrient data set contained the USGS CAWSC data as an additional data source, which was due to the CAWSC data only being available for the more recent years. Additionally, we did not include the Suisun Marsh region in any of the models for the nutrient parameters because this region had a large gap in its long-term record and recent data only for 2017-2021.

The fit and conformity to assumptions of each model were assessed by visually assessing the normality of the residuals, inspecting a plot of residuals and predicted values for any pattern, and validating that the predicted and observed values were correlated. Some of the parameters (Delta outflow, secchi depth (except for the seasonal-year model), and all three nutrient parameters) needed to be natural log-transformed to meet the assumption of normally distributed residuals. The USGS Cache Slough flow data was offset prior to a log transformation for normality to account for negative net flow across the mean seasonal net flows in the spring, summer, and fall seasons of 2015. For the nutrient data, we also ran a Box-Ljung test on the model residuals to check for autocorrelation. We added lag terms to the nutrient models as needed to reduce autocorrelation in the residuals.

Chlorophyll-a and Microcystis

Component Data Sets

Chlorophyll-a concentration and *Microcystis* rating data were gathered from several different sources. The main source was from a data package from the [Environmental Data Initiative](#) (EDI) archive (Bashevkin 2022). This package contains data from the Environmental Monitoring Program (EMP), Summer Towntnet Trawl (STN), Stockton Deepwater Shipping Channel Dissolved Oxygen Monitoring (SDO), Fall Midwater Trawl (FMWT), and U.S. Geological Survey (USGS) San Francisco Bay Research Monitoring Project (USGS-SFBRMP). Where possible, data not yet available on EDI was obtained directly from the Principal Investigators at DWR's North Central Regional Office (NCRO) (Amanda Maguire, DWR, pers. comm).

Discrete water samples were collected at 1-meter depth from a boat with a Van Dorn-type water sampler or a through-hull pump. Sample water was filtered through glass fiber filters with a nominal pore size of 0.7 μm for all monitoring programs except NCRO, which used filters with an average pore size of 1.0 μm . All samples were analyzed fluorometrically for chlorophyll-a pigment concentration. Information on the specific analytical techniques used for each program can be found in the metadata file associated with the EDI archive. All data and analysis code can be found on the IEP Drought

Synthesis GitHub repository:

<https://github.com/InteragencyEcologicalProgram/DroughtSynthesis/tree/main/PrimaryProducerTeam>.

Data analysis methods

For the short-term analysis, chlorophyll-*a* concentration data collected between 2011 and 2021 were averaged for each station by month. Only stations which had data for an average of greater than 6 months per year were used in the analysis. The resulting data file included 35 stations and 4627 samples (Figure 6). The number of samples differed among years and was greater between 2016 and 2019 (Supplemental Figure 1). The Delta was divided into 5 regions for analysis: Confluence, North Delta, South-Central, Suisun Bay and Suisun Marsh. These regions contained between 1 and 18 stations each (Figure 6).

To evaluate the influence of water-year type on the chlorophyll-*a* concentration, data were binned into three water year classifications: Wet (2011, 2017, 2019), Neutral (2012, 2016, 2018), and Drought (2013, 2014, 2015, 2020, 2021). These 3 classifications were derived from the 5 water-year classifications for the Sacramento River watershed (wet, above normal, below normal, dry, critically dry; cdec4gov.water.ca.gov/reportapp/javareports?name=WSIHIST). Monthly chlorophyll-*a* concentration data were also binned into four seasons: winter (December to February), spring (March through May), summer (June through August) and fall (September through November).

The long-term analysis used average monthly chlorophyll-*a* concentration for each station by month between January and December. Water samples for these data were collected at two-week and four-week intervals by the DWR/CDFW EMP during 1975-2021 and the U.S. Geological Survey San Francisco Bay Research and Monitoring Program during 1977-1980 and 1988-2021. These data included 35 stations partitioned among the Confluence (15 stations), North Delta (2 stations), South-Central Delta (10 stations) and Suisun Bay (8 stations) (Figure 7). There were not enough stations for Suisun Marsh to include it in the long-term analysis. Stations included in the analysis had at least 10 years of data and at least 12 samples per year. The resulting dataset contained 15,072 records that included 12,170 records from EMP and 2,902 records from the U. S. Geological Survey (Supplemental Figure 2).

Significant differences in average monthly chlorophyll-*a* concentration among regions, water years and seasons for both short-term and long-term

analysis were determined by a mixed effect model using the R packages lme4 and lmerTest (Bates et al. 2020; Kuznetsova et al. 2017). The chlorophyll-*a* concentration dataset was \log_{10} transformed to produce a normal distribution. The log-average chlorophyll-*a* concentration was calculated by taking the arithmetic mean of the \log_{10} transformed chlorophyll-*a* values and then, back-transforming to the original scale by raising 10 to the previously calculated arithmetic mean value ($10^{(\text{arithmetic mean of } \log_{10} \text{ chlorophyll-}a)}$). The log-average is equivalent to the geometric mean of the chlorophyll-*a* values. Region, water year, and season were included in the model as fixed effects with a random intercept for station. Pairwise comparisons between predictor variables were computed with the emmeans R package (Lenth et al. 2021). All analyses were performed in R (R Core Team, 2021).

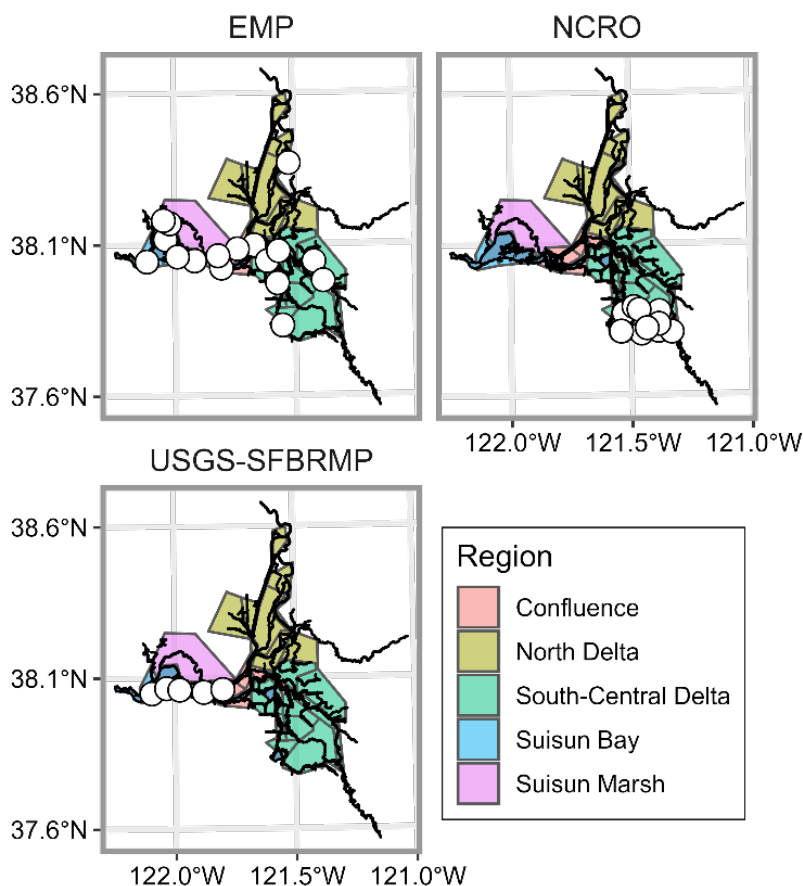


Figure 6. Map of station locations in the upper San Francisco Estuary used for the short-term (2011-2021) analysis of chlorophyll-*a* concentration.

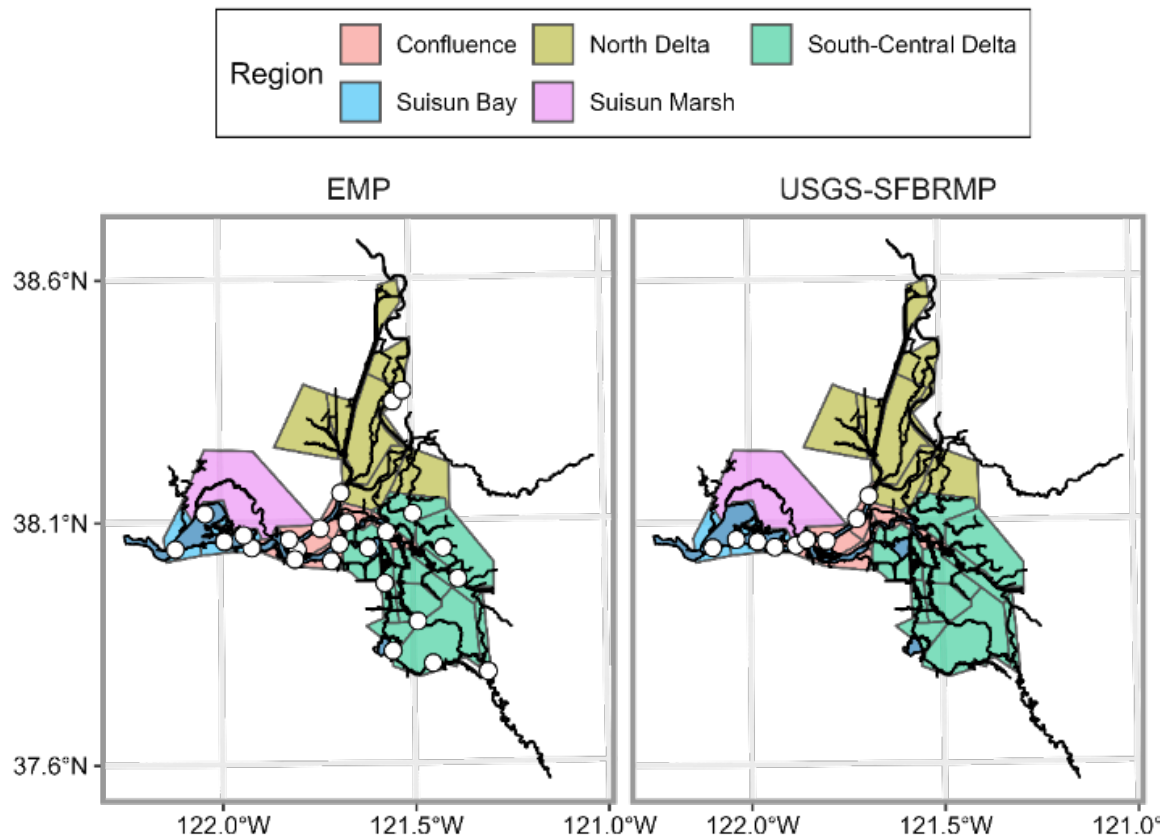


Figure 7. Map of sampling stations used for the long-term analysis of chlorophyll-*a* concentration measured between 1975 and 2021.

***Microcystis* index analysis**

Microcystis is the dominant cyanobacterium in the upper San Francisco Estuary and is a toxic bloom forming species (Lehman et al. 2005).

Microcystis is difficult to quantify with traditional water quality sampling at 1 m because it primarily occurs in large colonies on the surface film of the water (Lehman et al. 2021). Because the colonies move quickly away from samplers with any disturbance of the surface water due to surface tension, they are difficult to quantify with traditional discrete water sampling. As a result, the quantity of *Microcystis* is routinely estimated using a visual index. The index ranges from 1 to 5, with 1 indicating no colonies observed and 5 indicating a dense mat of colonies observed on the surface (Figure 7).

We only analyzed *Microcystis* index data collected during 2011–2021. Long-term analysis (1975–2021) of *Microcystis* index scores was not conducted because data were not collected until 2007. Previous research indicated *Microcystis* primarily occurred between June and November (Lehman et al. 2008), therefore we only analyzed Summer (June–August) and Fall (September–November) data. Only stations that averaged greater than 3 measurements per year during the summer and fall season were included in the data set. This resulted in 3,321 data records across 110 stations. The number of stations per region ranged between 6 and 56 (Figure 7). There was an increase in records in 2017 in the South-Central Region when the North Central Regional Office of DWR (NCRO) began collecting *Microcystis* index data (Supplemental Figure 3). Because the index is subjective and collected by many people, differences in the interpretation of the five index categories could bias the analysis. Therefore, we binned the index data into three visually very different categories: none (index rating 1), low (index ratings 2 and 3) and high (index ratings 4 and 5, Fig. 2). For each station, the maximum rating value measured for each month between June and November during 2011–2021 was used in the analysis.

Differences in the probability of having a high or low *Microcystis* surface index score among water year types were analyzed by fitting an ordinal model to the data using a Bayesian adjacent category ordinal model (Bürkner and Vuorre 2019) in the BRMS R package (Bürkner 2018). The model used water year type, region, and season as fixed effects, with a random intercept for station, to estimate the probability of observing a *Microcystis* index of none, low, or high. Differences in Bayesian model estimates were considered significant if the 95% credible intervals did not overlap. The results of these Bayesian analyses were verified using analysis of similarity, a non-parametric statistical analysis, which is also appropriate for ordinal data (PRIMER-e, (Clarke and Gorley 2015)).

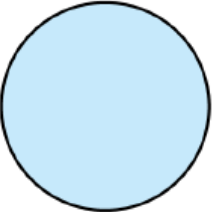
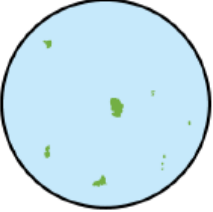
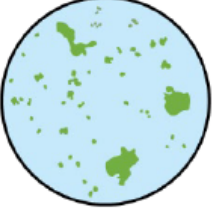
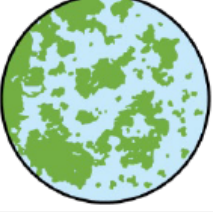
	<p>1 – Absent No visible <i>Microcystis</i> colonies</p>
	<p>2 – Low Visible but widely scattered <i>Microcystis</i> colonies.</p>
	<p>3 - Medium Adjacent colonies of <i>Microcystis</i>.</p>
	<p>4 - High Contiguous colonies of <i>Microcystis</i>.</p>
	<p>5. Very High Concentrated contiguous colonies of <i>Microcystis</i> forming mats or scum.</p>

Figure 8. The *Microcystis* visual surface colony rating index used by IEP surveys ranges from 1 for no colonies observed to 5 for a dense mat of colonies on the surface of the water.

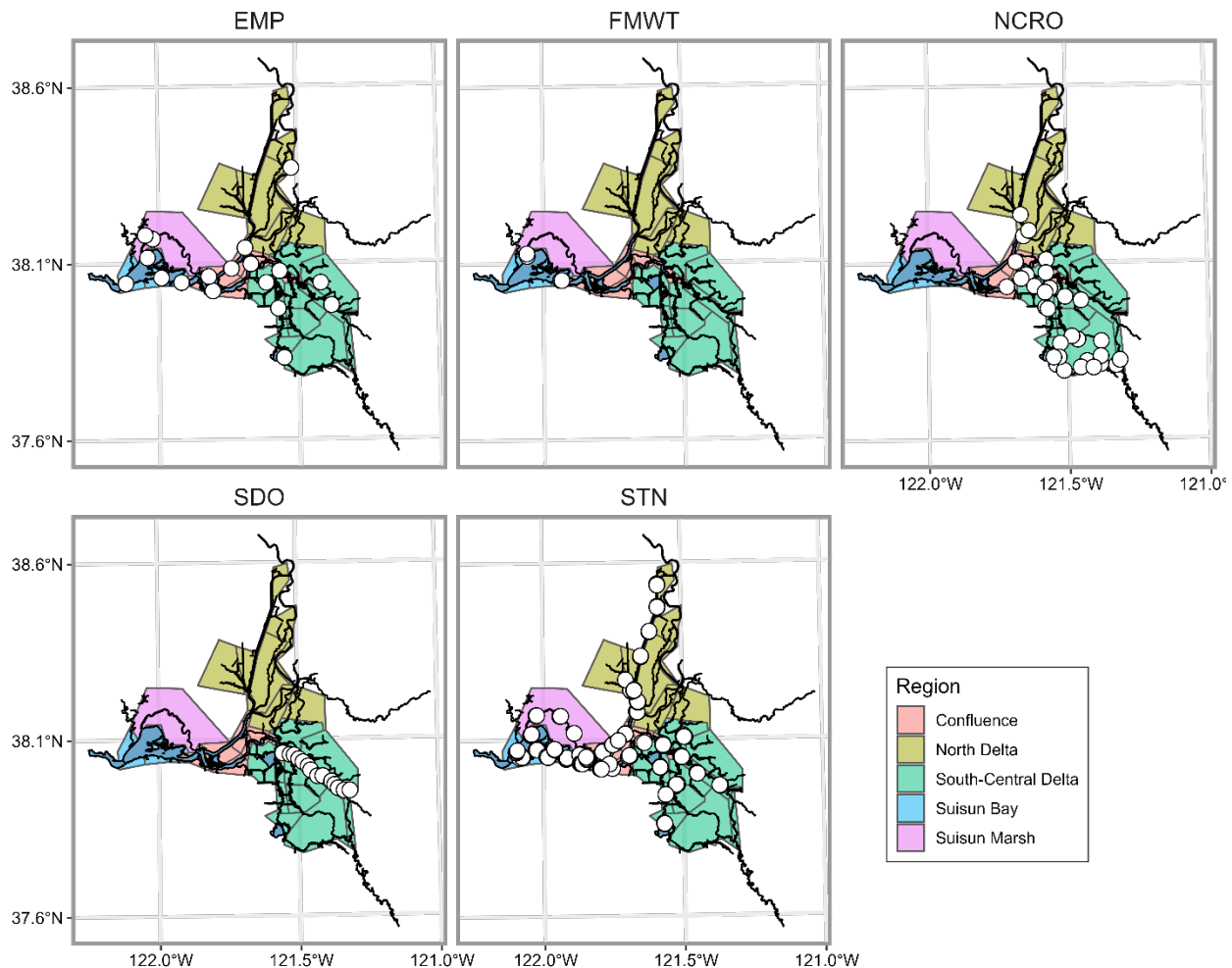


Figure 9. Map of stations in the upper San Francisco Estuary used in the *Microcystis* visual index analysis.

Aquatic Vegetation

State agencies have funded the Center for Spatial Technologies and Remote Sensing (CSTARS) at the University of California, Davis to conduct landscape scale surveys of aquatic vegetation in the Delta annually during the majority of years since 2004. These surveys consist of hyperspectral airborne imagery, which can differentiate among growth forms such as submersed aquatic vegetation (SAV) and floating aquatic vegetation (FAV). The spatial extent of the surveys has varied among years but has most consistently included a composite region comprised of large portions of the North and Central Delta (~18,000 hectare of waterways; 79% of Delta waterway area).

Analysis of raw imagery data to categorize areas by vegetation type typically takes about a year from the time of data collection, so the 2020 data are provisional, and the 2021 data will not be available until spring 2022. Therefore, we cannot yet evaluate the impacts of the current drought or associated management actions. In addition, the results we present in this report are limited to summary statistics because there are not sufficient data to perform a rigorous statistical analysis.

Invertebrates

Component data sets

Zooplankton Catch Per Unit Effort (CPUE, organisms/m³) data was downloaded using the `zooper` package (<https://github.com/InteragencyEcologicalProgram/zooper>), an R package that synthesizes zooplankton data from multiple IEP studies. Using R we joined CPUE data for macro (500-505 µm mesh), meso (150-160 µm mesh), and micro (43 µm mesh) nets into one data frame, and then joined biomass lookup data for meso and micro zooplankton, which use fixed biomass conversions for each taxon (BPUE, µg/m³). Sampling data used in analysis excluded winter months (December – February) due to inconsistent sampling of winter in the 1970s and 1980s. BPUE for macro zooplankton was calculated using length-weight equations. Sampling stations were assigned to regions based on the `R_EDSM_Subregions_Mahardja` shapefile from the `Deltamapr` package (Bashevkin 2021), and data from the “North” region was excluded due to lack of consistent long-term sampling in the region.

Data analysis

We grouped our analysis into three different sections: 1) Long-term (LT) analysis, covering zooplankton data from 1975-2021 using only EMP sampling; 2) short-term (ST) analysis, covering zooplankton data from 2011-2021 using both EMP and FMWT survey data; and 3) Taxa specific analysis using data from 1994-2021 from the EMP surveys. For all our metrics we calculated water year for each sample so that water year X = December (X-1) – November X. Long-term analysis used metrics of total BPUE of all taxa for each sample and then calculated three BPUE averages, one each for season, region, and year total. Short-term analysis used metrics of total BPUE of all taxa for each sample and calculated monthly BPUE averages for each region. Taxa specific analysis used total BPUE for 15 different taxa in each sample and calculated yearly average BPUE for each

taxa for years 1994-2021, as a few of the non-native species were not introduced to the region until the late 1980s and early 1990s.

We used the above BPUE averages to create five different models to detail how zooplankton biomass was impacted by drought in the upper estuary:

1. Model 1 (Long Term): BPUE \sim Drought (Year type)
 - a. Using yearly averages, overall Delta zooplankton BPUE modeled by Drought Year type classification (Wet Period, Neutral, Dry).
2. Model 2 (Long Term): $\log(\text{BPUE}) \sim \text{Drought} + \text{Season}$
 - a. Using seasonal averages BPUE is modeled by Drought Year type and Season.
3. Model 3 (Long Term): $\log(\text{BPUE}) \sim \text{Drought} + \text{Region} + \text{Drought} * \text{Region}$
 - a. Using yearly regional averages, regional BPUE is modeled by Drought Year type, Region, and their interaction.
4. Model 4 (Short Term): $\log(\text{BPUE}) \sim \text{Year} * \text{Region} + \text{Month}$
 - a. Using the short-term monthly averages, BPUE is modeled by year, region, and month.
5. Model 5: Taxa specific BPUE \sim Sacramento Valley Annual Water Index
6. Taxa specific yearly BPUE average is modeled by Sacramento Valley Annual Water Index, an estimate of yearly runoff through the Delta
7. Community ordination was performed using non-metric multidimensional scaling (NMDS), breaking up communities by Drought Year type for years 1994-2020.
 - a. NMDS compares community differences across multi-dimensional space on a reduced number of dimensions by using Bray-Curtis dissimilarities between community points. Permutational analysis of variance (PERMANOVA) was then used to determine if community groupings by Drought Year type were significantly different.

Our short-term (ST) analysis covers zooplankton data from 2011-2021 using both EMP and FMWT survey data. We calculated water year for each sample so that water year X = December (X-1) – November X. Our ST analysis used metrics of total BPUE of all taxa for each sample and calculated monthly BPUE averages for each region. We used year, region, and month to model the log transformed monthly BPUE so that: $\log(\text{BPUE}) \sim \text{Year} * \text{Region} + \text{Month}$.

Jellyfish

Data on gelatinous zooplankton (ctenophores and cnidarians) were queried from Fall Midwater Trawl (FMWT), 20mm, and Bay Study databases. Data on gelatinous zooplankton are collected by these surveys, but generally not made available online in their public-facing databases. Therefore, data were requested from the primary investigators. Total catch of all gelatinous zooplankton species (Table 2) was calculated for each trawl and converted to CPUE by dividing catch by volume of trawl. For Bay Study's otter trawl, where CPUE is calculated as area, not volume, this was converted to volume by multiplying by the mouth area of the trawl. Sampling stations were assigned to regions based on the R_EDSM_Subregions_Mahardja shapefile from the deltamapr package. We calculated water year for each sample so that water year X = December (X-1) – November X. We calculated monthly averages for each region and month and present the data graphically. These data will be combined with data from the UC Davis Suisun Marsh survey and compared statistically in the final version of the report.

Table 2. Gelatinous zooplankton taxa collected by IEP surveys used in this analysis.

Common Name	Scientific Name	20mm	FMWT	BayStudy
Unknown Jelly		x	x	x
Moon Jellies	<i>Aurelia sp.</i>	x	x	x
Maeotius	<i>Maeotius marginata</i>	x	x	x
Bell Jelly	<i>Polyorchis penicillatus</i>	x	x	x
Giant Bell Jelly	<i>Scrippsia pacifica</i>	x	x	x
Sea Gooseberry	<i>Pleurobrachia bachei</i>	x	x	x
Crystal Jelly	<i>Aequorea sp.</i>		x	x
Black Sea Jelly	<i>Blackfordia virginica</i>	x	x	x
Purple striped jelly	<i>Chrysaora colorata</i>			x
Chrysaora	<i>Chrysaora sp</i>			x
Sea Nettle	<i>Chrysaora fuscescens</i>			x
Aglauroopsis	<i>Aglauroopsis aeora</i>			x
Moerisia	<i>Moerisia sp.</i>	x		

Clams

For the short-term analysis, data on invasive clams were queried from the DWR, Reclamation, and USGS Generalized Random Tessellation Stratified (GRTS) program, along with 10 annually sampled sites from DWR's EMP benthic survey. Analyses focused on two invasive clam species, *Potamocorbula amurensis* and *Corbicula fluminea*. Sampling stations were assigned regions based on the R_EDSM_Subregions_Mahardja shapefile from the `deltamapr` package (Bashevkin 2021). Data included range from 2011-2019, with sampling data once in May and once in October, though sampling was highly variable during these sampling periods (Supplemental Figure 4). No GRTS data were available for 2013 and 2016, so these years were omitted. Our analysis covers metrics of density, and grazing rate for each species. Grazing rate was calculated using methods from (Thompson et al. 2008), and is a function of species-specific pumping rates, temperature, biomass, and density.

We assessed the data for normality and zero inflation and found that both grazing rates and densities were highly zero-inflated. Therefore, we used zero-inflated negative binomial models using the R package `glmmTMB` (Magnusson et al. 2019). We constructed four models on subsets of the data to see whether the two species' grazing rates and densities differed by year and region of the estuary.

Number of clams per area (meter squared) or grazing rate (cubic meters of water filtered per meter squared per day) was modeled against year and region with month as a random effect. Zero inflation was modeled against region, since most of the zeros resulted from sampling in regions outside of the range for each species. We used the package `emmeans` to perform pairwise comparisons to determine which years were significantly different from one another (Lenth et al. 2021). The model for *C. fluminea* was fit using the entire data set, but the model of *P. amurensis* would not converge with the entire data set due to lack of catch in the North Delta and South Central delta. Therefore, *P. amurensis* data was subset to only include Suisun Marsh, Suisun Bay, and the Confluence.

For the long-term analysis, we only used data from EMP's long-term benthic monitoring. We calculated the average annual density and grazing rate for each species and performed a linear model on the metric of interest versus year type (Drought, Neutral, or Wet). Because *P. amurensis* was not

introduced until 1986, the *P. amurensis* model was run on only 1986-2019. We also looked to see whether the range of *P. amurensis* shifts with outflow by calculating the center of distribution of *P. amurensis* in kilometers from the Golden Gate using the 'ggdist' function in the 'spacertools' package (<https://github.com/sbashevkin/spacertools>) and performing a regression on the center of distribution versus the Sacramento Valley Index and the previous year's Sacramento Valley Index.

Fish

Species-specific analyses

The goals for the species-specific analyses were to:

- Compare hatchery winter-run Chinook Salmon survivorship for 2021 to the previous two years using acoustic tag data
- Compare cohort replacement rates (CRR) among Drought, Neutral and Wet Period years for winter-run, spring-run and fall-run Chinook Salmon
- Examine the timing of outmigration during Drought, Neutral, and Wet Period years for Chinook Salmon
- Test for temporal autocorrelation in population indices for Threadfin Shad American Shad, Delta Smelt, Longfin Smelt, and Striped Bass (age-0)
- Compare population indices among Drought, Neutral and Wet Period years for Threadfin Shad American Shad, Delta Smelt, Longfin Smelt, and Striped Bass (age-0)

We used four data sources for our analyses, based on the length of the time series available, suitability for addressing ecological questions, and the availability of key fish species in those data sets. The species selected for analysis, Chinook Salmon (*Oncorhynchus tshawytscha*), Threadfin Shad (*Dorosoma petenense*), American Shad (*Alosa sapidissima*), Delta Smelt (*Hypomesus transpacificus*), Longfin Smelt (*Spirinchus thaleichthys*), and Striped Bass (age-0, *Morone saxatilis*), were chosen based on data availability and the importance of these species either to conservation and management or to their value as ecological indicators.

The Central Valley Enhanced Acoustic Tagging project (data and information available here: <https://oceanview.pfeg.noaa.gov/CalFishTrack/index.html>) provides information on the direct measurement of juvenile, anadromous

fish migrations in the Central Valley. The CDFW Grandtab escapement data (Azat 2021) provides a long-term dataset that can be used to identify the strength of recruitment for a particular Central Valley salmon run and that run's returning year class's contribution to the population's overall abundance. Year over year escapement can be used to calculate a population's "cohort replacement rate" (CRR), which is the measure of the number of future spawners produced by each spawner. Chinook salmon (*Oncorhynchus tshawytscha*), are indeterminate semelparous (Begon et al. 1986), where adults return to spawn between 1 and 4 years after hatching such that each cohort is not an independent subpopulation. The age-structure of the returning population is therefore influential in estimating the CRR, as that returning population will include multiple cohorts that would have experienced different environmental conditions during their outmigration. For Sacramento River Winter Run Chinook (SRWRC) salmon, the age structure of the returning population is dominated by age-3 (90%) fish, but also includes 7% age-1-2 returns and 2% age-4 (Satterthwaite et al. 2017). Similarly, most CVSRC return to spawn as age-3 (73%) fish, with 9% returning as age-1-2 and 17% returning as age-4. Central Valley fall-run Chinook (CVFRC) display the most diverse age structure with 63% returning to spawn at age-3, 18% at age-1-2 and 19% at age-4 (Satterthwaite et al. 2017).

To further explore potential drought effects on Chinook Salmon, we accessed salmon monitoring data from the Delta Juvenile Fish Monitoring Program (DJFMP) in the San Francisco Bay-Delta through a combination of trawling and beach seines from the late 1970s to present. Catch data from trawls conducted at Sherwood Harbor (38.5334833, -121.5239083) and Chipps Island (38.04365479, -121.9112847) were downloaded from the Delta Juvenile Fish Monitoring Program website (https://www.fws.gov/lodi/juvenile_fish_monitoring_program/).

We used data from 1988 to 2021 to standardize time periods between the two trawl locations. Currently, the Sherwood Harbor Trawl samples the Sacramento River October to March using a Kodiak trawl and during the months of April to September with a mid-water trawl. The Chipps Island Trawl site in Suisun Bay is sampled year-round with a mid-water trawl. Sampling frequency differs between months, and some sampling differences have also occurred across the multi-decadal data time period. Data include both Kodiak trawl and mid-water trawl catches and marked and unmarked fish. Depending on the question(s) addressed, data for all run-types were combined or were subset to focus only on juvenile winter-run, spring-run, or fall-run Chinook Salmon.

The DJFMP uses a database program that assigns length-at-date criteria to assign salmon race (see "Race Table" under the data tab, <http://www.fws.gov/stockton/jfmp/>). Chinook salmon that were not measured between August 1, 1977 and July 31, 1992 are not able to be raced nor are they able to be associated with any measured fish. Fish that are not measured are designated with a fork length of "0" and a summed count of "1" or greater. Fish whose length was not measured, but recorded as zero, were removed from the dataset when plotting fish lengths.

Table 3. Trawl sample sizes/catch numbers (1988 - 2021)

Run-type	Sherwood Harbor Catch	Chippis Island Catch
Fall-run Chinook	227,609	266,656
Winter-run Chinook	2,344	4,022
Spring-run Chinook	22,578	57,329

Fall Midwater Trawl fish indices (1967-2020) for Threadfin Shad, American Shad, Delta Smelt, Longfin Smelt, and Striped Bass (age-0) were downloaded from the CDFW website on July 21, 2021. These indices were calculated by CDFW and are derived from sampling data generally collected during September, October, November, and December of each year with missing data for 1974 and 1979. The indices are effectively a catch-per-unit-effort (CPUE) estimate, based on weighted catches from each of 17 areas over the four-month sampling period (September-December). Details for the calculations, as well as the complete catch data from this program, are available from CDFW (<https://wildlife.ca.gov/Conservation/Delta/Fall-Midwater-Trawl>). Both data sets were joined to annual drought year classifications (described above).

To test for serial randomness, we ran a non-parametric runs test (package: DescTools) to determine if there was evidence of temporal autocorrelation for the Threadfin Shad, American Shad, Delta Smelt, Longfin Smelt, and Striped Bass (age-0) indices. The indices for these fishes were not normally distributed, and were log-transformed ($\ln(x)$, $\ln(x+1)$ for Delta Smelt) for subsequent statistical analyses. We used an ANOVA on the transformed indices to test the hypothesis that the apparent abundance of these species was affected by drought year classification (i.e., drought, normal or wet), and conducted pairwise comparisons on the estimated marginal means

(package: emmeans (Lenth et al. 2021)) in the model to identify, where appropriate, which year-type pairs appeared to be significantly different.

Fish community analyses

The first goal of the analysis was to identify sub-community assemblages (of fishes surveyed by the Fall Midwater Trawl Study) in the San Francisco Estuary after accounting for space and time.

The second goal of the analysis was to identify a representative from the sub-community assemblages and test whether and, if so, how catch varies among categorical water-year types and across a continuous drought metric. Specifically, we tested whether catch varies among three water-year types: Droughts, Wet Periods, and Neutral years and tested whether catch in time t varies across the Sacramento Water Year Index in time t and time $t-1$.

The analytical workflow was as follows:

Goal 1: Identifying Sub-Community Assemblages and Representative Species

1. Reduce the dataset to years during which the majority of stations were surveyed
 - a. Keep data from 1977 - 2020 (with the exception of 1979), resulting in 43 years of data
2. Eliminate stations that were not surveyed every included year
 - a. This resulted in the inclusion of 86 stations ranging from station 305 through station 912
3. Remove non-fish species from the dataset
4. Reduce the dataset to the most commonly survey months (September - December)
5. Eliminate fishes that were detected, on average, ≤ 10 times per year
 - a. That is, fishes with ≤ 430 records in the dataset across all stations and all included years were removed from the analysis
 - b. This resulted in the inclusion of 15 fish species
6. Spatiotemporally aggregate species-specific catch to the annual and sub-region levels
 - a. That is, the catch was summed for each species per sub-region and per-year
7. Scale the catch data to meet requirements of subsequent analyses. Data were natural log + 1 transformed and then scaled by species-specific centering and dividing by the species-specific standard deviation.

8. Perform a Principal Tensor Analysis (PTA) on the full, scaled dataset
9. Use the PTA output as an input for a hierarchical clustering algorithm to identify species relationship (i.e., a dendrogram) and use silhouette widths to identify the optimal number of clusters (i.e., sub-community assemblages)
10. For each sub-community assemblage:
 - a. Subset the scaled data to include only species within the sub-community assemblage
 - b. Remove sub-regions in which the species were never detected
 - c. Perform a PTA
 - d. Determine whether the sub-community assemblages are related to drought
 - i. Identify the tensor most associated with the temporal mode (i.e., year)
 - ii. Regress the temporal mode anomalies against the annual Sacramento Valley Index and Drought MAST team identified water-year types 1) The PTA anomaly of the temporal mode is the relative principal tensor distance of a given year to all other years after accounting for the other modes of sub-region and species. In other words, the relative catch of the sub-community assemblage systematically shifts as anomalies move away from zero
11. Identify a sub-community assemblage representative species based on silhouette width and data suitability for a regression analysis

Goal 2: Drought and Representative Species Catch

1. Develop a zero-inflated negative binomial (to account for zeros in catch data) mixed effects (to account for repeated measure of sub-region) Bayesian regression model to predict representative species catch across water-year types
2. Develop a zero-inflated negative binomial (to account for zeros in catch data) mixed effects (to account for repeated measure of sub-region) Bayesian regression model to predict representative species catch across Sacramento Valley Index

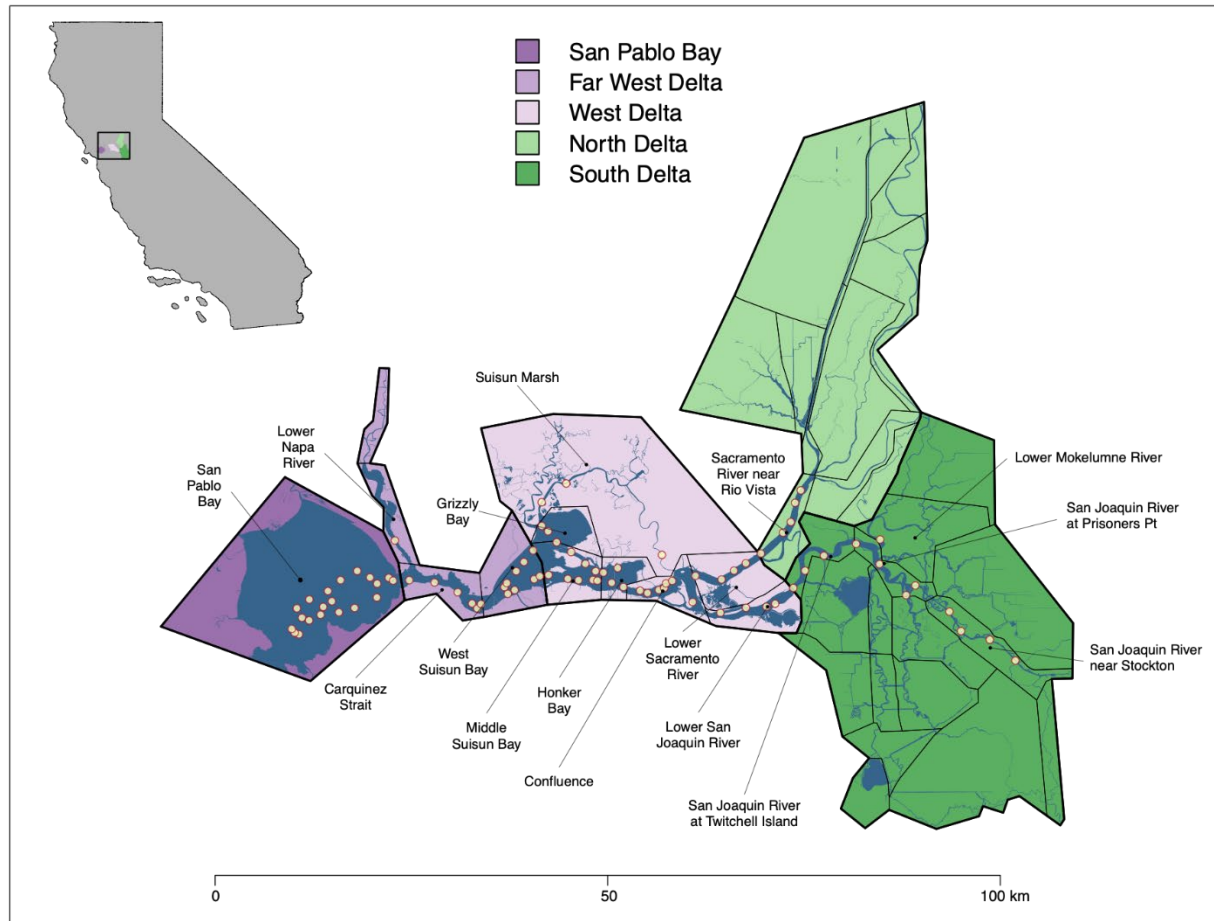


Figure 10. Map of the Delta with regions denoted by thick bordered and colored polygons, sub-regions denoted by thin bordered polygons, and Fall Midwater Trawl Study stations included in the analysis denoted by red bordered yellow points. Only sub-regions with Fall Midwater Trawl Study stations are labeled. Inset map illustrates the study region relative to the state of California.

Goal 1: Identifying Sub-Community Assemblages and Representative Species

Principal tensor analysis (PTA) is an ordination-based multi-mode data reconstruction method used to identify patterns in a single mode after accounting for the variability associated with the other modes (Cichocki et al. 2015; Leibovici 2010). In this analysis, the modes are space (i.e., sub-region), time (i.e., year), and taxa (i.e., fish species). Refer to IEP Technical Report #96 chapter 5 (specifically, pages 130 - 134) for thorough methods description (IEP Long-term Survey Review Team 2021).

We performed a hierarchical cluster analysis on the Euclidean distances between species scores of these three dominant principal tensors after

accounting for space (sub-region) and time (year) with the optimal number of clusters (3) being identified via average silhouette width.

The silhouette width indicates how suitable a species is for the sub-community assemblage in which it has been assigned. The silhouette width of a single species i approaches 1 when three conditions are met:

1. species i is highly related to the other species in the sub-community assemblage
2. the other species in the sub-community assemblage are highly related
3. species i is rarely related to species **not** in the sub-community assemblage to which it has been assigned

The silhouette width of a single species i approaches 0 when the species is not strongly related to any cluster. The silhouette width of a single species i approaches -1 if the hierarchical clustering algorithm misclassified the species.

Once the sub-community assemblages were identified, we performed a subsequent PTA on each assemblage to evaluate the relationship between Sacramento Valley Water Year Index and the assemblages. We visually assessed the dominant tensors after decomposing for species to determine which dominant tensor was related to the temporal mode (i.e., year). We then regressed the anomalies of this temporally dominant tensor (after decomposing for the modes of space and species) against the drought year classification as well as the Sacramento Valley Index using a simple linear regression framework.

Goal 2: Drought and Representative Species Catch

We used the silhouette width analysis to identify representative species for each cluster and evaluate whether and, if so, how catch of these species changes across categorical and continuous drought metrics. Because FMWT catch data for a given species is usually zero-inflated (e.g., Supplemental Figure 18, Appendix A), we used “zero-inflated models” (Shafira and Lestari 2020; Workie and Azene 2021) that simultaneously fit two model components: the first component predicts whether or not an event will be a zero and the second component predicts the value when the catch is non-zero. We, therefore, used a zero-inflated negative binomial (ZINB) regression to predict catch after accounting for Delta sub-region (Figure 10) using a multilevel Bayesian framework in R using the ‘brms’ package (version 2.16.1) following methods described by Bürkner (2018) with the addition of an autoregressive moving average residual correlation structure to account for the timeseries nature of the data (i.e., the annual timestep).

Representative Species Catch Associated with a Categorical Drought Metric

We selected a representative species from each sub-community assemblage (e.g., the species with the highest silhouette width per assemblage or a species of management interest and tested whether catch for the representative species, and, therefore, the sub-community assemblage the species represents, differed among the Drought MAST Team identified drought year classifications (Drought, Wet Periods, and Neutral periods Figure 11). We used a Bayesian framework (brms package, see Statistical Inference in a Bayesian Framework, in supplemental information, Appendix A) to develop a zero-inflated negative binomial mixed effects model to predict species catch during Droughts, Wet Periods, and Neutral years. The model included an autoregressive moving average correlation structure to account for the time-series nature of the dataset and an offset term to account for varying effort (i.e., trawling events or tows) across space and time. We did not perform this analysis on the marine cluster as the sampling locations of the FMWT survey are more suitable to evaluating brackish and freshwater fishes of the San Joaquin and Sacramento Rivers Delta.

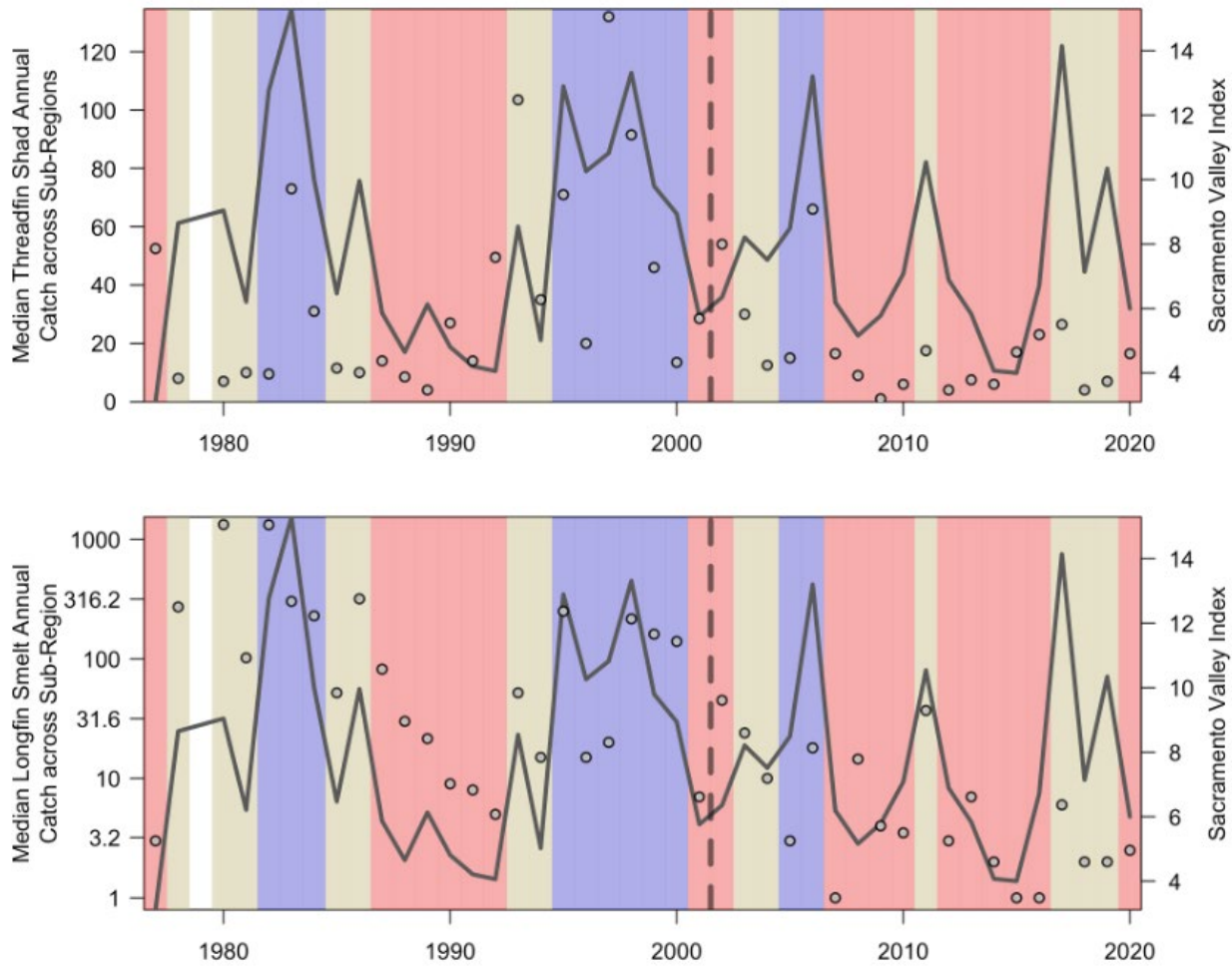


Figure 11 Median annual catch (points) for (top) Threadfin Shad and (bottom) Longfin Smelt, the selected sub-community assemblage representatives, across sub-regions. Colored backgrounds indicate annual water year category of Droughts (red), Wet Periods (blue), and other (i.e., Neutral; tan) year types. No data were collected in 1979. Gray line (right-axis) indicates annual Sacramento Valley Index. The vertical dashed line denotes the separation of Pre-POD era from the Post-POD era as defined by Thomson et al. (2010)). NOTE: Longfin Smelt catch (b) is log₁₀-scaled.

Threadfin Shad - White Catfish Cluster: Threadfin Shad

Threadfin Shad were selected as the representative of the freshwater Threadfin Shad - White Catfish cluster due to their silhouette width and management relevance relative to White Catfish. Due to the limited spatial range of the species, we removed sub-regions from the analysis that

averaged <10 individuals observed per year across the 43-year record, resulting in the inclusion of the following sub-regions:

1. Carquinez Strait
2. Grizzly Bay
3. Honker Bay
4. Lower Sacramento River
5. Lower San Joaquin River
6. Mid Suisun Bay
7. Sacramento River near Rio Vista
8. San Joaquin River at Prisoners Point
9. San Joaquin River at Twitchell Island
10. San Joaquin River near Stockton
11. San Pablo Bay
12. Suisun Marsh

The analysis was performed using 3 MCMC chains of 40,000 iterations with 20,000 burn-in (i.e., warm-up) iterations.

Fresh to Brackish Cluster: Longfin Smelt

Longfin Smelt were selected as the representative of the freshwater to brackish cluster due to their silhouette width and status as a species of management relevance (Figure 87). Due to the limited spatial range of the species, we removed sub-regions from the analysis that averaged <10 individuals observed per year across the 43 year record, resulting in the inclusion of the following sub-regions:

1. Carquinez Strait
2. Confluence
3. Grizzly Bay
4. Honker Bay
5. Lower Napa River
6. Lower Sacramento River
7. Mid Suisun Bay
8. Sacramento River near Rio Vista
9. San Pablo Bay
10. Suisun Marsh
11. West Suisun Bay

The analysis was performed using 3 MCMC chains of 40,000 iterations with 20,000 burn-in (i.e., warm-up) iterations.

Representative Species Catch Associated with a Continuous Drought Metric

To examine more nuanced flow-abundance relationships, we analyzed representative species catch across the continuous variable of Sacramento Valley Index (Figure 89). Furthermore, pelagic organisms, such as our representative species, across the San Francisco Estuary were reported to precipitously decline in 2000s, a phenomenon known as the Pelagic Organism Decline or, simply, "POD" (Mac Nally et al. 2010; Sommer et al. 2007; Thomson et al. 2010). We, hypothesized the relationship between representative species catch a drought may differ before and after the onset of the POD, which is considered to be around 2002 (Thomson et al. 2010).

We used the same Bayesian framework described above to predict representative species catch across Sacramento Valley Index in Year_t and Sacramento Valley Index_{t-1} in Year pre- and post-POD using a tensor product smoother (i.e., non-linear Sacramento Valley Index in Year_t, non-linear Sacramento Valley Index in Year_{t-1}, and their interaction) by POD time-period. The results of the model can be interpreted as the typical catch after accounting for effort in the average sub-region where the species is caught.

[Threadfin Shad - White Catfish Cluster: Threadfin Shad](#)

Threadfin Shad were selected as the representative of the freshwater Threadfin Shad - White Catfish cluster, and we removed sub-regions from the analysis that averaged <10 individuals observed per year across the 43-year record. The analysis was performed using 3 MCMC chains of 40,000 iterations with 20,000 burn-in (i.e., warm-up) iterations.

[Fresh to Brackish Cluster: Longfin Smelt](#)

Longfin Smelt were selected as the representative of the freshwater to brackish cluster, and, as with Threadfin Shad, we removed sub-regions from the analysis that averaged <10 individuals observed per year across the 43-year record. The analysis was performed using 3 MCMC chains of 40,000 iterations with 20,000 burn-in (i.e., warm-up) iterations.

Summary plot

To put analyses of all metrics together into a single figure, we converted the coefficients from the long-term drought models to qualitative degrees of drought response on a scale of 0 (no response) to 5 (strong response). We plotted these impact levels for some of the most important ecological parameters on a circular bar plot and color-coded the plot for increases or decreases in response to drought. We also assessed the qualitative degree to which the parameter values in 2021 were similar or different to previous

droughts on a scale of 0 (same as previous droughts) to 5 (very different from previous droughts).

Results

Hydrology

Delta Outflow

Delta Outflow from the Dayflow model was slightly lower in 2021 relative to 2020 but within the range of previous drought years (Figure 12). Year, season, and drought were all factors that significantly affected Delta outflow (Table 4). As expected, Delta Outflow was significantly lower in the Drought periods than Neutral or Wet periods and was significantly lower in the summer and fall seasons relative to the winter and spring seasons (Figure 13). Across seasons and drought year classification, 2021 had a lower median outflow relative to previous drought years (Figure 14).

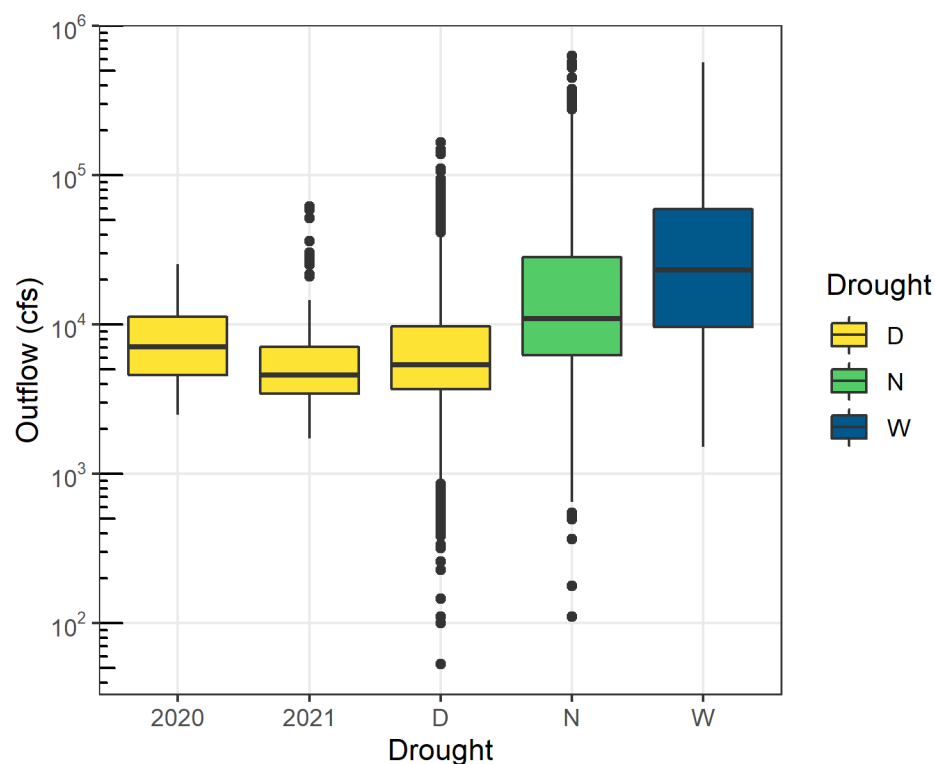


Figure 12. Boxplots of Delta Outflow from the Dayflow model for each value of the Drought year classification (Drought period [D], Neutral [N], and Wet period [W]), with 2020 and 2021 shown separately. Note that the y-axis is scaled to log₁₀ units (19 negative values are not displayed).

Table 4 Summary ANOVA outputs for both models of Delta Outflow from the Dayflow model. Sum of squares (Sum Sq), degrees of freedom (Df), ratio of two variances (F-value), and probability-value (Pr(>F)).

Model	Parameter	Sum Sq	Df	F value	Pr(>F)
Seasonal_Year	Year	97.61146	46	11.4898	< 0.001
Seasonal_Year	Season	72.68083	3	131.1807	< 0.001
Seasonal_Year	Residuals	25.48634	138		
Seasonal_Drought	Drought	63.91413	2	98.2735	< 0.001
Seasonal_Drought	Season	72.68083	3	74.5020	< 0.001
Seasonal_Drought	Residuals	59.18366	182		

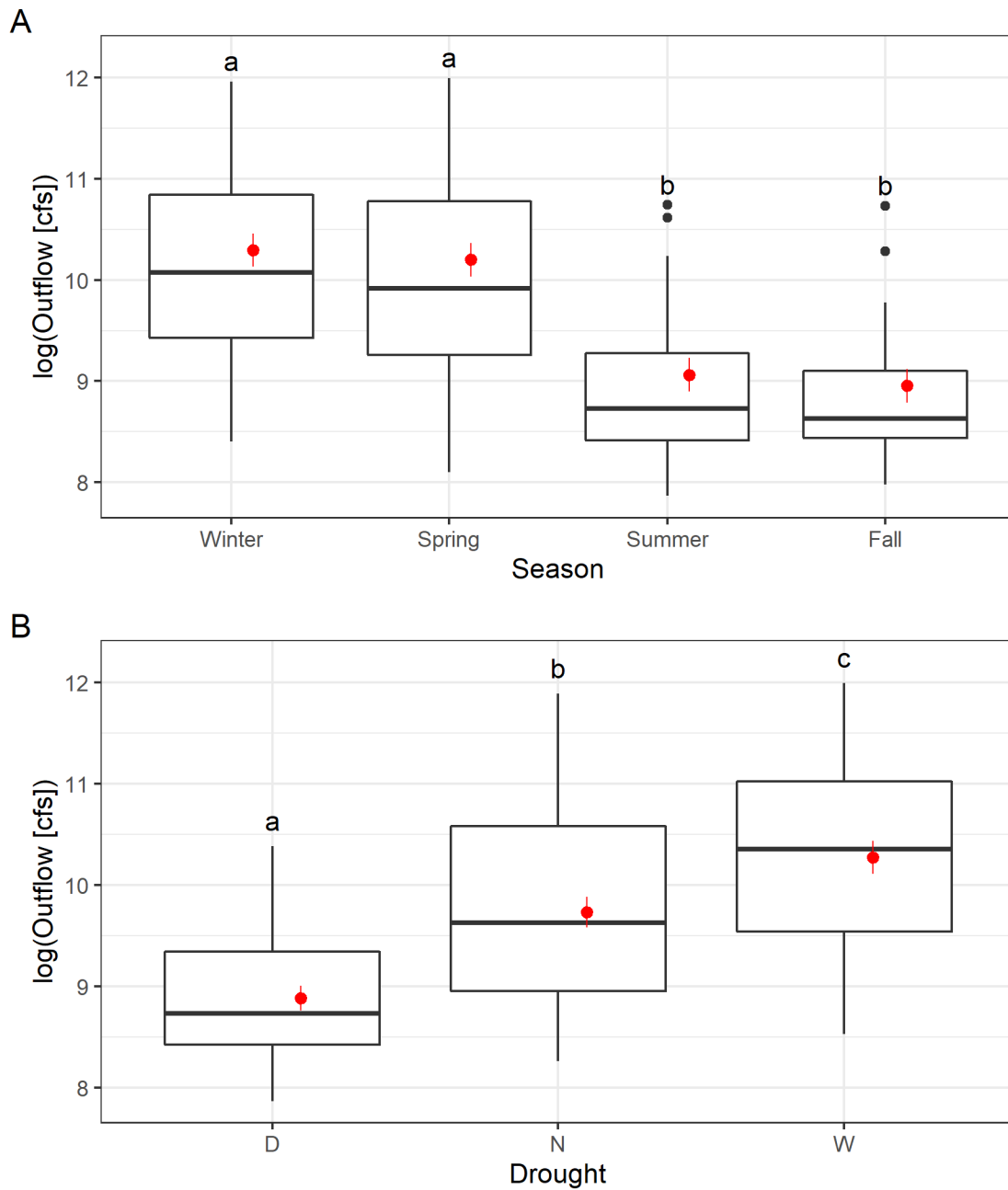


Figure 13 Observed (boxplots) and model-predicted (red points \pm 95% confidence intervals) log-transformed Delta outflow (Dayflow) for the seasonal-drought model by A) season and B) Drought year classification (Drought period [D], Neutral [N], and Wet period [W]). Different letters above the box plots identify statistically significant ($p < 0.05$) differences from a Tukey post-hoc test.

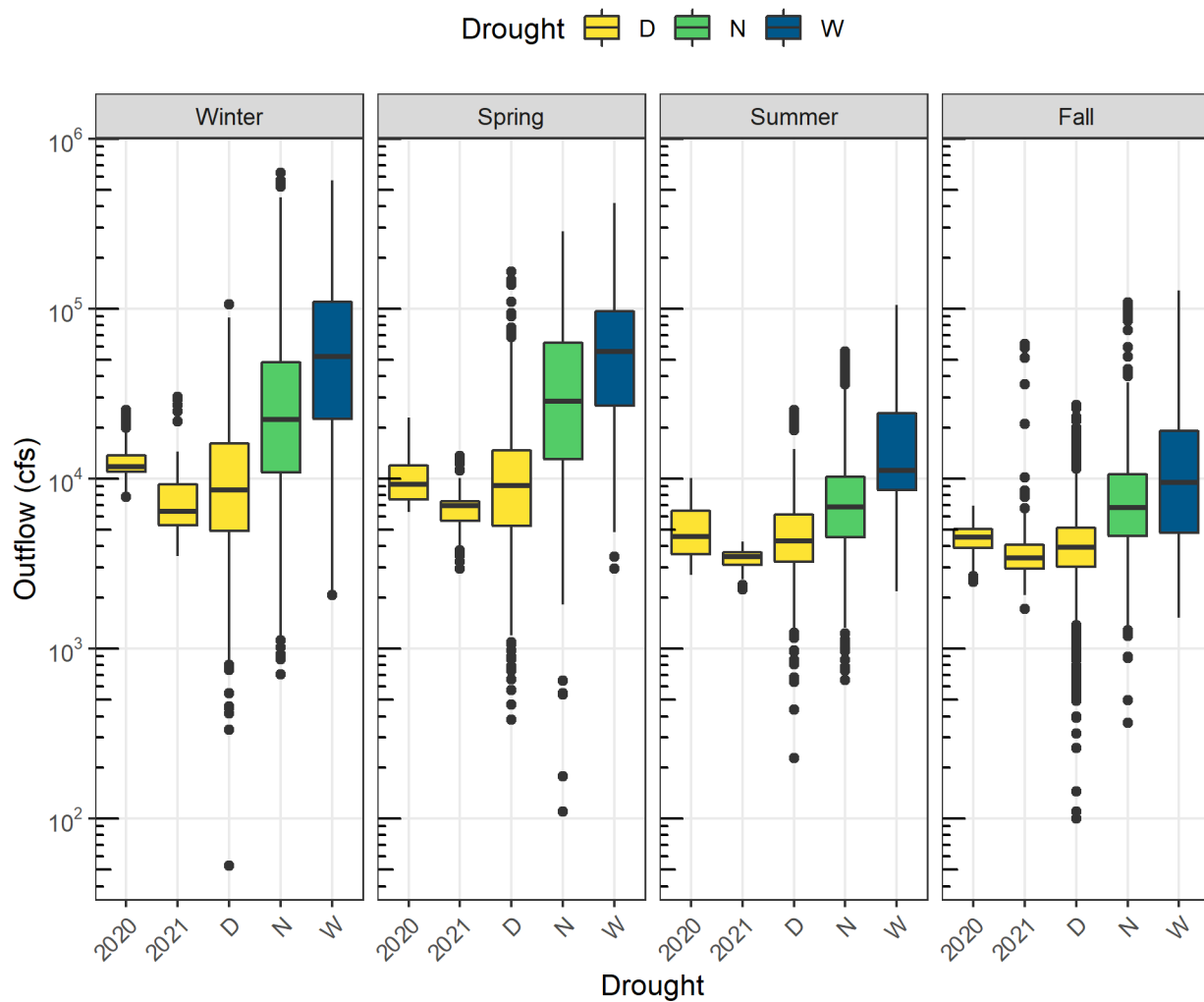


Figure 14. Boxplots of Delta Outflow from the Dayflow model of the Drought year classification (Drought period [D], Neutral [N], and Wet period [W]), with 2020 and 2021 shown separately grouped by season. Note that the y-axis is scaled to log₁₀ units (19 negative values are not displayed).

Whereas drought years are characterized by lower Delta outflow from the Dayflow model, a comparison of this output to combined USGS outflow at four monitoring stations, can be made (Figure 15). For the short-term record of WY2011 – 2021, the linear fitting of Dayflow outflow with USGS computed outflow is strong across all flow conditions with $R^2 = 0.929$ and a RMSE of 9,391 cfs. Below 10,000 cfs Delta outflow, however, the fit is poor ($R^2 = 0.077$ and a RMSE of 1,854 cfs) (Figure 15). Dayflow outflow less than 10,000 cfs makes up approximately 59% of the short-term record.

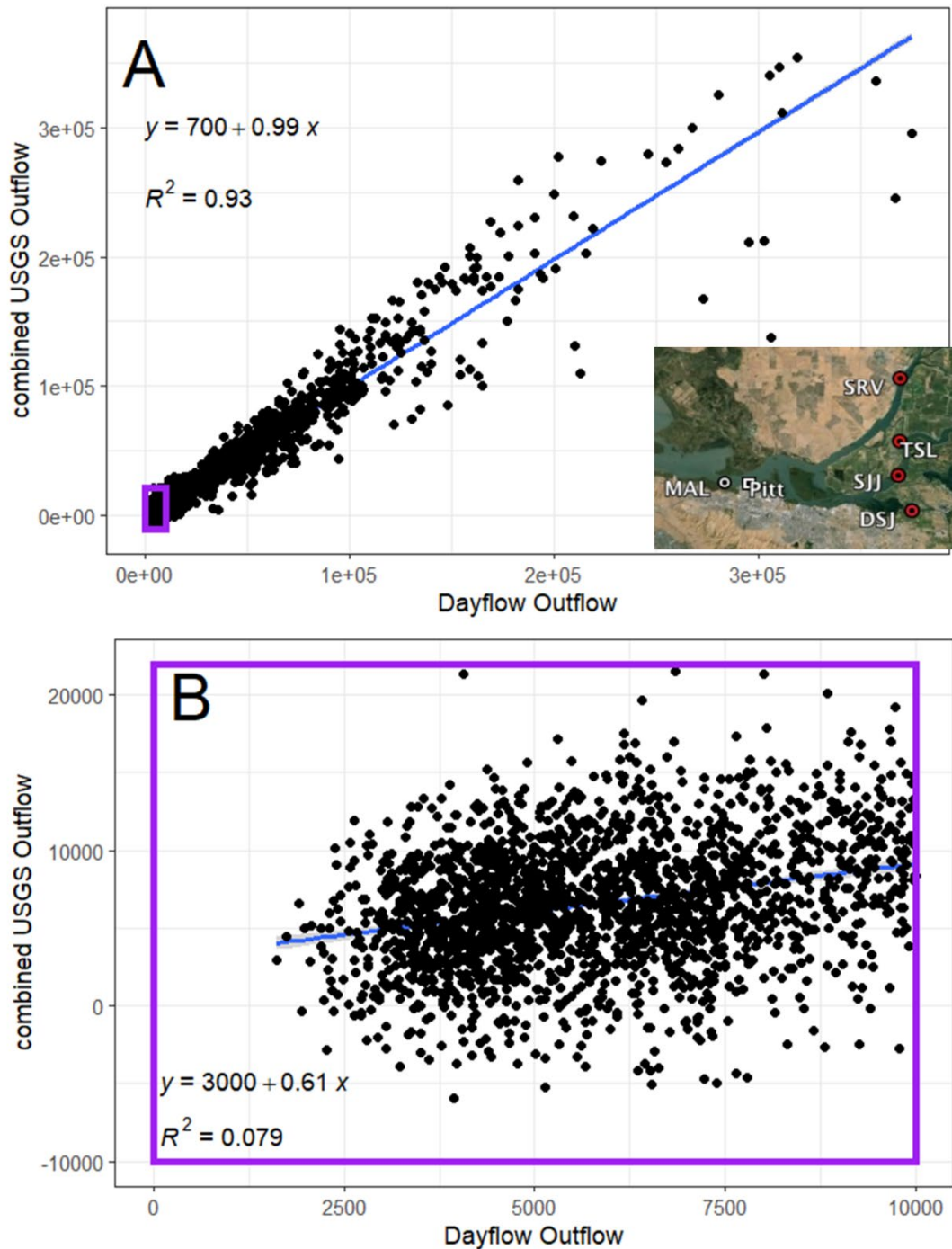


Figure 15. Comparison of Dayflow outflow and combined USGS outflow computed from four continuous monitoring stations between 2011 – 2021 during (A) all flow conditions and (B) low flow conditions (<10,000 cfs; inset). Purple bounding box in top panel represents low-flow conditions in bottom panel. Dayflow outflow <10,000 cfs represents ~59% of short-term

record. Adopted from Monismith (2016). Inset map of USGS continuous monitoring station in the Western Delta (red circles) Image from Google Earth.

Despite the poor relationship across the short-term record between Dayflow outflow and combined USGS outflow during low-flow conditions (Figure 15), the seasonal-year model of the log-transformed combined USGS outflow identifies that 2020 and 2021 net flows were lower relative to Neutral years of 2011, 2017, and 2019 (Figure 16). Results of both seasonal-year and seasonal-drought models were statistically similar between Dayflow and combined USGS outflow data sets (Table S1) in both the long and short-term analyses. Winter and Spring outflows are significantly higher relative to Summer and Fall (Figure 16).

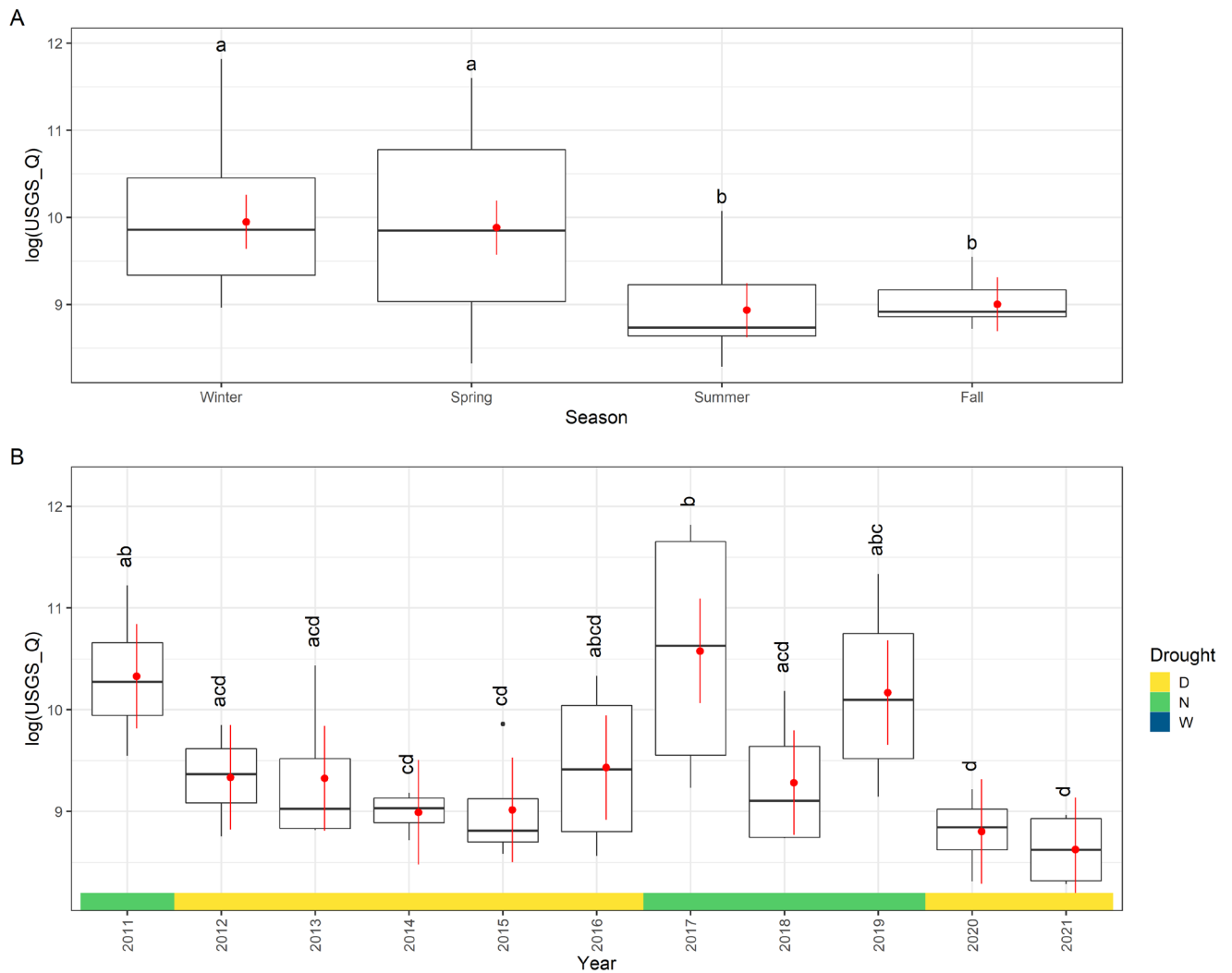


Figure 16. Observed (boxplots) and model-predicted (red points $\pm 95\%$ confidence intervals) log-transformed combined net outflow for the seasonal-year model across the short-term record. Different letters above the box plots identify statistically significant ($p < 0.05$) differences from a Tukey post-hoc test.

Moving upstream of the low-salinity zone toward the Cache Slough Complex, net discharge at the Cache Slough station exhibits unique patterns across years and seasons relative to the Dayflow outflow metric. Across the short-term record, the seasonal-year model identified that 2021 and 2020 Cache Slough net flows were similar to all years except 2015 (Figure 17). Seasonal effect was only significantly different between summer and winter flows. In the seasonal-drought model, Cache Slough flow differed significantly

between Neutral and Drought years (Table 5) which is similar to Dayflow outflow and combined USGS outflow model results (Table S1).

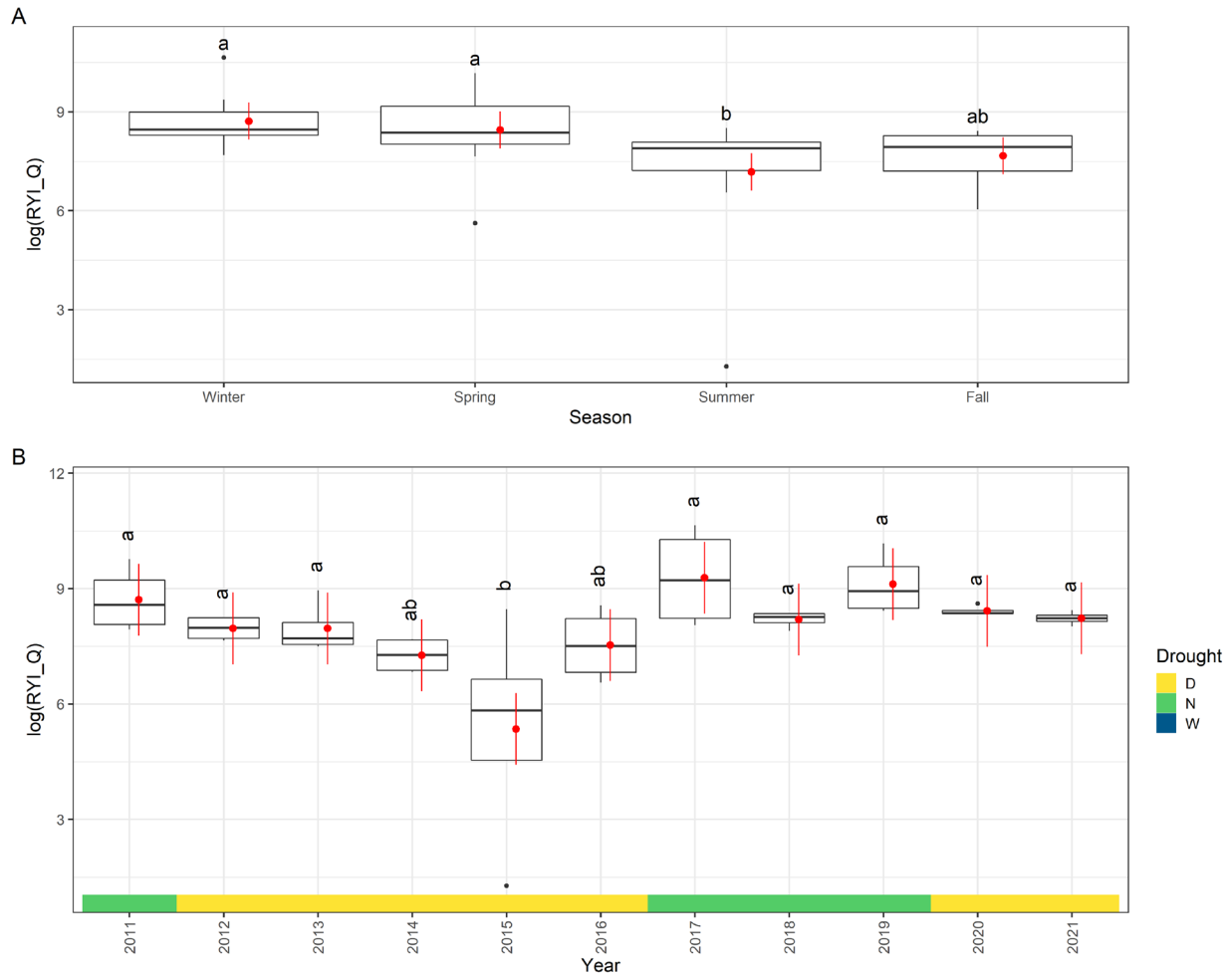


Figure 17. Observed (boxplots) and model-predicted (red points \pm 95% confidence intervals) log-transformed Cache Slough net flow for the seasonal-year model. Different letters above the box plots identify statistically significant ($p < 0.05$) differences from a Tukey post-hoc test.

Table 5. Summary ANOVA outputs for Cache Slough flow models

Model	Parameter	Sum Sq	Df	F value	Pr(>F)
Seasonal_Year	Year	53.016	10	4.628	< 0.001
Seasonal_Year	Season	18.753	3	5.457	0.0041
Seasonal_Year	Residuals	34.364	30		
Seasonal_Drought	Drought	18.343	1	10.362	0.0026
Seasonal_Drought	Season	18.753	3	3.531	0.0235
Seasonal_Drought	Residuals	69.036	39		

Export

Water exports at the pumping facilities in 2021 were lower relative to 2020 as well as other drought years (Figure 18). Across the long-term record, 2021 exports were significantly different from most wet years (Figure 19). Exports are significantly different across year and season (Table 6) with spring exports significantly lower relative to other seasons (Figure 19, Figure 20).

The model-predicted summer exports are below the 95 percentile of observed exports (Figure 19). Exports during Drought are lower and significantly different relative to Neutral and Wet years (Figure 20). Exports in Neutral and Wet years were not significantly different in the seasonal-drought model

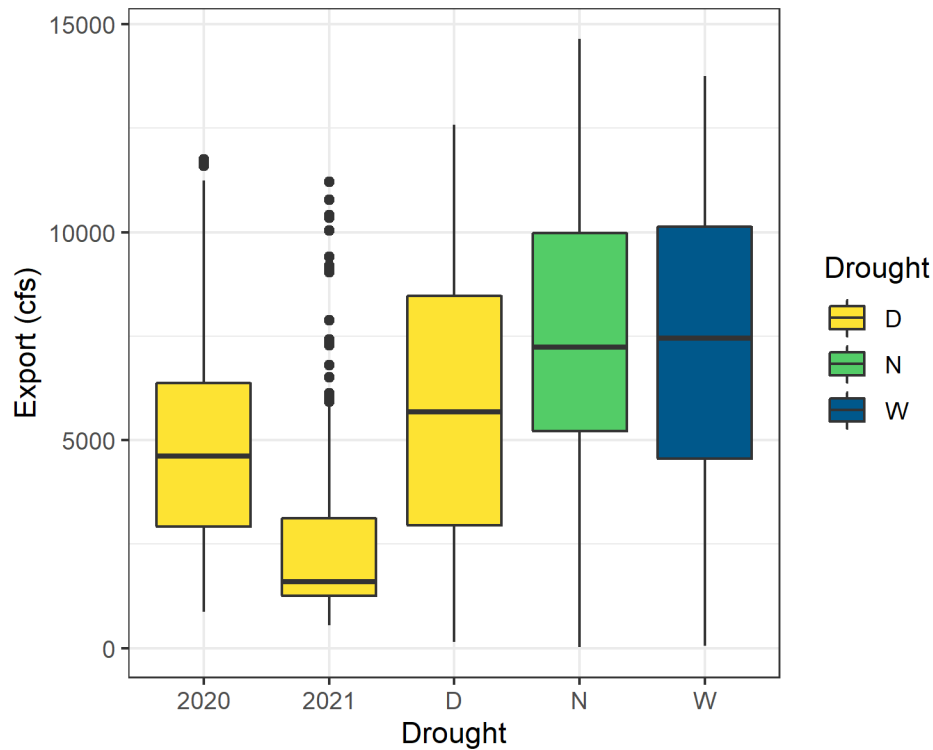


Figure 18. Boxplots of export by Drought year classification (Drought [D], Neutral [N] and Wet Periods [W]), with 2021 and 2020 shown separately.

Table 6. Summary ANOVA outputs for both export models

Model	Parameter	Sum Sq	Df	F value	Pr(>F)
Seasonal_Year	Year	5.88E+08	46	4.409	< 0.001
Seasonal_Year	Season	1.77E+08	3	20.372	< 0.001
Seasonal_Year	Residuals	4E+08	138		
Seasonal_Drought	Drought	1.35E+08	2	14.360	< 0.001
Seasonal_Drought	Season	1.77E+08	3	12.593	< 0.001
Seasonal_Drought	Residuals	8.53E+08	182		

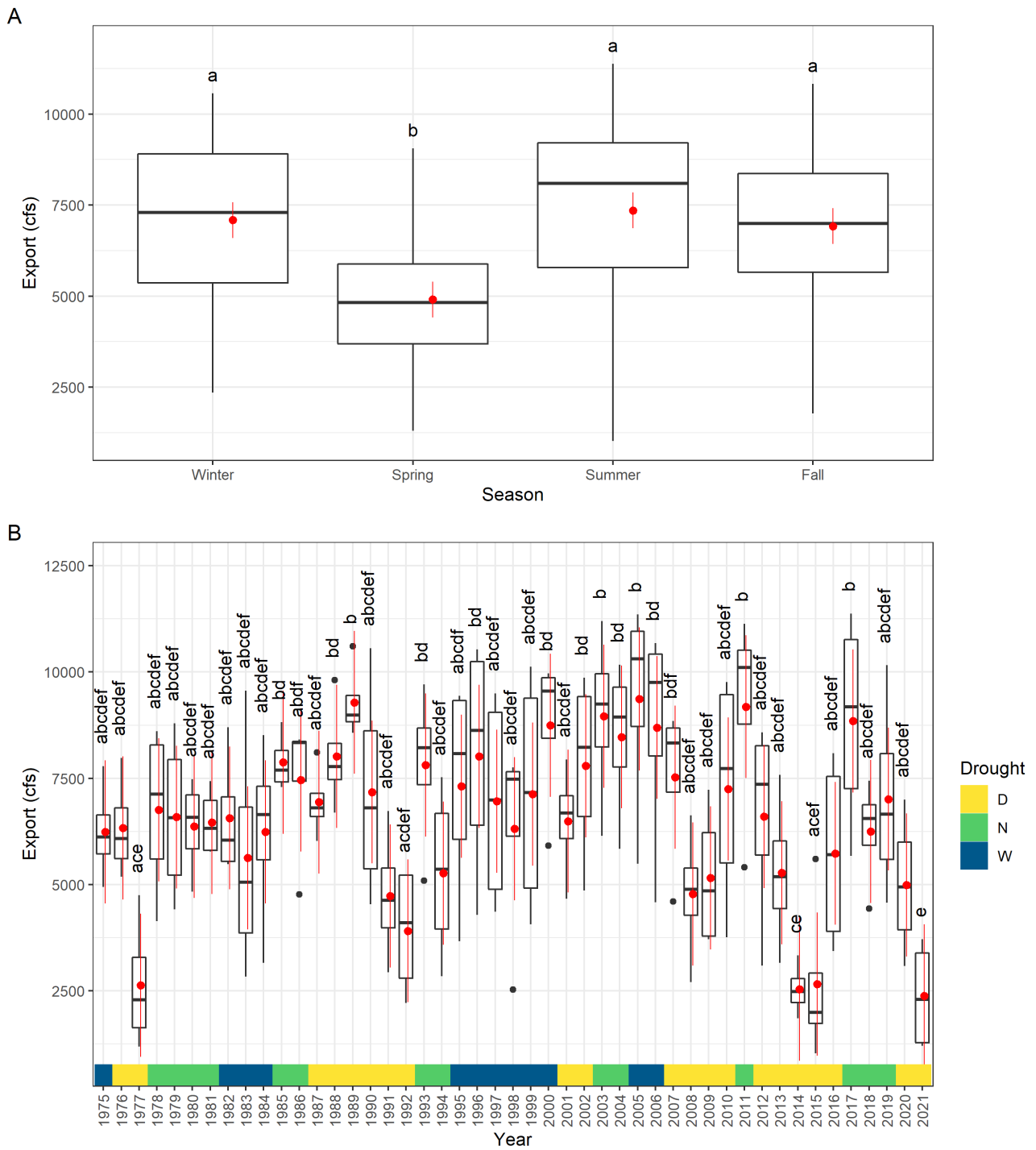


Figure 19. Observed (boxplots) and model-predicted (red points \pm 95% confidence intervals) exports for the seasonal-year model. Different letters above the box plots identify statistically significant ($p < 0.05$) differences from a Tukey post-hoc test.

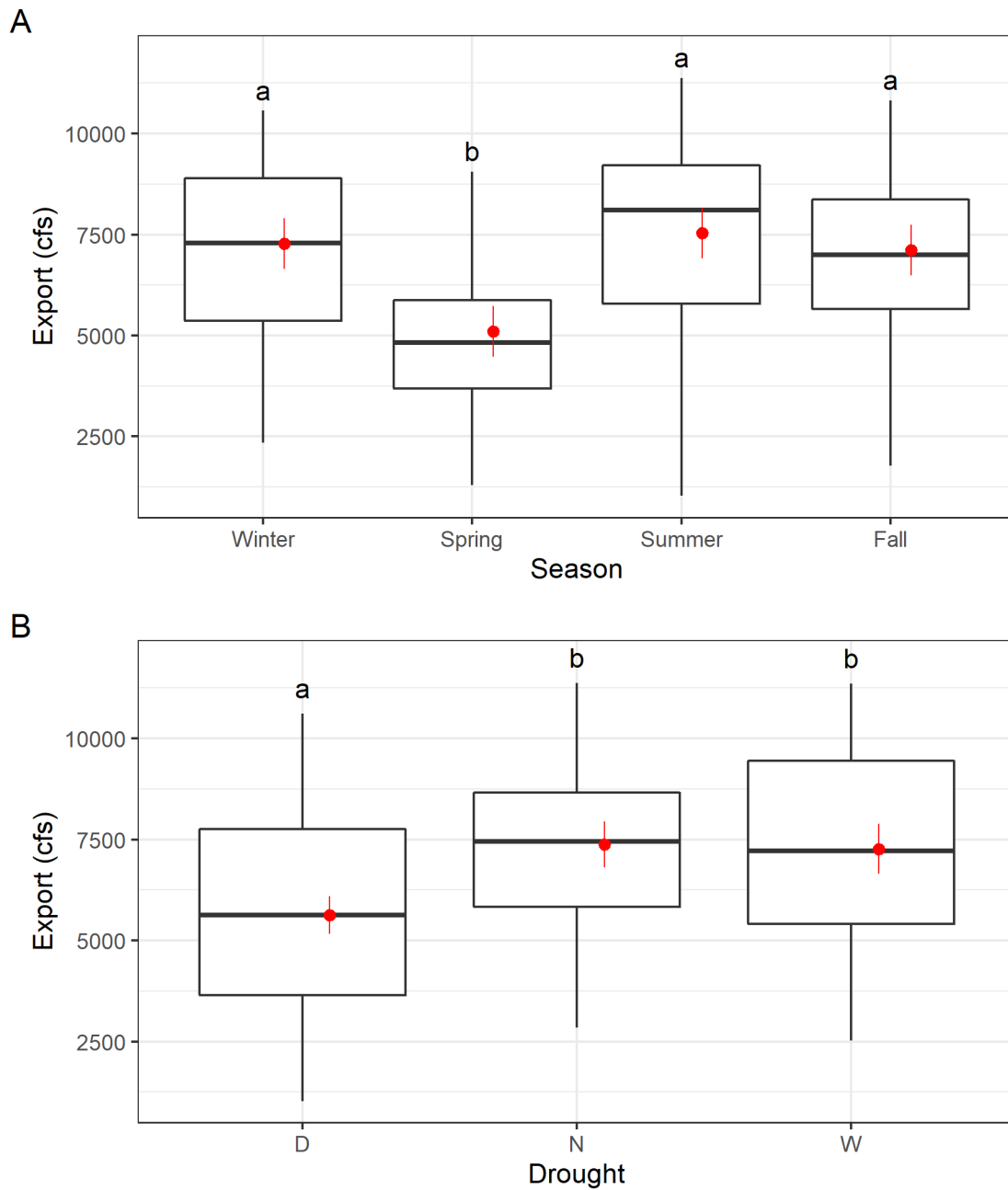


Figure 20. Observed (boxplots) and model-predicted (red points $\pm 95\%$ confidence intervals) exports for the seasonal-drought model by A) season and B) Drought year classification (Drought period [D], Neutral [N], and Wet period [W]) Different letters above the box plots identify statistically significant ($p < 0.05$) differences from a Tukey post-hoc test.

X2

The median position of X2 in 2021 fell within the range of previous drought years and was upstream of the median value of 2020 (Figure 21). Across all seasons, the position of X2 was farther upstream relative to all drought years (Figure 22). The seasonal-year model identified that the X2 position varied significantly across years and that 2021 was like 2014, 2015, and other drought years in the long-term record (Figure 23). The position of X2 was significantly different across the year, season, and drought factors in both models (Table 7).

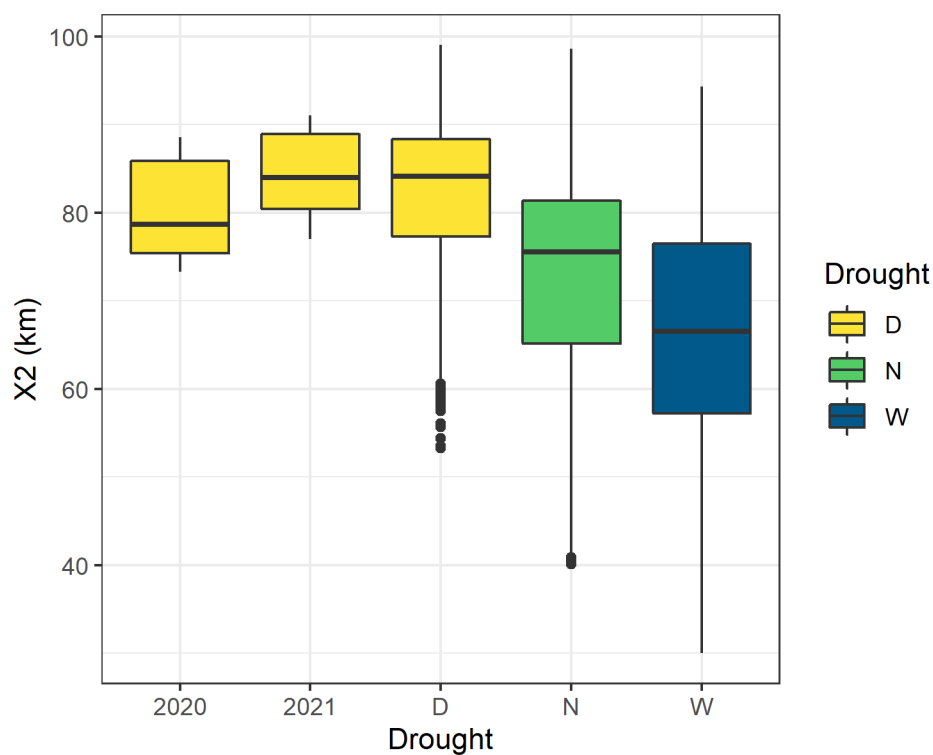


Figure 21. Boxplots of X2 (km) for each value of the Drought year classification (Drought period [D], Neutral [N], and Wet period [W]), with 2021 and 2020 shown separately.

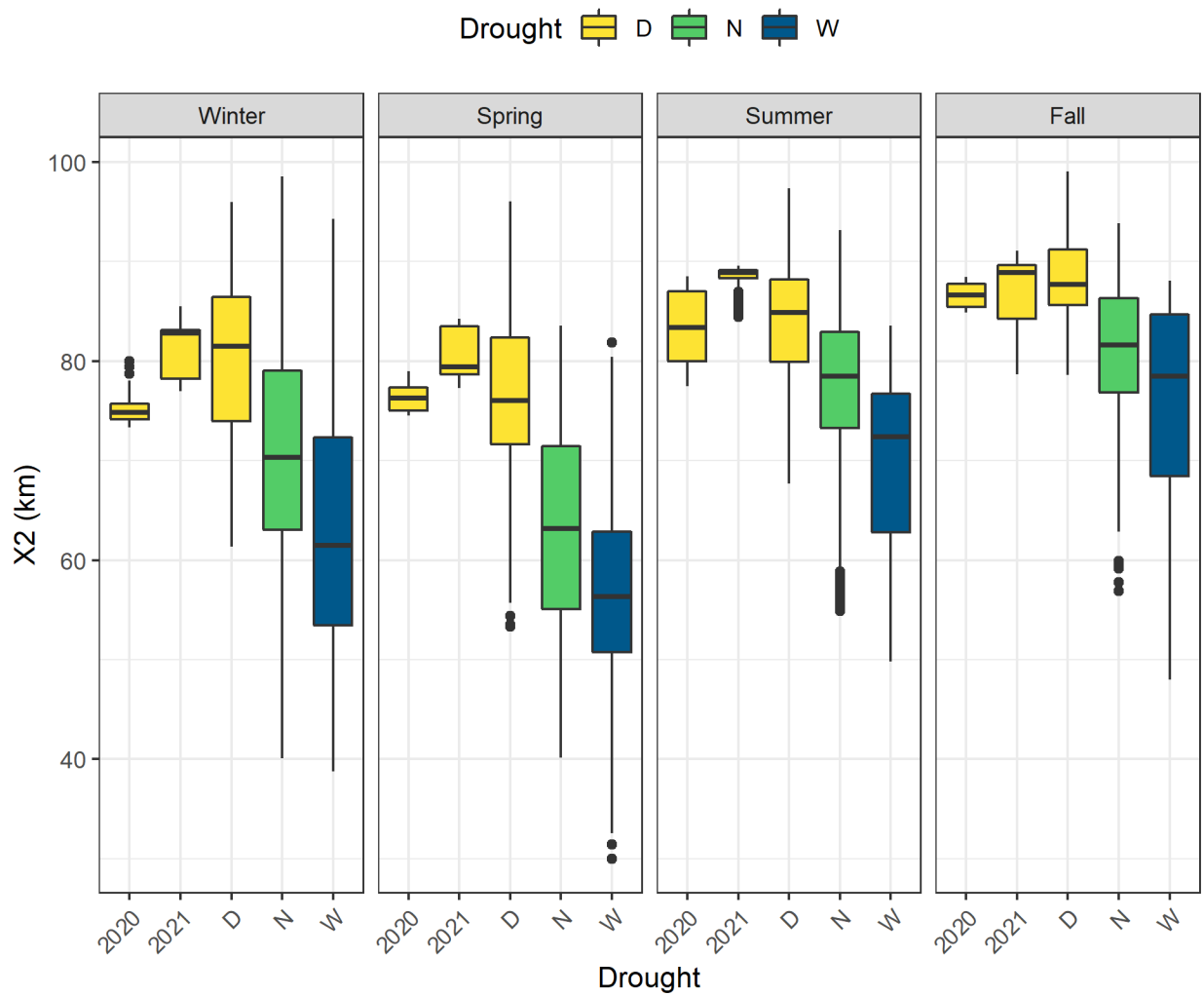


Figure 22. Boxplots of X2 of the Drought year classification (Drought period [D], Neutral [N], and Wet period [W]), with 2020 and 2021 shown separately grouped by season.

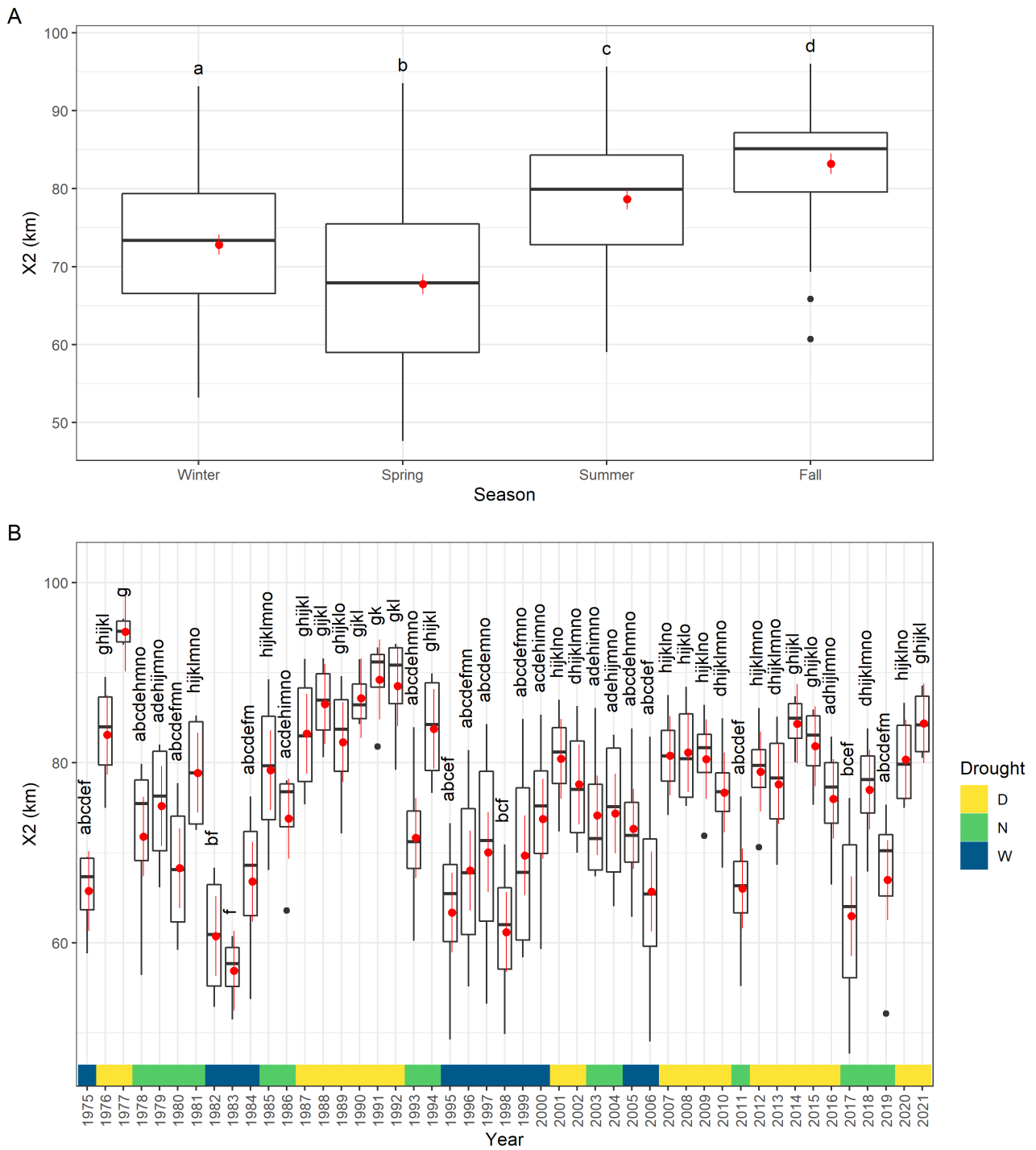


Figure 23. Observed (boxplots) and model-predicted (red points ±95% confidence intervals) X2 for the seasonal-year model. Different letters above the box plots identify statistically significant ($p < 0.05$) differences from a Tukey post-hoc test.

Table 7. Summary ANOVA outputs for both X2 models

Model	Parameter	Sum Sq	Df	F value	Pr(>F)
Seasonal_Year	Year	13243.12	46	14.36604	< 0.001
Seasonal_Year	Season	6406.007	3	106.5542	< 0.001
Seasonal_Year	Residuals	2765.506	138		
Seasonal_Drought	Drought	8715.136	2	108.7377	< 0.001
Seasonal_Drought	Season	6406.007	3	53.28466	< 0.001
Seasonal_Drought	Residuals	7293.489	182		

Water quality

Temperature

Water temperatures were similar in 2020 and 2021 (although data for 2021 is only included through September). Temperatures in both years were higher than those from prior years of any drought year classification or year type. Generally, temperatures were higher in drier years (Figure 24).

In all the temperature models, all factors significantly impacted water temperatures ($p < 0.001$, Table 8). In both regional ANOVAs, temperatures were significantly the highest in the South-Central region and the lowest in the North region ($p < 0.05$, Figure 25, Figure 26). In just the regional-year ANOVA, Suisun Bay was significantly cooler than Suisun Marsh and the Confluence. In both seasonal ANOVAs, seasonal temperatures were all significantly different from one another. The seasonal temperatures ordered from lowest to highest are: winter, spring, fall, and summer (Figure 27, Figure 28).

In both models of the drought year classification, Drought years had significantly higher temperatures than Neutral or Wet years ($p < 0.05$, Figure 25, Figure 27). In the regional-drought model, Neutral years were significantly warmer than Wet years, but they were equivalent in the seasonal-drought model (Figure 25, Figure 27). When accounting for regions or seasons in the seasonal-year and regional-year models, 2021 temperatures were higher than most prior years, although not always significantly so (Figure 26, Figure 28).

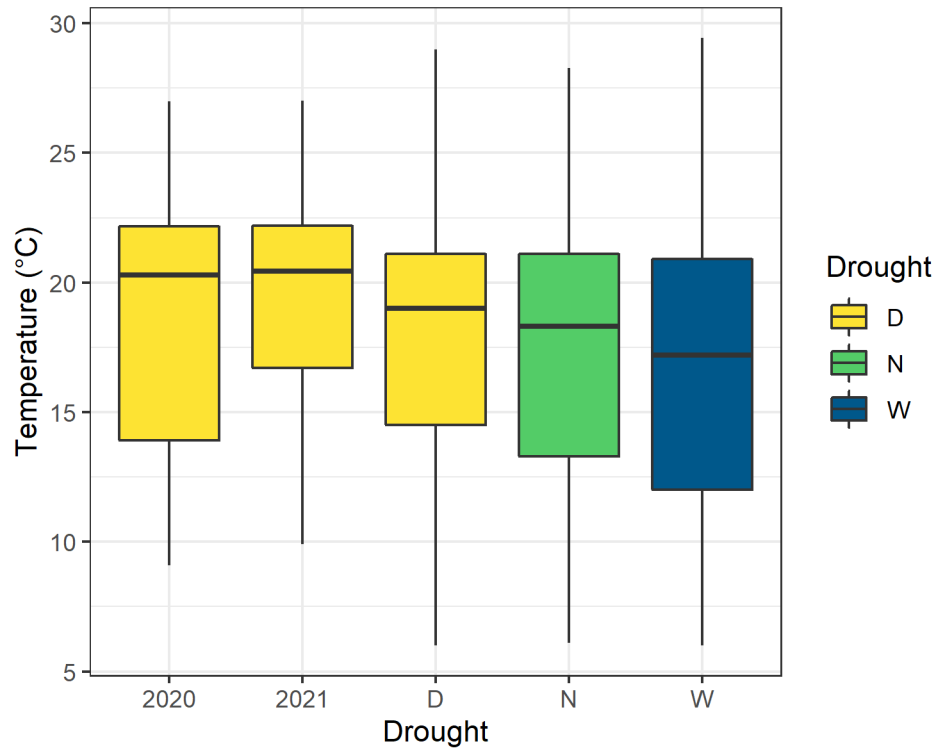


Figure 24. Boxplots of temperature for each value of the Drought year classification (Drought period [D], Neutral [N], and Wet period [W]), with 2020 and 2021 shown separately.

Table 8. Summary ANOVA outputs for each of the four temperature models.

Model	Parameter	Sum Sq	Df	F value	Pr(>F)
Regional_Drought	Drought	24.29536	2	30.77683	< 0.001
Regional_Drought	Region	51.95627	4	32.90854	< 0.001
Regional_Drought	Residuals	85.65034	217		
Regional_Year	Year	87.99068	46	15.0727	< 0.001
Regional_Year	Region	51.37079	4	101.1972	< 0.001
Regional_Year	Residuals	21.95502	173		
Seasonal_Drought	Drought	13.33979	2	10.07663	< 0.001
Seasonal_Drought	Season	3107.538	3	1564.917	< 0.001
Seasonal_Drought	Residuals	112.526	170		
Seasonal_Year	Year	61.74506	46	2.637647	< 0.001
Seasonal_Year	Season	3096.019	3	2027.938	< 0.001
Seasonal_Year	Residuals	64.12071	126		

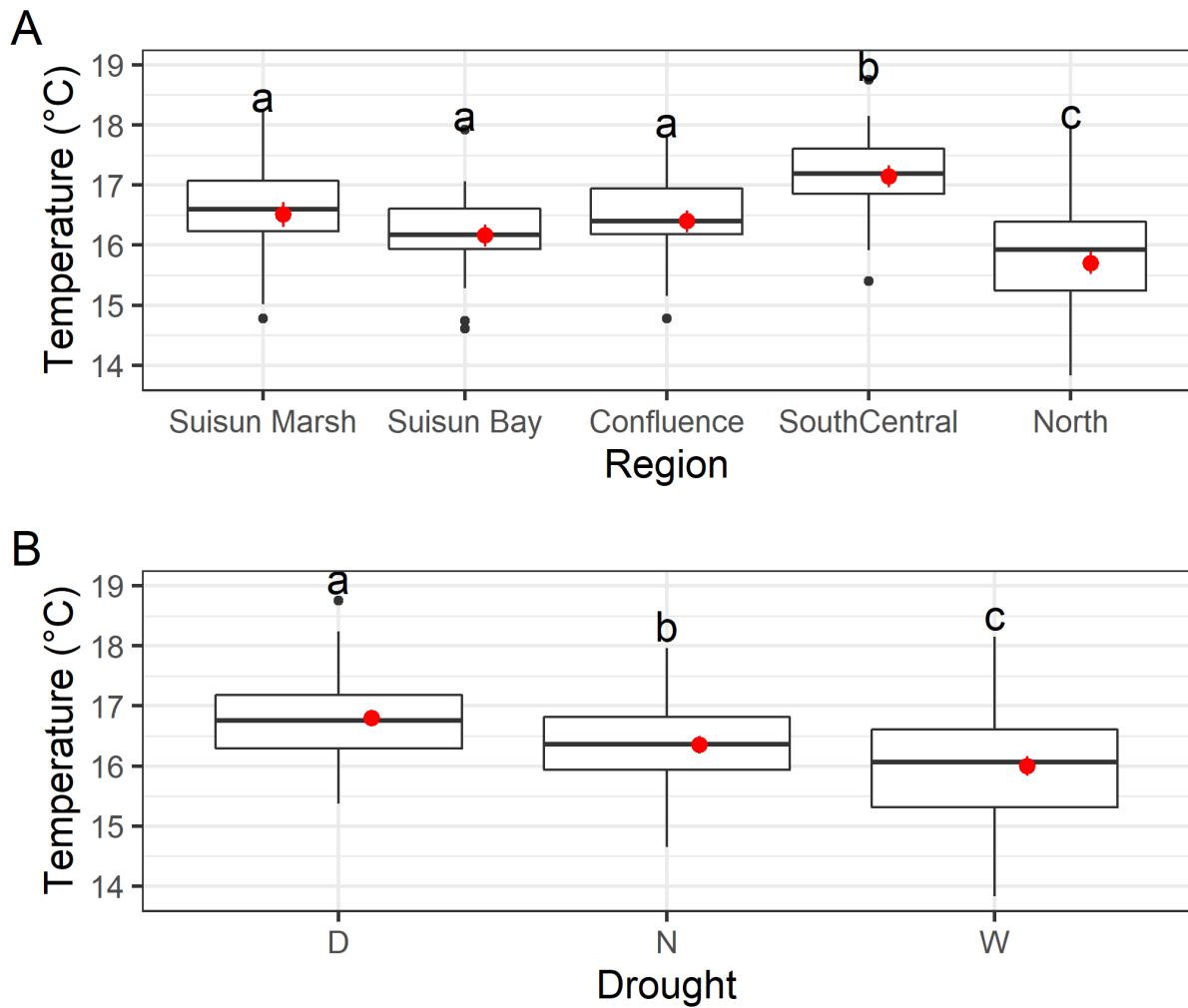


Figure 25. Observed (boxplots) and model-predicted (red points $\pm 95\%$ confidence intervals) temperatures for the regional-drought model by A) Region and B) Drought year classification (Drought period [D], Neutral [N], and Wet period [W]). Different letters above boxplots identify statistically significant ($p < 0.05$) differences from a Tukey post-hoc test.

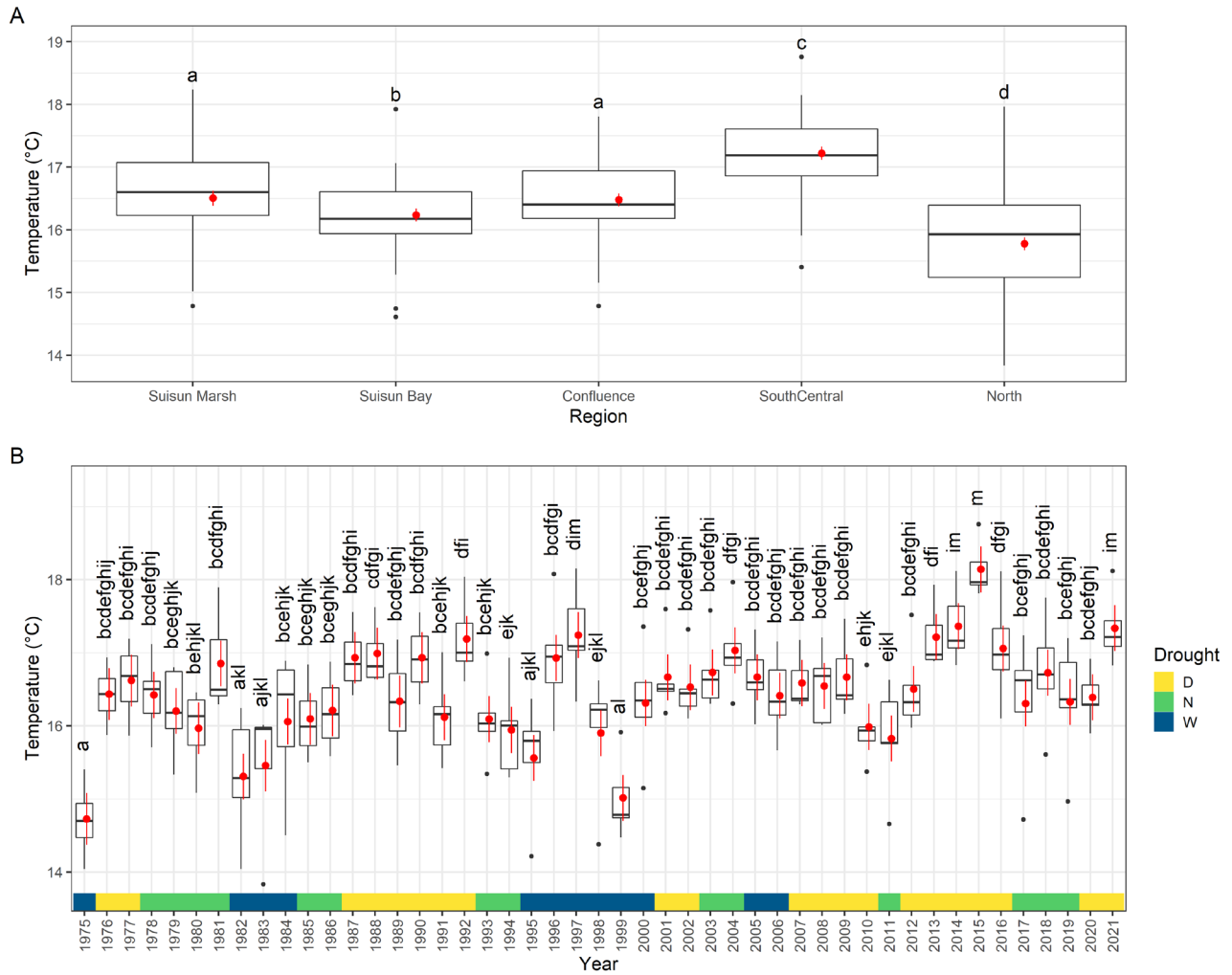


Figure 26. Observed (boxplots) and model-predicted (red points $\pm 95\%$ confidence intervals) temperatures for the regional-year model. Different letters above boxplots identify statistically significant ($p < 0.05$) differences from a Tukey post-hoc test.

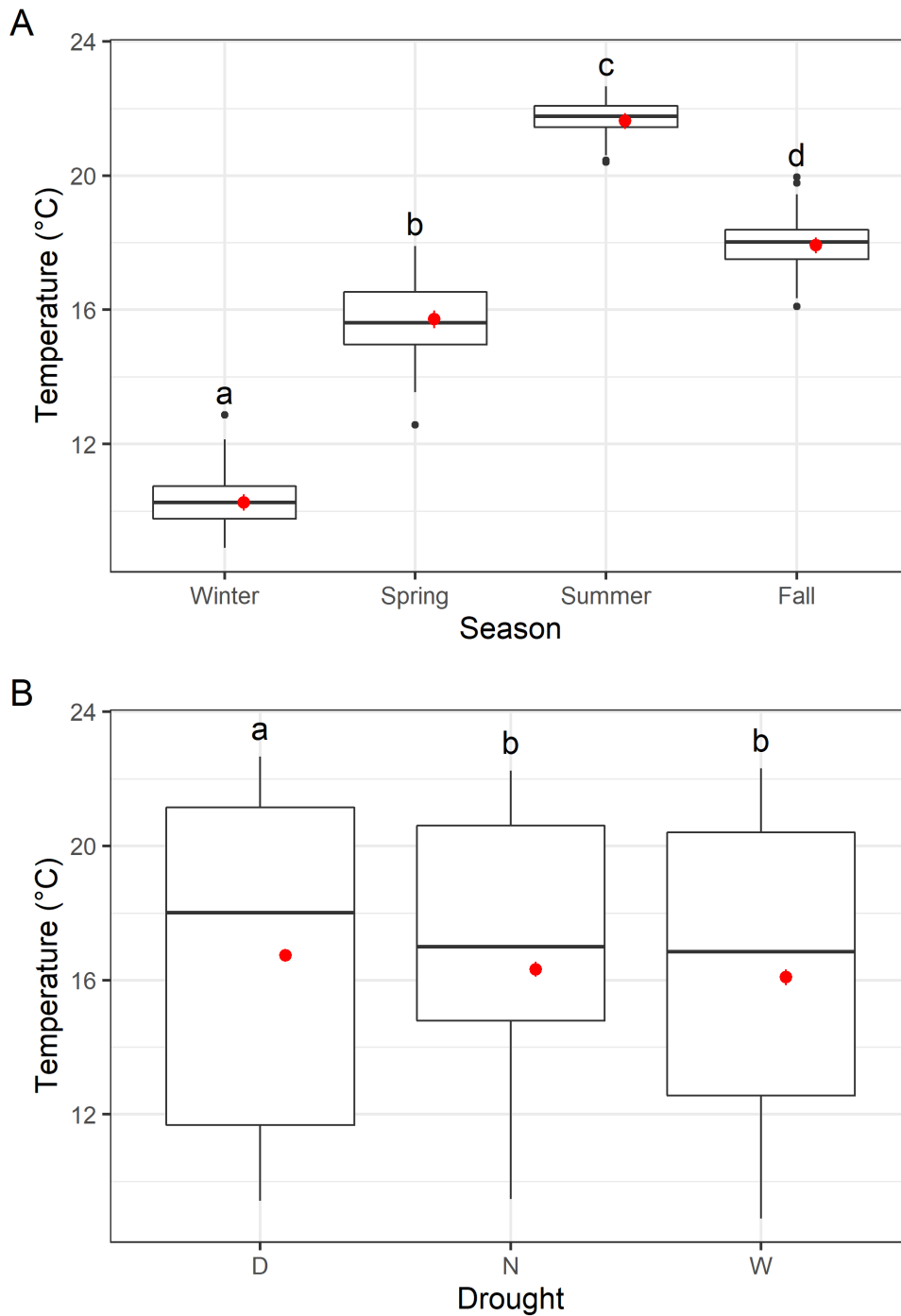


Figure 27. Observed (boxplots) and model-predicted (red points $\pm 95\%$ confidence intervals) temperatures for the seasonal-drought model by A) season and B) Drought year classification (Drought period [D], Neutral [N],

and Wet period [W]). Different letters above boxplots identify statistically significant ($p < 0.05$) differences from a Tukey post-hoc test.

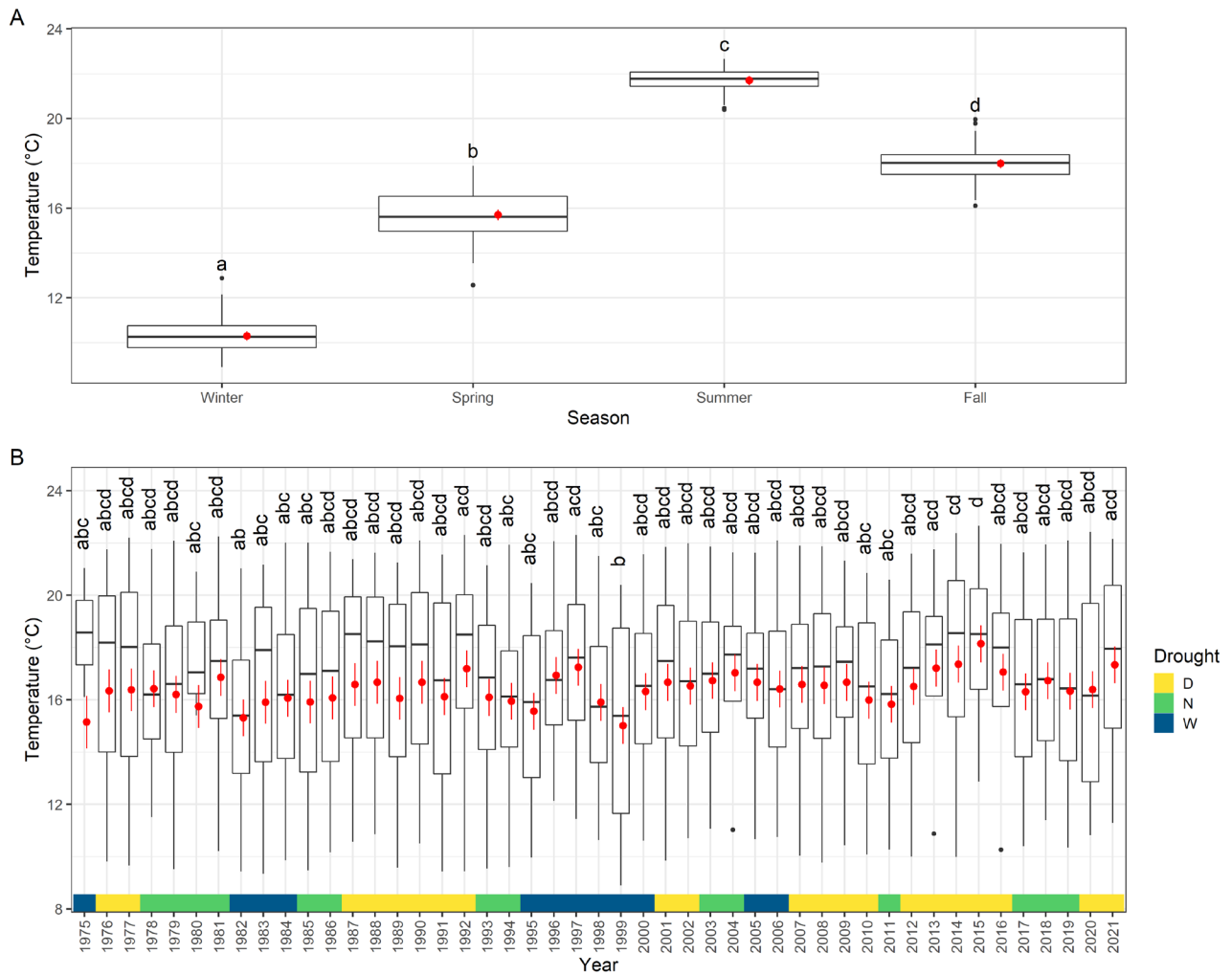


Figure 28. Observed (boxplots) and model-predicted (red points $\pm 95\%$ confidence intervals) temperatures for the seasonal-year model. Different letters above boxplots identify statistically significant ($p < 0.05$) differences from a Tukey post-hoc test.

Salinity

Salinities observed in 2021 were higher than those in 2020 or in a typical Drought-designated year. Salinity in 2020 more closely resembled a typical Drought year, which was higher than a Neutral year, and itself, in turn, higher than a typical Wet period year (Figure 29).

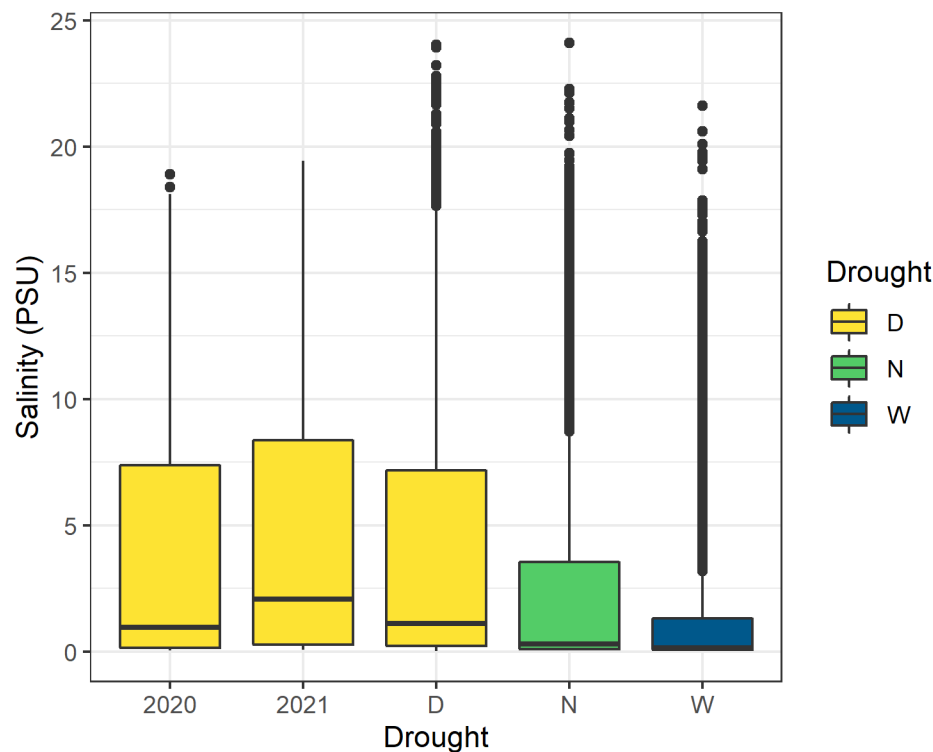


Figure 29. Boxplots of salinity for each Drought year classification (Drought period [D], Neutral [N], and Wet period [W]) alongside 2020 and 2021.

For each regional and seasonal model, the component factors of Drought year classification and year each had a significant effect on salinity, with each having a p value < 0.001 (Table 9).

ANOVA models for regional salinity showed Suisun Marsh, Suisun Bay, and Confluence were each significantly different from any other region, while South Central and North were significantly lower than the three other downstream regions, but not significantly different from each other (Figure 30, Figure 31). In the regional-drought model, each year type was significantly different from one another and matched observed distributions in the collected data, namely that Drought years showed higher salinity than

Neutral years, which, in turn, had higher salinity than Wet period years (Figure 30). The regional-year model showed that 2021 had higher salinity than most previous years, including many Drought-designated years, and most closely resembled 1991, 2014, and 2015 (Figure 31).

ANOVA models for seasonal salinity showed that fall was significantly higher and spring was significantly lower than all other seasons, while winter and summer were not significantly different from one another (Figure 32, Figure 33). Consistent with the regional-drought model, each year type was significantly different from one another in the seasonal-drought model and matched observed distributions in the collected data, namely that Drought years showed higher salinity than Neutral years, which, in turn, had higher salinity than Wet Period years (Figure 32). The seasonal-year model showed that 2021 had higher salinity than most previous years, though 1977, 2014, and 2015 appeared to have higher, though not statistically different salinity than 2021 (Figure 33).

Table 9. Summary of ANOVA outputs for models of regional and seasonal salinity by drought year classification and year (as a factor).

Model	Parameter	Sum Sq	Df	F value	Pr(>F)
Regional_Drought	Drought	176.888	2	50.688	< 0.001
Regional_Drought	Region	1663.163	4	238.294	< 0.001
Regional_Drought	Residuals	380.381	218		
Regional_Year	Year	249.428	46	3.065	< 0.001
Regional_Year	Region	1658.593	4	234.37	< 0.001
Regional_Year	Residuals	307.841	174		
Seasonal_Drought	Drought	45.670	2	83.085	< 0.001
Seasonal_Drought	Season	27.772	3	33.68192	< 0.001
Seasonal_Drought	Residuals	46.998	171		
Seasonal_Year	Year	215.144	46	10.339	< 0.001
Seasonal_Year	Season	77.429	3	57.057	< 0.001
Seasonal_Year	Residuals	57.448	127		

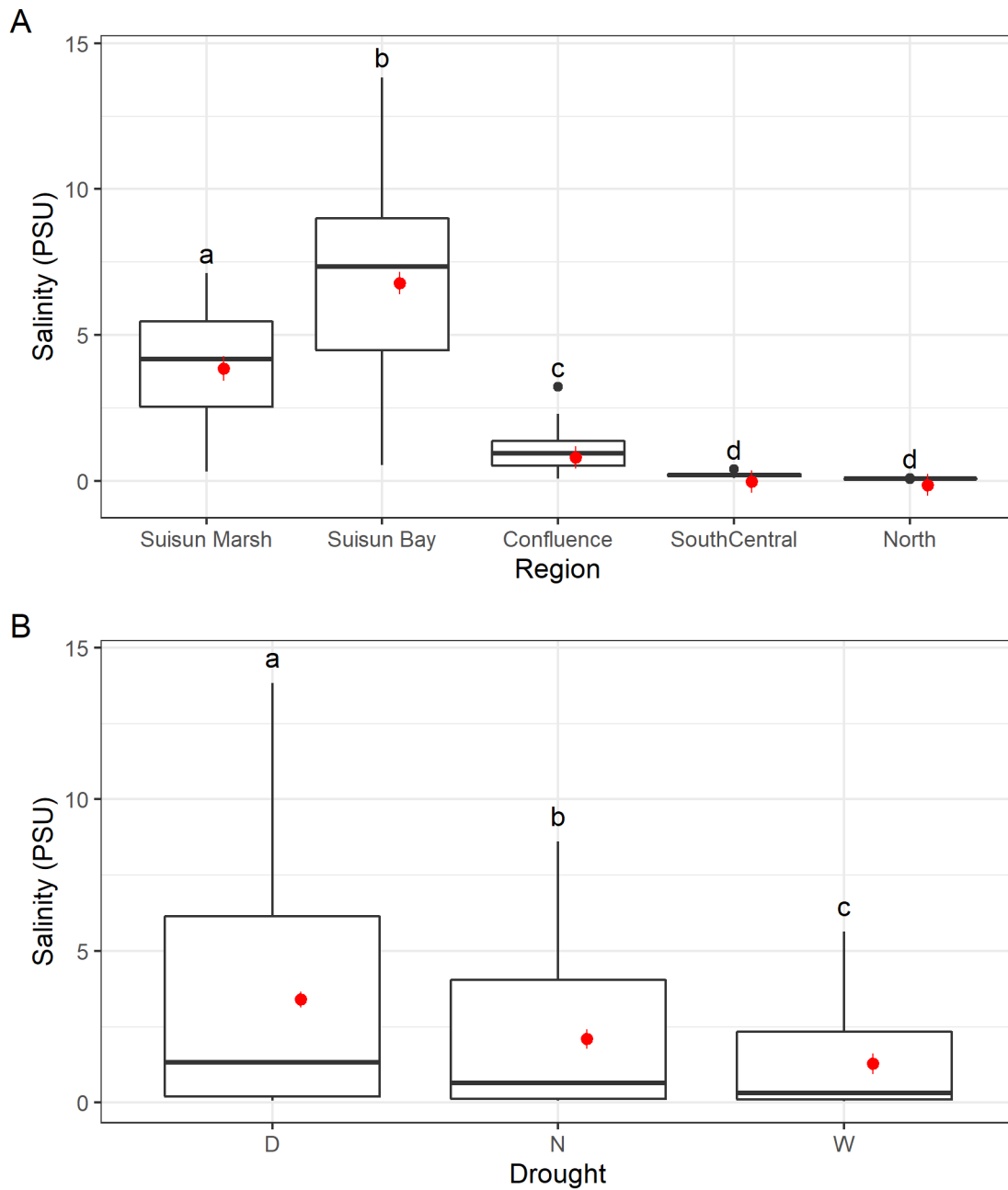


Figure 30. Observed (boxplots) and model-predicted (red points $\pm 95\%$ confidence intervals) salinities for the regional by Drought year classification model. Different letters above the box plots identify statistically significant ($p < 0.05$) differences from a Tukey post-hoc test.

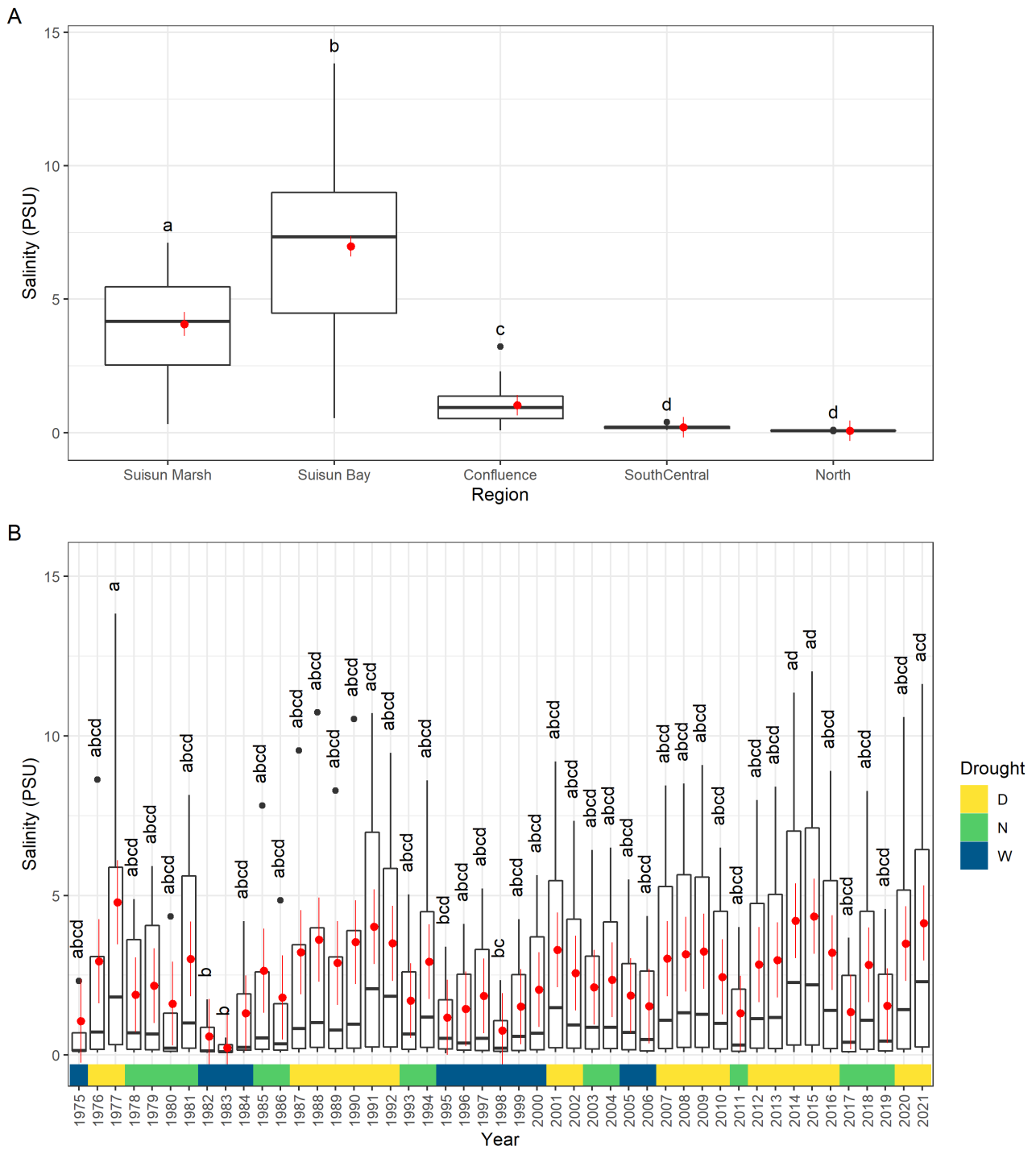


Figure 31. Observed (boxplots) and model-predicted (red points \pm 95% confidence intervals) salinities for the regional by year model. Different letters above the box plots identify statistically significant ($p < 0.05$) differences from a Tukey post-hoc test.

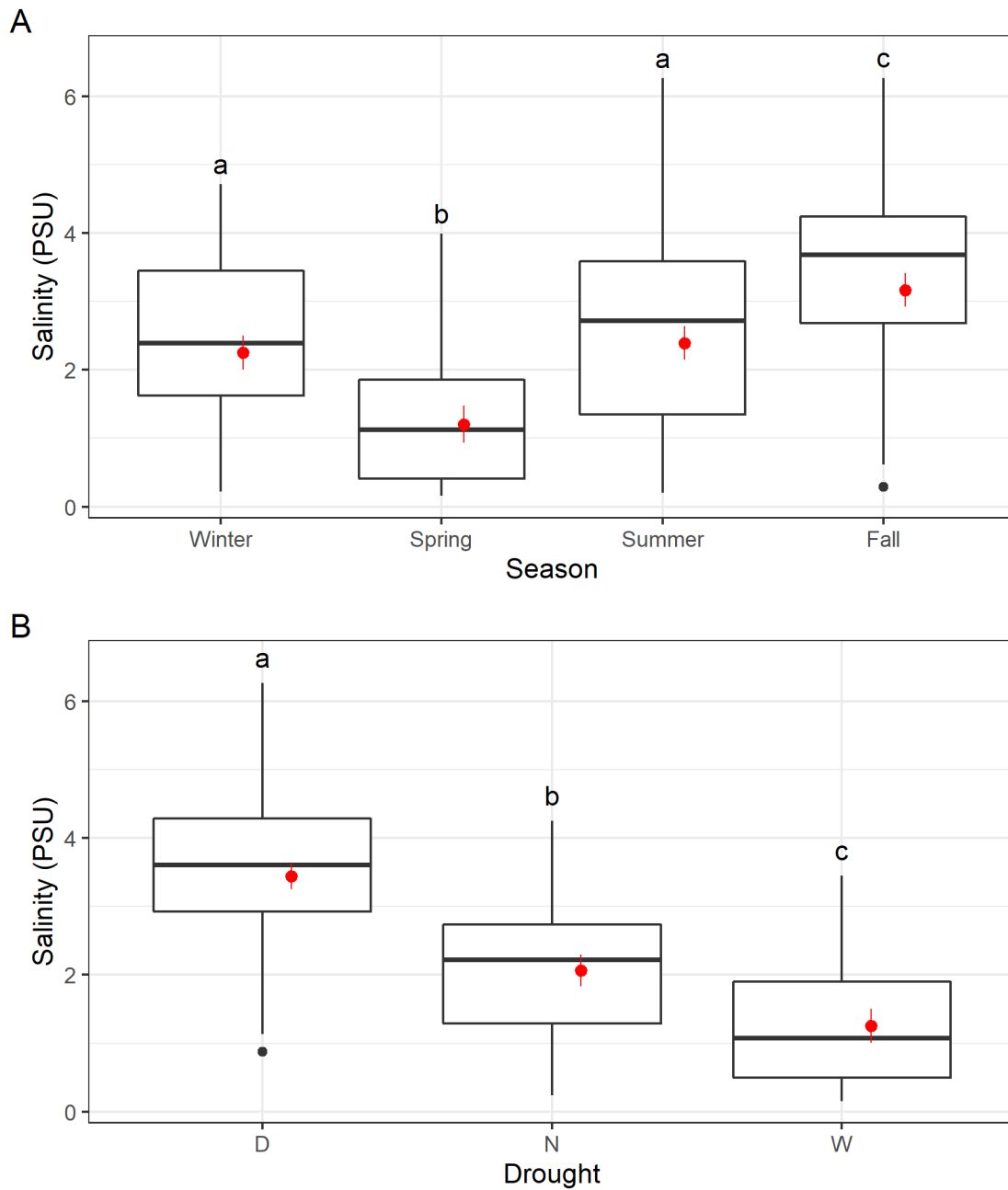


Figure 32. Observed (boxplots) and model-predicted (red points \pm 95% confidence intervals) salinities for the seasonal by Drought year classification model. Different letters above the box plots identify statistically significant ($p < 0.05$) differences from a Tukey post-hoc test.

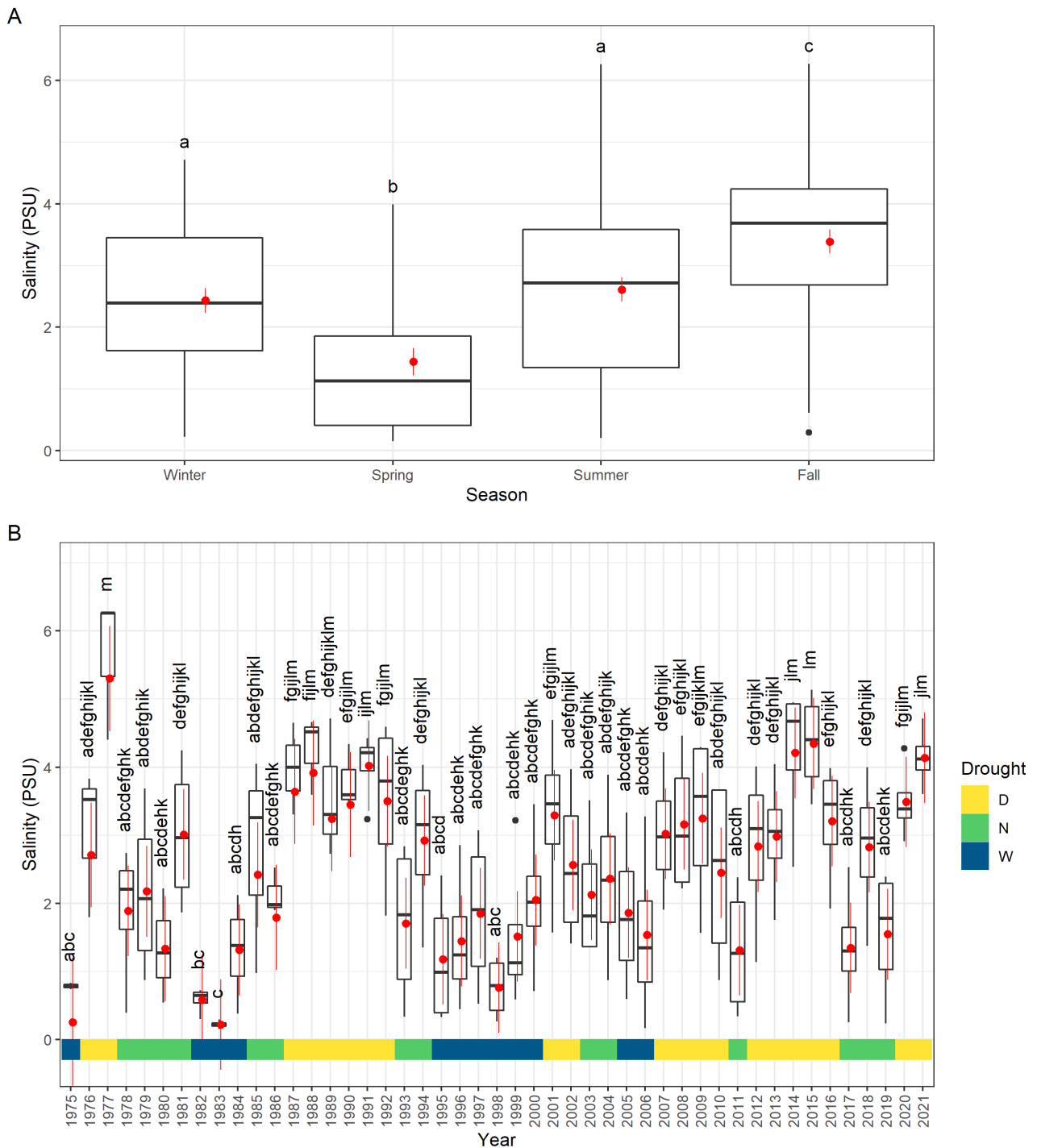


Figure 33. Observed (boxplots) and model-predicted (red points \pm 95% confidence intervals) salinities for the seasonal by year model. Different letters above the box plots identify statistically significant ($p < 0.05$) differences from a Tukey post-hoc test.

Secchi Depth

Secchi depth measurements observed in 2021 were lower than those in 2020 but higher than in a typical Drought designated year which in turn was higher than a Neutral year, and itself, in turn, higher than a typical Wet Period year (Figure 34).

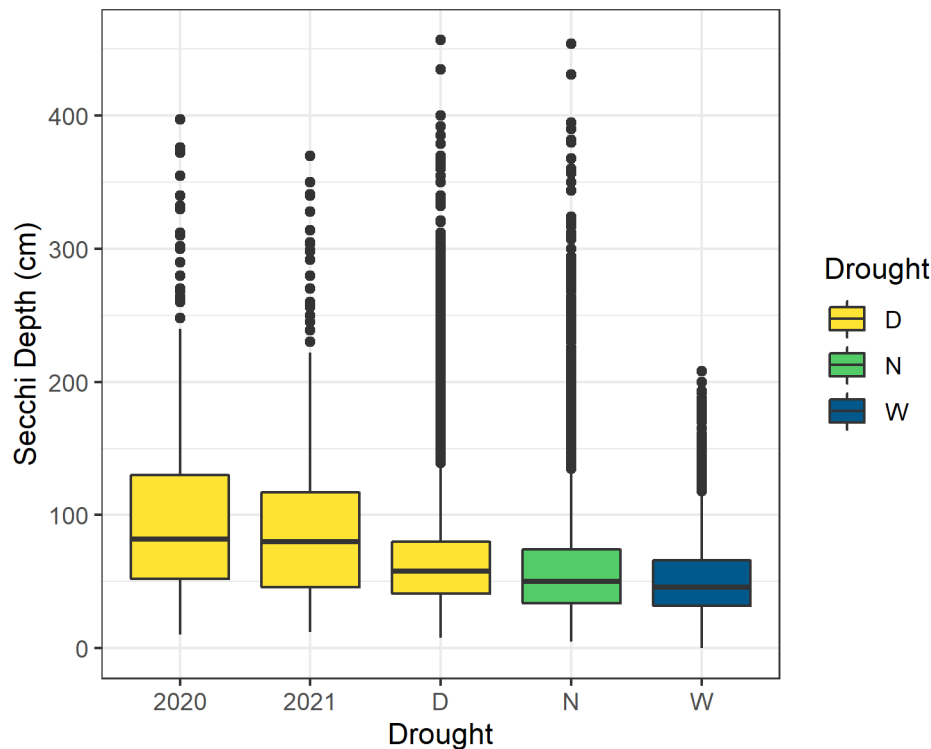


Figure 34. Boxplots of secchi depth for each Drought year classification type alongside 2020 and 2021

For each regional and seasonal model, the component factors of Drought year classification and year each had a significant effect on the secchi depth, with each having a p value < 0.001 (Table 10).

ANOVA models for regional secchi depth showed Suisun Marsh, Suisun Bay, and Confluence were each significantly different from any other region, while South Central and North were significantly higher than the three other downstream regions, but not significantly different from each other (Figure 35, Figure 36). In the regional-drought model, each year type was significantly different from one another and matched observed distributions in the collected data, namely that Drought years showed higher secchi depth

than Neutral years, which, in turn, had higher secchi than Wet Period years (Figure 35). The regional-year model showed that 2021 had higher secchi depth than many previous years, including many Drought designated years, but was not significantly different from 2020 nor from any Drought, Wet Period or Neutral year since 2006 (Figure 36).

ANOVA models for seasonal secchi depth showed that fall was significantly higher than winter, spring, and summer, and that winter, spring, and summer were not significantly different from one another (Figure 37, Figure 38). Consistent with the regional-drought model, each year type was significantly different from each other in the seasonal-drought model and matched observed distributions in the collected data, namely that Drought years showed higher secchi depth than Neutral years, which, in turn, had higher secchi than Wet Period years (Figure 37). The seasonal-year model showed that 2021 was not statistically higher than 2014, 2016, and 2018-2020, but was significantly higher than all other previous years (Figure 38).

Table 10. Summary of ANOVA outputs for models of regional and seasonal secchi depth by drought year classification and year (as a factor)

Model	Parameter	Sum Sq	Df	F value	Pr(>F)
Regional_Drought	Drought	4.6819	2	33.58393	< 0.001
Regional_Drought	Region	26.84664	4	96.2874	< 0.001
Regional_Drought	Residuals	14.84705	213		
Regional_Year	Year	13.69726	46	8.629155	< 0.001
Regional_Year	Region	29.50082	4	213.7305	< 0.001
Regional_Year	Residuals	5.831689	169		
Seasonal_Drought	Drought	4.292528	2	31.17063	< 0.001
Seasonal_Drought	Season	3.988735	3	19.30973	< 0.001
Seasonal_Drought	Residuals	11.08571	161		
Seasonal_Year	Year	60144.74	46	12.49691	< 0.001
Seasonal_Year	Season	17363.66	3	55.32009	< 0.001
Seasonal_Year	Residuals	12241.17	117		

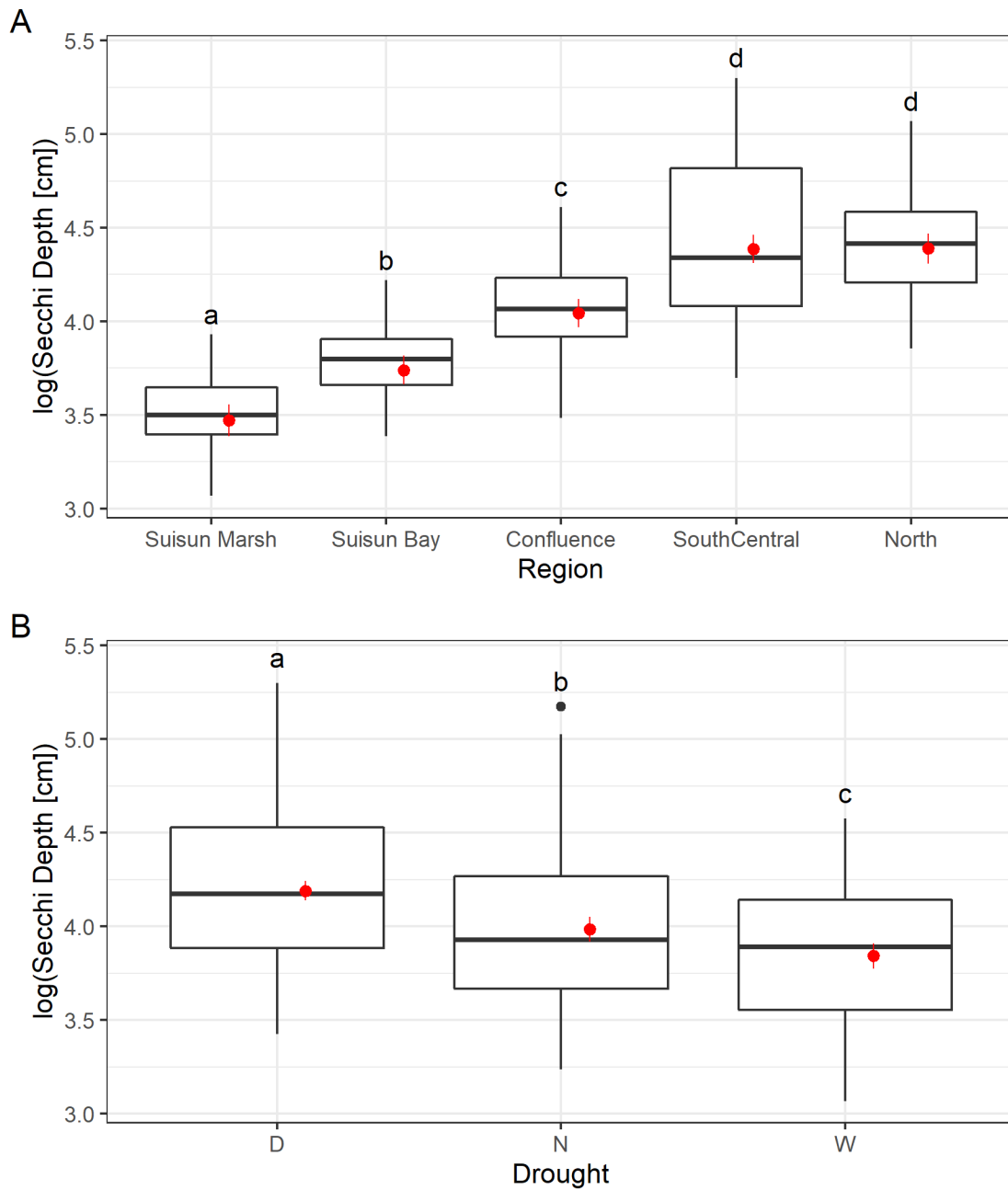


Figure 35. Observed (boxplots) and model-predicted (red points \pm 95% confidence intervals) log-transformed secchi depth for the regional by Drought year classification model. Different letters above the box plots identify statistically significant ($p < 0.05$) differences from a Tukey post-hoc test.

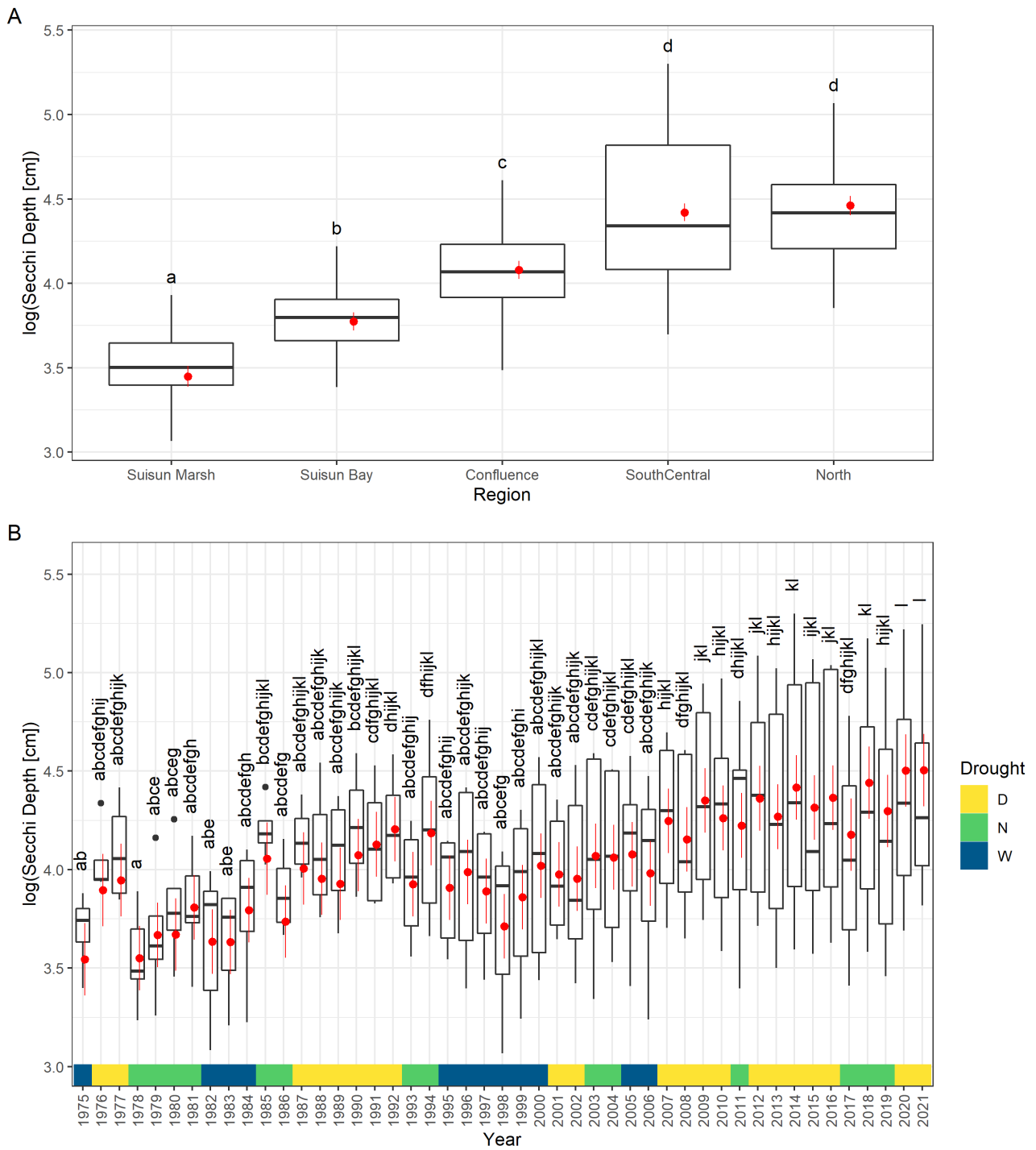


Figure 36. Observed (boxplots) and model-predicted (red points \pm 95% confidence intervals) log-transformed secchi depth for the regional by year model. Different letters above the box plots identify statistically significant ($p < 0.05$) differences from a Tukey post-hoc test.

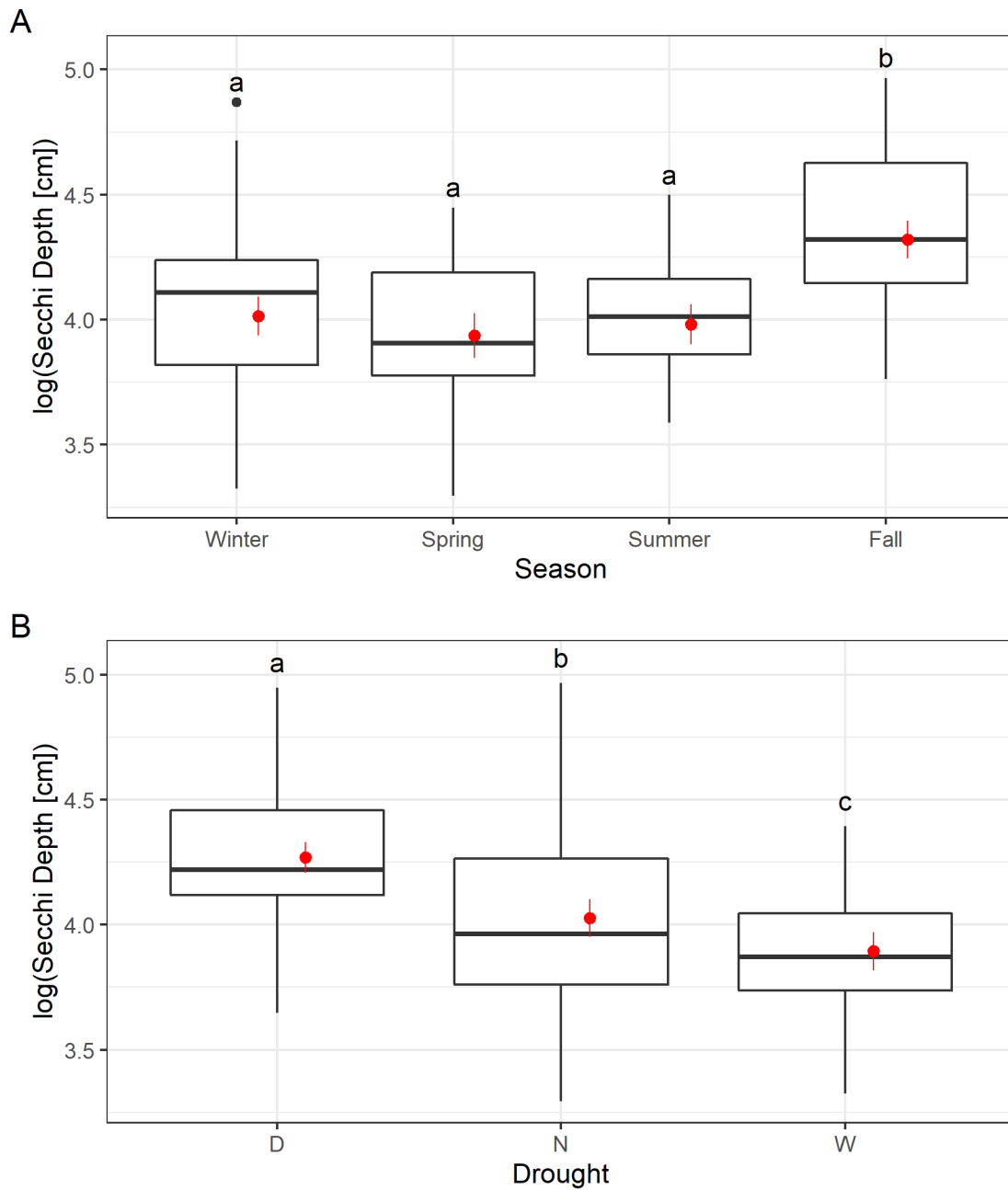


Figure 37. Observed (boxplots) and model-predicted (red points \pm 95% confidence intervals) log-transformed secchi depth for the seasonal by Drought year classification model. Different letters above the box plots identify statistically significant ($p < 0.05$) differences from a Tukey post-hoc test.

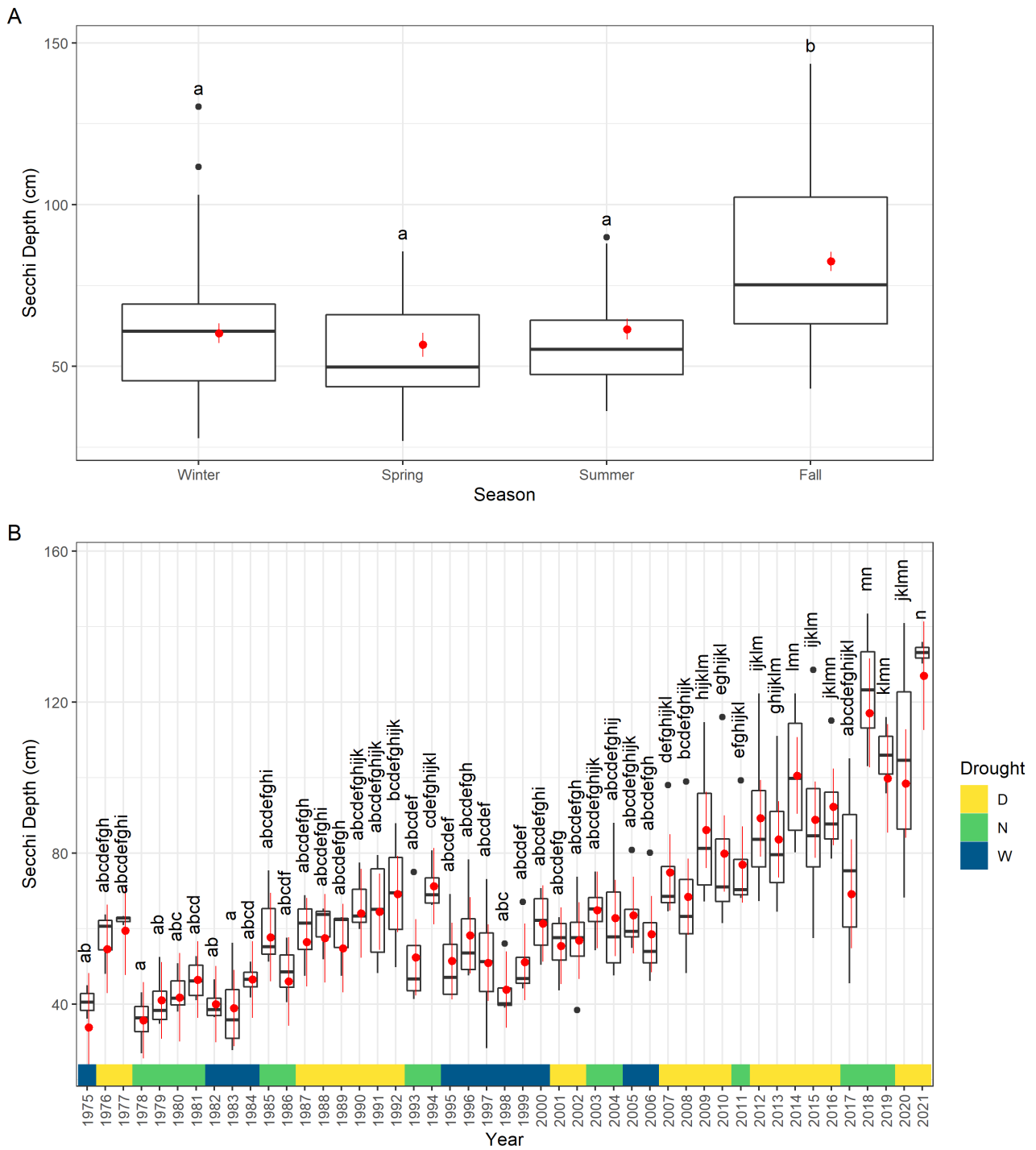


Figure 38. Observed (boxplots) and model-predicted (red points \pm 95% confidence intervals) secchi depth for the seasonal by year model. Different letters above the box plots identify statistically significant ($p < 0.05$) differences from a Tukey post-hoc test.

Dissolved Ammonia

Dissolved ammonia values were similar in 2020 and 2021 (2021 is only through September). However, maximum values in 2021 were lower than both 2020 and other critical (water year type) and Drought (drought year classification) years (Figure 39, Figure 40). Generally, dissolved ammonia values did not visually differ between year types or drought year classifications, so the lower maximum 2021 values are notable.

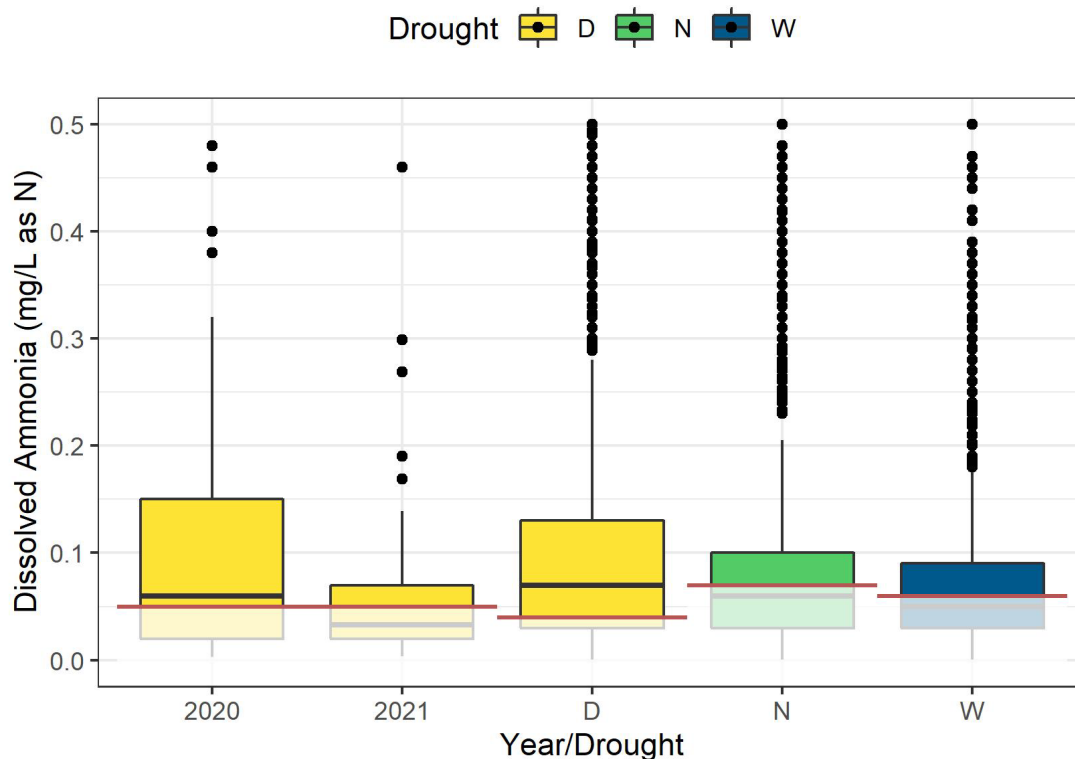


Figure 39. Boxplots of dissolved ammonia for each Drought year classification (Drought period [D], Neutral [N], and Wet period [W]) value with 2020 and 2021 shown separately from other Dry values. Data plotted prior to simulations. Red lines represent the highest reporting limit of censored data. Y-axis was cut off at 0.5 so boxplots were more visible; no outliers for 2020 and 2021 were above this value.

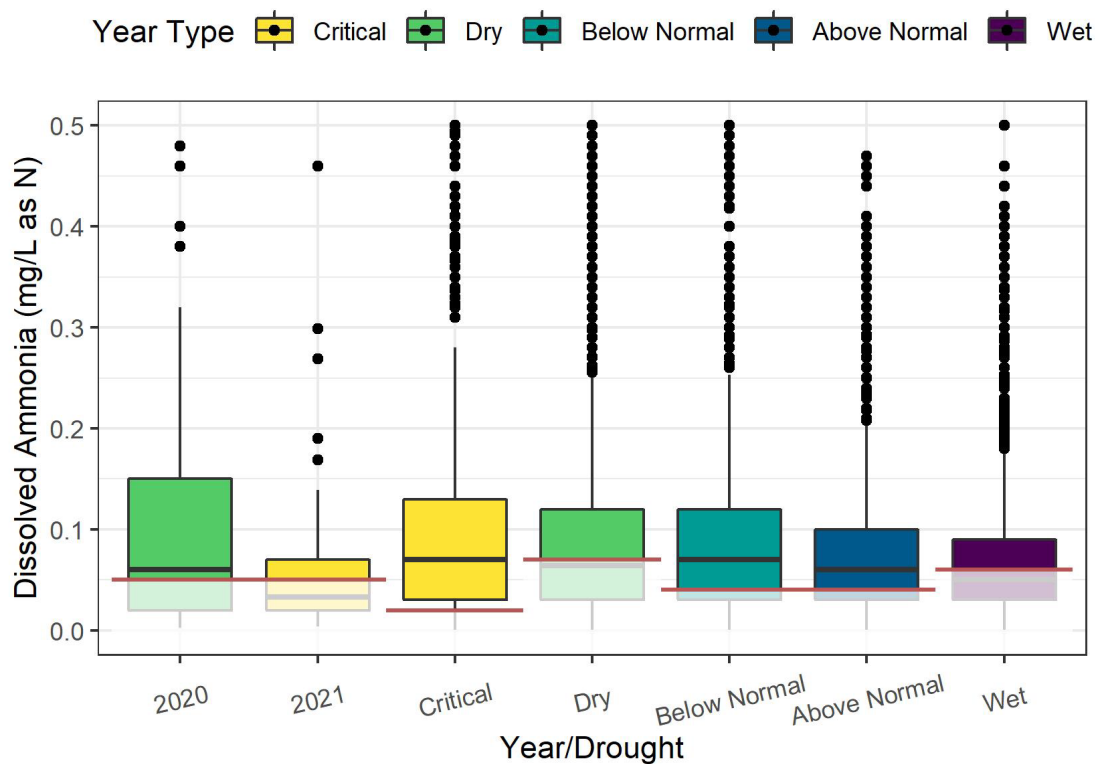


Figure 40. Boxplots of dissolved ammonia for each Year Type value with 2020 and 2021 shown separately from other Dry values. Red lines represent the highest reporting limit of censored data. Y-axis was cut off at 0.5 so boxplots were more visible; no outliers for 2020 and 2021 were above this value.

In the seasonal ANOVAs, neither Drought year classification nor Year significantly impacted log-transformed dissolved ammonia values ($p > 0.05$) (Table 11). Season was significant in both ANOVAs, with Winter and Fall having the highest values (Figure 41).

In the regional ANOVAs, Drought year classification significantly impacted log-transformed dissolved ammonia values, with Drought values being higher than Wet Periods (Figure 42), while Year did not (Table 11). Region was significant in the short-term (2013 – present) model, with South-Central being significantly lower than the other three regions.

Table 11. ANOVA results for dissolved ammonia. Four ANOVAs were run, with one explanatory variable being either season or region and the other drought year classification or year.

Model	Parameter	Sum Sq	Df	F value	Pr(>F)
Seasonal_Drought	Drought	0.082	2	2.709	0.070
Seasonal_Drought	Season	2.819	3	62.272	< 0.001
Seasonal_Drought	Residuals	2.444	162		
Seasonal_Year	Year	0.390	8	2.0347	0.085
Seasonal_Year	Season	0.687	3	9.569	< 0.001
Seasonal_Year	Residuals	0.575	24		
Regional_Drought	Drought	0.1306	2	3.710	0.027
Regional_Drought	Region	0.0573	3	1.086	0.357
Regional_Drought	Residuals	2.727	155		
Regional_Year	Year	0.272	8	2.049	0.083
Regional_Year	Region	0.858	3	17.22	< 0.001
Regional_Year	Residuals	0.399	24		

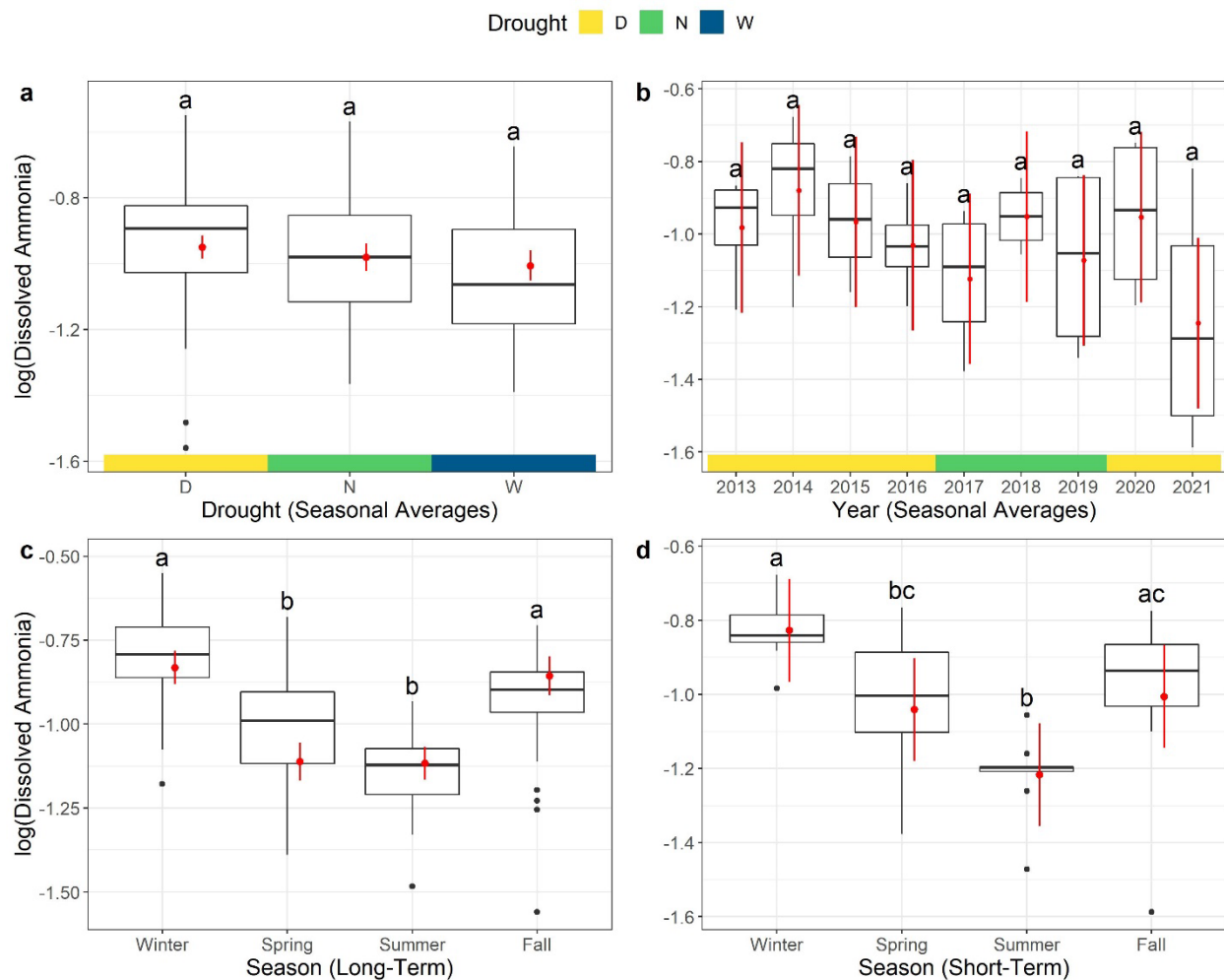


Figure 41. Boxplots of observed log-transformed dissolved ammonia (mg/L as N) values by (a) drought year classification (Drought period [D], Neutral [N], and Wet period [W]) (b) year type (c) season (long-term dataset) and (d) season (short-term dataset). Model-predicted values using seasonal averages with 95% confidence intervals are displayed as red points. Values below reporting limits were estimated via simulation. Letters represent different groups based on pairwise comparisons.

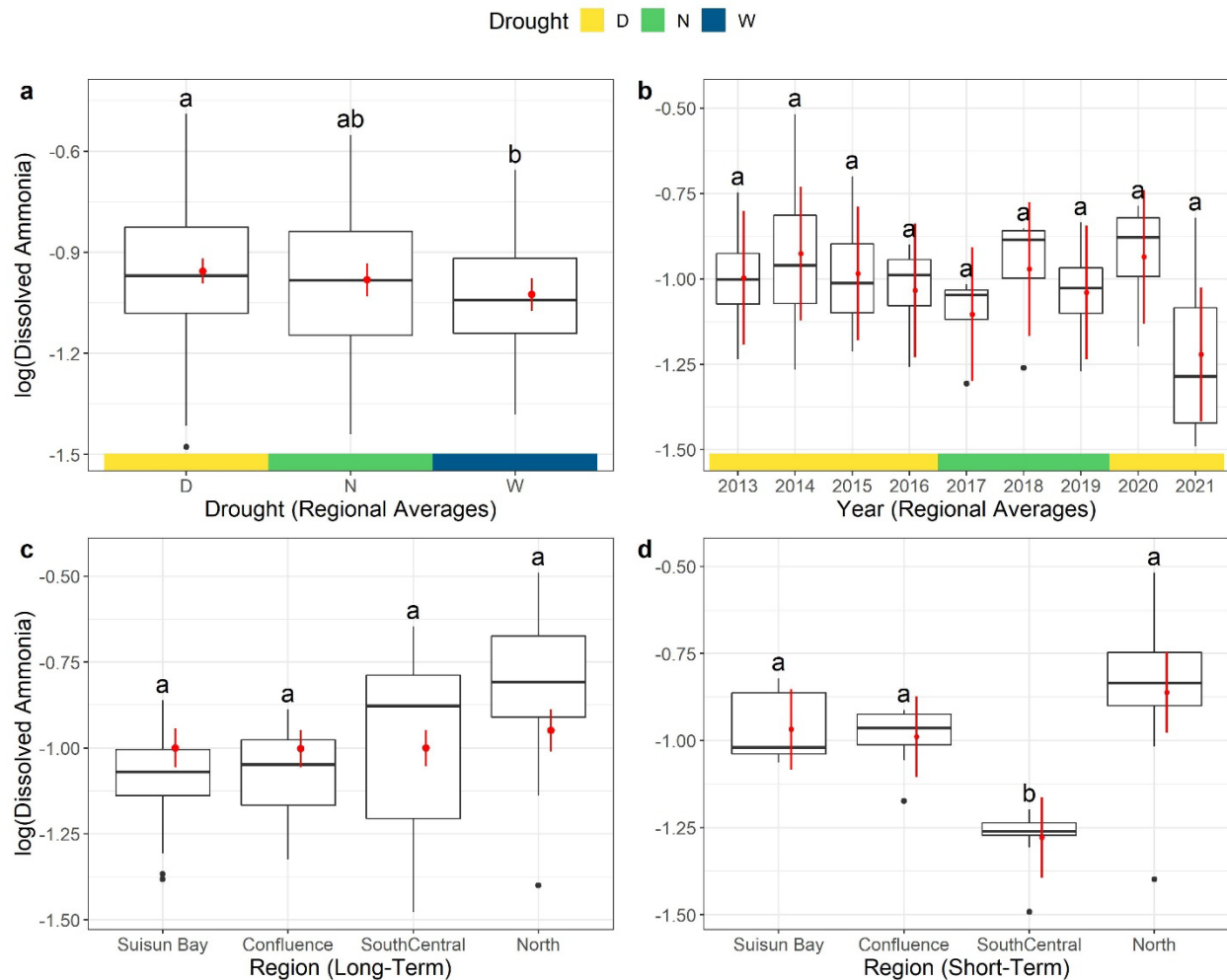


Figure 42. Boxplots of observed log-transformed dissolved ammonia (mg/L as N) values by (a) drought year classification (Drought period [D], Neutral [N], and Wet period [W]) (b) year type (c) region (long-term dataset) and (d) region (short-term dataset). Model-predicted values using regional averages with 95% confidence intervals are displayed as red points. Values below reporting limits were estimated via simulation. Letters represent different groups based on pairwise comparisons.

Dissolved Nitrate Nitrite

Dissolved nitrate nitrite values were similar in 2020 and 2021 (2021 is only through September), with the median of the 2021 values being slightly lower (Figure 43, Figure 44). 2021 values were also lower than other critical and dry years, though only slightly.

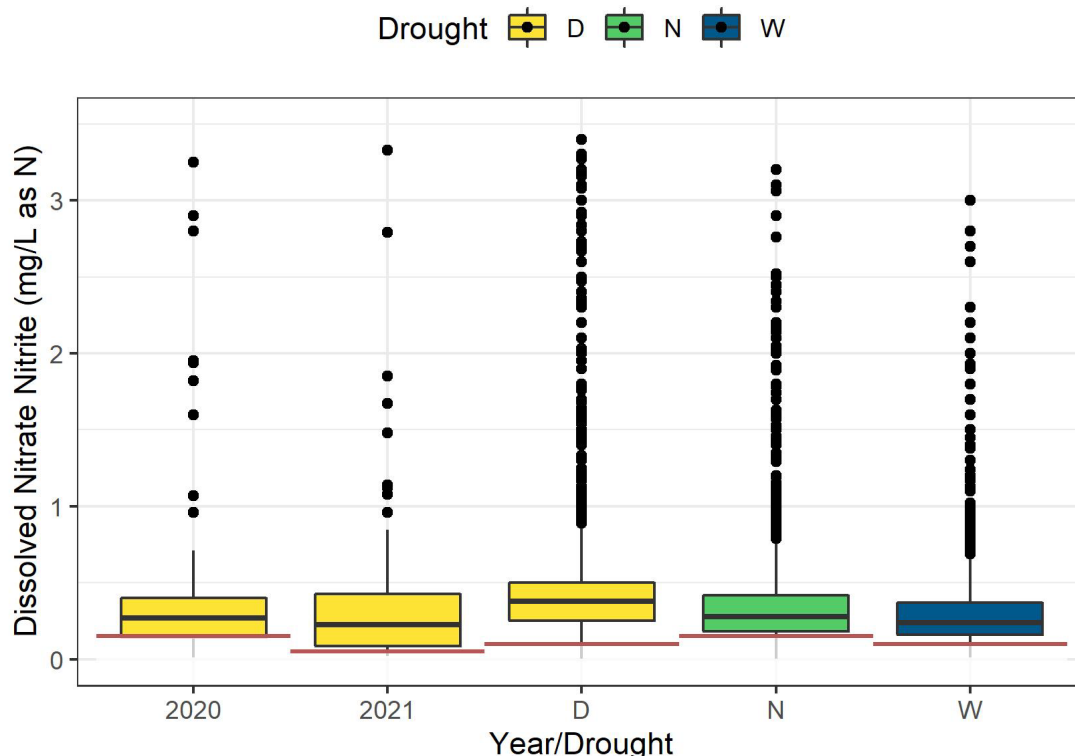


Figure 43. Boxplots of dissolved nitrate nitrite for each Drought year classification (Drought period [D], Neutral [N], and Wet period [W]) value with 2020 and 2021 shown separately from other Dry values. Red lines represent the highest reporting limit of censored data. Y-axis was cut off at 3.5 so boxplots were more visible; no outliers for 2020 and 2021 were above this value.

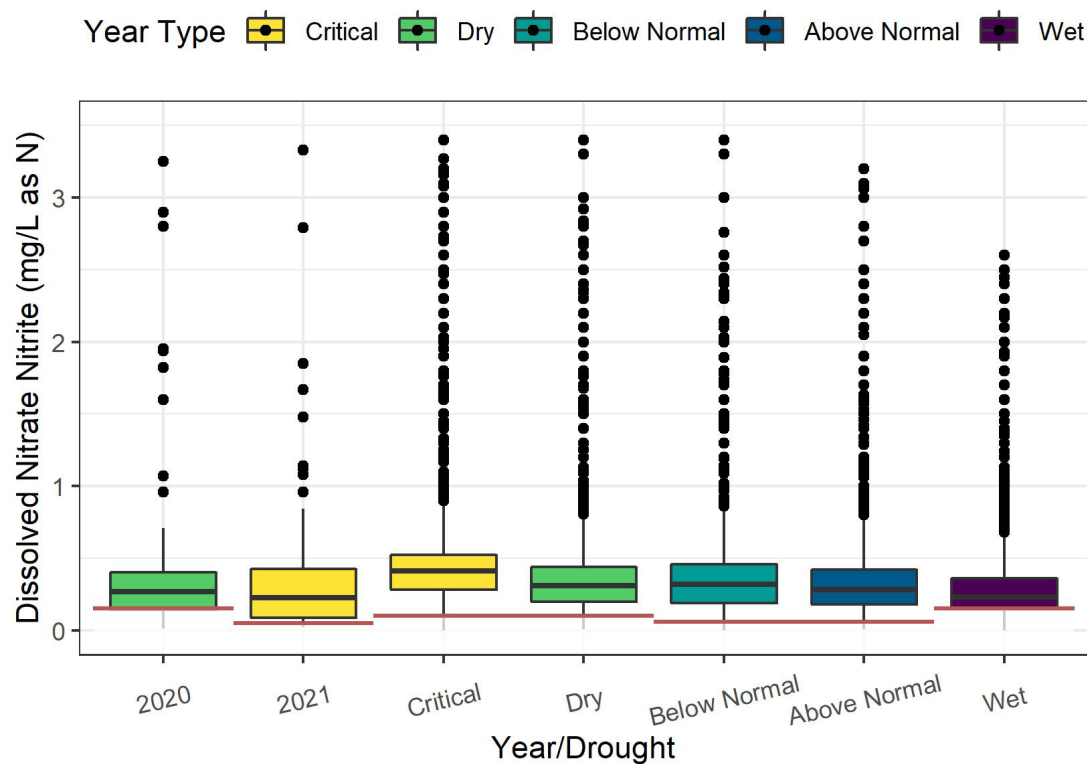


Figure 44. Boxplots of dissolved nitrate nitrite for each Year Type value with 2020 and 2021 shown separately from other Dry values. Red lines represent the highest reporting limit of censored data. Y-axis was cut off at 3.5 so boxplots were more visible; no outliers for 2020 and 2021 were above this value.

In the seasonal ANOVAs, both Drought year classification and Year significantly impacted log-transformed dissolved nitrate nitrite values (Table 12). Post-hoc estimated marginal means (EMM) tests revealed a significant difference ($p < 0.05$) between dry and neutral/wet years according to the Drought year classification, with dry year values being greater than wet and neutral (Figure 45). Both 2020 and 2021 were similar to multiple other dry and some neutral years. Season was significant in both ANOVAs with Winter having the highest values.

In the regional ANOVAs, both Drought year classification and Year significantly impacted log-transformed dissolved nitrate nitrite values (Table 12). Similar to the seasonal ANOVAs, EMM tests indicated a significant difference between dry and neutral/wet years with dry year values being the highest (Figure 46). 2021 was similar to 2017 and 2019, but not to previous

(2013-2016) dry years, while 2020 was similar to all years 2016-2021. Region was significant in both ANOVAs, with Confluence and Suisun Bay having no significant difference from each other and North and South Central being significantly different than other regions (Figure 46).

Table 12. ANOVA results for dissolved nitrate nitrite. Four ANOVAs were run, with one explanatory variable being either season or region and the other drought year classification or year.

Model	Parameter	Sum Sq	Df	F value	Pr(>F)
Seasonal_Drought	Drought	0.162	2	10.873	< 0.001
Seasonal_Drought	Season	1.551	3	69.612	< 0.001
Seasonal_Drought	Residuals	1.293	174		
Seasonal_Year	Year	0.193	8	2.906	0.025
Seasonal_Year	Season	0.104	3	4.167	0.019
Seasonal_Year	Residuals	0.165	20		
Regional_Drought	Drought	0.307	2	23.630	< 0.001
Regional_Drought	Region	0.692	3	35.442	< 0.001
Regional_Drought	Residuals	1.132	174		
Regional_Year	Year	0.314	8	32.223	< 0.001
Regional_Year	Region	1.118	3	305.491	< 0.001
Regional_Year	Residuals	0.0293	24		

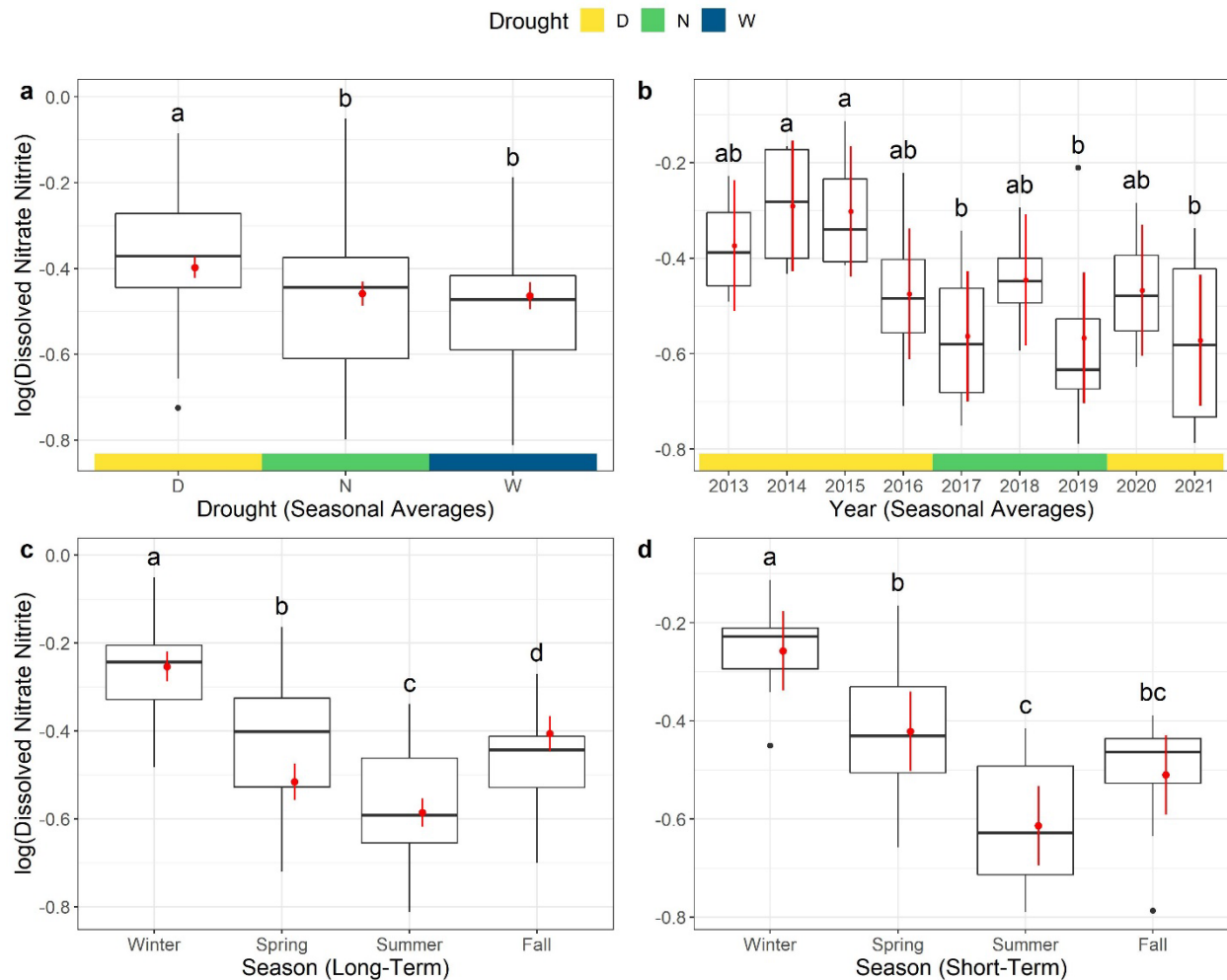


Figure 45. Boxplots of observed log-transformed dissolved nitrate nitrite (mg/L as N) values by (a) drought year classification (b) year type (c) season (long-term dataset) and (d) season (short-term dataset). Model-predicted values using seasonal averages with 95% confidence intervals are displayed as red points. Letters represent different groups based on pairwise comparisons.

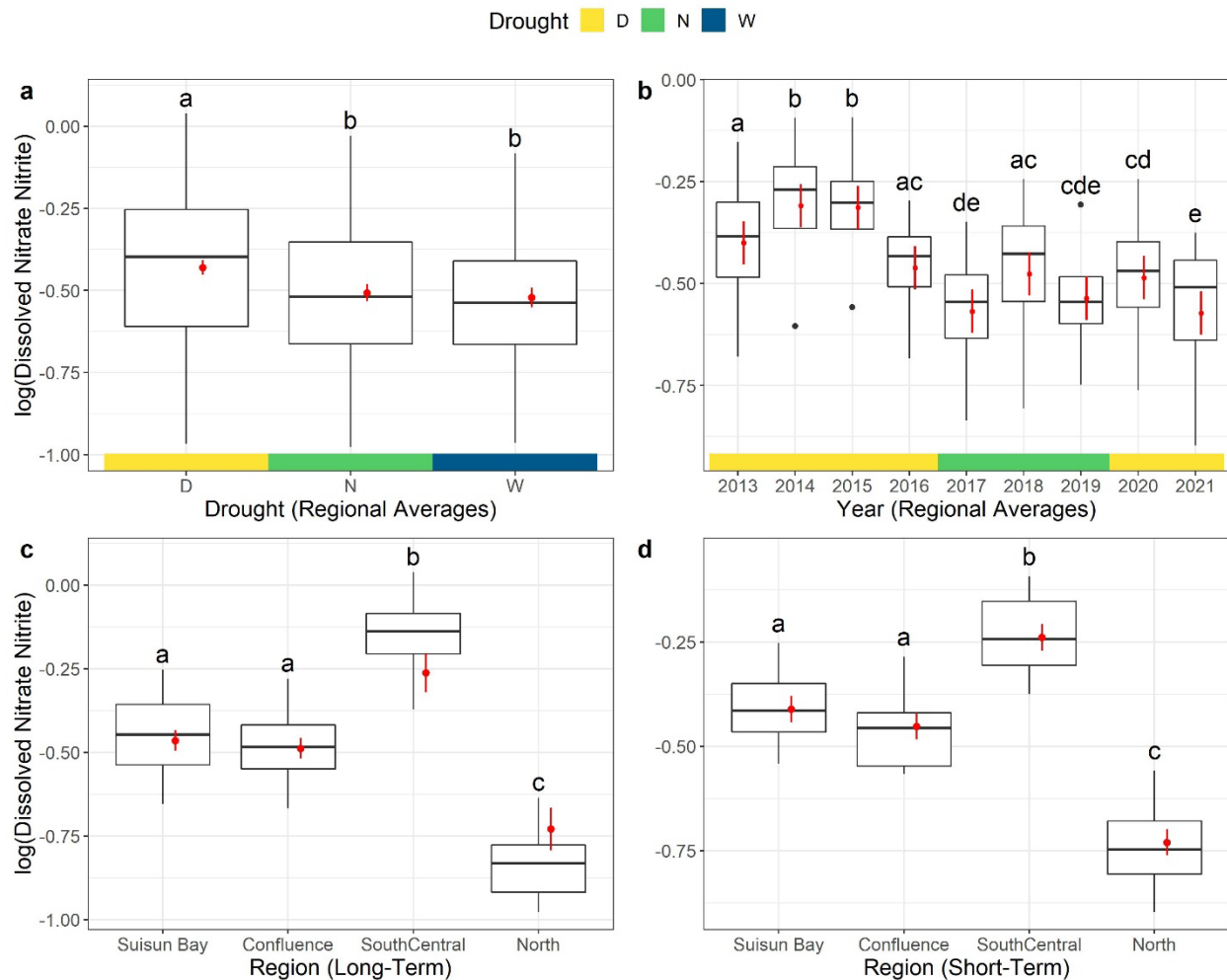


Figure 46. Boxplots of observed log-transformed dissolved nitrate nitrite (mg/L as N) values by (a) drought year classification (b) year type (c) region (long-term dataset) and (d) region (short-term dataset). Model-predicted values using regional averages with 95% confidence intervals are displayed as red points. Values below reporting limits were estimated via simulation. Letters represent different groups based on pairwise comparisons.

Dissolved Orthophosphate

Dissolved orthophosphate values were similar in 2020 and 2021 (2021 is only through September), with 2021 values being slightly higher (Figure 47, Figure 48). 2021 values were on par with other dry and critical years.

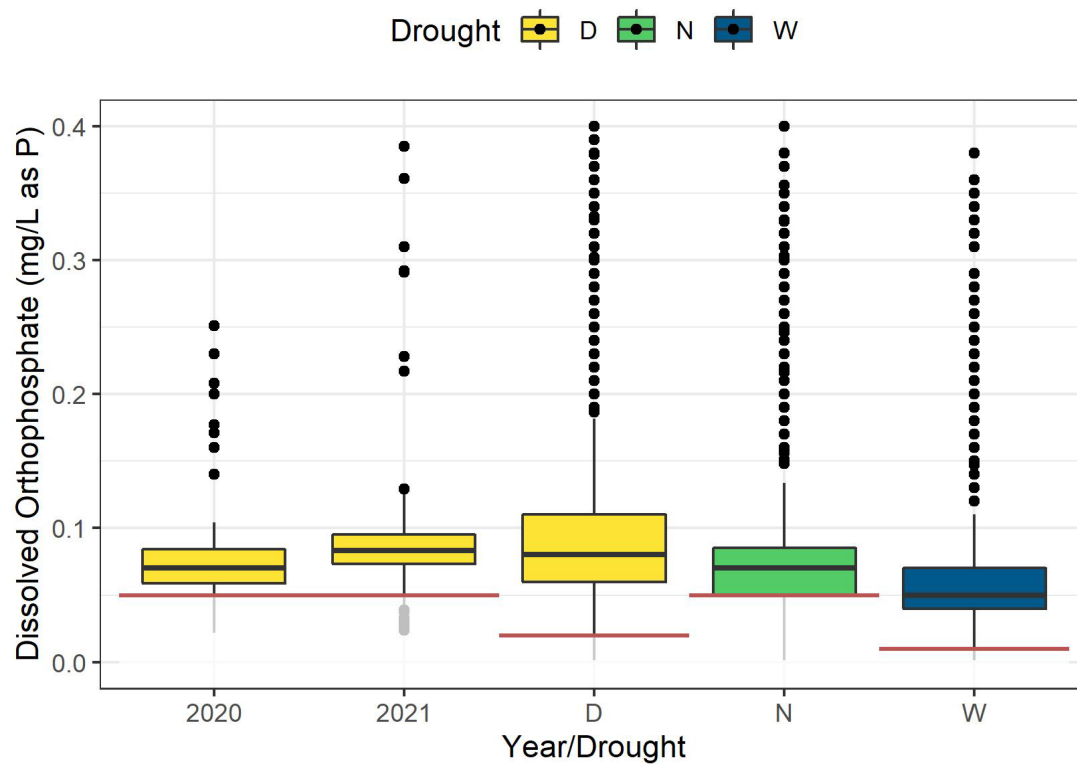


Figure 47. Boxplots of dissolved orthophosphate for each Drought year classification value with 2020 and 2021 shown separately from other Dry values. Red lines represent the highest reporting limit of censored data. Y-axis was cut off at 0.4 so boxplots were more visible; no outliers for 2020 and 2021 were above this value.

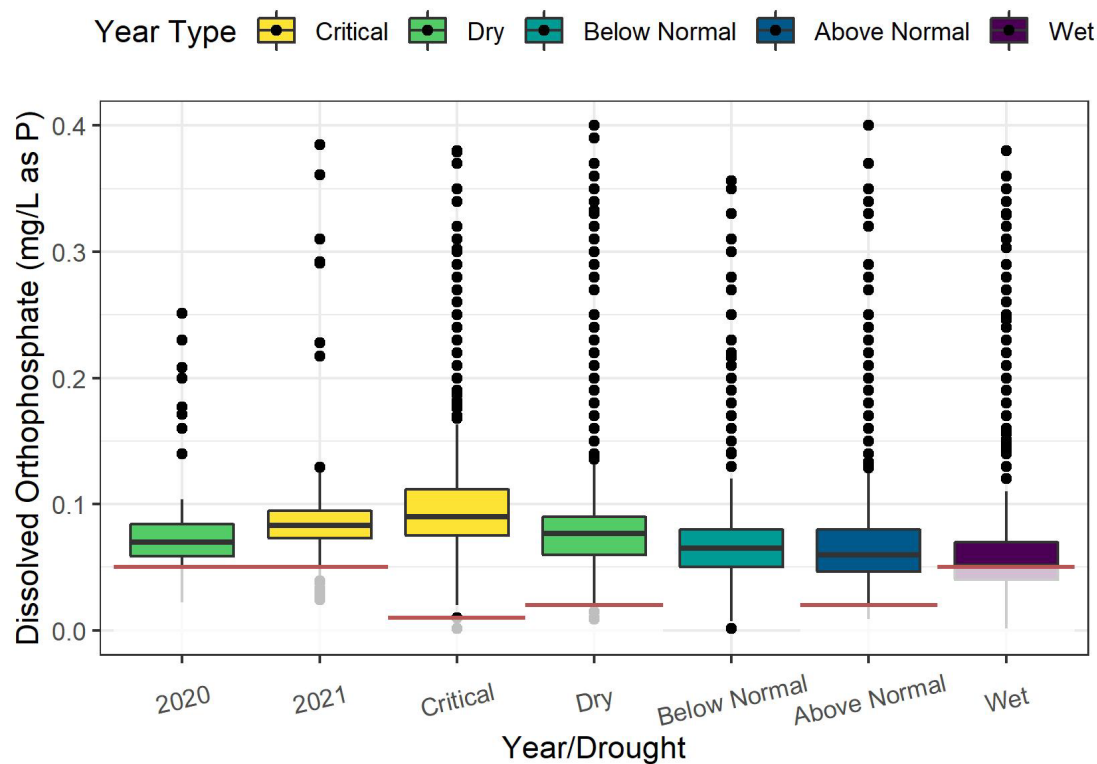


Figure 48. Boxplots of dissolved orthophosphate for each Year Type value with 2020 and 2021 shown separately from other Dry values. Red lines represent the highest reporting limit of censored data. Y-axis was cut off at 0.4 so boxplots were more visible; no outliers for 2020 and 2021 were above this value.

In the seasonal ANOVAs, Drought year classification and Year both significantly impacted log-transformed dissolved orthophosphate values (Table 13). Post-hoc EMM tests revealed a significant difference ($p < 0.05$) between dry and wet years, with dry years having higher values (Figure 49). Season was significant in both ANOVAs, with Spring having significantly lower values than other seasons in the long-term model.

In the regional ANOVAs, both Drought year classification and Year significantly impacted log-transformed dissolved orthophosphate values (Table 13). EMM tests indicated a significant difference between all Drought year classification types with dry years having the highest values and wet years the lowest (Figure 50). 2021 was not significantly different from any year, while 2020 was similar to all years except for 2015. Region was significant in both ANOVAs, with South Central having the highest values.

Table 13. ANOVA results for dissolved orthophosphate. Four ANOVAs were run, with one explanatory variable being either season or region and the other drought year classification or year. Df = degrees of freedom.

Model	Parameter	Sum Sq	Df	F value	Pr(>F)
Seasonal_Drought	Drought	0.110	2	9.590	< 0.001
Seasonal_Drought	Season	0.430	3	24.984	< 0.001
Seasonal_Drought	Residuals	1.022	178		
Seasonal_Year	Year	0.099	8	4.970	0.001
Seasonal_Year	Season	0.043	3	5.730	0.004
Seasonal_Year	Residuals	0.060	24		
Regional_Drought	Drought	0.385	2	25.944	< 0.001
Regional_Drought	Region	0.234	3	10.573	< 0.001
Regional_Drought	Residuals	1.309	176		
Regional_Year	Year	0.096	8	8.969	< 0.001
Regional_Year	Region	0.124	3	30.937	< 0.001
Regional_Year	Residuals	0.032	24		

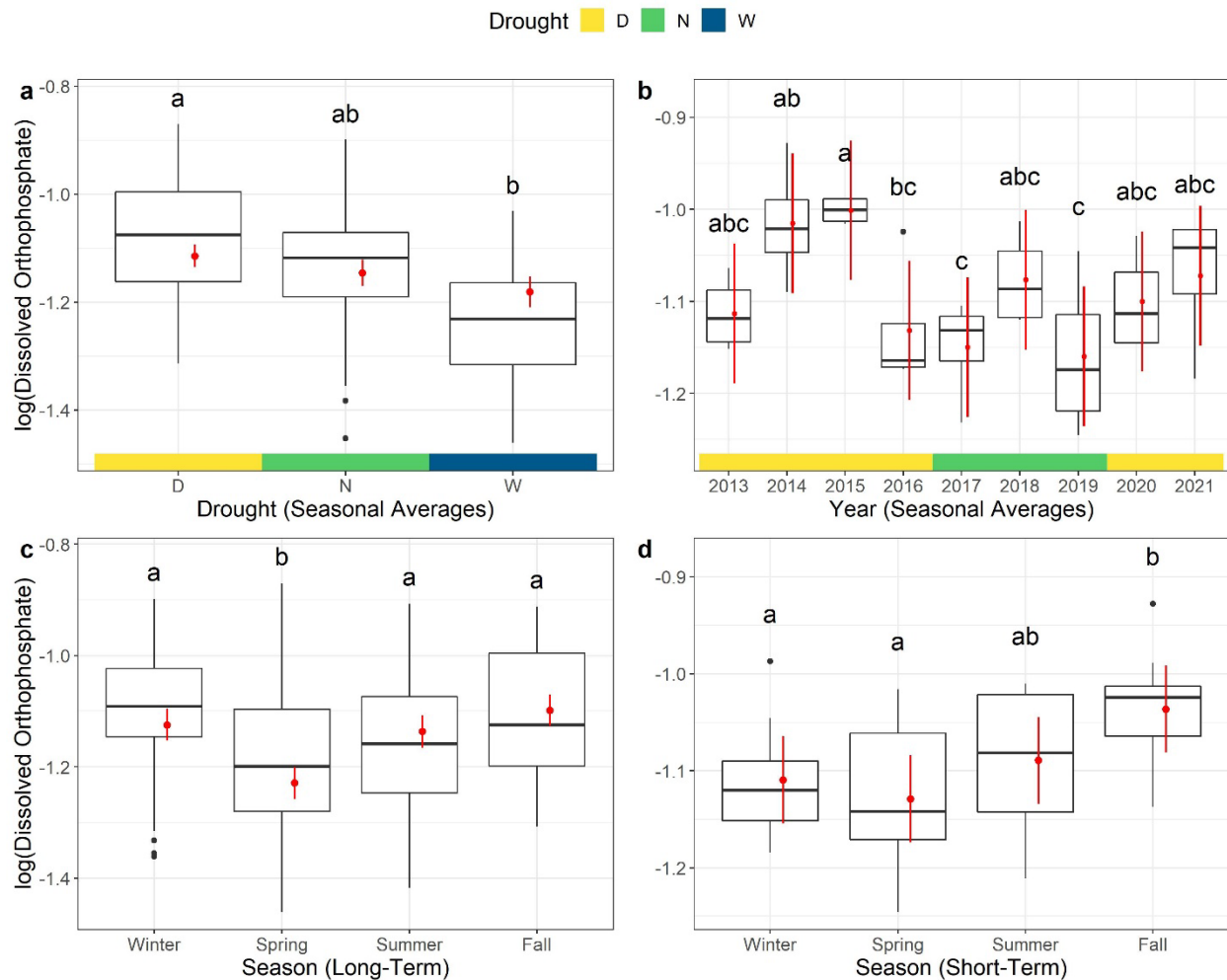


Figure 49. Boxplots of observed log-transformed dissolved orthophosphate values (mg/L as P) by (a) drought year classification (b) year type (c) season (long-term dataset) and (d) season (short-term dataset). Model-predicted values using seasonal averages with 95% confidence intervals are displayed as red points. Letters represent different groups based on pairwise comparisons.

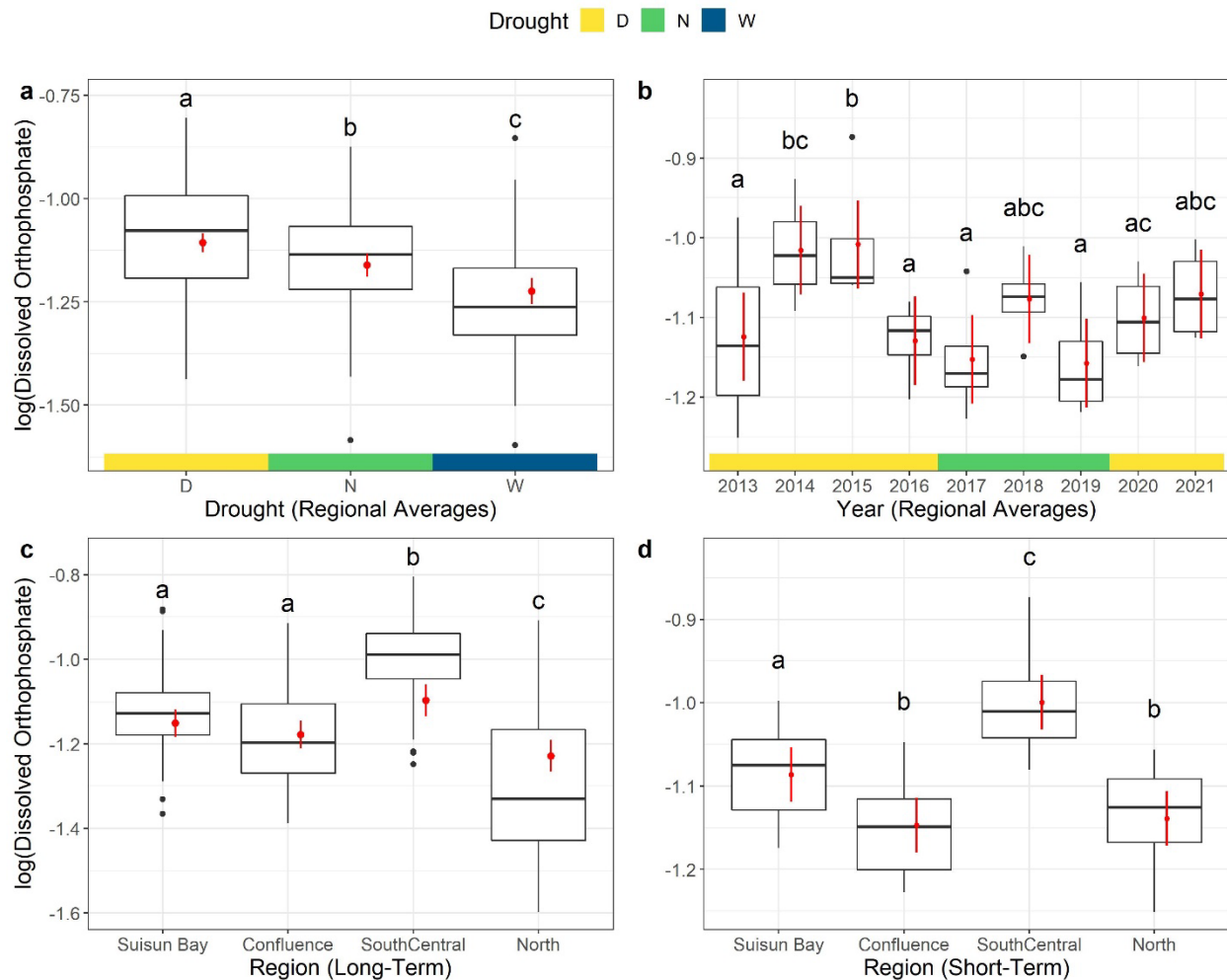


Figure 50. Boxplots of observed log-transformed dissolved orthophosphate (mg/L as P) values by (a) drought year classification (b) year type (c) region (long-term dataset) and (d) region (short-term dataset). Model-predicted values using regional averages with 95% confidence intervals are displayed as red points. Letters represent different groups based on pairwise comparisons.

Dissolved Oxygen

Since approximately 2013, high-frequency (15-minute) dissolved oxygen (DO) measurements were made at selected USGS continuous monitoring stations in the system (USGS 2016). The DO timeseries measured on the lower Sacramento River and the Toe Drain represent seasonal and annual patterns inherent to ecosystem metabolism in two distinct channel reaches

(Figure 51). Generally, the smaller and more landward reach (TOE) exhibits a greater range of concentrations with a lower mean concentration relative to the seaward (DEC) location.

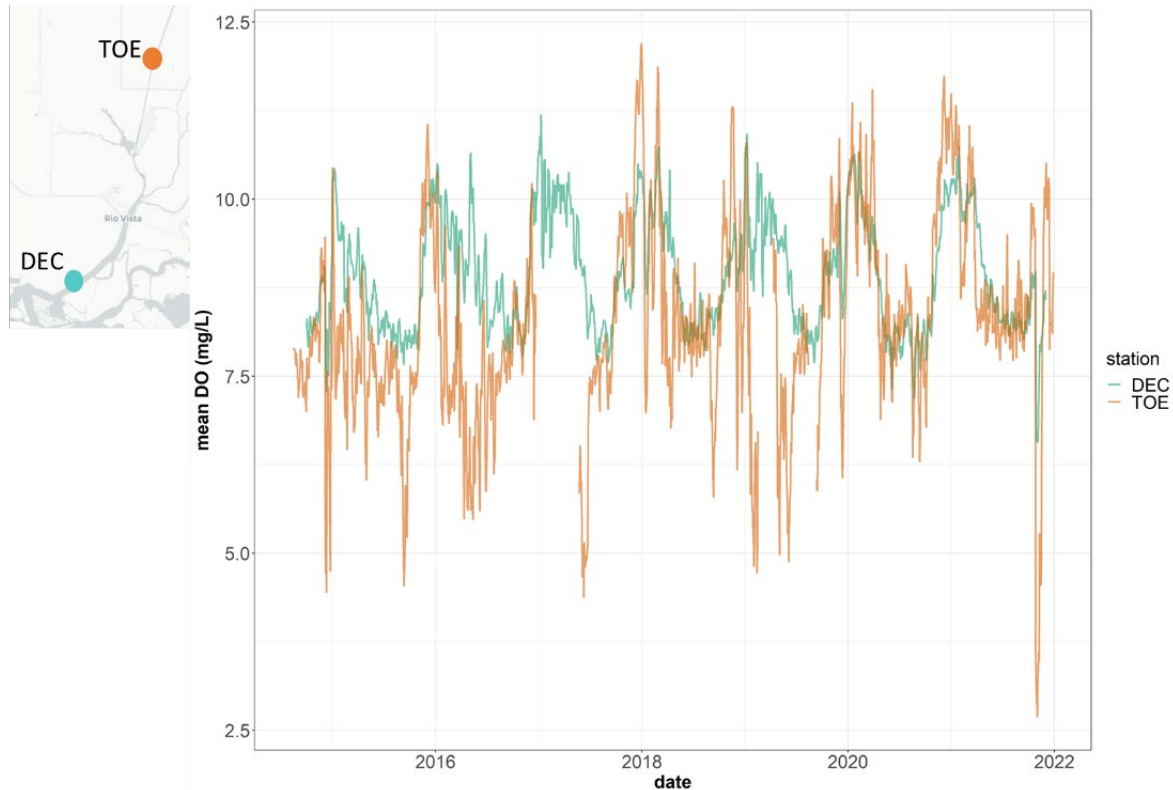


Figure 51. Dissolved Oxygen timeseries at stations representing the lower Sacramento River (DEC; USGS stations 11455478 and 11455485, teal) and the Toe Drain (TOE; USGS stations 11455139 and 11455140, orange). Inset map of station locations.

The DO timeseries at both reaches by water year identify periodic decreases in concentrations. The variation of DO between water years appears more distinct in the Toe Drain relative to the lower Sacramento station (Figure 52 and Figure 53). The DO declines in both reaches at the start of water year 2022 – represented by Year 2021 in the analyses of this report - represent the lowest concentrations in the short-term record.



Figure 52. Toe Drain dissolved oxygen timeseries across water years (2014 – present).

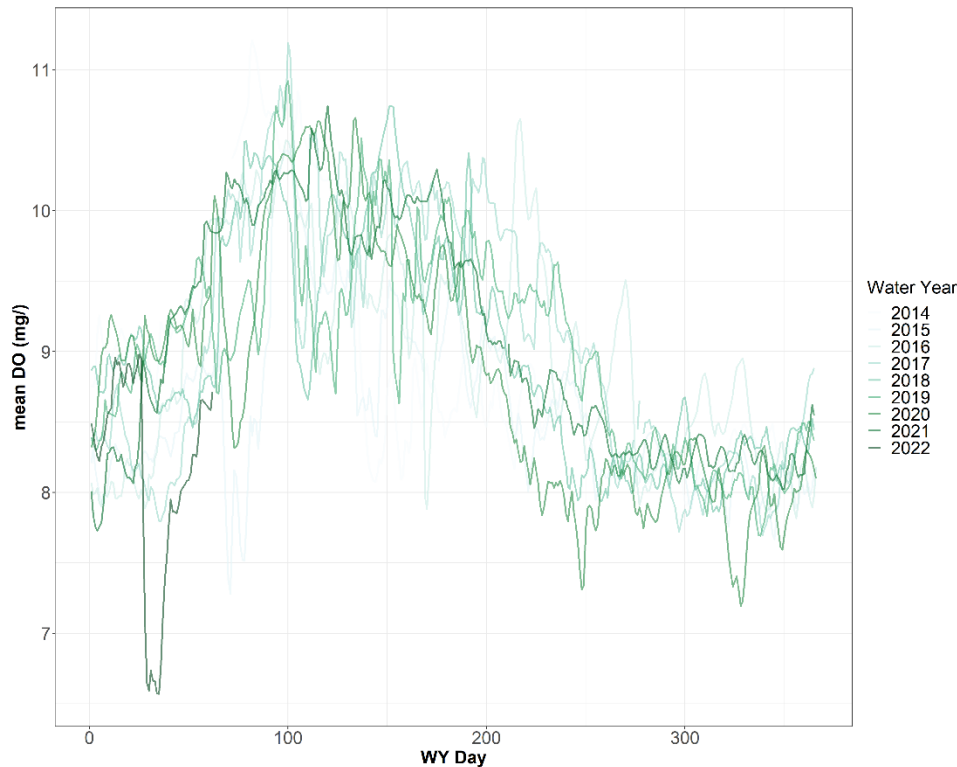


Figure 53. Lower Sacramento River timeseries across water years (2014 – present)

Chlorophyll-a

Short-term analysis

The log-average (i.e. geometric mean) chlorophyll-*a* concentration was commonly between 1 and 10 $\mu\text{g/L}$ among regions for all water year types between 2011 and 2021 (Figure 54). Concentrations were not significantly different among regions within the ANOVA model ($p < 0.05$, Table 14a). However, concentrations did differ among drought year classifications ($p < 0.01$, Table 14a and Figure 55). Pairwise comparisons indicated the highest chlorophyll-*a* concentration occurred in Neutral years compared with Wet and Drought years (Table 14b). Interestingly, chlorophyll-*a* concentration in Wet years was not significantly different from that in Drought years ($p > 0.05$).

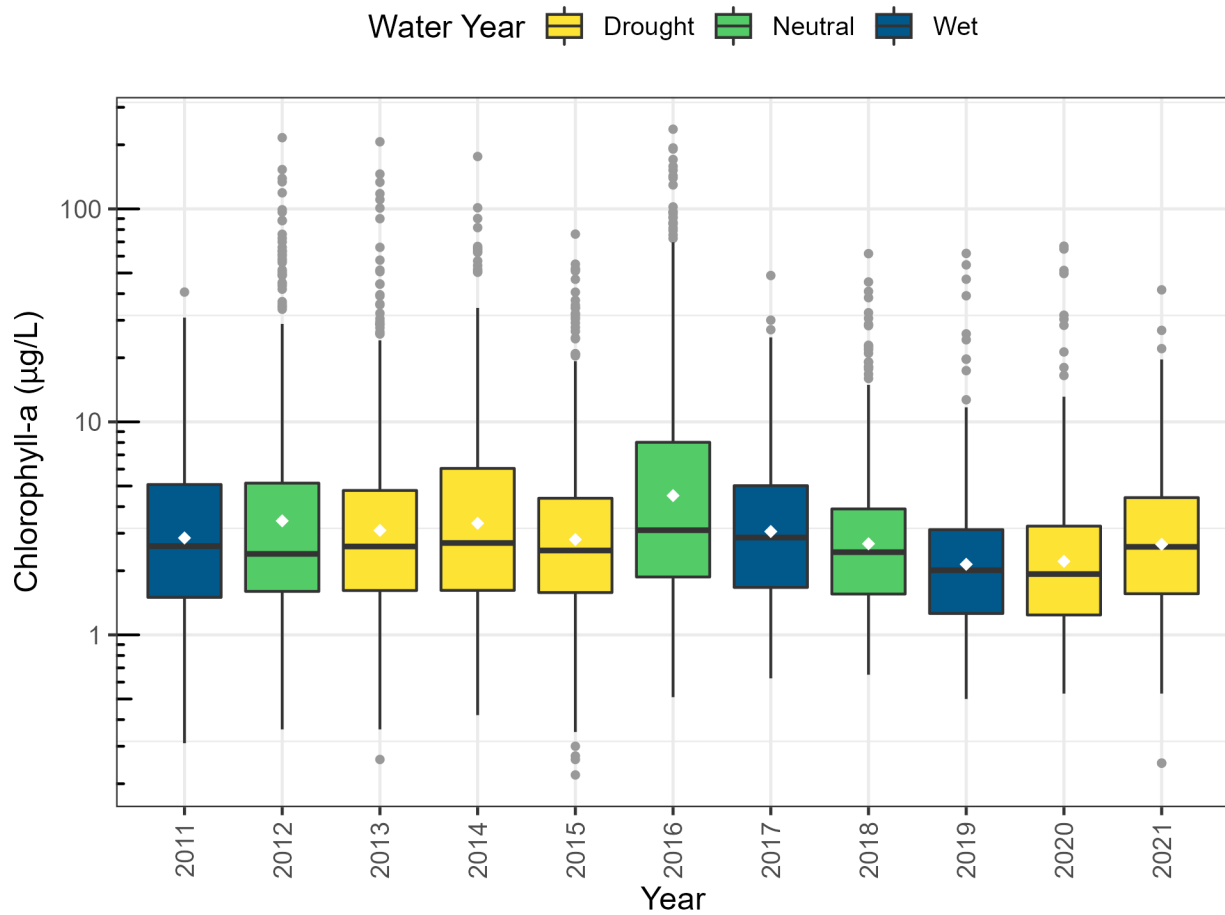


Figure 54. Boxplots showing the log-average (white diamond), median (bar), interquartile range between the 25th and 75th percentile (box), 1.5 times the interquartile range (whiskers), and outliers (points) of chlorophyll-a concentration for each year between 2011 – 2021. Y-axis scaled by log₁₀.

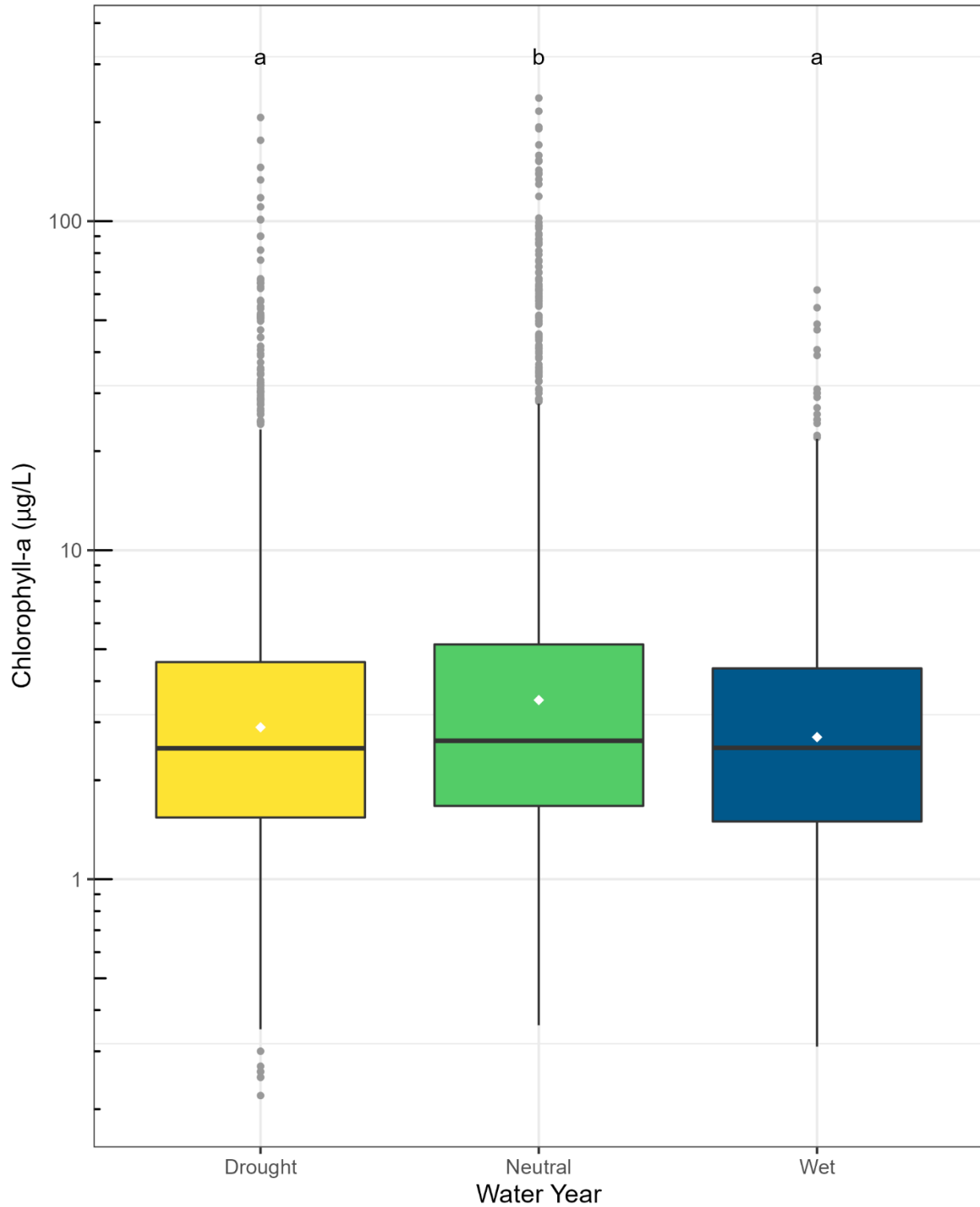


Figure 55 Boxplots showing the log-average (white diamond), median (bar), interquartile range between the 25th and 75th percentile (box), 1.5 times the

interquartile range (whiskers), and outliers (points) of chlorophyll-*a* concentration for wet, neutral, and drought year classifications during 2011 – 2021. Different letters above boxplots represents significant differences in marginal means at the 0.05 significance level. Y-axis scaled by \log_{10}

Chlorophyll-*a* concentration differed among drought year classifications for all seasons ($p < 0.05$, Figure 56). Pairwise comparisons indicated chlorophyll-*a* concentration also differed between some water years for a given season ($p < 0.05$, Figure 57, non-overlapping red arrows). However, chlorophyll-*a* concentration did not differ between wet and drought years ($p > 0.05$, Figure 57, overlapping red arrows) during the spring, summer, fall or winter.

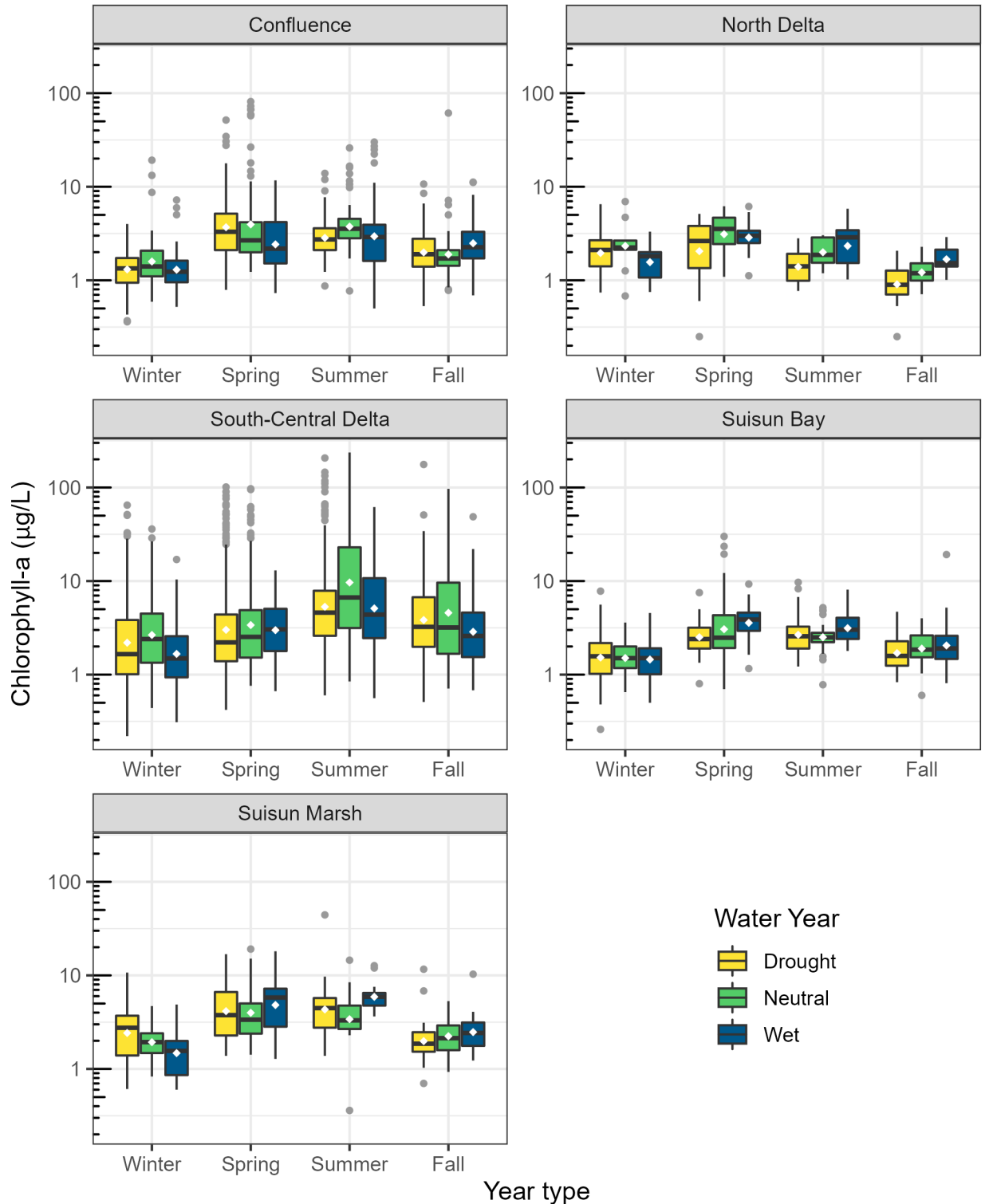


Figure 56 Boxplots showing the log-average (white diamond), median (bar), interquartile range between the 25th and 75th percentile (box), 1.5 times the

interquartile range (whiskers), and outliers (points) of chlorophyll-a concentration for three water year types by region and season. Y-axis scaled by \log_{10} .

Table 14. Analysis of variance model (ANOVA) results (a) and pairwise estimated marginal means comparisons (b) for the prediction of monthly average \log_{10} chlorophyll-a concentration for year type, season and region measured within 5 regions of the upper San Francisco Estuary during wet, below average and drought years between 2011 and 2021.

a.

Model Term	Sum Sq	Mean Sq Error	Num. Df	Den. Df	F-value	Pr(>F)
Water Year	8.18	4.09	2	4588.2	34.48	<0.01
Season	93.30	31.10	3	4587.4	262.04	<0.01
Region	0.98	0.25	4	30.3	2.07	0.11

b.

Contrast	Estimate	SE	Df	t-ratio	Pr(>F)
Wet - Below Avg	-0.0985	0.0145	4591	-6.795	<0.01
Wet - Drought	-0.0193	0.0134	4592	-1.433	0.3238
Below Avg - Drought	0.0793	0.0131	4591	6.048	<0.01

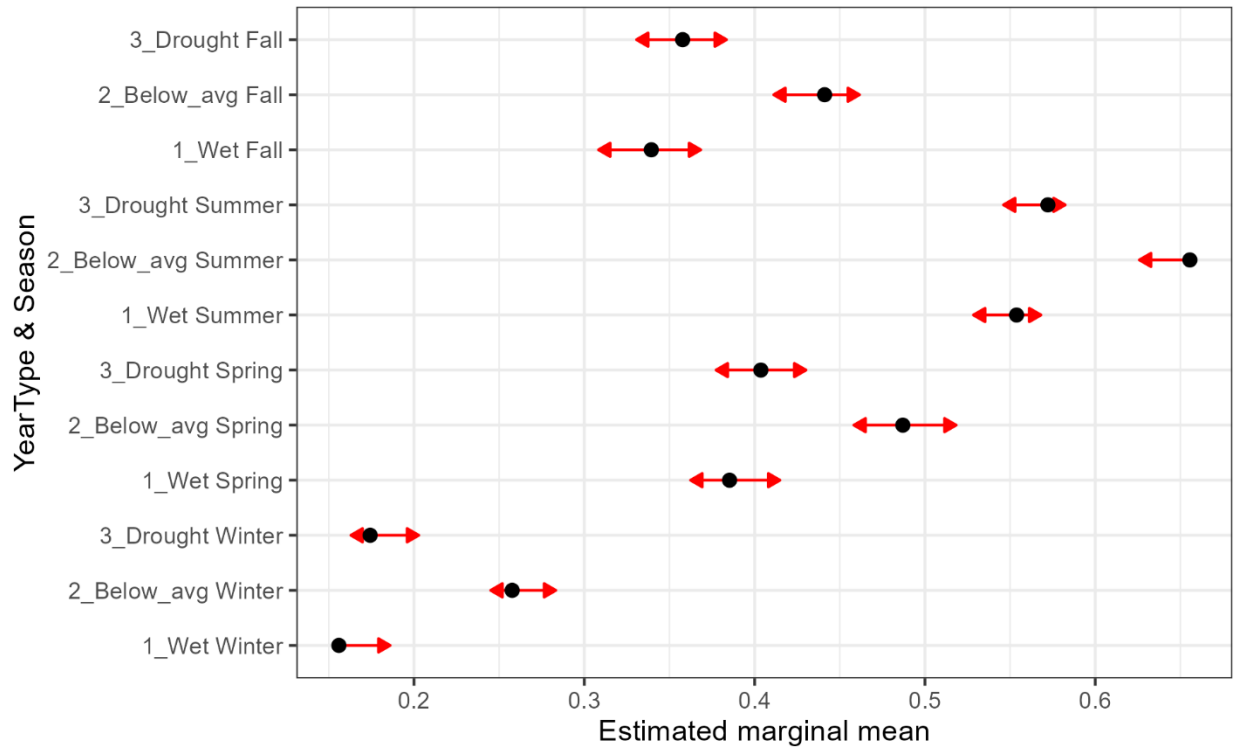


Figure 57. Pairwise comparisons for differences in water year type within and between seasons. Estimated marginal means (black dot) and estimated error around differences between the means (red arrow) for chlorophyll-*a* concentration measured for wet, below average and drought years during 2011-2021. Red arrows that do not overlap indicate that the means differ at the 0.05 level of significance.

Long-term analysis

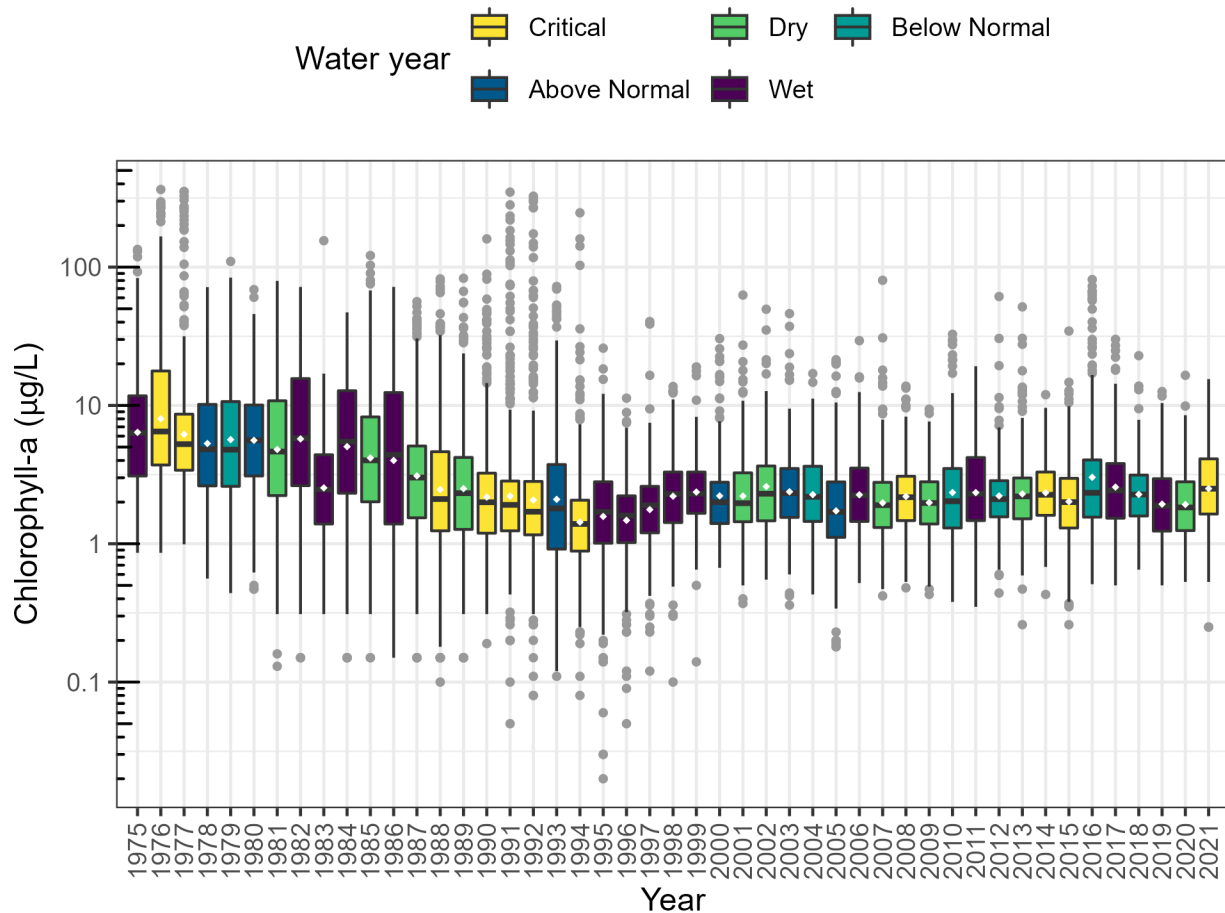


Figure 58 Yearly log-average (white diamond), median (bar), inter-quartile range between 25th and 75th percentiles (box), 1.5 times the interquartile range (whiskers), and outliers (circles) for chlorophyll-*a* concentration measured during 1975 - 2021 for four regions of the upper San Francisco Estuary. Colors show water year types for each water year. Y-axis scaled by log₁₀.

Yearly log-average chlorophyll-*a* concentration varied between 2 and 10 µg/L for most years between 1975 and 2021 (Figure 58). The ANOVA model results for average monthly chlorophyll-*a* concentration were similar to those for the short-term analysis with significant differences computed for water year ($p < 0.01$) and season ($p < 0.01$). However, unlike in the short-term analysis region was significant at the 0.05 level (Table 15).

Table 15. Type III analysis of variance model results for comparison of monthly average \log_{10} chlorophyll-*a* concentration among water years, regions, and seasons for 1975-2021.

	Sum Sq	Mean Sq	Num. DF	Den. DF	F value	Pr(>F)
Year	50.118	50.118	1	12490.7	770.1593	< 0.001
Region	0.643	0.214	3.000	30.700	3.294	0.03355
Season	163.218	54.406	3.000	12459.700	836.051	< 0.001

Log-average chlorophyll-*a* concentration was below 5 $\mu\text{g/L}$ and did not differ between dry years and either critical or wet years during 1975-2021 when all regions were combined ($p > 0.05$, Figure 62). Mean chlorophyll-*a* concentration for critical, dry, and wet years, however, was lower than for above and below normal years ($p < 0.05$).

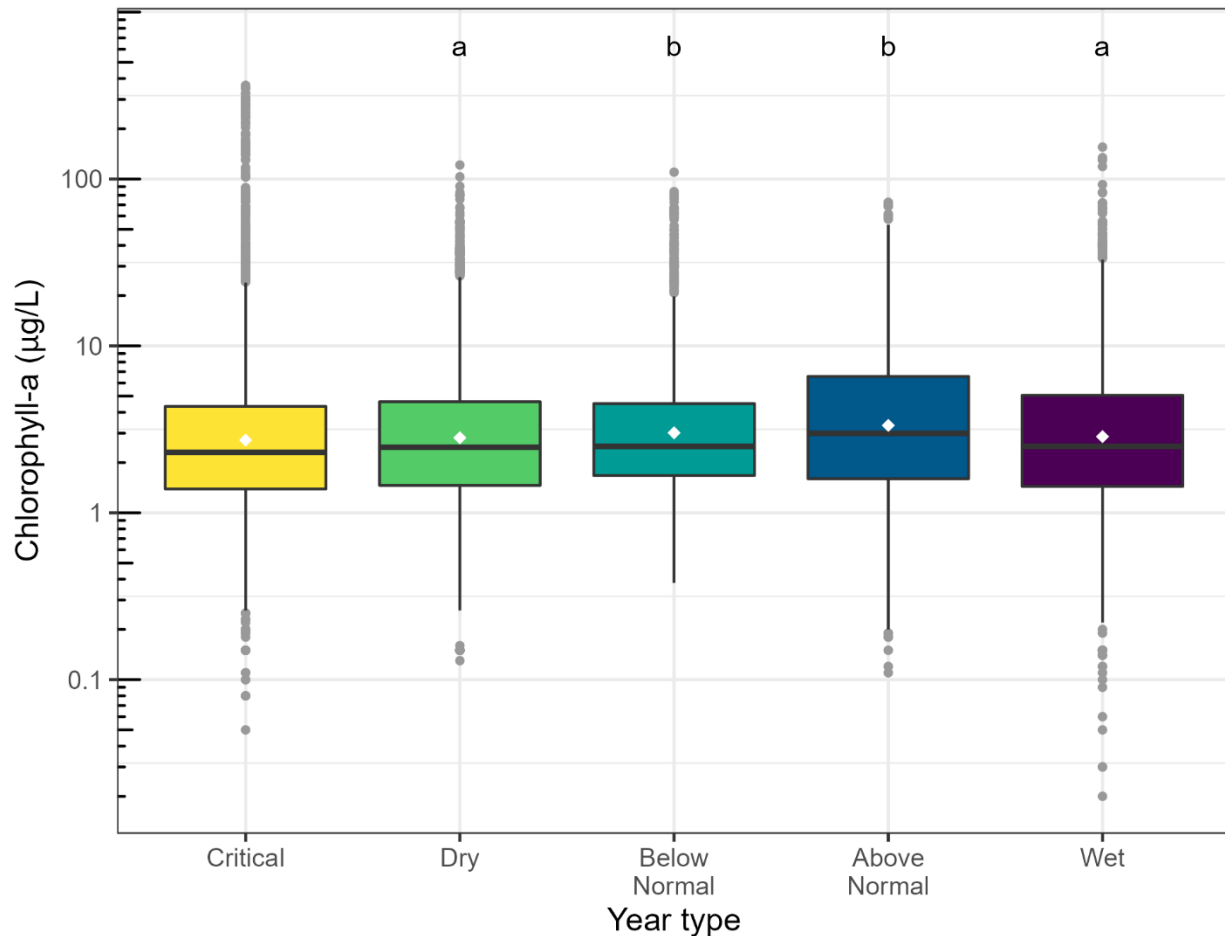


Figure 59. Log-average (white diamond), median (bar), inter-quartile range between 25th and 75th percentiles (box), 1.5 times the interquartile range (whiskers), and outliers (circles) for chlorophyll-*a* concentration measured during 1975-2021 in the upper San Francisco Estuary. Different letters above boxplots represents significant differences in marginal means at the 0.05 significance level. Y-axis scaled by \log_{10} .

The log-average chlorophyll-*a* concentration was below 10 $\mu\text{g/L}$ for water years within seasons for each region during 1975-2021 (Figure 60). The ANOVA model showed a significant difference in mean \log_{10} chlorophyll-*a* concentration among regions ($p < 0.05$, Table 15). However, post-hoc tests found no significant pairwise difference between regions ($p > 0.05$), suggesting the differences are small. Visually, the South-Central Delta had the highest chlorophyll-*a* concentration, with many upper whisker values approaching 100 $\mu\text{g/L}$ for all years and exceeding 100 $\mu\text{g/L}$ in critical water

years (Figure 60). The North Delta appeared to have the lowest chlorophyll-*a* concentration, with the upper whisker values never exceeding 11 µg/L.

The ANOVA model also showed a significant effect of season on \log_{10} chlorophyll-*a* concentration ($p < 0.05$, Figure 60). The post-hoc analysis found significant pairwise differences between all seasons ($p < 0.05$). Interesting patterns between water year type and season occurred among the regions. For example, in the Confluence and South-Central Delta, chlorophyll-*a* concentration decreased with wetter years in the spring but increased with wetter years in the summer. For Suisun Bay and North Delta, chlorophyll-*a* concentration during spring and summer was lower in critical and below normal years than in wet and above normal years (Figure 60).

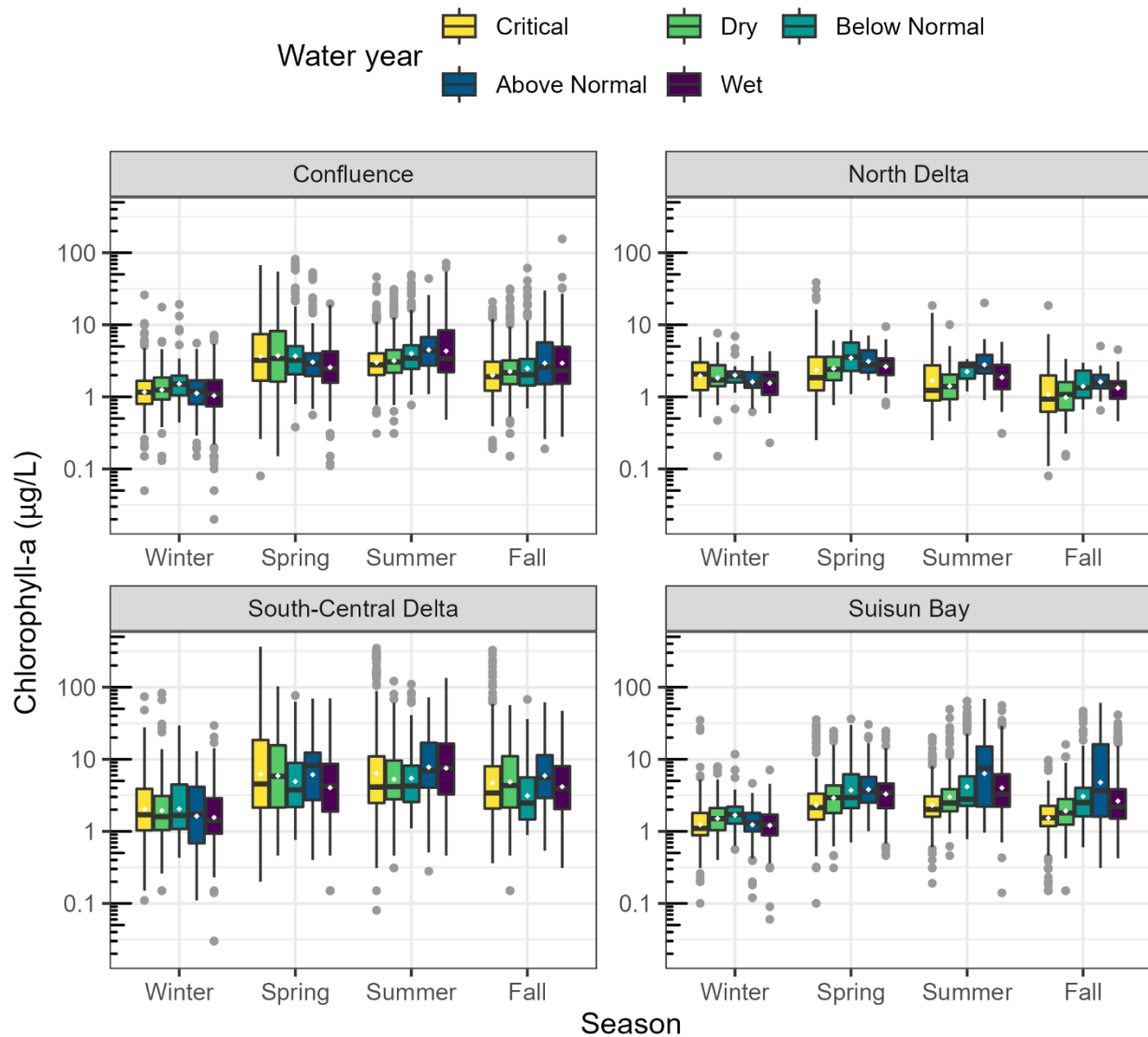


Figure 60. Log-average (white diamond), median (bar), inter-quartile range between 25th and 75th percentiles (box), 1.5 times the interquartile range (whiskers), and outliers (circles) for chlorophyll-*a* concentration among water years by region and season for data collected between 1975 and 2021. Y-axis scaled by log₁₀.

Microcystis index

Short-term analysis

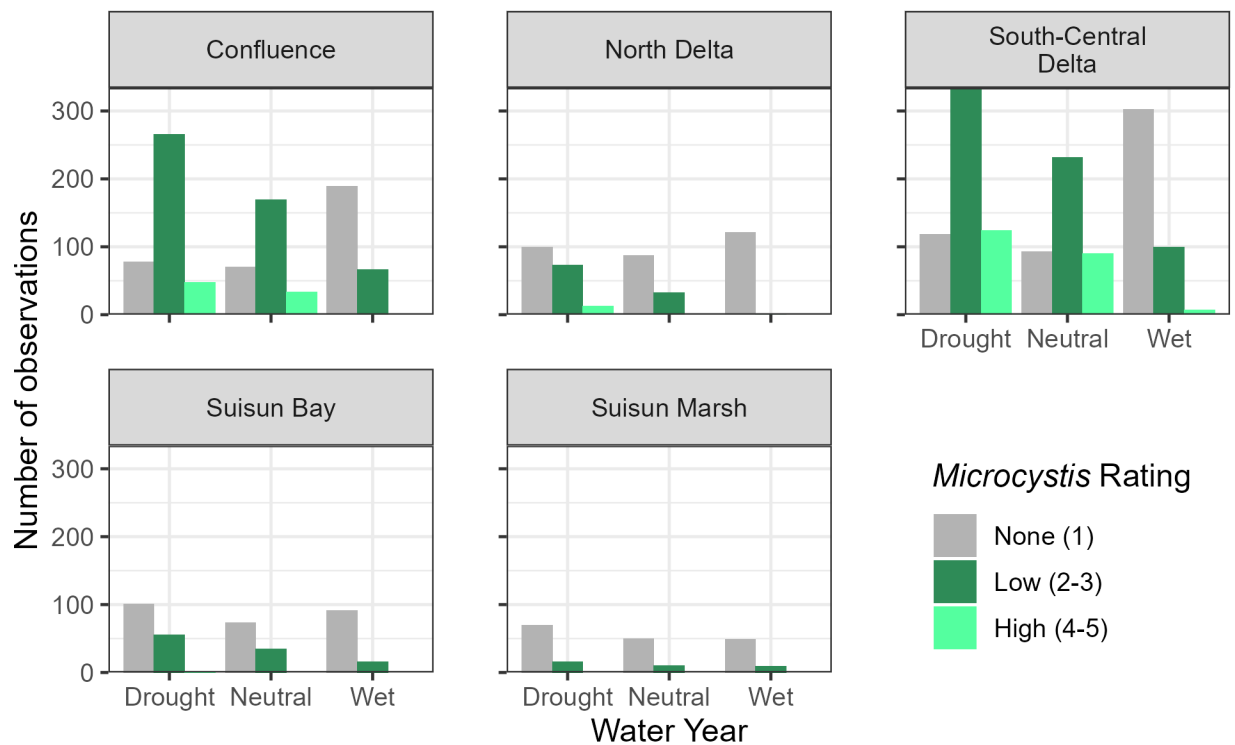


Figure 61 Number of *Microcystis* index scores observed for none, low and high biomass among regions for wet, below average and drought water year types during 2011-2021.

Table 16. Percentage of *Microcystis* index values observed in each drought year classification. Total number of observations in each year type are given in parentheses.

	None	Low	High
Drought (n = 1397)	33.4%	53.3%	13.4%
Neutral (n = 974)	38.3%	49.2%	12.6%
Wet (n = 950)	79.2%	20.1%	0.01%

In drought year types between 2011-2021, over 60% of observations were assigned to Low plus High *Microcystis* Index scores (Figure 61 and Table 16). This pattern was reversed in Wet years when about 20% of observations were assigned a Low score. Based on analysis of similarity (ANOSIM), there was no significant difference among *Microcystis* index scores for regions (Figure 61). However, *Microcystis* index scores differed among water year types. Index scores were lower for wet years than below average or drought years ($p < 0.01$). There was no significant difference between index scores for below average and drought years.

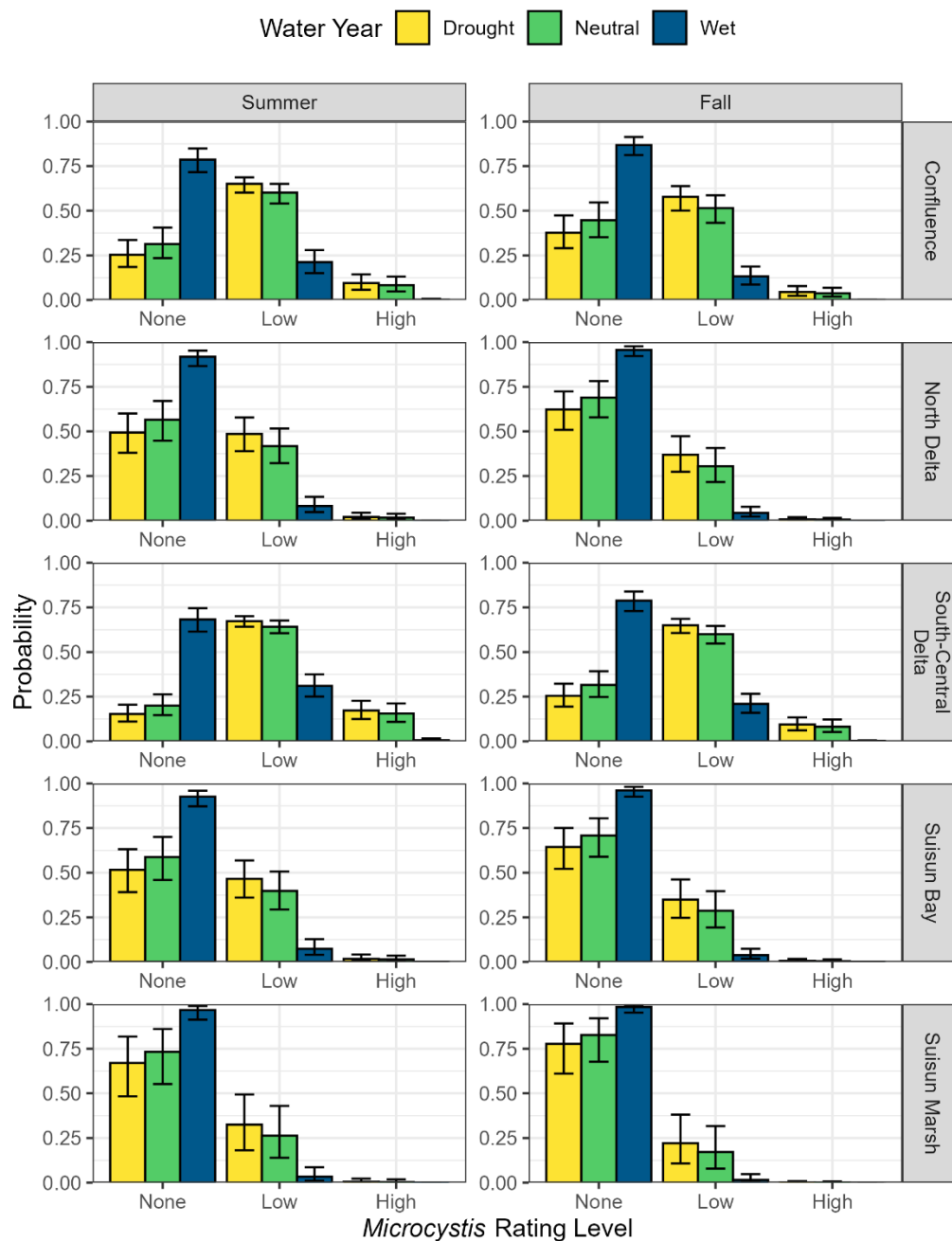


Figure 62. Probability of obtaining a low or high *Microcystis* index score for wet, below average and drought water year types during 2011-2021 among regions based on an ordinal model. The probability of scores in each combination of year type and season sum to 1. Error bars indicate the 95% credible interval for the probability estimate. Non-overlapping credible intervals are considered different at the 5% level of significance.

The ordinal model with water year, region, and season as predictor variables of *Microcystis* index scores identified water year and season as significant explanatory variables, but region was not significant (Figure 62). Neutral and drought years had a higher probability of a low *Microcystis* index score than wet years for all regions (non-overlapping credible intervals, Figure 62). Like the ANOSIM analysis, there was no difference (overlapping credible intervals) in the probability of a low *Microcystis* index score between below average and drought year types. High *Microcystis* index scores were less likely to occur than low *Microcystis* index scores across all regions. In addition, high *Microcystis* scores were less likely to occur in wet years. Instead, wet years had a higher probability of a *Microcystis* score of none compared with other years.

Aquatic Vegetation

Aquatic vegetation coverage has generally increased over time (Figure 63), occupying 8.0% of waterway area in 2004 and 12.6% in 2020 (2021 data were not ready in time for this report). In addition, the three highest values have been recorded within the last six years of the time series (2015 = 14.9%, 2017 = 19.9%, 2018 = 16.6%). SAV coverage of waterways (17.5%) is consistently higher than FAV coverage (3.6%). Also, variation in SAV coverage (standard deviation [SD] = 6.5%) is higher than that of FAV coverage (SD = 1.6%).

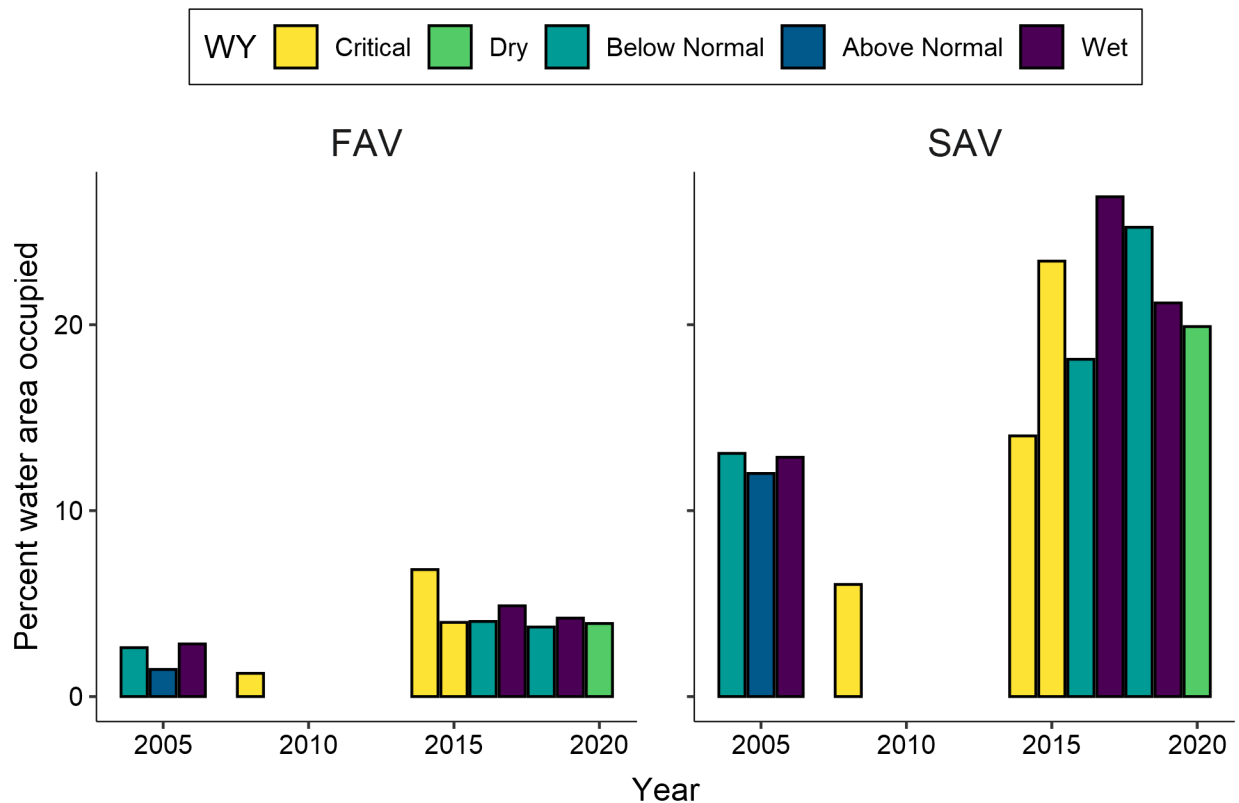


Figure 63. Time series of aquatic vegetation coverage in a region that includes the North and Central Delta and is based on annual remote sensing surveys. FAV = floating aquatic vegetation (includes *Eichhornia crassipes* and *Ludwigia* spp.). SAV = submersed aquatic vegetation (includes many species not distinguishable from remote sensing). Years without bars indicate those without data.

Based on the 11 years of data available for the period 2004-2020, there is not a simple pattern of higher aquatic vegetation coverage during drier year types (Figure 64). For example, mean coverage for FAV during critically dry years (4.0%) is the same as that for wet years (4.0%). For SAV, mean coverage during wet years (20.3%) is higher than that of critically dry years (14.5%). Critically dry years are more variable than the other four water year types in coverage for both FAV (SD: critical = 2.8%, dry = NA, below normal = 0.7%, above normal = NA, wet = 1.0%) and SAV (SD: critical = 8.7%, dry = NA, below normal = 6.1%, above normal = NA, wet = 7.0%). It is important to note that sample sizes for each water year type are very low, ranging from one to three data points (Figure 63).

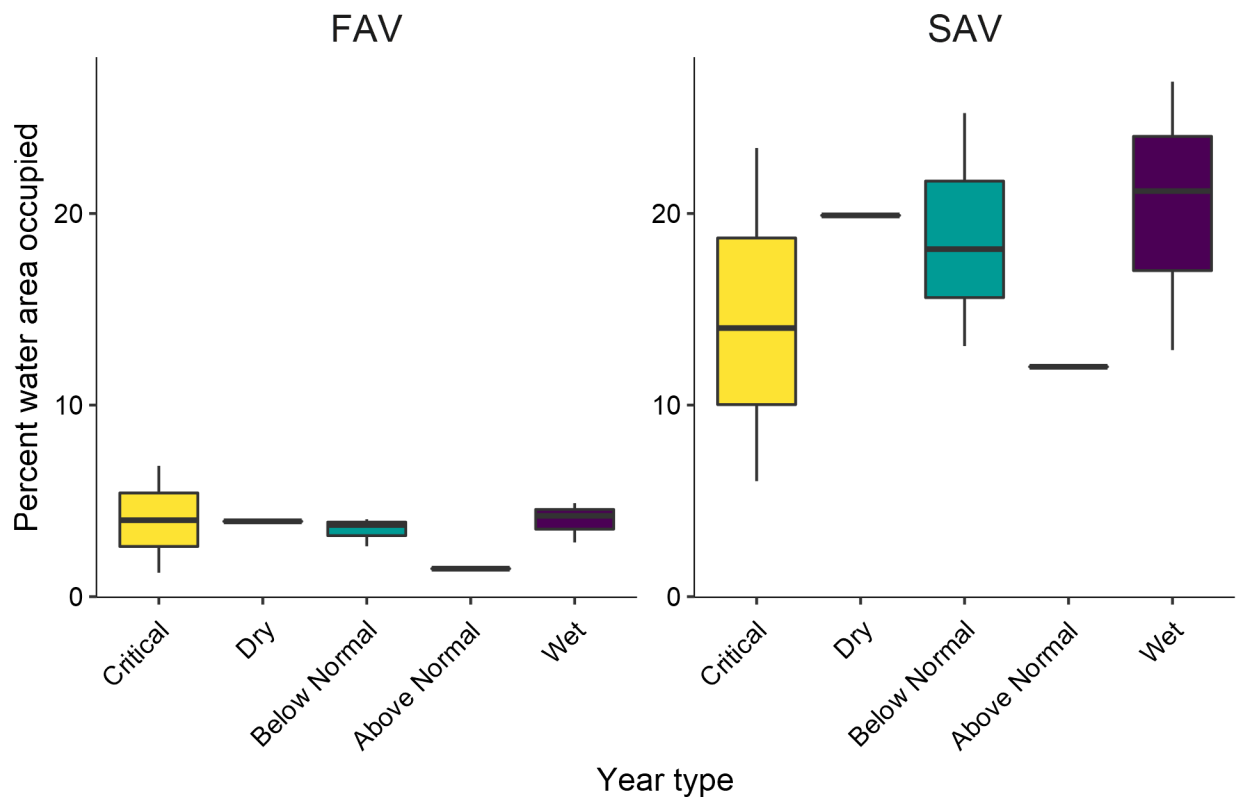


Figure 64. Comparison of aquatic vegetation coverage among water year types based on annual remote sensing surveys conducted over the North and Central Delta in 11 years during 2004-2020. FAV = floating aquatic vegetation (includes *Eichhornia crassipes* and *Ludwigia* spp.). SAV = submersed aquatic vegetation (includes many species not distinguishable from remote sensing).

Patterns of aquatic vegetation coverage in Franks Tract (Figure 64) are qualitatively similar to those for the broader Delta (Figure 62). The 2021 coverage data were not available in time for this report, so impacts of the Emergency Drought Barrier on the spread of aquatic weeds remain unclear.

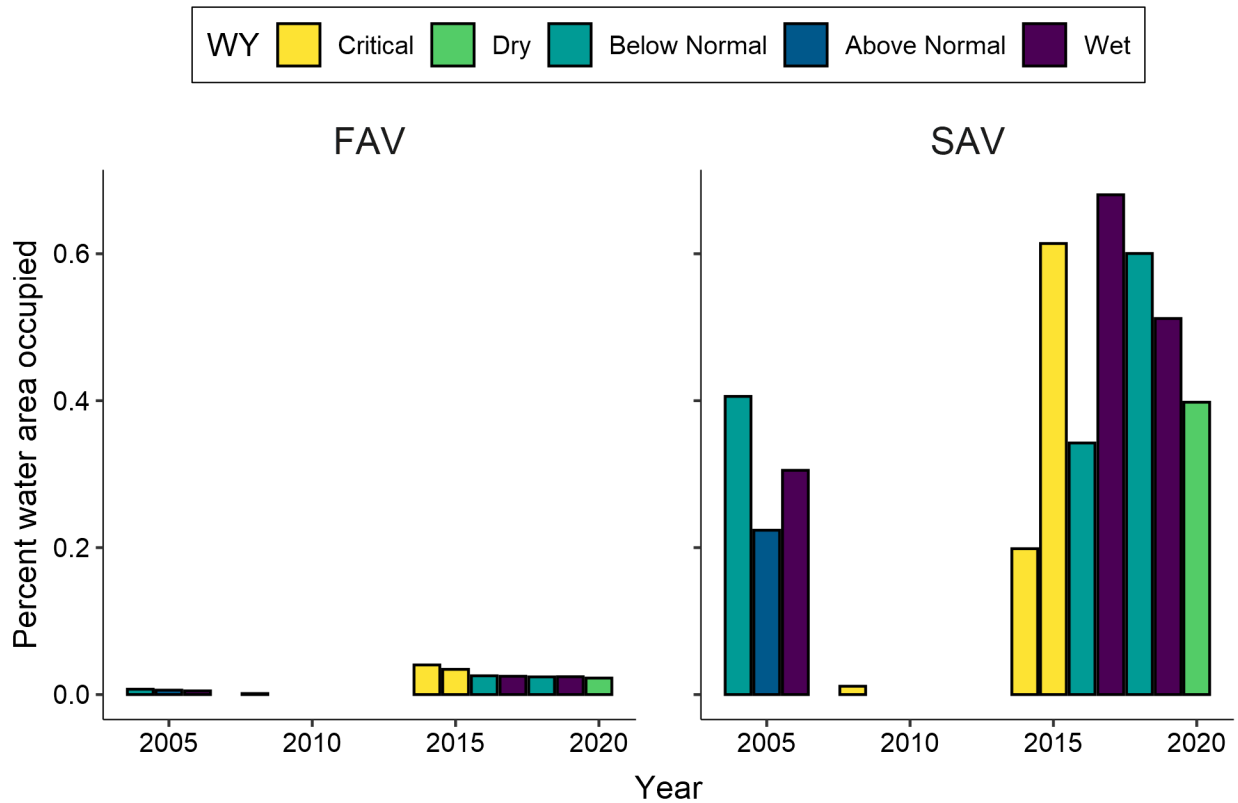


Figure 65. Time series of aquatic vegetation coverage in Franks Tract based on annual remote sensing surveys. FAV = floating aquatic vegetation (includes *Eichhornia crassipes* and *Ludwigia* spp.). SAV = submersed aquatic vegetation (includes many species not distinguishable from remote sensing). Years without bars indicate those without data.

Zooplankton

Our findings showed significant differences in zooplankton biomass in the upper estuary when accounting for year types and season (Table 17, Figure 68), with Neutral summer months producing more biomass and Wet springs producing the lowest values, which could be linked to high outflows and shorter residence time, resulting in greater export of zooplankton from the system. When examining regional results, we saw that in Suisun Bay, Wet and Neutral years had higher zooplankton biomass, while in the south-Central Delta Drought years were the most productive (Figure 69, Table 18).

For the short-term analysis covering the last decade, we found that in the South-Central Delta zooplankton biomass was highest in the Drought years of 2013 through 2016, and decreased in 2017, a year of heavy precipitation

(Table 19, Figure 70). That trend was reversed in Suisun Marsh, with 2017 having the biomass in the estuary for that year.

Several of the taxa examined had significant correlations with the yearly Sacramento Valley Index (Fig. 23). The native calanoid copepod *Acartia* did show significantly higher densities in drier years, likely due to higher salinity conditions expanding its range from the Bay Area further into the sampling area. The cladocera *Daphnia* and *Diaphanosoma* both saw more than 35% of their biomass variance explained by water year index, having higher densities when the water index was lower. We saw the opposite trend for the non-native calanoid copepod *Pseudodiaptomus forbesi*, with higher densities of adults and juveniles correlated with a higher water index. The native mysid *Neomysis mercedis*, whose population significantly declined in the 1980s, also saw a strong positive correlation between BPUE and water index. PERMANOVA showed 26% (Table 20) of the variation in community structure was correlated with Drought year classification, and the communities separated out by Drought year classification in the NMDS Plot (Figure 66). Wet year communities had more biomass composed of the mysids *Hyperacanthomysis longirostris* and *Neomysis mercedis*, while dry years had more of the cladocerans *Diaphanosoma* and *Daphnia*.

Table 17. Analysis of variance comparing long-term seasonal average log transformed BPUE and Drought year type.

Model Term	Sum Sq	Mean Sq Error	Num. Df	F-value	Pr(>F)
Drought	2.48	1.240	2	4.569	0.012
Season	7.82	3.909	2	14.401	<0.0001

Table 18. Analysis of variance comparing long-term log transformed BPUE between Drought year type, region, and their interaction

Model Term	Sum Sq	Mean Sq Error	Num. Df	F-value	p-value
Drought	2.08	1.0394	2	2.460	0.0884
Region	6.34	2.1122	3	4.999	0.0024

Drought:Region	12.22	2.0374	6	4.822	0.0001
----------------	-------	--------	---	-------	--------

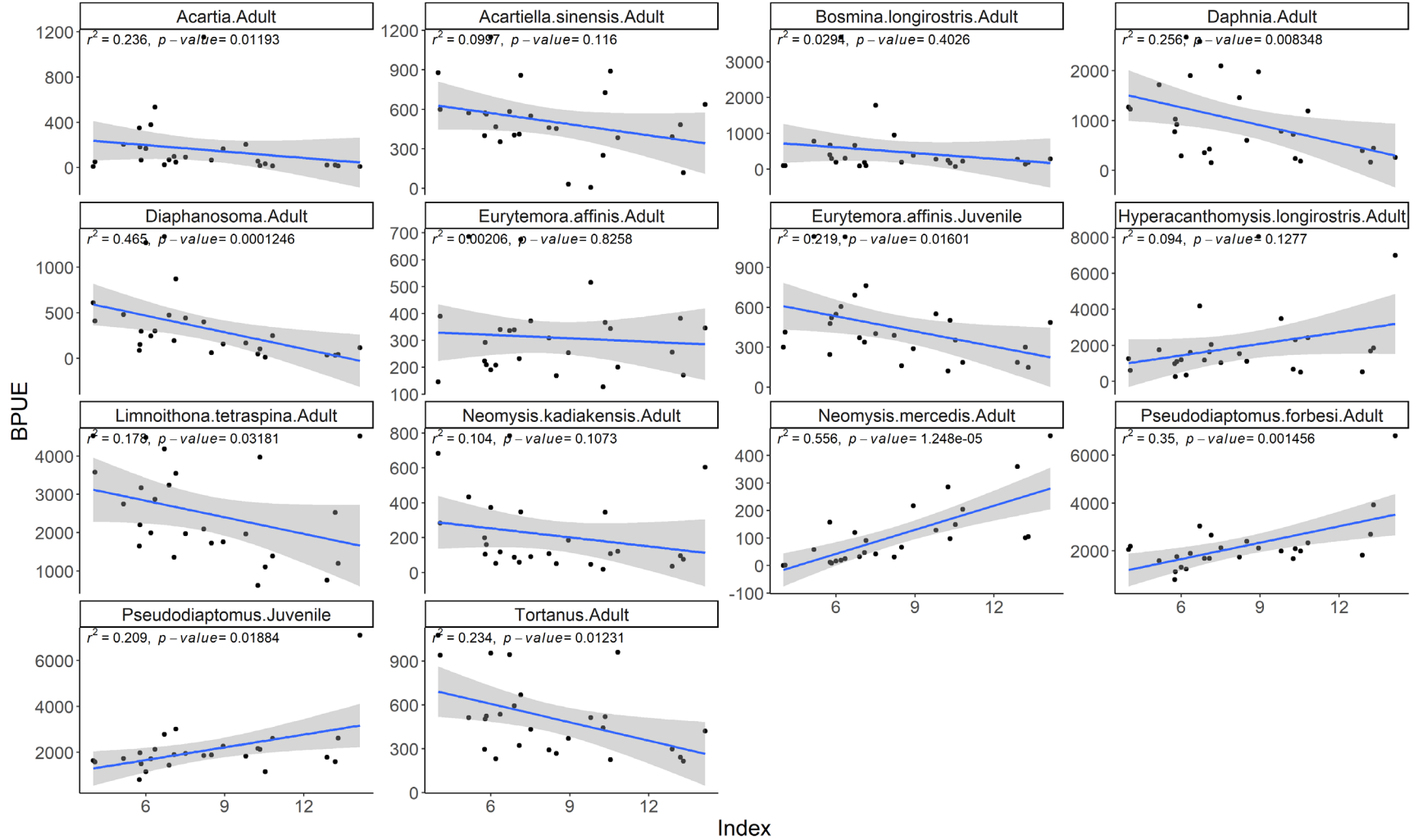
Table 19. Analysis of variance comparing short-term log transformed monthly BPUE by region and water year.

Model Term	Sum Sq	Mean Sq Error	Num. Df	F-value	Pr(>F)
Water Year	70.1	7.01	10	5.666	<0.0001
Region	47.9	15.98	3	12.909	<0.0001
Month	112.0	112.04	1	90.536	<0.0001
Water Year:Region	36.1	1.29	28	1.041	0.409

Table 20 Permutational multivariate analysis of variance of zooplankton community between Drought year types

Model Term	Sum Sq	R2	Num. Df	F-value	Pr(>F)
Drought	0.1091	0.2593	2	4.0263	<0.001

Taxa BPUE by Water Year Index



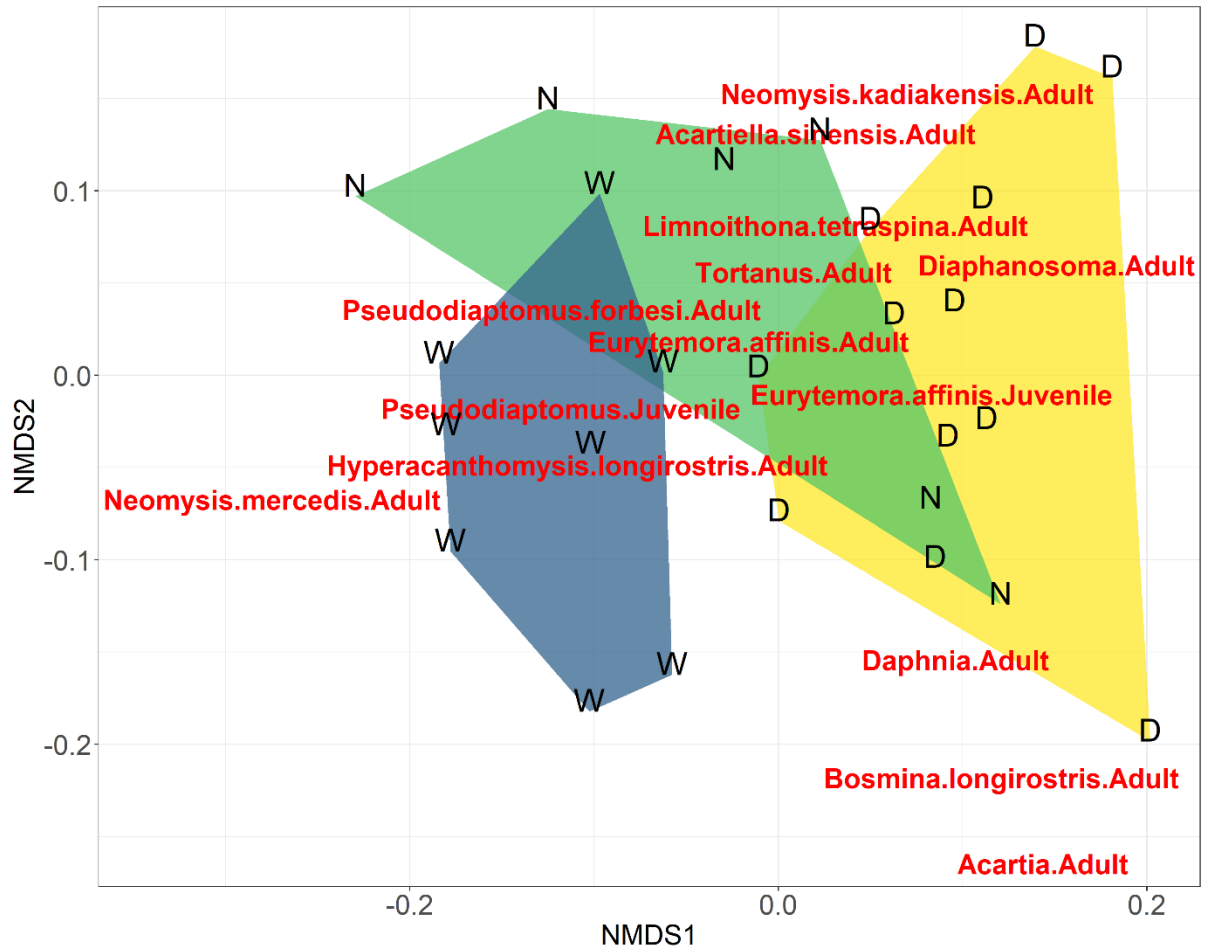


Figure 67. Non-metric multi-dimensional scaling plot of zooplankton community composition by drought year classification (Drought period [D], Neutral [N], and Wet period [W]).

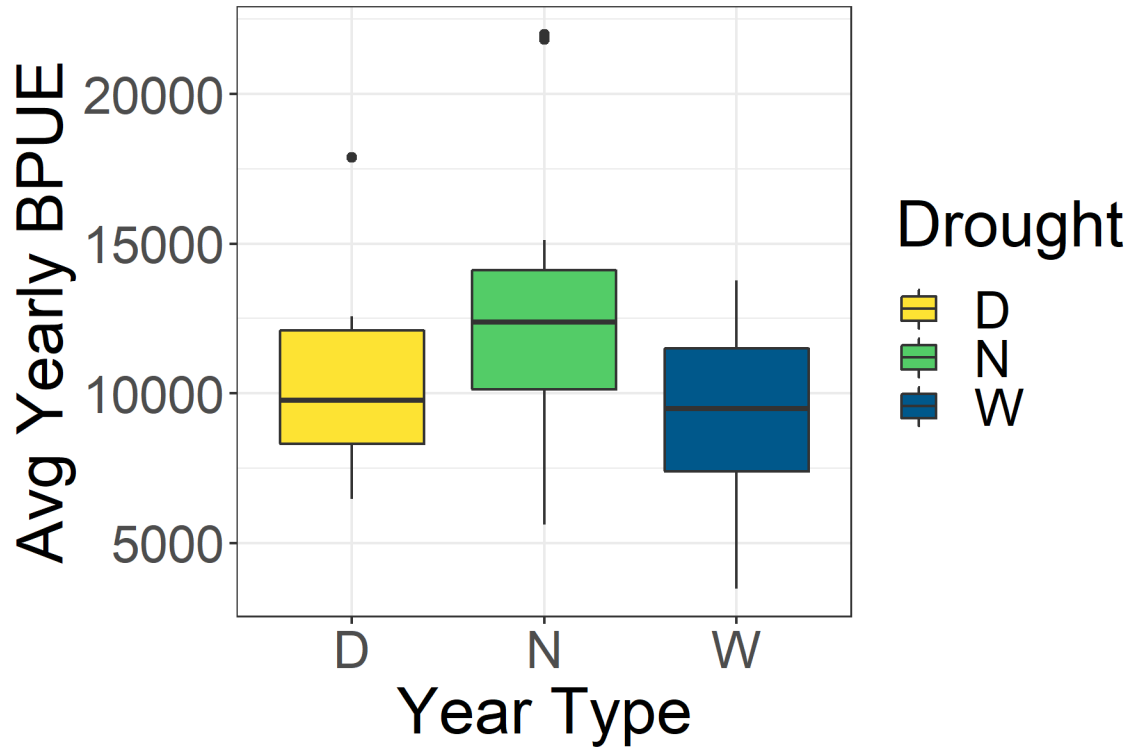


Figure 68. Average total zooplankton biomass per unit effort biomass by drought year classification (Drought period [D], Neutral [N], and Wet period [W]). Drought year classification on its own was not significantly different (ANVOA $f = 3.006$, $p = 0.06$)

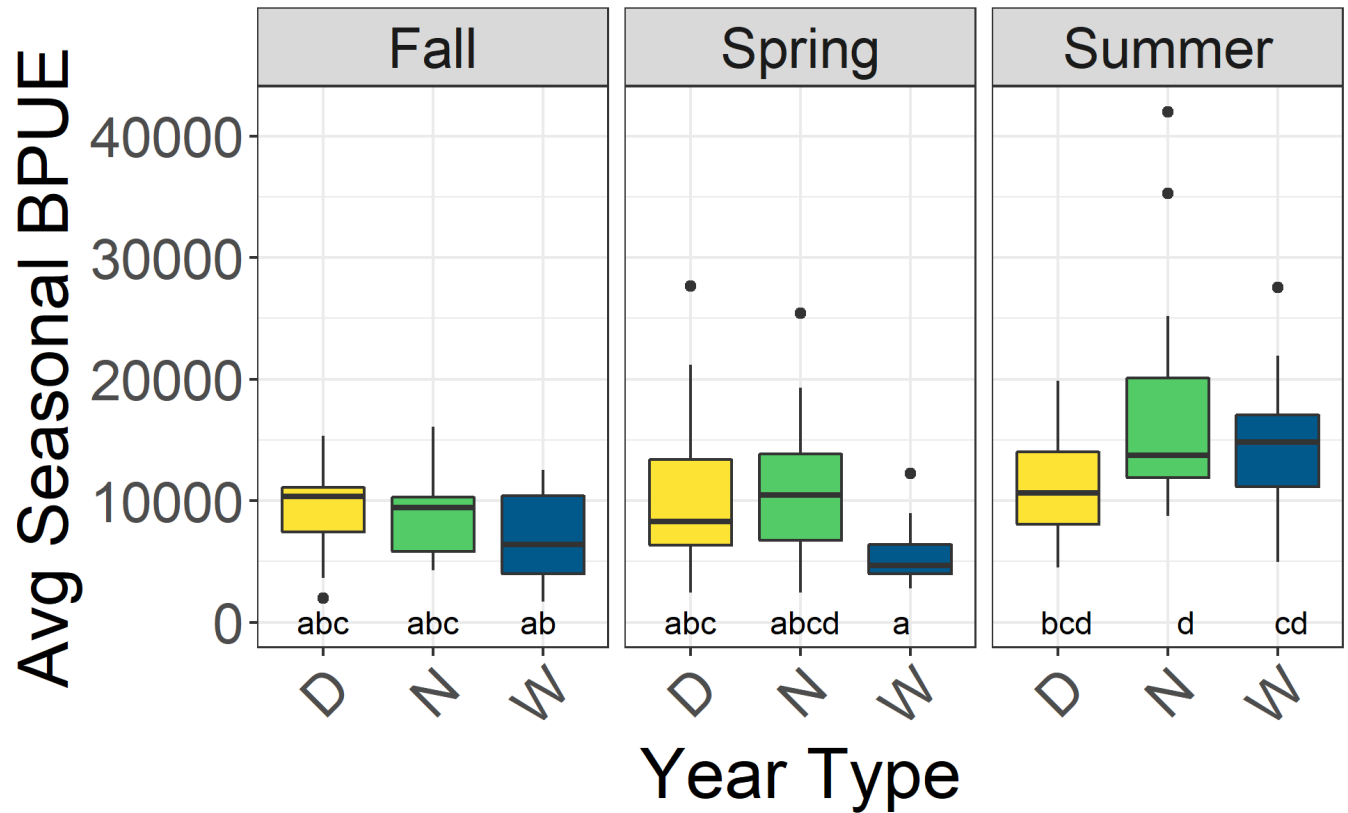


Figure 69. Average zooplankton biomass by biomass by drought year classification (Drought period [D], Neutral [N], and Wet period [W]) and season. Letters indicate groups not significantly different at the $p < 0.05$ level.

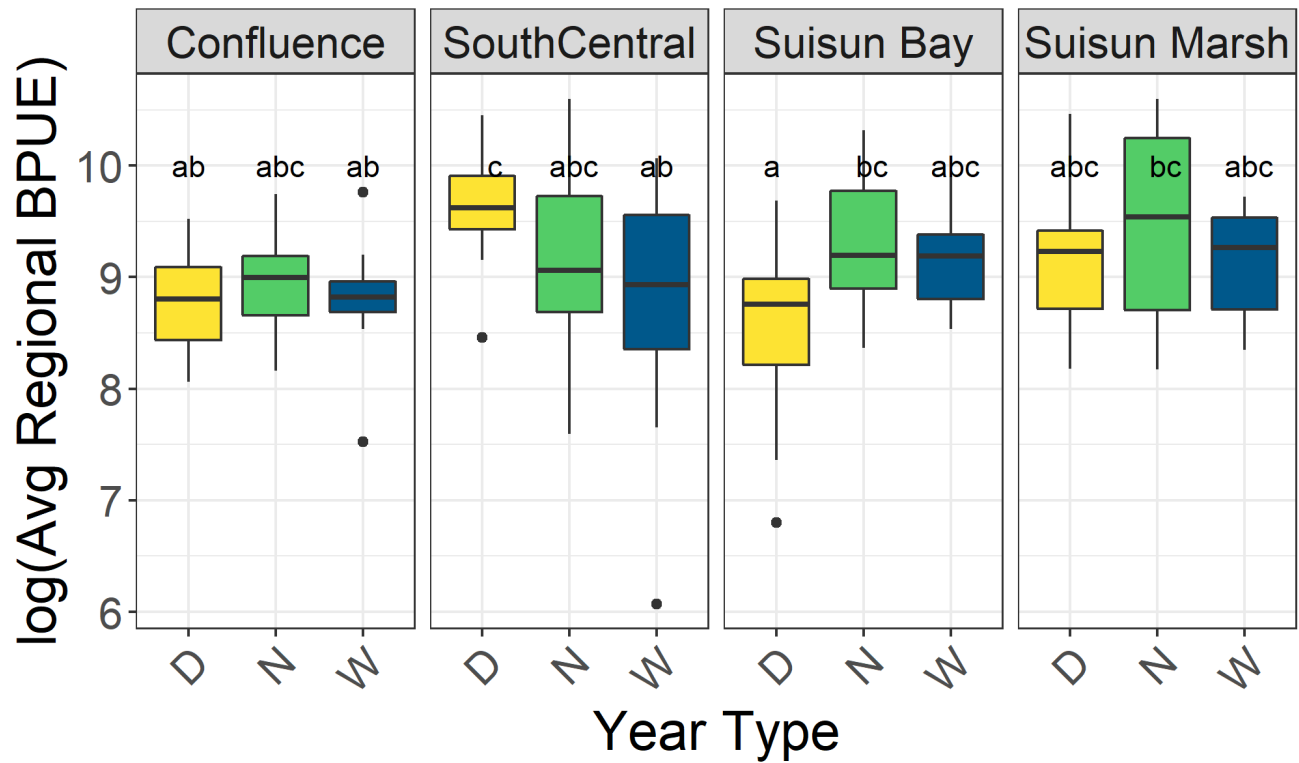


Figure 70. Average zooplankton biomass by drought year classification (Drought period [D], Neutral [N], and Wet period [W]) and region. Letters indicate groups not significantly different at the $p < 0.05$ level.

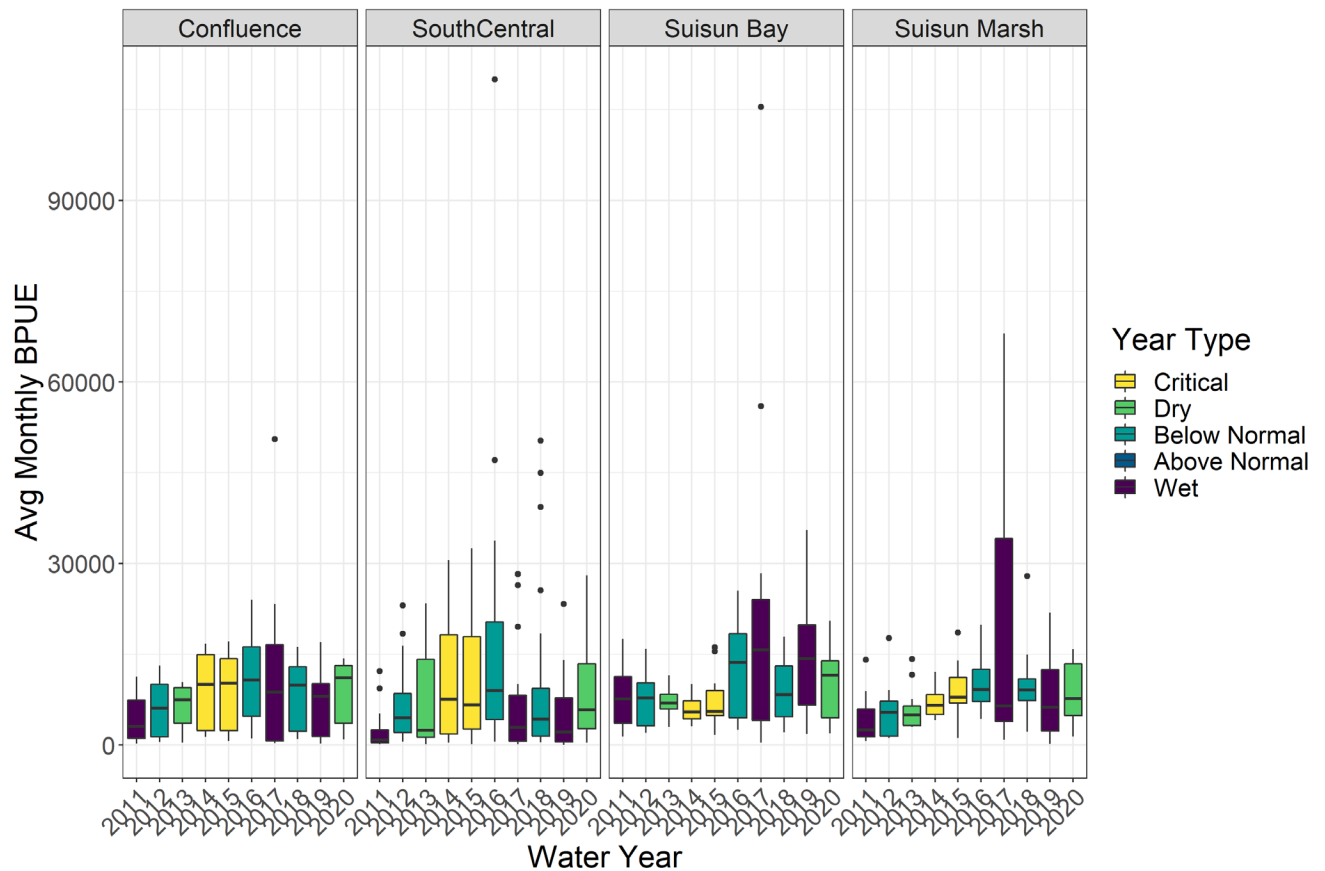


Figure 71. Average zooplankton biomass by region and year for 2011-2020

Jellyfish were most abundant in the Confluence, Suisun Bay, and Suisun Marsh regions, reaching highest abundances in Suisun Bay in 2017 and 2019 (Figure 71). A full statistical analysis of these data has not been completed, but the general trend is for highest abundances of jellyfish to occur during wet periods (Figure 72). However, the rare occurrences of jellyfish in the freshwater regions of the South-Central and North regions all occurred during droughts (Figure 71).

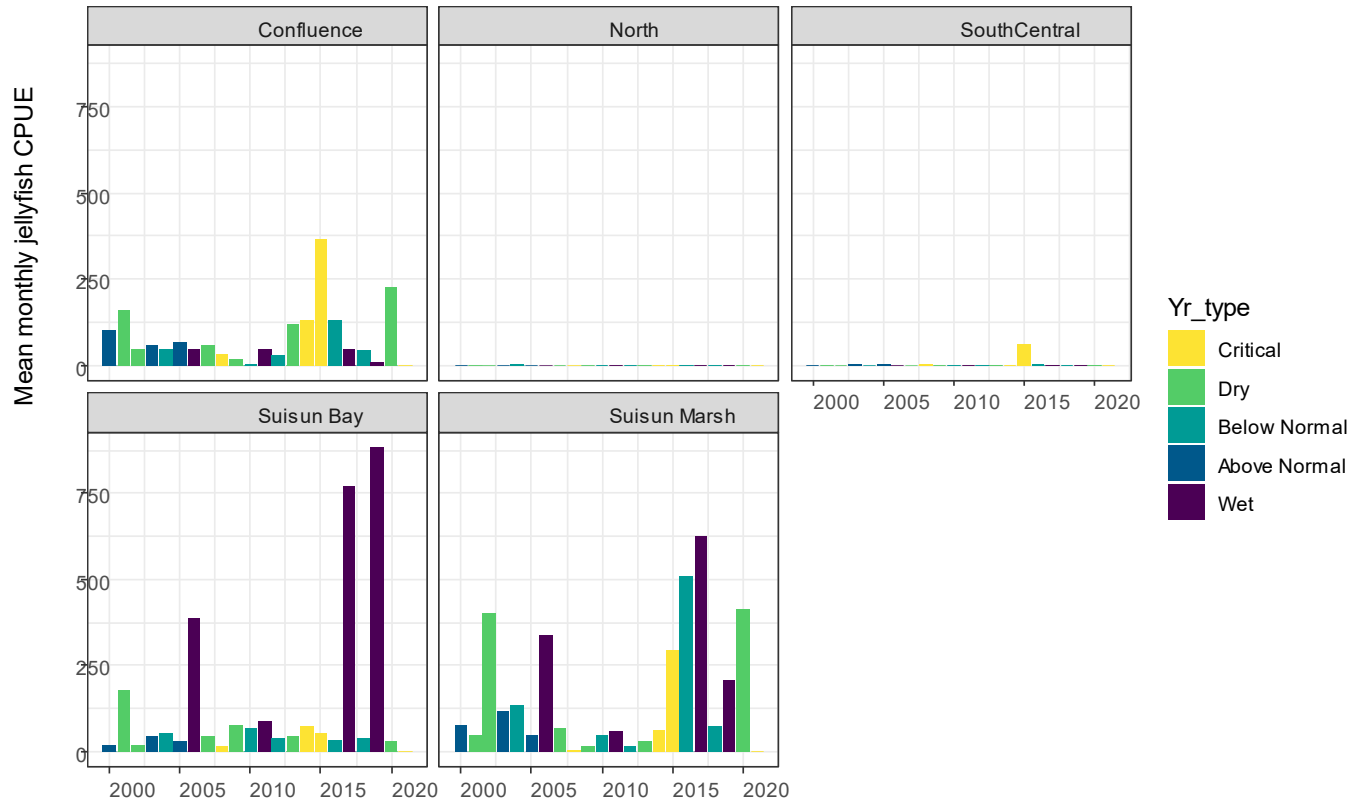


Figure 72. Annual mean monthly jellyfish CPUE by region.

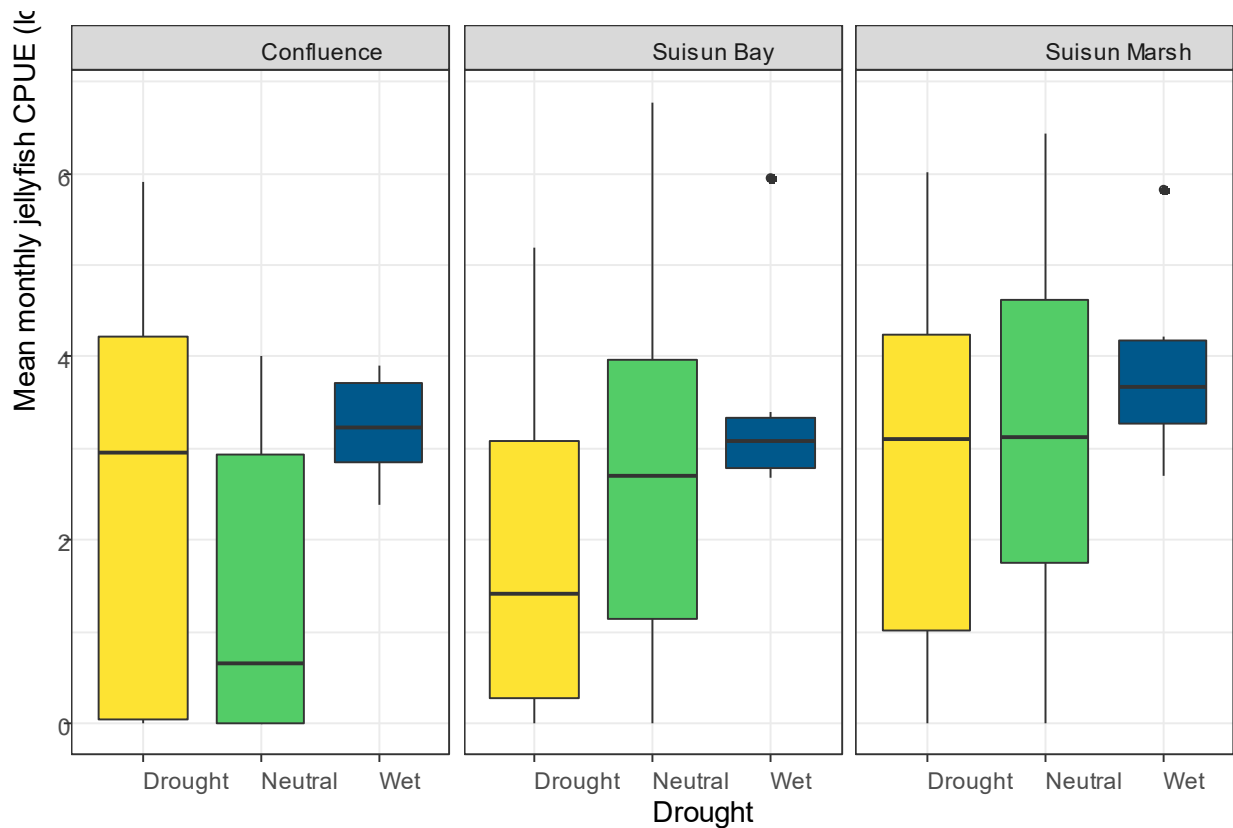


Figure 73. Mean monthly Jellyfish CPUE for June-October, 2000-2021, separated by region and Drought year classification. The North Delta and South-Central regions were omitted due to extremely low jellyfish catch.

From 2011-2019, both clam species showed changes to density and grazing rate between years, with some patterns relating to water year type. *C. fluminea* had highest density in the wet years of 2011, 2017, and 2019, but also showed similar density during the dry year of 2018, possibly due to carry over from the previous year. The drought years of 2012-2016 had somewhat lower density and grazing rate, but with very high variability. Conversely, *P. amurensis* had the lowest density during the wet years of 2011, 2017, and 2019 and the highest density and grazing rates during the critically dry years of 2014 and 2015.

Long-term trends were similar to the more recent trends with a strong increase in grazing rates in *P. amurensis* during droughts and no response in *C. fluminea* (Supplemental Figure 6, Supplemental Figure 7, Figure 76).

P. amurensis distribution also responded to drought, but there was a significant lag in the shift in distribution. While there was no significant impact of multi-year droughts or wet periods (results not shown), or the Sacramento Valley index in the year data was collected (results not shown), the annual center of *P. amurensis* distribution did have a significant negative relationship with the previous year's Sacramento Valley Index (Figure 77). Linear model coefficient -962, Adjusted R-squared: 0.2921 F-statistic: 14.21 on 1 and 31 Df, p-value: 0.000691).

Table 21. Analysis of deviance table for models of density and grazing rates for *P. amurensis* and *C. fluminea* from zero-inflated negative binomial models on data from 2011-2019. The interaction between region and year was not modeled because the model would not converge when the interaction was included. Data from 2013 and 2016 were too sparse to include in the model

Species	Model	Model Term	Df	Chisq	Pr(>Chisq)
<i>P. amurensis</i>	Density	Year	6	204.8	<0.0001
<i>P. amurensis</i>	Density	Region	2	271.2	<0.0001
<i>C. fluminea</i>	Density	Year	6	78.9	<0.0001
<i>C. fluminea</i>	Density	Region	4	371.4	<0.0001
<i>P. amurensis</i>	Grazing	Year	6	63.57	<0.0001
<i>P. amurensis</i>	Grazing	Region	2	60.466	<0.0001
<i>C. fluminea</i>	Grazing	Year	6	28.5	<0.0001
<i>C. fluminea</i>	Grazing	Region	4	150.77	<0.0001

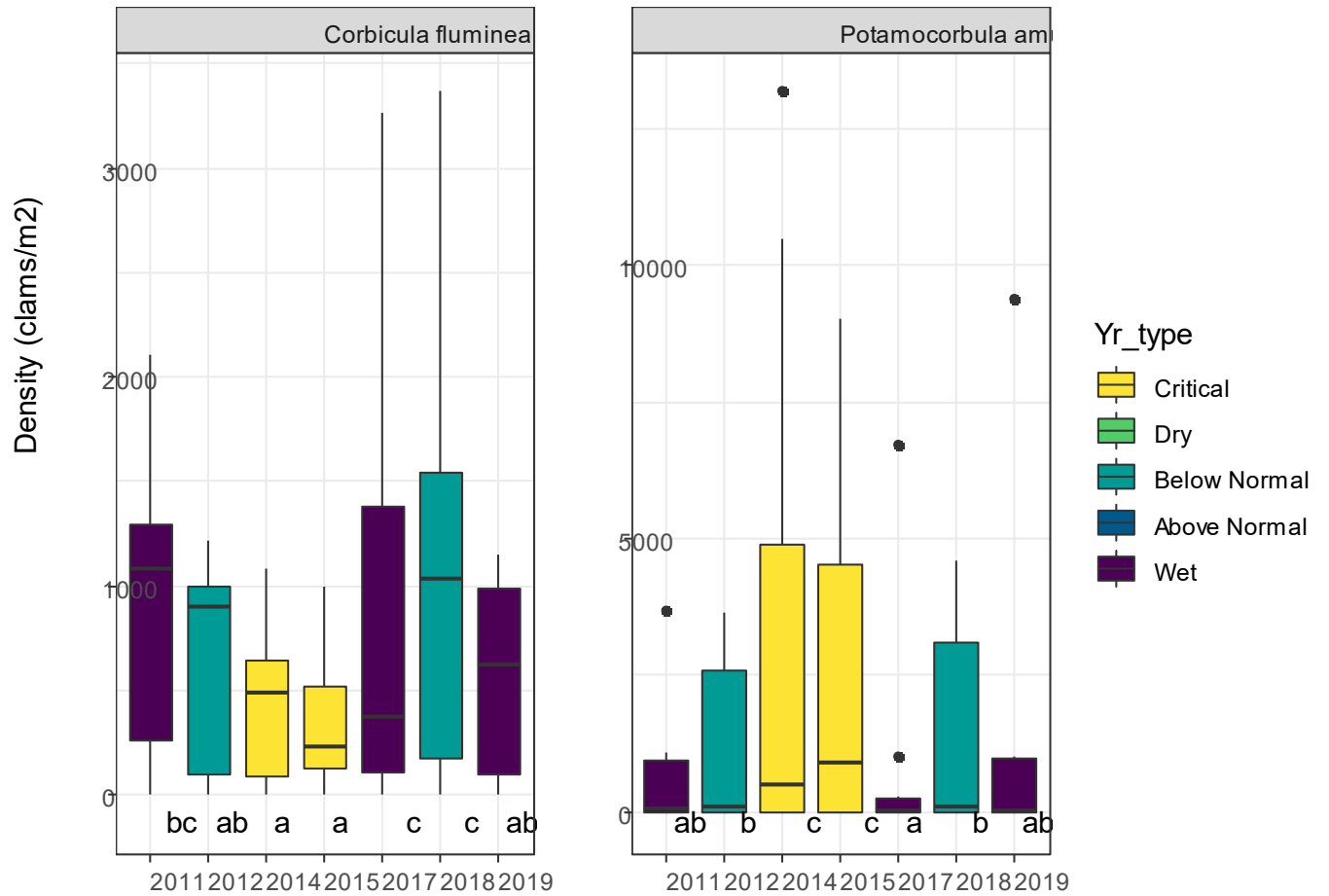


Figure 74. Monthly average density (clams/m²) of invasive clams measured by GRTS and EMP by year. Letters denote groups with significantly different abundance (results of zero-inflated negative binomial model, (Table 21)). 2013 and 2016 were omitted due to small sample size.

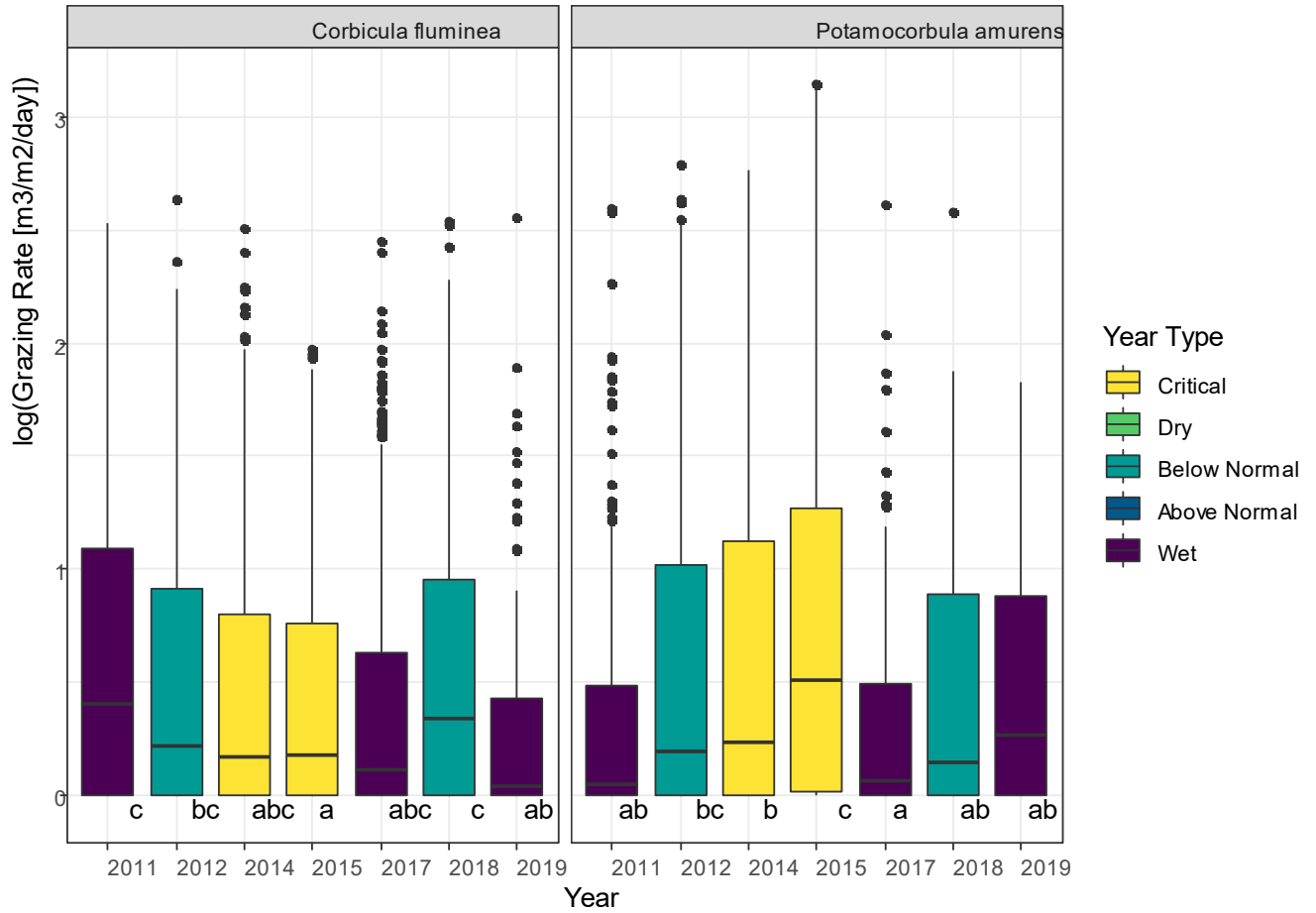


Figure 75. Monthly grazing rate of invasive clams as measured by GRTS and EMP by year for 2011-2019. Letters denote groups that are not significantly different at the $p < 0.05$ level. (Table 21)

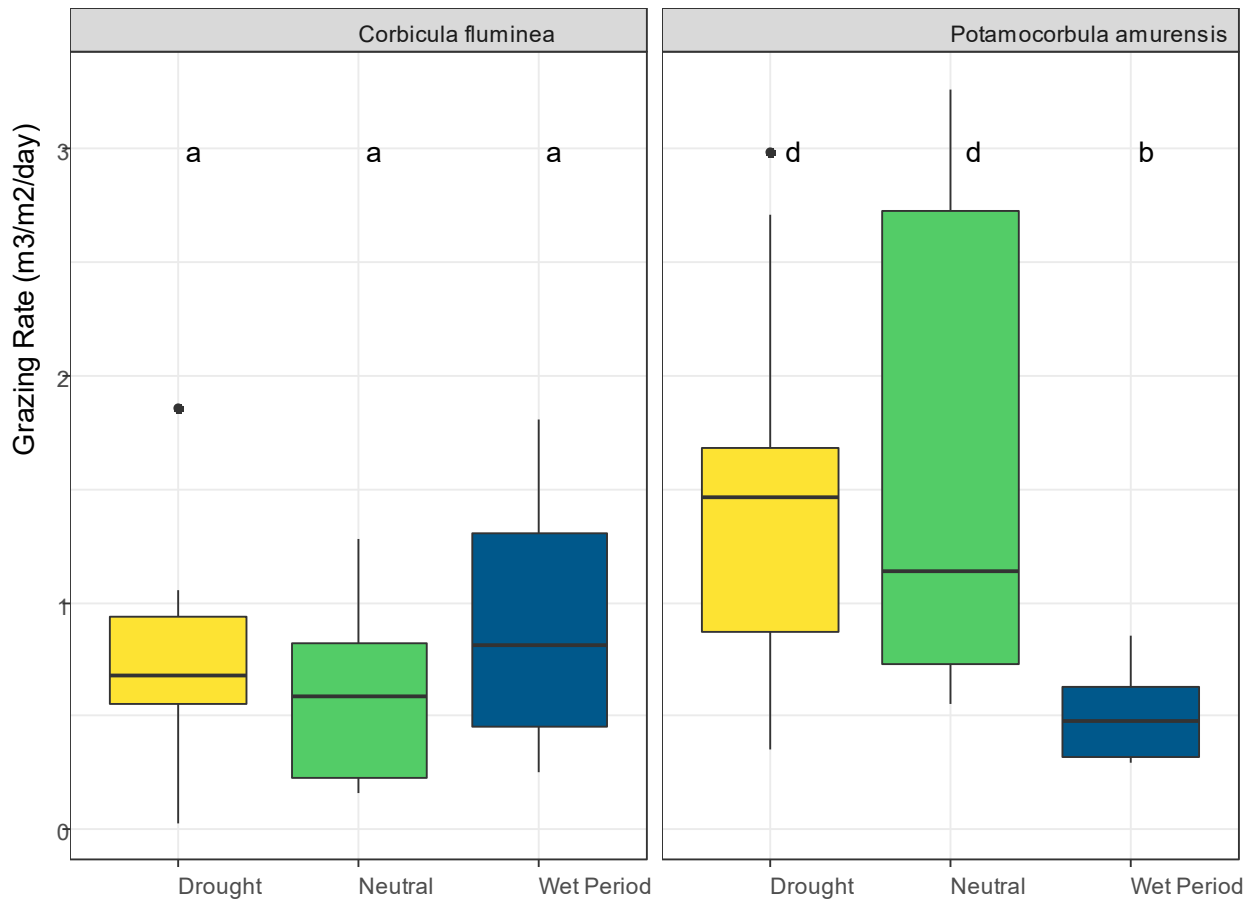


Figure 76. Average annual grazing rates for two species of invasive clams, 1976-present (*C. fluminea*) and 1987-present (*P. amurensis*) across the estuary by year type. Letters indicate groups without statistically significant differences. *C. fluminea* ANOVA F-value 1.028 on 2 and 37 Df. $p = 0.367$. *P. Amurensis* ANOVA F-value 6.81 on 2 and 28 Df, $p = 0.0039$.

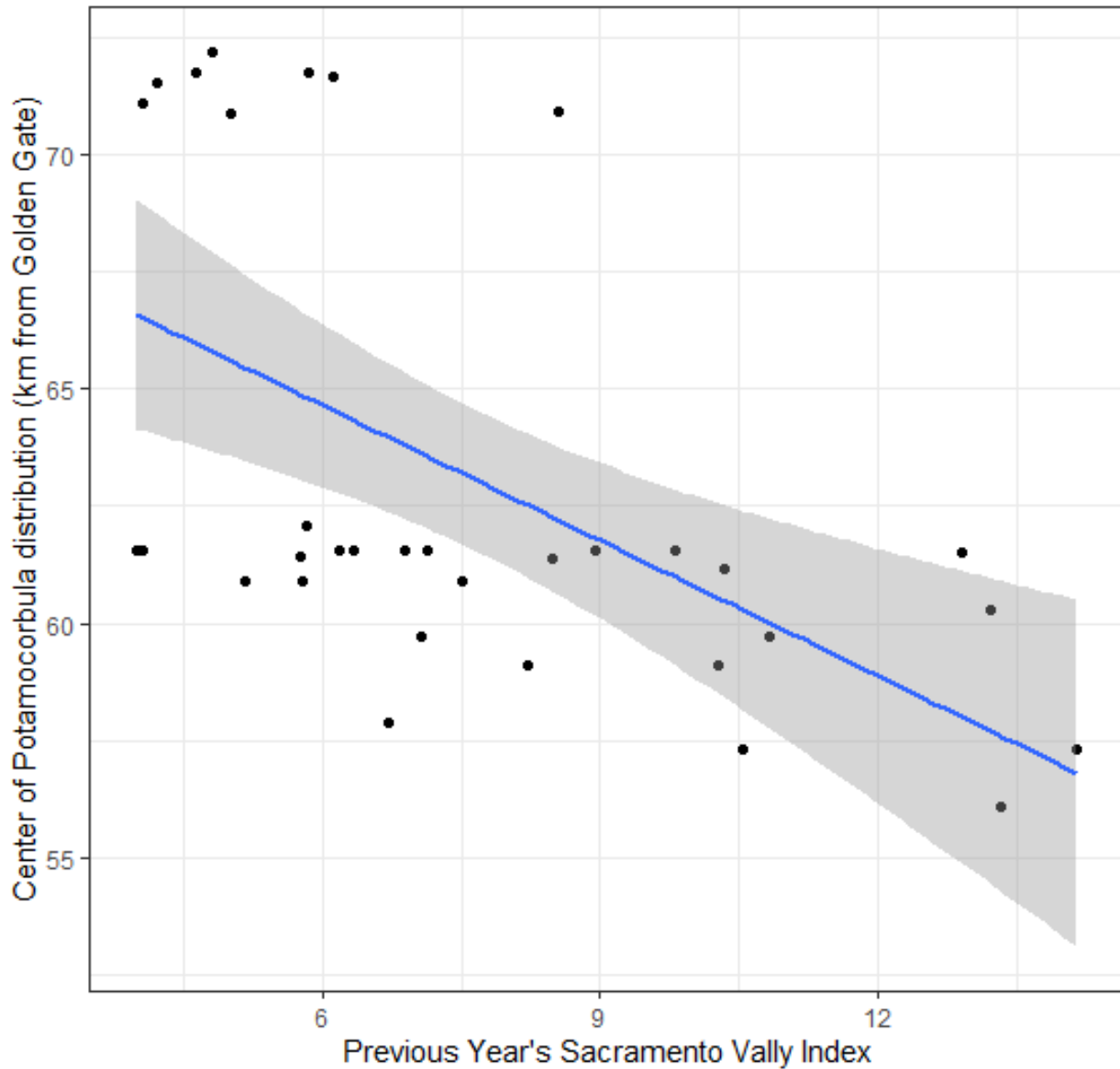


Figure 77. Center of distribution (km from the Golden Gate) for *P. amurensis* versus the previous year’s Sacramento Valley Water Year index. Linear model of annual average distance versus the previous year’s Sacramento Valley index (coefficient -962, Adjusted R-squared: 0.2921 F-statistic: 14.21 on 1 and 31 DF, p-value: 0.000691)

Fish

Species-specific analyses

Winter-run survivorship, 2021

Acoustic receiver data from 2021 on hatchery produced SRWRC is shown in Table 22, includes three releases: a thiamine boosted release, a thiamine control, and a third release group. Detections at the Tower Bridge in Sacramento occurred between February 5, 2021, and March 28, 2021. Detections at Benicia occurred between March 7, 2021, and March 30, 2021.

Table 22. Minimum through-Delta survival: City of Sacramento to Benicia (using Cormack-Jolly-Seber survival model)

Release Group	Survival (%)	SE	95% lower C.I.	95% upper C.I.
ALL	35.7	6.4	24.3	49.0
Release 3	37.8	8.0	23.9	54.2
Thiamine Boost	40.0	15.5	15.8	70.3
Thiamine Control	22.2	13.9	5.6	57.9

Drought effects on CCR

Using the run-specific age structure described by Satterthwaite et al. (2017), Figure 78 shows the calculated CRR for SR winter-run Chinook by drought condition during juvenile migration. Figure 79, Figure 80 show the calculated CRR for CVSRC and CVFRC respectively, by drought condition during juvenile migration.

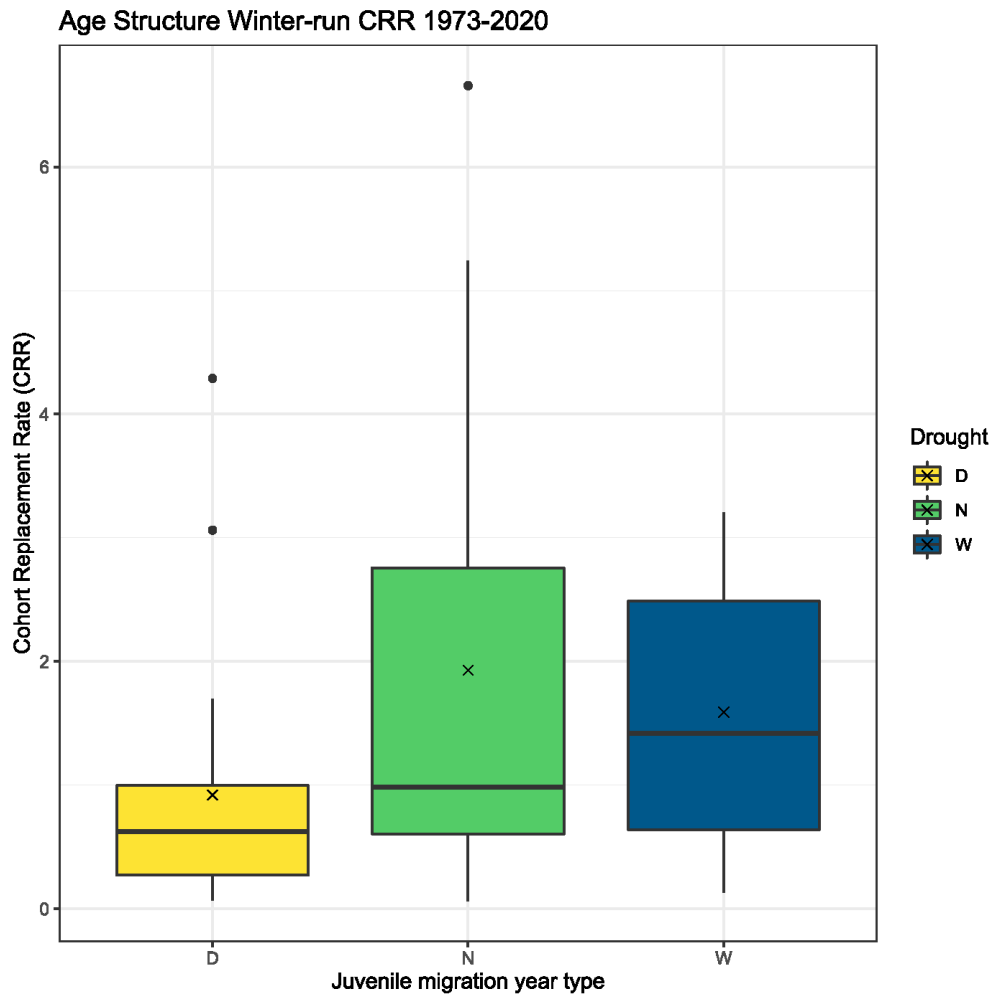


Figure 78. Sacramento River winter-run Chinook Cohort Replacement Rate (1973-2020) by juvenile migration condition (Drought period, Neutral, or Wet period).

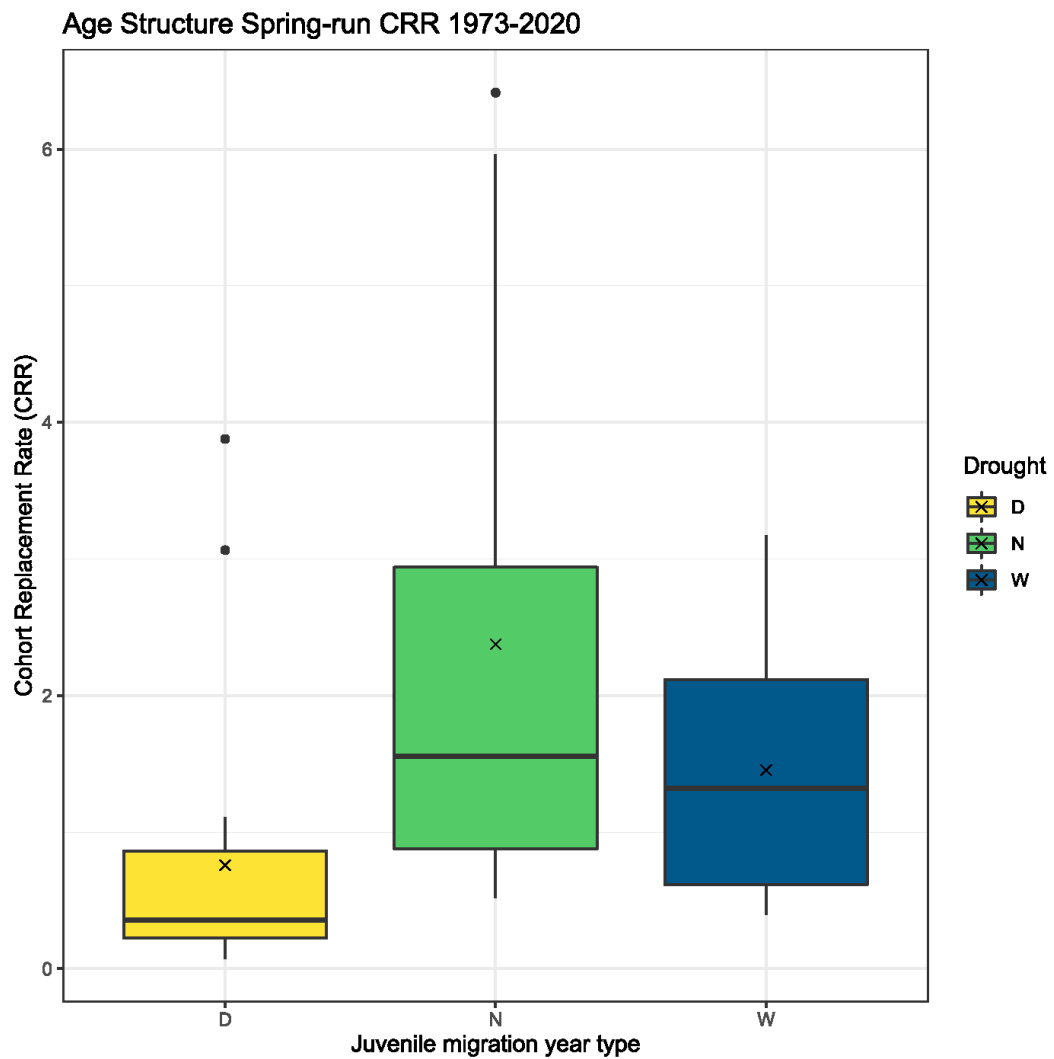


Figure 79. Central Valley spring-run Chinook Cohort Replacement Rate (1973-2020) by juvenile migration condition (Drought period [D], Neutral [N], or Wet period[W]).

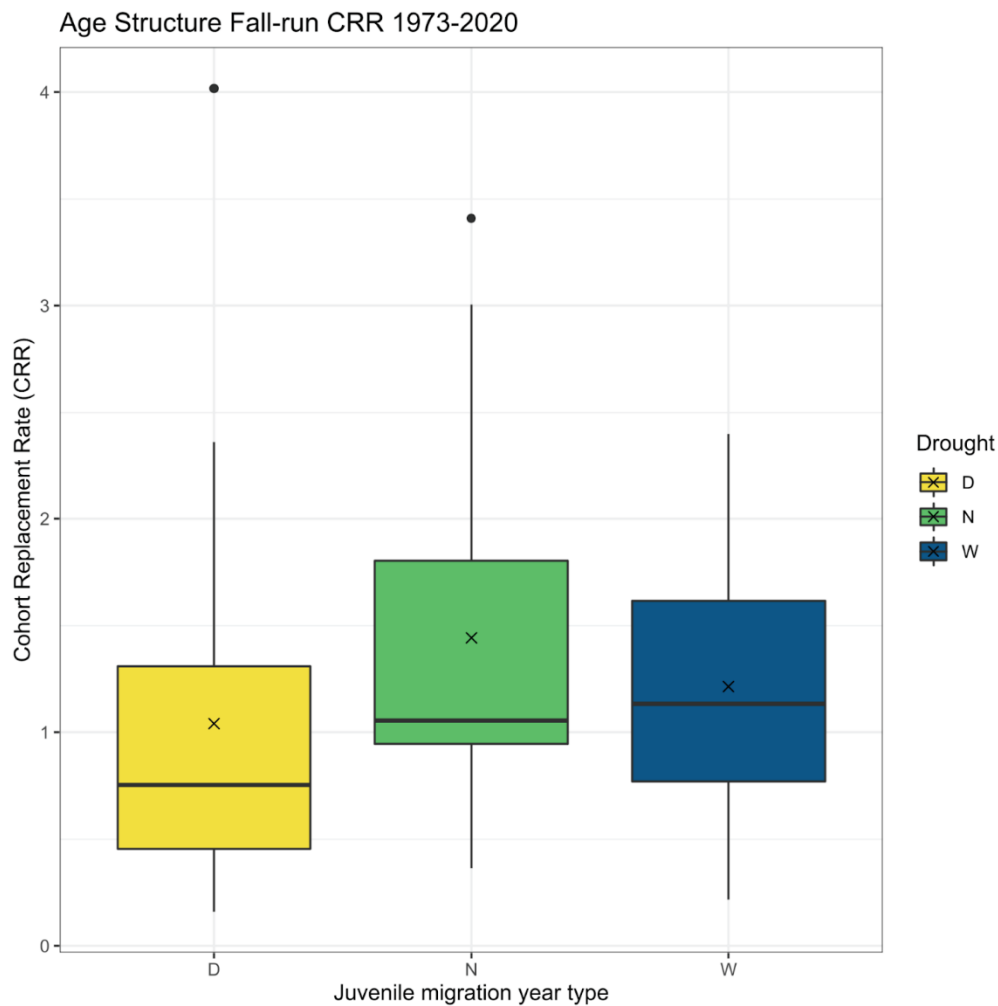


Figure 80. Central Valley fall-run Chinook Cohort Replacement Rate (1973-2020) by juvenile migration condition (Drought period [D], Neutral [N], or Wet period [W]).

Outmigration timing

Separating Chinook run types, Figure 81 and Figure 82 display distribution of migration timing of juvenile Chinook salmon caught at the Sherwood Harbor (Figure 81) and Chipps Island (Figure 82) trawl locations. These combine available trawl data from 1988 to 2021, grouped by the Drought year classification (Drought, Neutral, or Wet Periods).

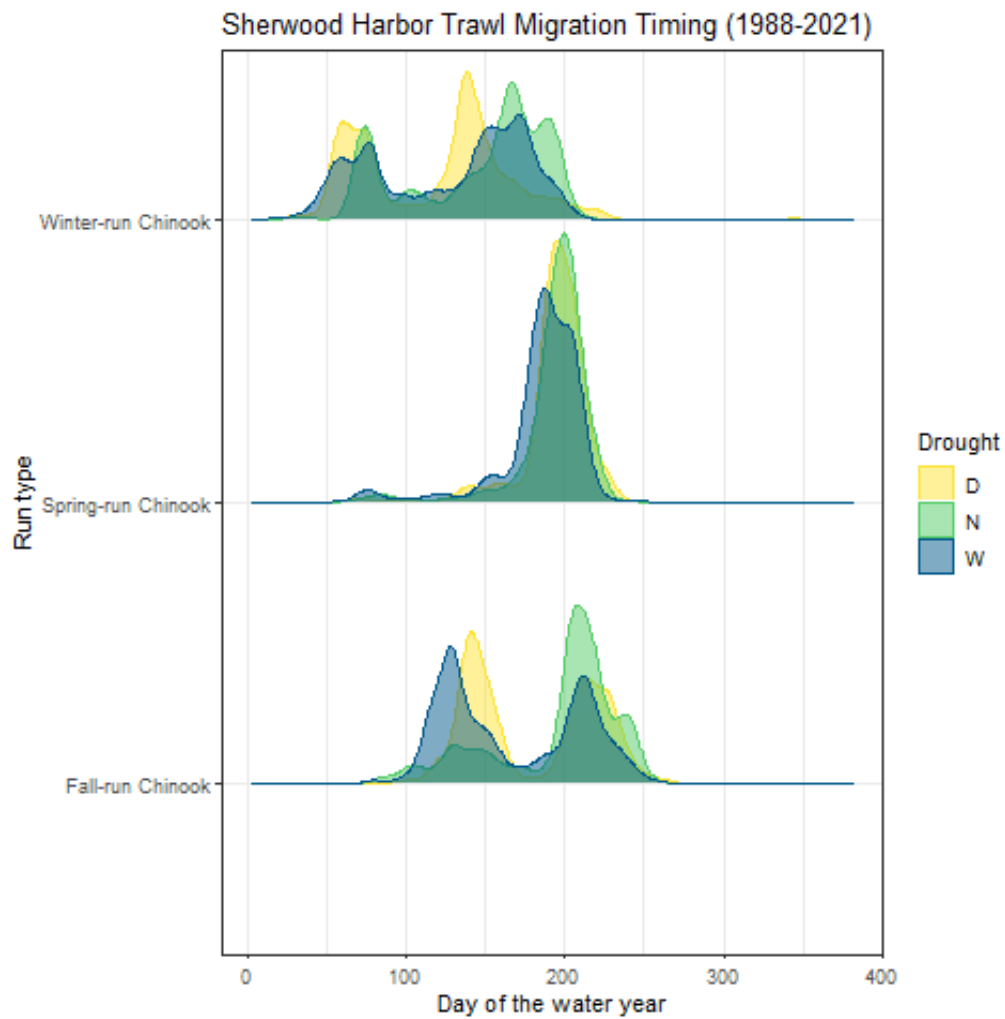


Figure 81. Probability distribution of Juvenile Chinook salmon migration timing at Sherwood Harbor trawls from 1988-2021 by drought period type (Drought [D], Neutral [N], or Wet period [W]).

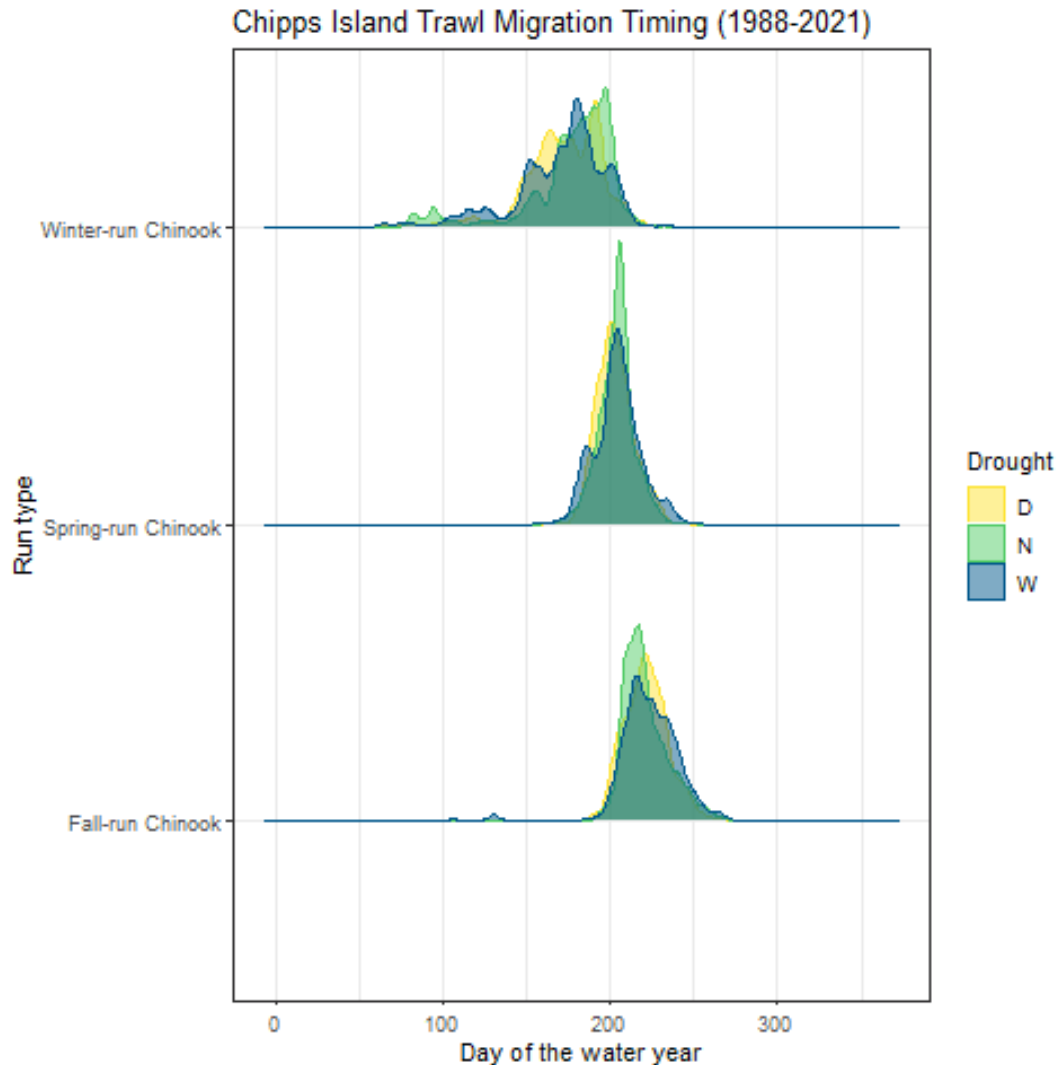


Figure 82. Probability distribution of Juvenile Chinook salmon migration timing at Chippis Island trawls from 1988-2021 by drought year classification (Drought [D], Neutral [N], or Wet period [W]).

Only winter-run Chinook salmon lengths, but not spring-run or fall-run, are shown in Figure 83 due to the considerable overlap in length distributions between spring- and fall-run resulting in a large proportion of incorrect run assignments of those runs by length-at-date criteria (Brandes et al. 2021; Harvey et al. 2014). Winter-run Chinook salmon have the most distinct length-at-date distribution, but the length-at-date race assignments still contain errors when checked against genetic data.

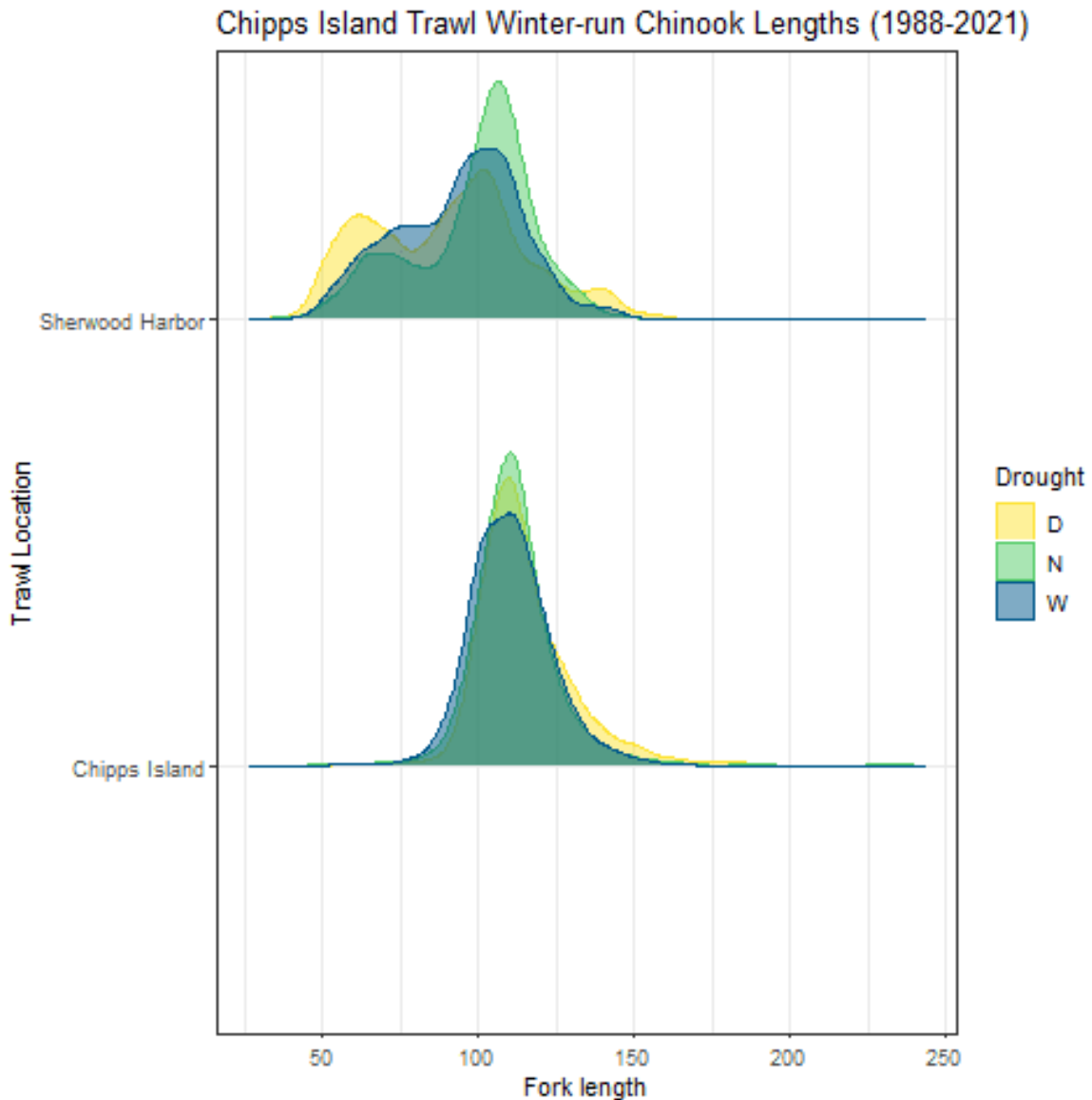


Figure 83. Distribution of lengths of juvenile winter-run-sized Chinook salmon caught at Sherwood Harbor and Chipps Island trawls from 1988 to 2021 by Drought year classification (Drought [D], Neutral [N], or Wet period [W]).

Temporal trends in population indices

Both recent trends of fish catch in the major CDFW surveys and long-term trends show many of the same patterns, with pelagic fish generally doing poorly in dry years (Figure 84). Age-0 Striped Bass hit a record low STN

index of 0.1 in 2021, and had lower SKT and 20mm indexes than 2020. The American Shad index was higher in 2021 than 2020 during the winter and spring, but lower than the wetter years of 2017 and 2019, and no American Shad were caught in the STN survey. Longfin Smelt had higher indexes of abundance in 2021 than 2020, which is somewhat surprising since Delta Outflow was lower than 2020, and Longfin Smelt are known to increase in abundance with outflow. There was no catch of Delta Smelt in any of the CDFW surveys in 2021.

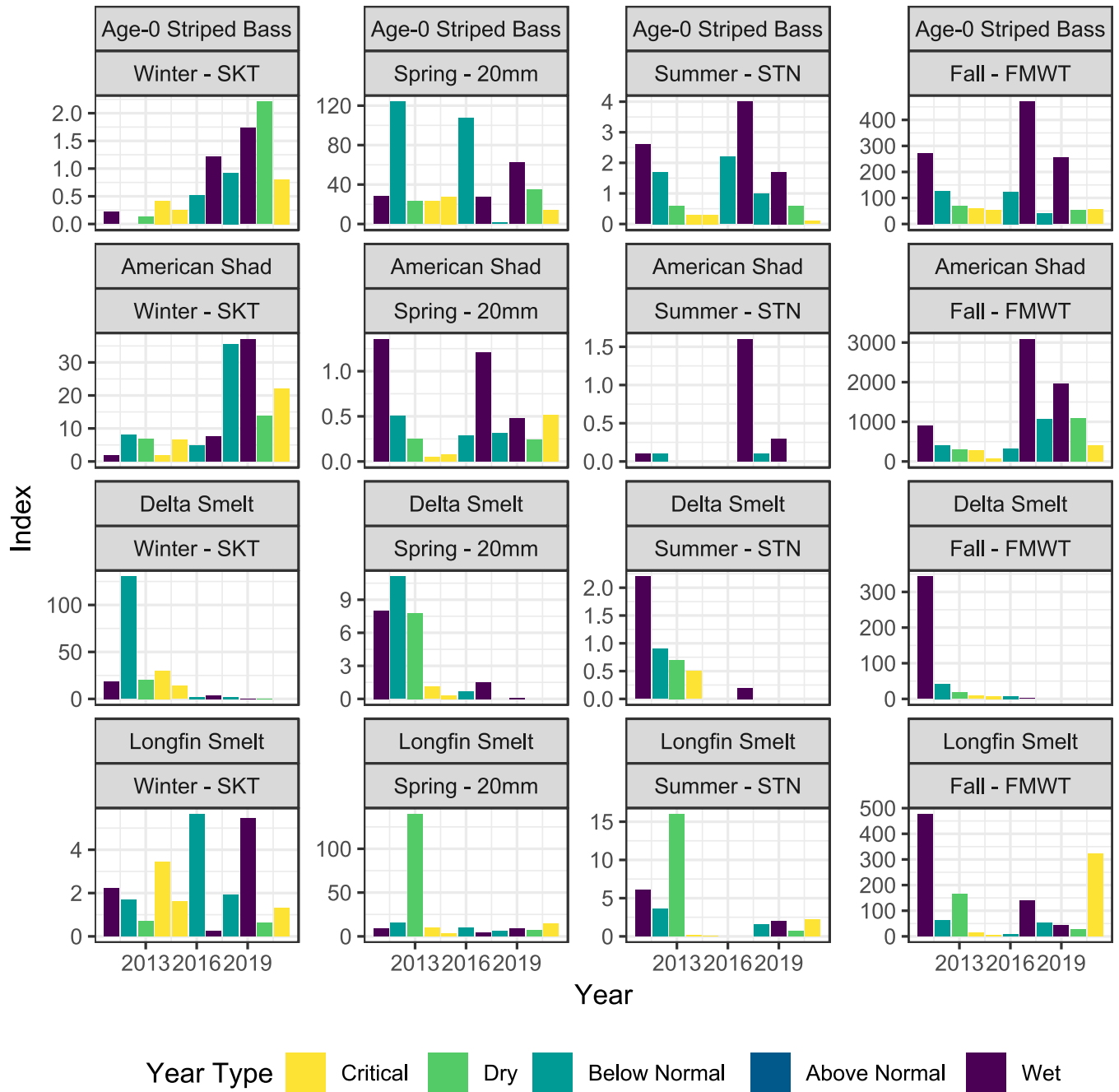


Figure 84. Annual abundance indices for Longfin Smelt, Delta Smelt, Striped Bass, and American Shad as calculated by CDFW for their Spring Kodiak Trawl survey, 20mm survey, Summer Towntnet survey, and Fall Midwater Trawl survey for 2011-2021.

Over the past 50 years, population fluctuations of Threadfin Shad, Delta Smelt, Striped Bass (age-0), and Longfin Smelt were non-random, but American Shad population fluctuations could not be distinguished from random (Table 23).

Table 23. Results of runs test for serial randomness on FMWT indices (1970-2020) for Threadfin Shad, American Shad, Delta Smelt, Striped Bass (age-0), and Longfin Smelt indices showed variable evidence of serial randomness.

Fish	runs	m	n	p-value
Threadfin Shad	14	25	24	0.0006
American Shad	23	25	24	0.282
Delta Smelt	14	25	24	0.0006
Striped Bass (Age-0)	8	25	24	<0.0001
Longfin Smelt	12	25	24	<0.0001

Drought effects

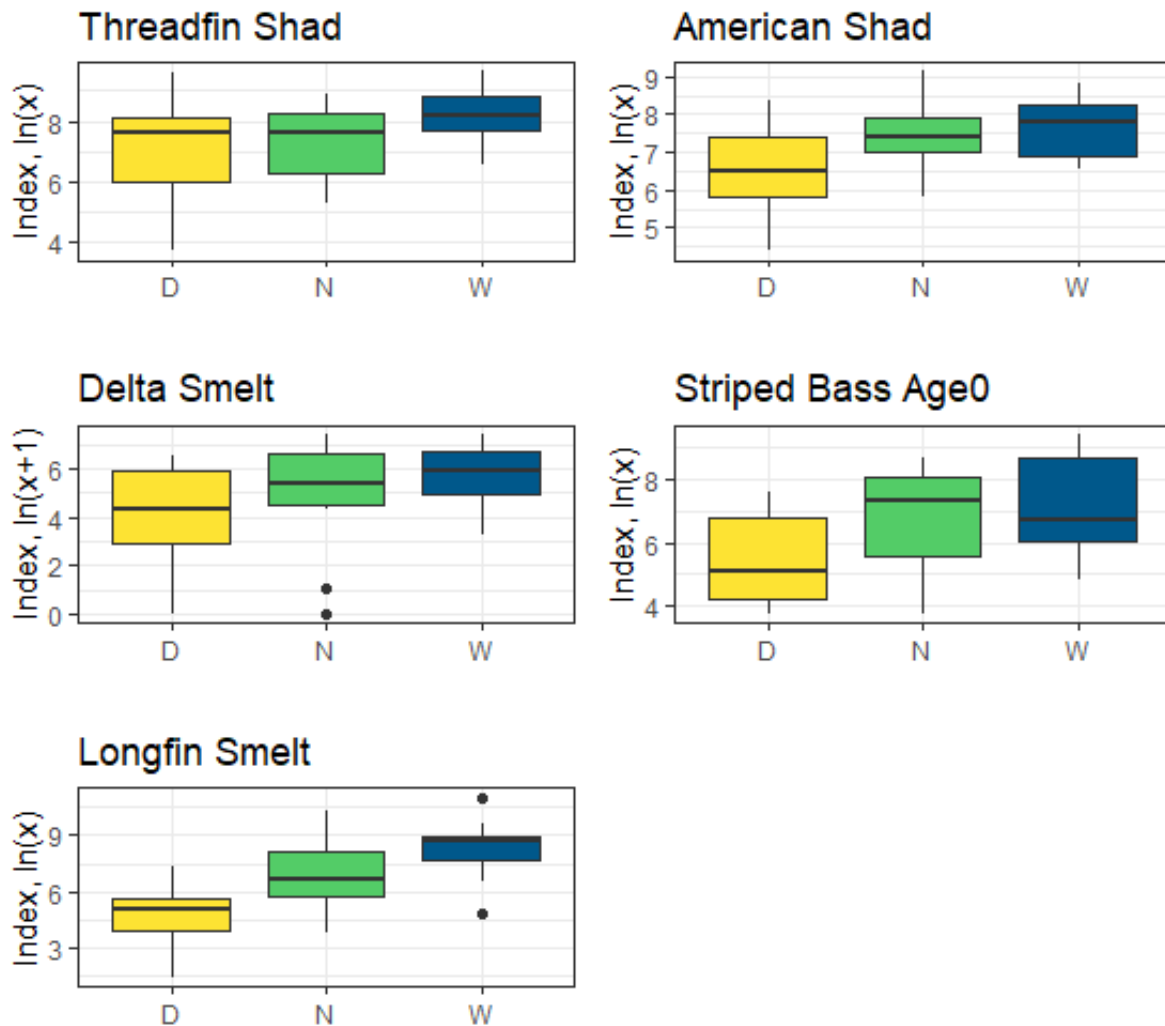


Figure 85. Fall Midwater Trawl indices grouped by drought year classification (Drought period [D], Neutral [N], and Wet period [W]) for five pelagic fish species.

Table 24. Results of ANOVAs run on the log-transformed FMWT index for each fish species. The Delta Smelt model was run on log(index + 1), due to zeros in the data set.

Fish	Model Term	Sum Sq	Mean Sq Error	Num. Df	Den. Df	F-value	P(>F)
------	------------	--------	---------------	---------	---------	---------	-------

Thread fin	Drought	11.172	5.586	2	46	2.9159	0.064
Thread fin	Residuals	88.125	1.916				
American Shad	Drought	11.483	5.742	2	46	7.5921	0.001
American Shad	Residuals	34.788	0.756				
Delta Smelt	Drought	20.874	10.437	2	46	2.8134	0.07
Delta Smelt	Residuals	170.647	3.710				
Longfin	Drought	109.77	54.885	2	46	19.601	<0.0001
Longfin	Residuals	128.80	2.800				
Striped bass	Drought	28.669	14.334	2	46	6.3253	0.004
Striped Bass	Residuals	104.247	2.2662				

Table 25. Pairwise comparisons for the effect of Drought (D) versus Neutral (N) and Wet Periods (W) from ANOVAs presented in Table 24. Results are given on the log (not the response) scale. P value adjustment: tukey method for comparing a family of 3 estimates

Fish	contrast	estimate	SE	Df	t-ratio	P(>t)
Threadfin	D : N	-0.228	0.473	46	-0.483	0.8796

Threadfin	D : W	-1.134	0.482	46	-2.350	0.0589
Threadfin	N : W	-0.905	0.514	46	-1.760	0.1946
American Shad	D : N	-0.898	0.297	46	-3.024	0.0111
American Shad	D : W	-1.061	0.303	46	-3.501	0.0029
American Shad	N : W	-0.163	0.323	46	-0.503	0.8700
Delta Smelt	D : N	-0.625	0.658	46	-0.950	0.6117
Delta Smelt	D : W	-1.592	0.671	46	-2.372	0.0561
Delta Smelt	N : W	-0.967	0.716	46	-1.350	0.3751
Longfin	D : N	-2.02	0.572	46	-3.531	0.0027
Longfin	D : W	-3.60	0.583	46	-6.175	<0.0001
Longfin	N : W	-1.58	0.622	46	-2.545	0.0375
Striped Bass	D : N	-1.224	0.514	46	-2.380	0.0550
Striped Bass	D : W	-1.783	0.525	46	-3.398	0.0040
Striped Bass	N : W	-0.559	0.559	46	-0.999	0.5810

Fish community analyses

Goal 1: Identifying Sub-Community Assemblages and Representative Species

Three dominant tensors (analogous to ordination axes) derived from the community-level principal tensor analysis were identified via an assessment of a scree plot. These dominant tensors explained 44.9% of the variation in the FMWT community dataset. We performed a hierarchical cluster analysis on the Euclidean distances between species scores of these three dominant tensors after accounting for space (sub-region) and time (year) with the optimal number of clusters (3,[Figure 86]) being identified via average silhouette width (Figure 87). Our analysis suggests all species have been correctly assigned in their sub-community assemblage (Figure 87).

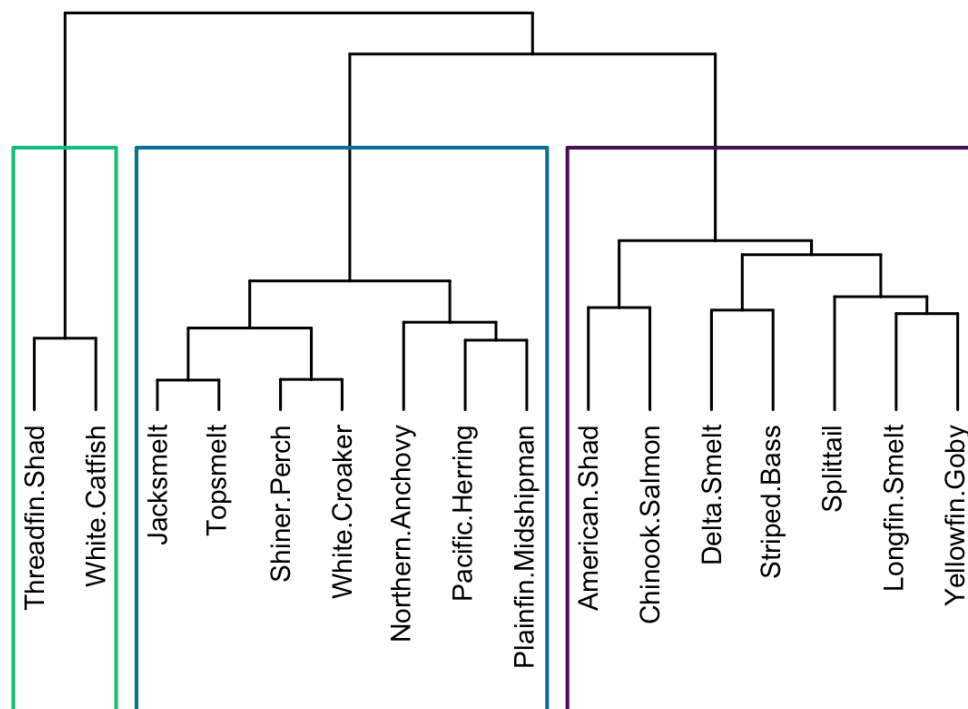


Figure 86. Dendrogram of the species included in this analysis with colored boxes denoting significantly distinct species clusters.

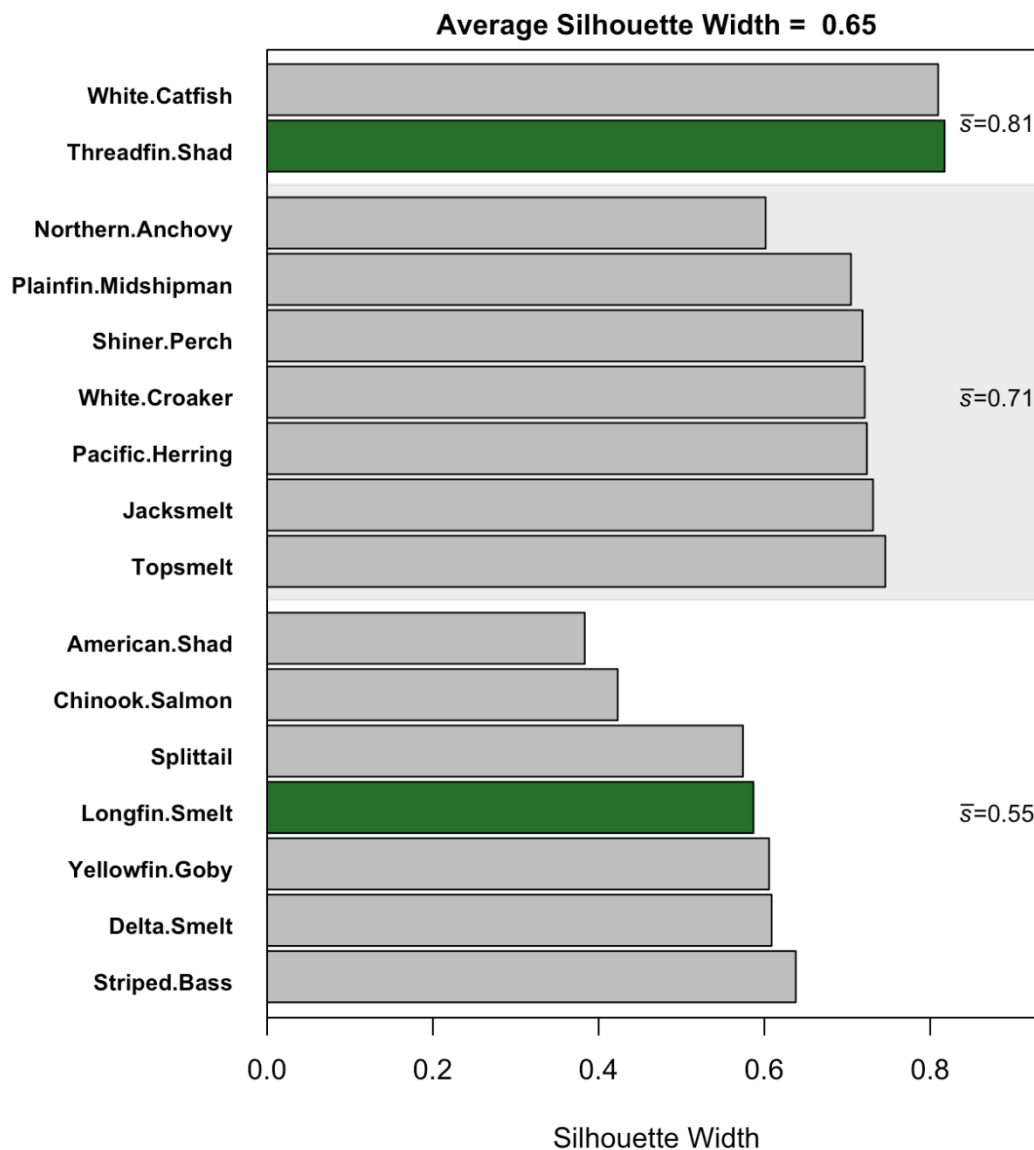


Figure 87. Species specific silhouette widths with sub-community assemblages denoted via background color. Green colored bars denote the selected representative species.

Once the sub-community assemblages were identified, we performed a subsequent PTA on each assemblage to evaluate the relationship between Sacramento Valley Index and the assemblages. The drought year classification analysis indicates that the community differed significantly (i.e., at the $\alpha \leq 0.05$) among year types after accounting for space and species (Figure 88). A significant regression (i.e., a p-value ≤ 0.05) indicates that the community significantly changed across the Sacramento Valley

Index after accounting for space and species (Figure 89). This method cannot indicate exactly how the community changed, only that it did change. Furthermore, the direction of the anomaly is meaningless; the relative change in magnitude of the anomaly, rather, is the key to interpretation.

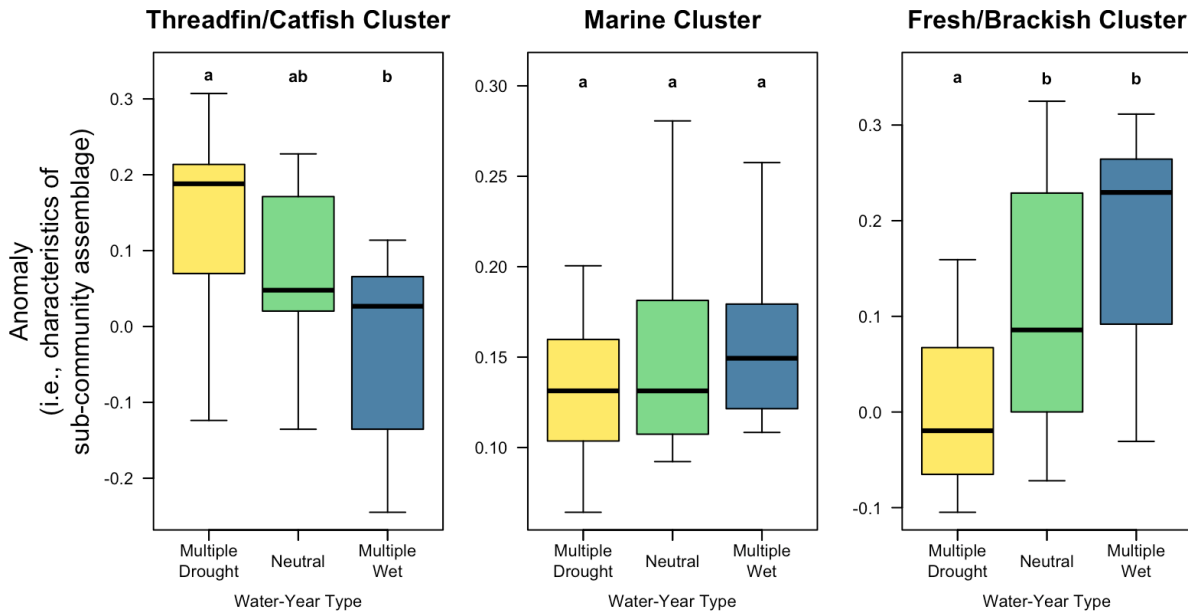


Figure 88. Linear model predicted temporally dominant tensor across drought year classification for (left) the Threadfin Shad/White Catfish cluster, (middle) the marine cluster, and (right) the freshwater/brackish cluster. Letters above boxes indicate significantly different catch after accounting for species and sub-region. Note: the directionality of the anomaly can be positively or negatively related to catch; additional analyses are necessary to identify the trend.

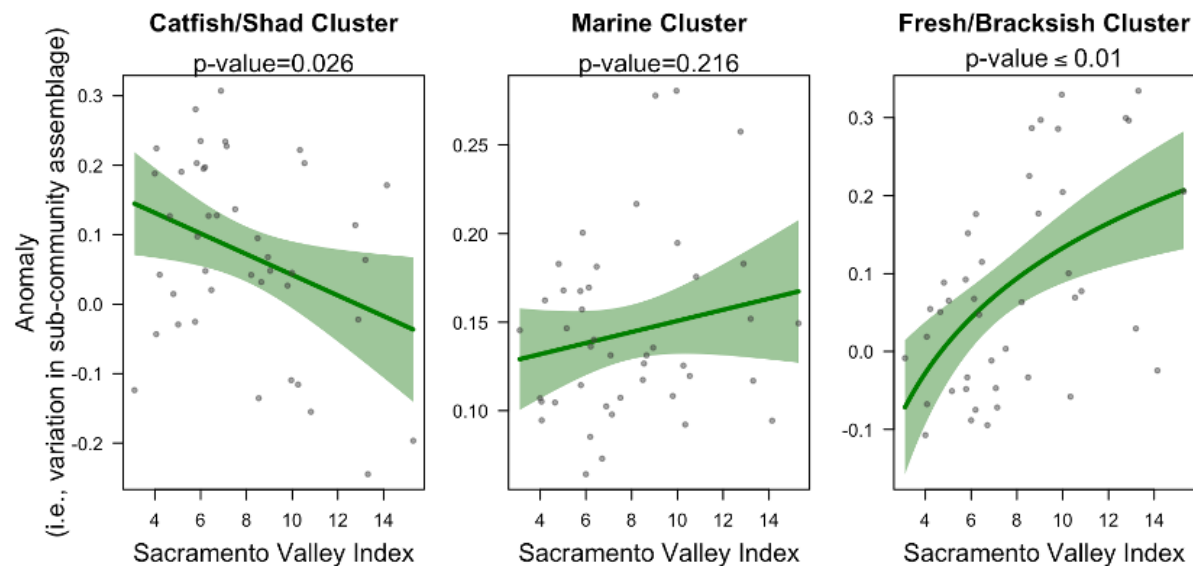


Figure 89. Linear model predicted mean temporally dominant tensor across the observed range of the Sacramento Valley Index for (left) the Threadfin Shad/White Catfish cluster, (middle) the Marine cluster, and (right) the freshwater/brackish cluster. Shown with model confidence interval (polygon) and data (points). A significant p-value (i.e., ≤ 0.05) indicates the catch within the cluster changed significantly with the Sacramento Valley Index after accounting for species and sub-region. Note: the directionality of the anomaly can be positively or negatively related to catch; additional analyses are necessary to identify the trend.

Goal 2: Drought and Representative Species Catch

Figure 89 and Figure 88 strongly suggest the fish community as detected by the Fall Midwater Trawl is associated with drought, but these PTA anomaly plots do not indicate how the community changes.

The ZINB analysis indicates that Threadfin Shad catch is equally low during Droughts and Neutral water-years but is significantly higher during Wet periods (Figure 90).

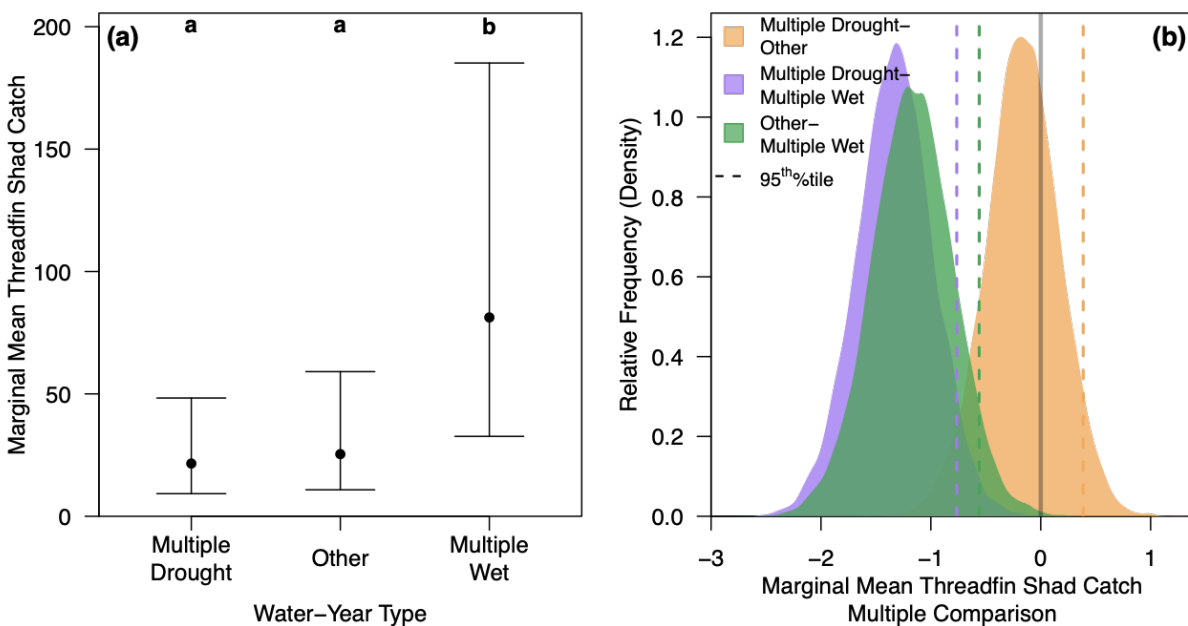


Figure 90. Threadfin Shad model results. (a) Marginal mean Threadfin Shad catch highest probably densities Drought year classifications (Multiple Drought (Elsewhere “Drought”), “Neutral”, and Multiple Wet (Elsewhere “Wet Period”)). Letters above points indicate significant differences. (b) Bonferroni-corrected multiple comparisons of marginal means among water year type. Pairs with $\geq 95\%$ of posterior comparisons < 0 are considered significantly different water year types.

The ZINB analysis indicates that Longfin Smelt catch is significantly lower during Drought years than the Neutral water year categories (Figure 91).

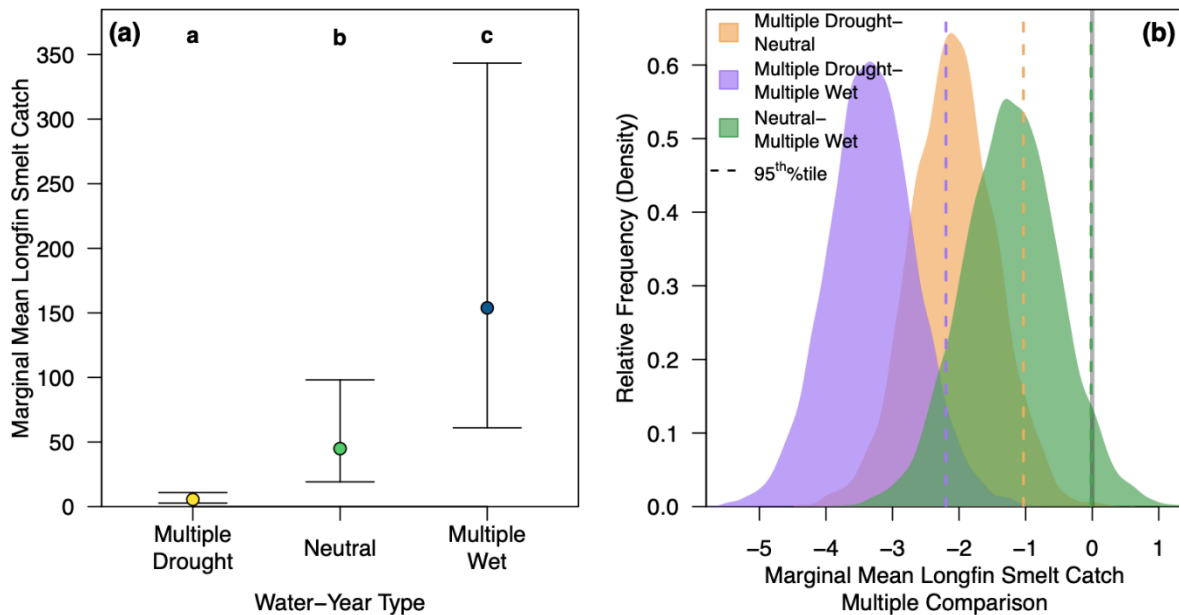


Figure 91. Longfin Smelt model results. (a) Marginal mean Longfin Smelt catch highest probably densities among Drought year classifications (Multiple Drought (Elsewhere “Drought”), “Neutral”, and Multiple Wet (Elsewhere “Wet Period”)). Letters above points indicate significant differences. (b) Bonferroni-corrected multiple comparisons of marginal means among water year type. Pairs with $\geq 95\%$ of posterior comparisons < 0 are considered significantly different water year types

Representative Species Catch Associated with a Continuous Drought Metric

The analysis indicates that, when holding other variables constant at their medians, Threadfin Shad catch was slightly higher pre-POD than post-POD (Figure 92); however, the pattern is not significant. When varying either Sacramento Valley Index in Year_t (Figure 93a) or Sacramento Valley Index in Year_{t-1} (Figure 93b) while holding the other variable constant at the Department of Water Quality water year hydrologic classification threshold value between Below Normal and Above Normal (i.e., Sacramento Valley Index = 7.8), the model confirms the pattern of no significant difference between pre- and post-POD. However, the non-linear interactive nature of the models allows for a more in-depth evaluation of the relationship between Threadfin Shad catch and drought. Specifically, the model highlights three interesting patterns:

1. Threadfin Shad is fairly constant at low to moderate values of Sacramento Valley Index in Year_t and Sacramento Valley Index in Year_{t-1}. However, catch increases sharply when Sacramento Valley

Index in Year_t and Sacramento Valley Index in Year_{t-1} are both $\sim \geq 11$ (Figure 94).

2. The San Francisco Estuary has not had conditions that are associated with these high catches in the post-POD era (Figure 94b, d, & e).
3. While catch at moderate values of Sacramento Valley Index in Year_t and Sacramento Valley Index in Year_{t-1} do not differ significantly between the pre- and post-POD eras (mean Sac Index_t = 8 and Sac Index_{t-1} = 10, asterisks in figures 94 and 95) and we lack the data to evaluate high values in the post-POD era, Threadfin Shad catch is significantly lower post-POD during extreme drought conditions relative to pre-POD (Figure 95).

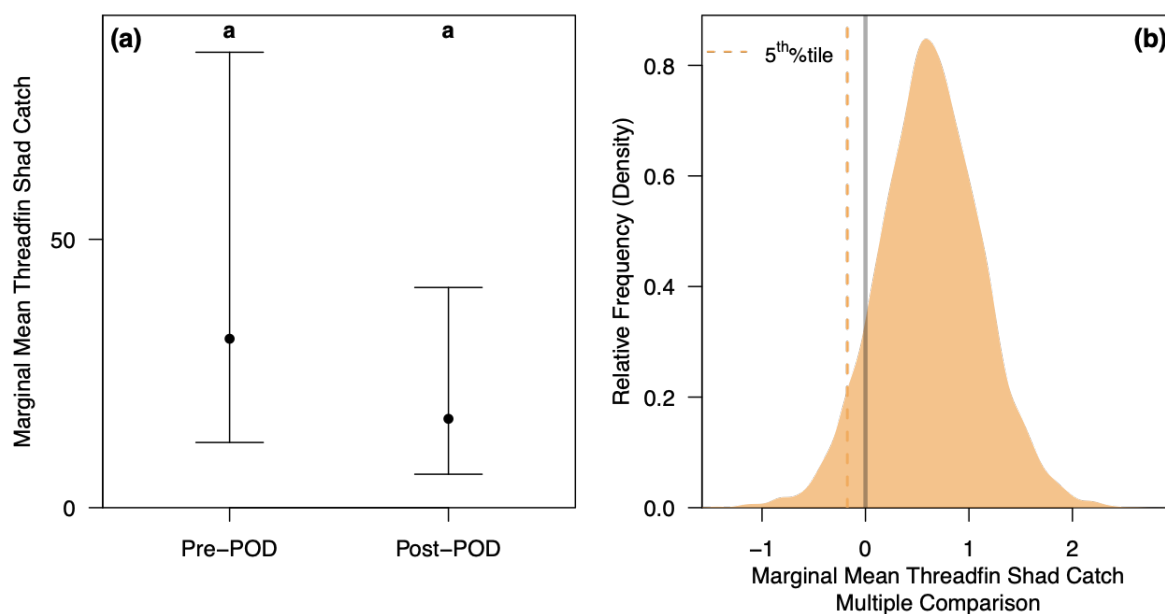


Figure 92. Threadfin Shad POD effect. (a) Threadfin Shad median catch Pre- and Post-POD (error bars represent 89% credible interval; categories labeled with different letters are significantly different). (b) Comparisons of catch between Pre- and Post-POD periods. A comparison with $\geq 95\%$ of posterior comparisons > 0 are considered significantly different. Model predictions are based on 2,000 posterior draws given the median of 20 sampling events per sub-region per year, the median Sacramento Valley Index in Year_t of 7.08, and the median Sacramento Valley Index in Year_{t-1} of 6.89.

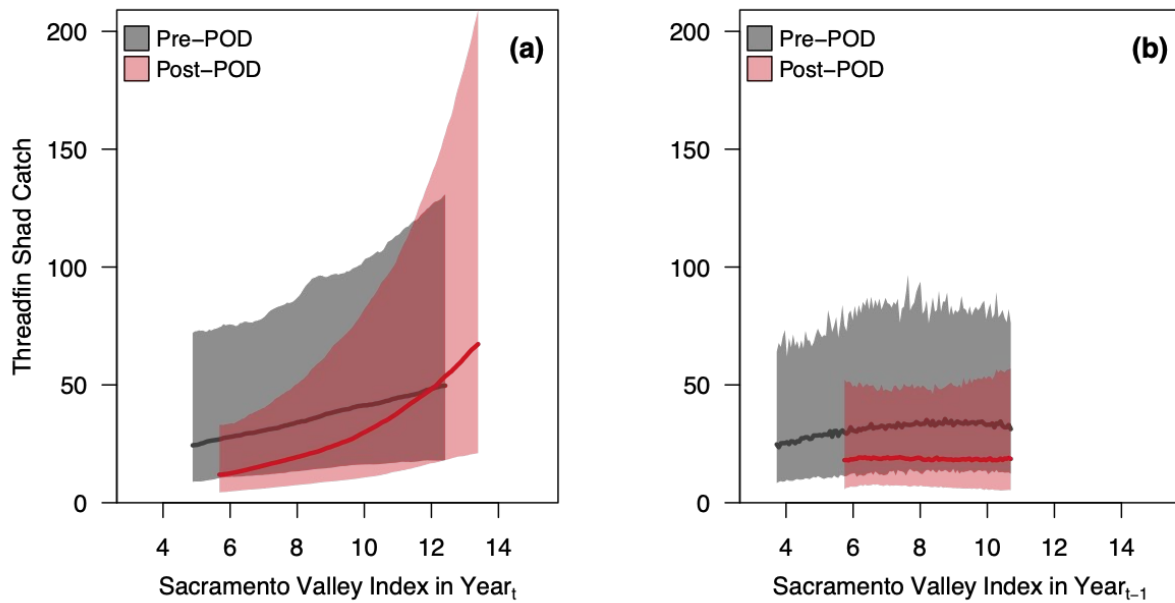


Figure 93 Threadfin Shad model prediction across (a) Sacramento Valley Index in Year_t given the Department of Water Quality water year hydrologic classification of threshold value between Below Normal and Above Normal (Sacramento Valley Index = 7.8) in Sacramento Valley Index in Year_{t-1} and (b) Sacramento Valley Index in Year_{t-1} given the hydrologic classification threshold value between Below Normal and Above Normal (Sacramento Valley Index = 7.8) in Sacramento Valley Index in Year_t. Lines represent median prediction and polygons represent 89% credible interval. Model predictions are based on 2,000 posterior draws given the median of 20 sampling events per sub-region per year. Data are constrained to the convex hull of observed values shown in Figure 94.

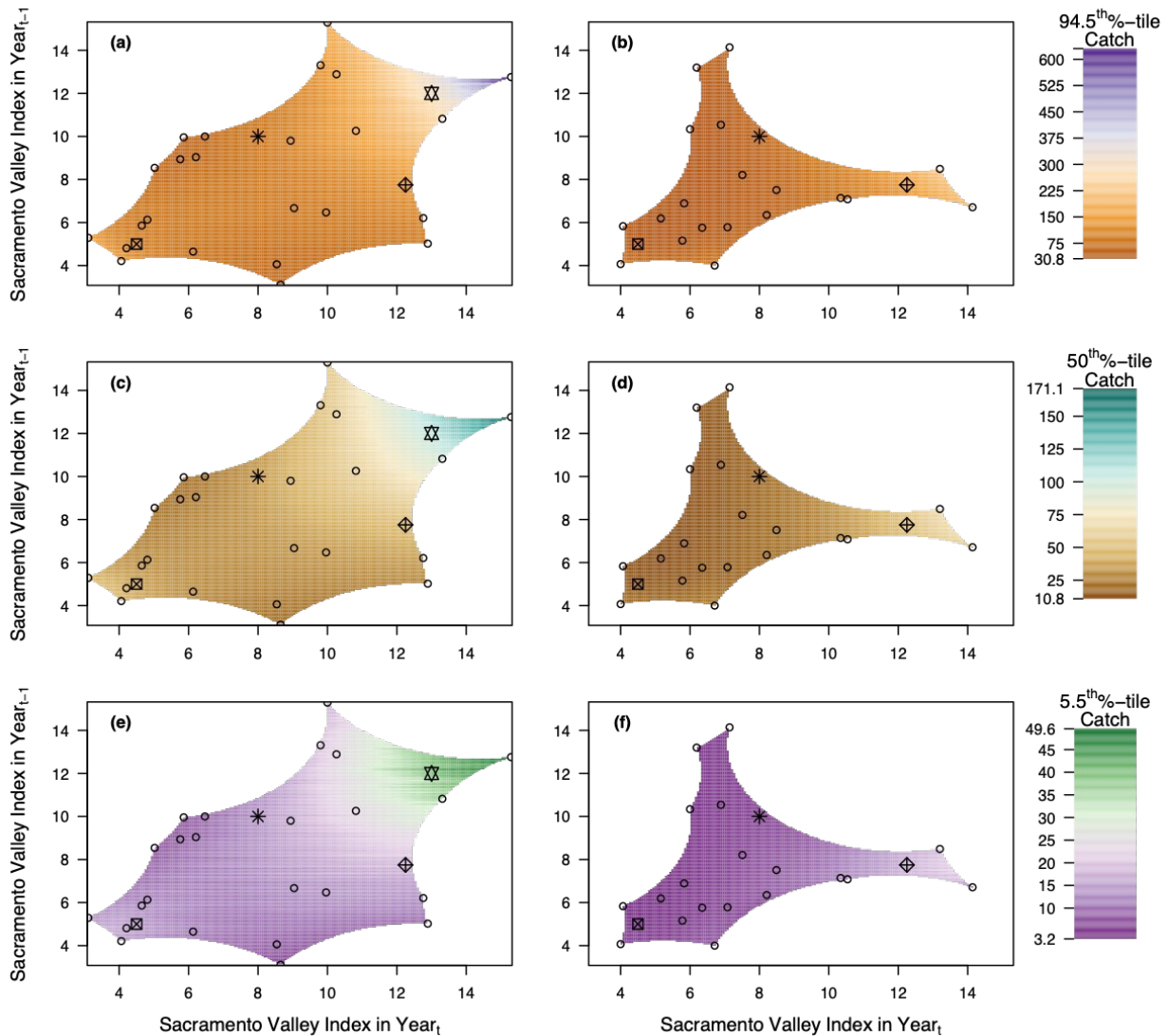


Figure 94 Threadfin Shad ZINB model (a, c, and e) pre- and (b, d, and f) post-POD (i.e., 2002) predicted (c and d) median catch, (a and b) upper 89% credible interval limit, and (e and f) lower 89% credible interval limit across Sacramento Valley Index in Year_t and Sacramento Valley Index in Year_{t-1} based on 2,000 posterior draws and given the median of 20 sampling events per sub-region per year. Open circles indicate observed values of Sacramento Valley Index in Year_t and Sacramento Valley Index in Year_{t-1}. The non-open circle points correspond to Sacramento Valley Index in Year_t and Sacramento Valley Index in Year_{t-1} scenarios predicted in Figure 95.

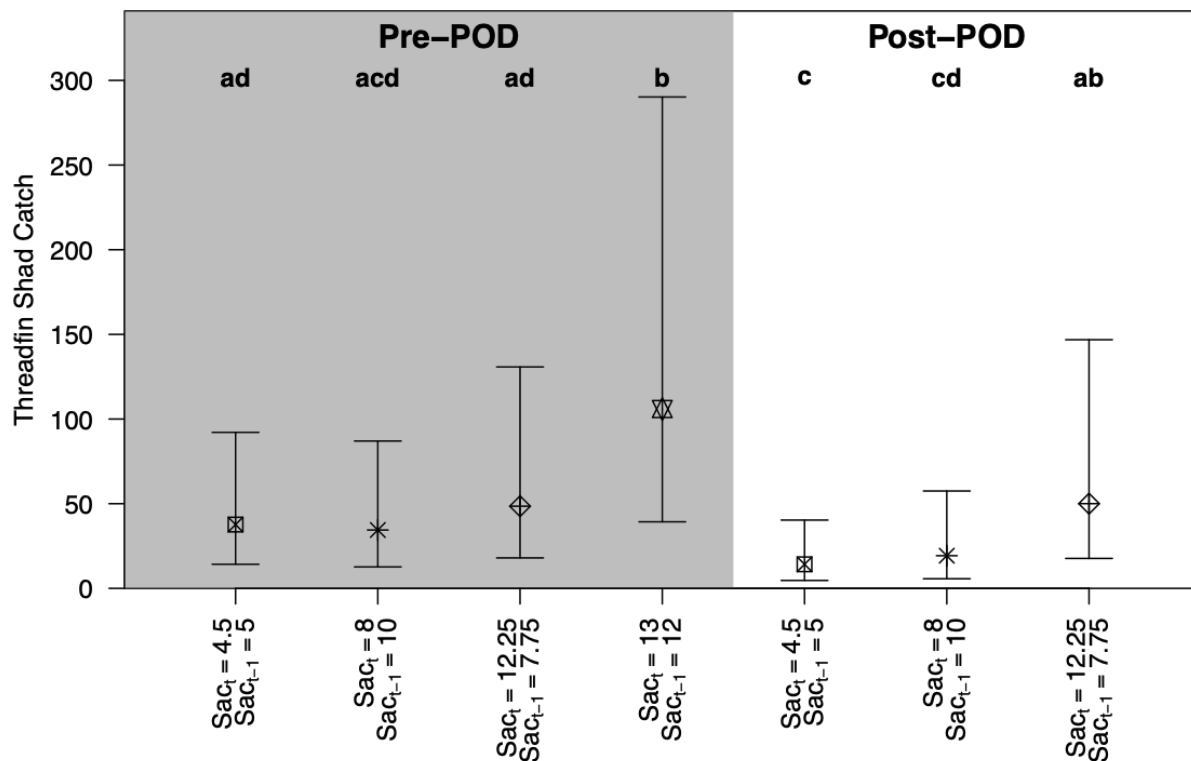


Figure 95. Threadfin Shad ZINB model marginal mean catch given specific values of Sacramento Valley Index in Year_t (Sac_t) and Sacramento Valley Index in Year_{t-1} (Sac_{t-1}). The point type corresponds to the same point type in Figure 94. Error bars represent 89% credible interval. Posterior draws are based on the median of 20 sampling events per sub-region per year

The analysis indicates that, when holding other variables constant at their medians, Longfin Smelt catch was significantly higher pre-POD than post-POD (Figure 96). Longfin Smelt catch increased with Sacramento Valley Index in Year_t while holding the Sacramento Valley Index in Year_{t-1} constant at 7.8 (threshold value between Below Normal and Above Normal; Figure 97a). However, Sacramento Valley Index in Year_{t-1} did not exhibit a strong relationship with catch when holding the Sacramento Valley Index in Year_t constant 7.8; (Figure 97b). When evaluating catch across the observed ranges of Sacramento Valley Index in Year_t and Sacramento Valley Index in Year_{t-1} our analysis highlights three interesting patterns:

1. Longfin Smelt catch increases steadily with increases Sacramento Valley Index in Year_t during the pre-POD era and only very weakly increases during the post-POD era (Figure 97).

2. Unlike Threadfin Shad, in the pre-POD era Longfin Smelt the above pattern weakens with increased Sacramento Valley Index in Year_{t-1} (Figure 98a, c, & e).
3. The San Francisco Estuary has not had conditions that are associated with high Longfin Smelt catches in the post-POD era (Figure 98b, d, & e).
4. However, Longfin Smelt catch in the pre-POD only significantly higher than the post-POD at moderate to high values of Sacramento Valley Index in Year_t (Figure 99), values rarely seen in the post-POD era (Figure 98).

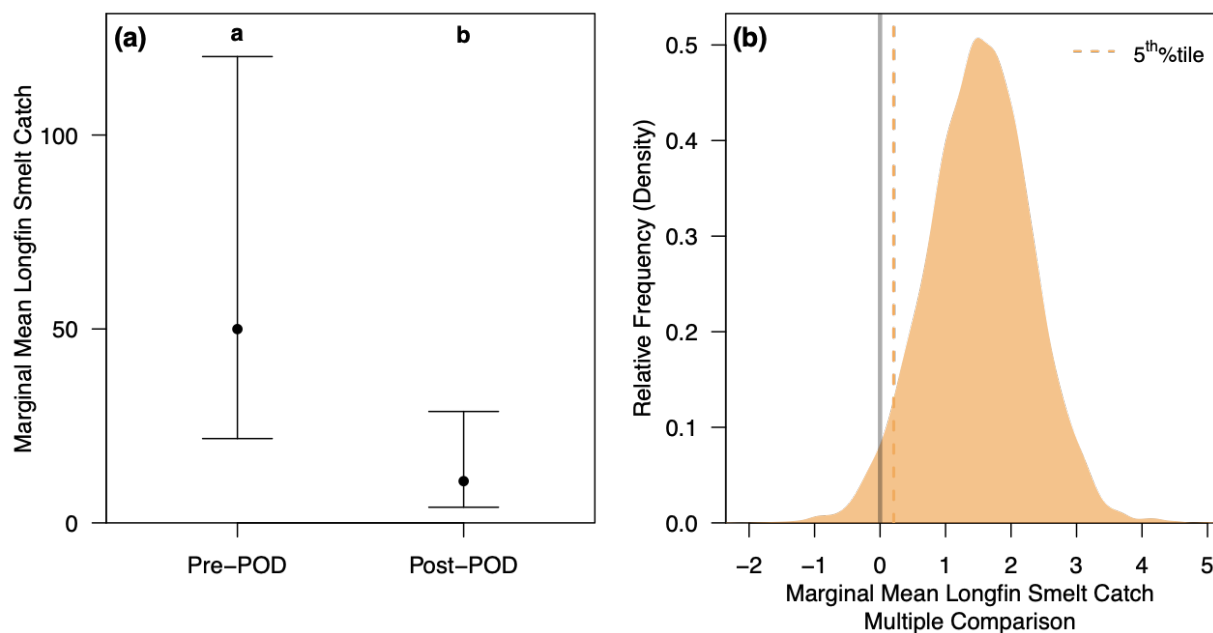


Figure 96. Longfin Smelt POD effect. (a) Longfin Smelt median catch Pre- and Post-POD (error bars represent 89% credible interval; categories labeled with different letters are significantly different). (b) Comparisons of catch between Pre- and Post-POD periods. A comparison with $\geq 95\%$ of posterior comparisons > 0 are considered significantly different. Model predictions are based on 2,000 posterior draws given the median of 20 sampling events per sub-region per year, the median Sacramento Valley Index in Year_t of 7.08, and the median Sacramento Valley Index in Year_{t-1} of 6.89.

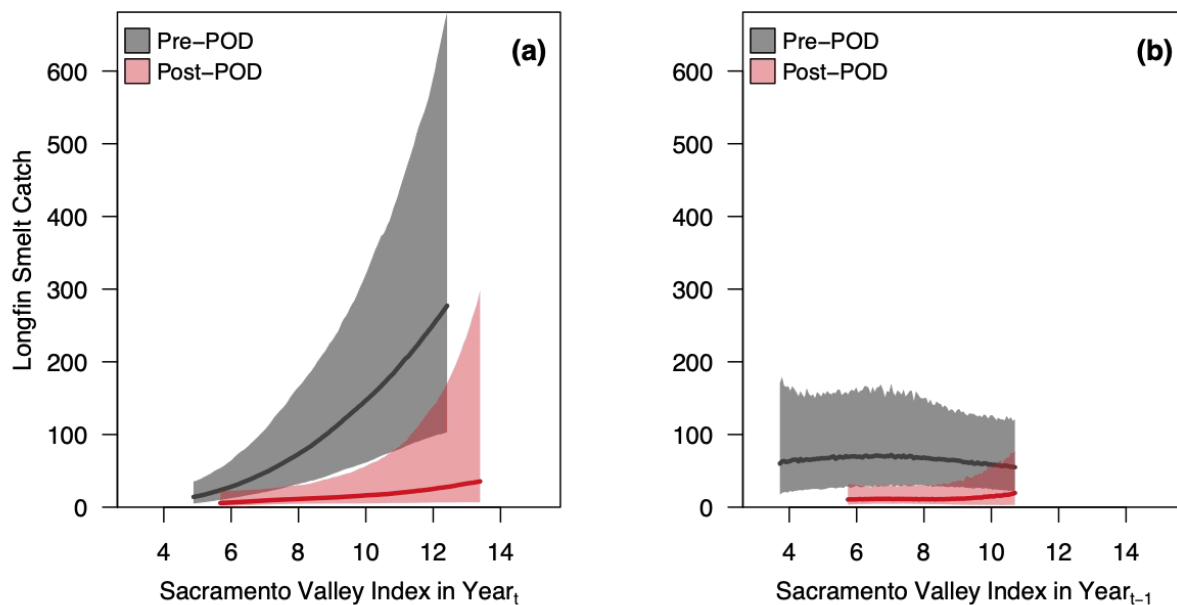


Figure 97. Longfin Smelt model prediction across (a) Sacramento Valley Index in Year_t given the Sacramento Valley Index of 7.8 in Year_{t-1} and (b) Sacramento Valley Index in Year_{t-1} given Sacramento Valley Index of 7.8 in Year_t. Lines represent median prediction and polygons represent 89% credible interval. Model predictions are based on 2,000 posterior draws given the median of 20 sampling events per sub-region per year. Data are constrained to the convex hull of observed values shown in Figure 98.

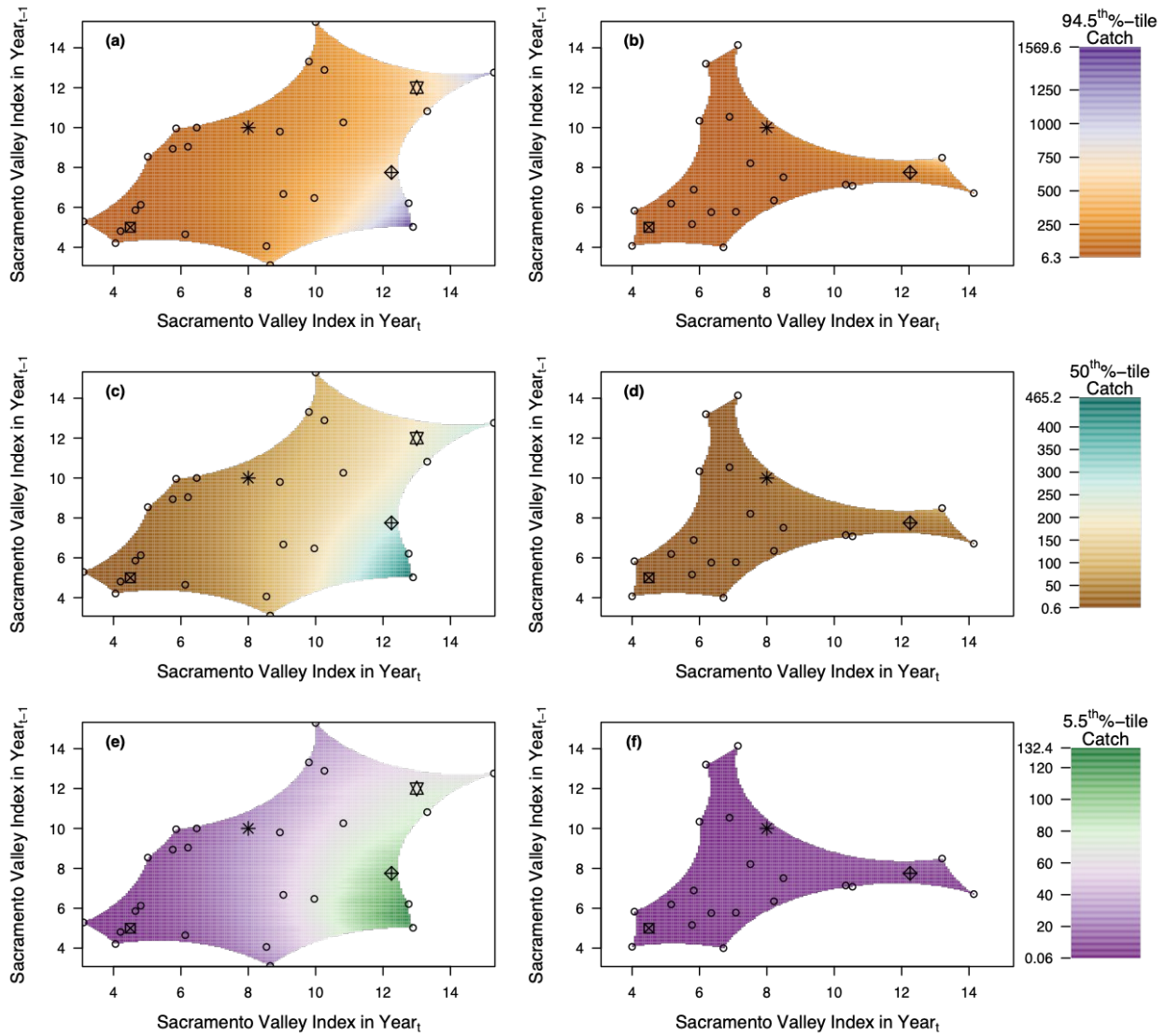


Figure 98 Longfin Smelt ZINB model (a, c, and e) pre- and (b, d, and f) post-POD (i.e., 2002) predicted (c and d) median catch, (a and b) upper 89% credible interval limit, and (e and f) lower 89% credible interval limit based on 2,000 posterior draws. Points indicate year-specific observed values of Sacramento Valley Index in Year_t and Sacramento Valley Index in Year_{t-1} based on 2,000 posterior draws and given the median of 20 sampling events per sub-region per year. Open circles indicate observed values of Sacramento Valley Index in Year_t and Sacramento Valley Index in Year_{t-1}. The non-open circle points correspond to Sacramento Valley Index in Year_t and Sacramento Valley Index in Year_{t-1} scenarios predicted in Figure 99.

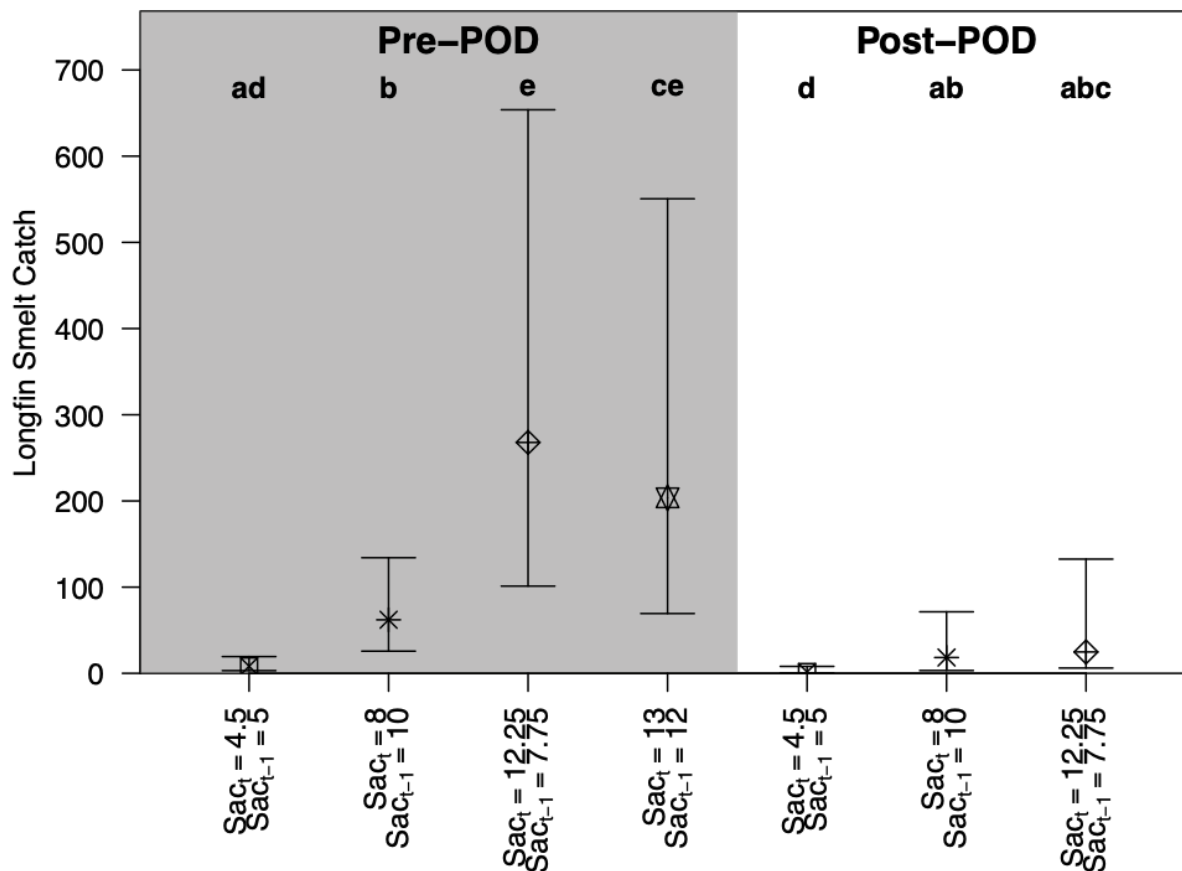


Figure 99. Longfin Smelt ZINB model marginal mean catch given specific values of Sacramento Valley Index in Year_t (Sac_t) and Sacramento Valley Index in Year_{t-1} (Sac_{t-1}). The point type corresponds to the same point type in Figure 98. Error bars represent 89% credible interval. Posterior draws are based on the median of 20 sampling events per sub-region per year.

Summary Plot

After qualitatively assessing the response of all the environmental parameters to droughts, a few stand out as most important to management (Figure 100). Decreases to outflow and increases to salinity and temperature drive increases in nutrients, *P. amurensis* grazing rates, and *Microcystis*. They also drive decreases in chlorophyll and pelagic fish populations. Zooplankton increase in the Central Delta and decrease in Suisun Bay. In

2021, many of these patterns held, but some parameters were greater or less than in historic droughts (Figure 101).

Ecosystem Responses to Drought

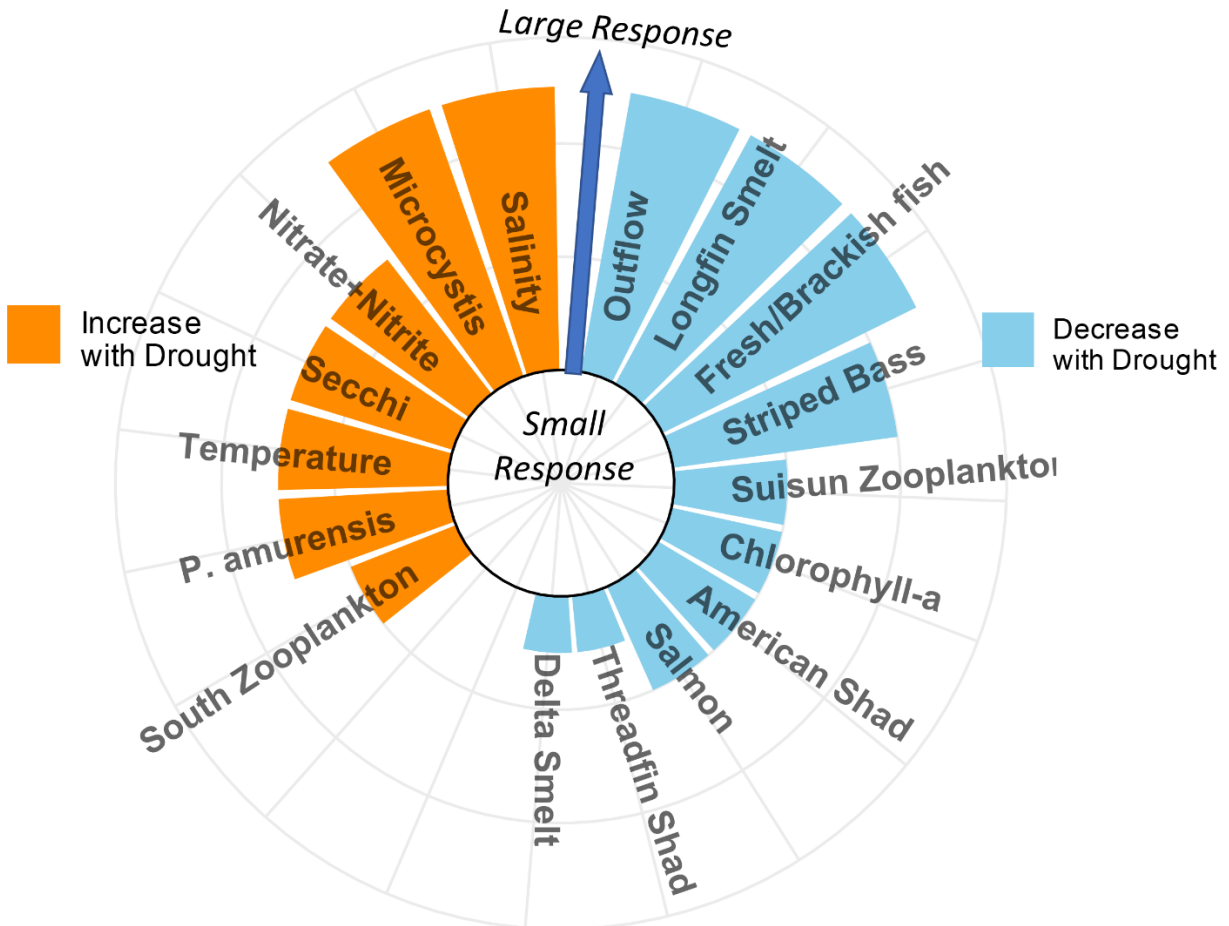


Figure 100. Plot of major ecological parameters and their relationship with Drought relationships were ranked on a qualitative scale of zero (no relationship) to 5 (large relationship) to multi-year droughts. Blue bars on the right side of the circle represent parameters with decreases during droughts. Orange bars on the left side of the circle represent parameters that increase during droughts.

Conditions in 2021 compared to previous droughts

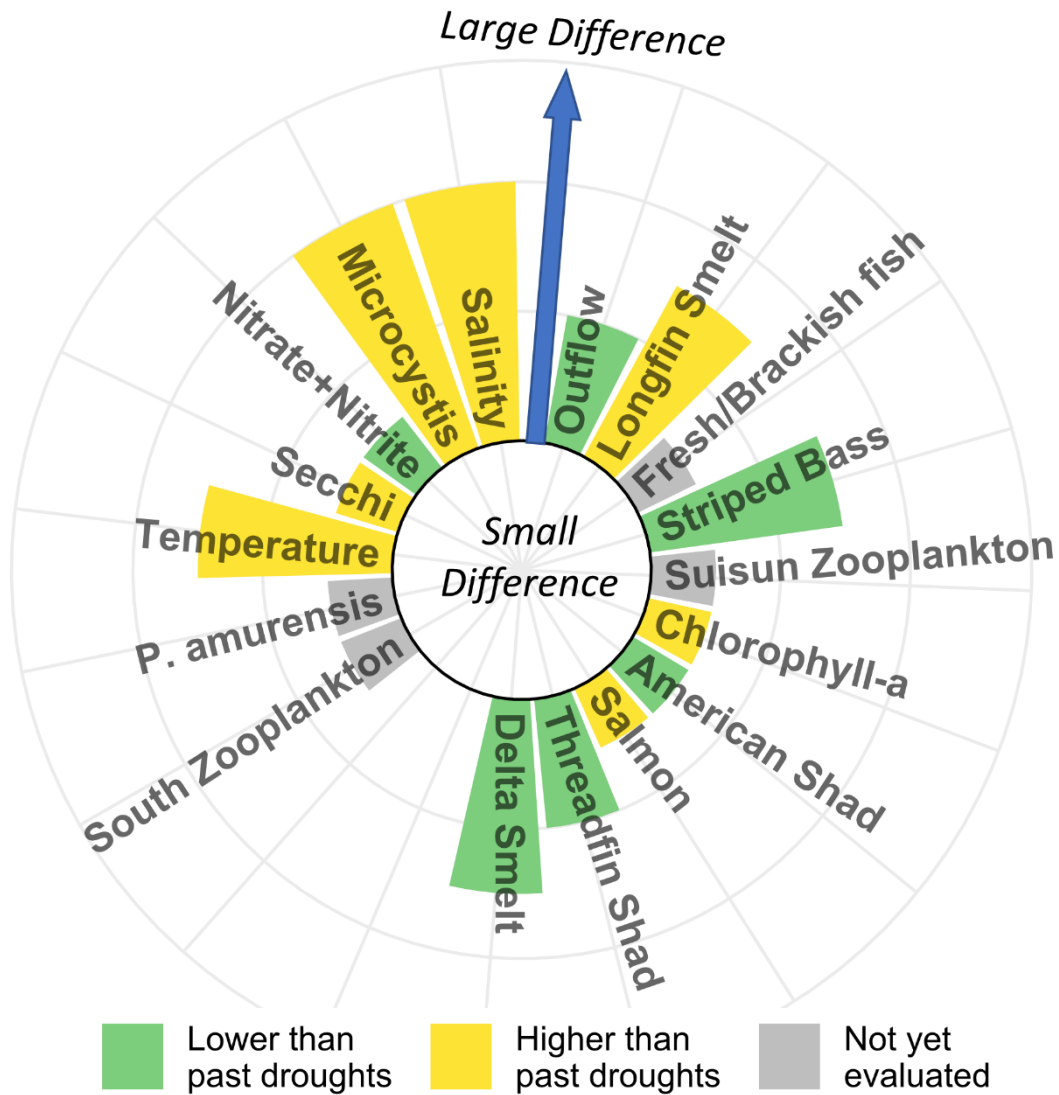


Figure 101. Plot of major ecological parameters in 2021 and their magnitude in comparison to previous droughts. Some of these differences may be due to the 2021 TUCP and/or Emergency Drought Barrier. Relationships were ranked on a qualitative scale of zero (similar to previous droughts) to 5 (very different from previous droughts). Green bars represent parameters that decreased relative to past droughts. Yellow bars represent parameters that increased relative to past droughts. Grey bars are parameters for which we have not completed data processing and analysis. Some parameters are

only available through September of 2021, so this plot should be considered preliminary.

Discussion

Drought in the Delta

The overall effect of drought in the Delta includes physical changes to hydrology and water quality, which have cascading effects on the ecosystem (as indicated in Figure 100). These include reduced flow, increased water clarity, and often increased nutrient concentrations. Zooplankton and phytoplankton increase locally, particularly at intermediate flows, but are low in most regions of the Delta during critically dry years. Most pelagic fish decline, and anadromous fishes change their migration patterns. With these changes, water resource managers decrease diversions from the Delta, shift outflow patterns, and attempt to balance human and environmental needs for an increasingly scarce water supply.

The drought of 2020 and 2021 stands out in being hotter than previous droughts, and some of the patterns we found for droughts in general became more extreme in 2021 (Figure 1010). Many stressors have been steadily increasing over the past several decades, so extracting which environmental stressors were due to the drought and which were due to other factors is difficult. Drought management actions in 2021, including construction of the Emergency Drought Barrier in West False River and the TUCP reducing Delta Outflow during the summer had localized flow and water quality effects. However, 2020 and 2021 experienced some of the highest water temperatures in our records. Harmful algal blooms and aquatic weeds reached new heights of density and abundance. Pelagic fishes continued their downward trends. Drought management actions were unlikely to affect these decadal trends, or system-wide drought response. Future management actions during droughts will need to take into account the impact of rising temperatures interacting with increasing precipitation variability when planning management responses to droughts.

Hydrology

Reduction in flow is one of the primary drivers behind all changes to the ecosystem during a drought. It was therefore not surprising that outflow, exports, and X2 differ significantly across years, season, and water year indices. 2021 had lower outflow and higher X2 than previous droughts, which was a direct result of the TUCP.

Delta outflow showed clear patterns, but other factors may be important during very dry conditions, including in-Delta water use and local conditions. Dayflow outputs may not be the best measure of hydrodynamics in the Delta under low flow conditions (<10,000 cfs). We compared Dayflow outflow to USGS combined outflow measured directly at four USGS continuous monitoring stations revealed a poor relationship during low flows between the two (as previously described by Monismith (2016)). More recently, the uncertainty of in-Delta water use described by Hutton and others (2021) is attributed to the uncertainty of Dayflow outflow at low-flow conditions (Monismith 2016).

Over the short-term record examined, approximately 59% of the Dayflow outflow values are at or below 10,000 cfs. Whereas the Dayflow outflow metric is influential for salinity standards and water management within the system (Rath et al. 2021), the use of Dayflow metrics such as outflow do not allow for a regional comparison of flow conditions within the Delta nor do they allow for a direct comparison of regional net flow conditions to food web dynamics. Tidal flows dominate the system during low flow conditions, especially during drought periods, so more nuanced metrics of flow may be important for food web investigations in future drought analyses. For example, a direct link between measured flow and salmon migration has been explored by (Romine et al. 2021) showing the influence of tidal variability to juvenile salmonoid passage.

Net flows at the USGS Cache Slough station across the short-term record found drought years 2021 and 2020 were only significantly different from drought year 2015 (Figure 17). The Cache Slough station analysis highlights that sub-regional flow regimes across water years and seasons may not match Delta outflow. Subregional flow regimes may largely be driven by water management activities and that flow on Cache Slough is different across water years in the short-term record is mostly likely due to Delta Cross Channel operation (see water management section) as well as reservoir outflow controls elsewhere in the system.

Although developing sub-regional flow metrics is beyond the scope of this report, it may be worth pursuing for future drought analyses. Identifying key stations throughout sub-regions may offer an opportunity to investigate flow

and foodweb dynamics and develop sub-regional constituent flux measurements where flow and water-quality measurements are co-located.

Water Quality

We found that drought periods have higher water temperatures than neutral or wet periods. This conforms with the results of a prior study, which found predominantly negative relationships between water temperature and inflow (Bashevkin and Mahardja in press). However, Bashevkin and Mahardja (in press) also found that the temperature-inflow relationship was variable seasonally and spatially, and positive temperature-inflow relationships were found in the winter and in the western Delta through Suisun from July through September. It is tempting to use the observed association of flow and temperature to ascribe a causal relationship (lower flow causes temperatures to rise), however, (as pointed out by Bashevkin and Mahardja) without incorporating air temperatures this would not be appropriate. Increased air temperature can increase evapotranspiration, and decreased cloud cover during droughts can further increase temperature. Therefore, higher temperatures may be causing lower flows, rather than vice-versa. Further study is needed to understand this relationship.

Warmer temperatures during drought periods cause stress to native fishes that are already living in stressful thermal conditions. Both the lethal and non-lethal impacts of high temperatures are important to consider to fully understand the implications of temperature variability. Chinook Salmon are at the warmest edge of their range in the San Francisco Estuary (Hecht et al. 2015). Warmer temperatures are especially damaging to the outmigrating juveniles in the wintertime, when high temperatures shorten the time they spend feeding and growing in the Delta, resulting in lower oceanic survival (Munsch et al. 2019). The timing of Delta Smelt spawning in the spring is determined by water temperature (Brown et al. 2016b), so higher temperatures could interfere with the timing and length of this window, potentially reducing reproductive output or larval survival.

Drought years had generally higher salinity than neutral years, which had higher salinity than wet years. 2021 had higher salinity than previous drought years, which was likely due, in part, to the TUCP and Barrier. This conforms with expectations, with years that had greater rainfall and inflow of fresh water from upstream sources diluting any localized and anthropogenic sources of salinity while helping hold back the upstream tidal pump of high salinity seawater. For the past 15 years there have been no "Wet periods", however low salinities can be seen even in Neutral years, except in winter

and fall, which have not had any yearly aggregated salinities below 1 PSU since 1997 and 1983, respectively (Figure 20).

Regional salinity patterns occurred as expected, with more upstream regions having lower salinity and more downstream and ocean-influenced regions having higher salinity waters. Having greater variability in regional salinity across the Delta, alongside greater variability in physical habitat and flow patterns, is thought to be beneficial in supporting the health of desirable fish species such as Delta Smelt, Chinook salmon, and Striped Bass (Moyle et al. 2010). However, this must be considered alongside preserving low salinity in interior Delta freshwater corridors for beneficial municipal and agricultural uses and to help avoid reverse salinity gradients that could interfere with the migratory cues and direction-finding abilities in some Delta fish species (CVRWQCB 2009).

A seasonal pattern is present across all drought year categories showing the spring season had the lowest salinity, with winter and summer having higher salinity occurring over a similar range, and the fall season having the highest salinity. This pattern was confirmed in both the drought year classification and year models for seasonal salinity. This finding matches expectations that the spring season, when rainfall and snowmelt should be at their highest, had the lowest salinity, while, fall, the season following the driest summer months and typically before the first major seasonal rainfall, when this system is most starved for freshwater inflows, had the highest general salinity.

Drought years had generally higher secchi depth measurements than Neutral years, which had higher secchi than Wet periods. This matches expectations, with wetter years leading to the increased runoff of sediment and leading to higher flows and the suspension and transport of sediment in the water column. 2021 was clearer than previous droughts, though it is unclear whether this is due to the TUCP and Barrier or a continuation of the steady decline in turbidity seen over the past 40 years. There have been no Wet periods (multiple wet years in a row) since 2006, which may help explain the increase in water clarity that seems to be on the rise since 1975 and is even more pronounced beginning in 2007. Wright and Schoellhamer (2004) observed a 50% decrease in sediment delivery from the Sacramento River to the San Francisco Bay and suggested several factors may have contributed, including a decline in the long-term effects of hydraulic mining, changes in land use, sediment deposition in reservoirs, and long term climatic shifts. Hestir et al. (2013) observed a similar decline in suspended sediment and suggest that the Delta is becoming sediment limited and point to a massive flow event in 1983 as a major contributor to increasing water clarity in the Delta. In general, increased water clarity had, and will continue to have,

negative impacts on survivability of native estuarine fishes including Delta smelt and other small young-of-the-year fishes at high risk from predation by exotic species (Nobriga et al. 2005).

Regional secchi depth occurred as expected, with more upstream regions having higher secchi. However, rather than being based on proximity to the ocean alone, Suisun Bay and to a greater extent, Suisun Marsh had lower secchi likely due to increased sediment suspension from both tidal agitation and increased wind and wave effects (Bever et al. 2018). The aquatic ecosystem is also shallower and more estuarine in Suisun Marsh whereas upstream in the North Delta and the interior South-Central Delta, where tidal forcing is less pronounced and channels have been straightened and deepened. As a consequence, Suisun is often important habitat for pelagic fishes that thrive on high turbidity (Ade et al. 2021).

The seasonal pattern in secchi depth largely matches expectations with the fall having generally clearer water, a season in which there is typically limited rainfall. Fall secchi measurements routinely exceeded 100 cm beginning in the late 2000s, and 3 of the last 5 years have exceeded 100 cm during winter, and while not significantly different, spring secchi values appeared to be lower than summer or winter. Spring and summer secchi depth values have not yet exceeded 100 cm, although it appears that secchi data is missing for the spring and summer months for the last 5 years, affecting the seasonal models for secchi and perhaps biasing those seasons low.

Dissolved ammonia was not significantly affected by Drought year classification type or Year. Dissolved ammonia values were highest in winter/fall (seasonally-averaged models) and the South Central region (regionally-averaged models). The variable reporting limit for ammonia may have interfered with our ability to detect differences between years types. Other analyses of long-term trends in ammonia suggest an increase over the period of record (Cloern 2019). However, upgrades to the Stockton Wastewater Treatment Plant are linked to the decrease in ammonium in 2006 (Beck et al. 2018), and the Sacramento County Wastewater Treatment Plant completed in early 2021 may explain the lower ammonia in 2021 (Saleh and Domagalski 2021).

Dissolved nitrate/nitrite and orthophosphate was significantly higher in Drought years compared to Neutral or Wet years, which were not significantly different from each other. Dissolved nitrate/nitrite values were highest in Winter and the South-Central region and lowest in the Summer and North regions. While there were no notable seasonal trends in phosphate, orthophosphate values in the South-Central region were

significantly higher than in others. Increased nutrient concentrations in dry years may relate to lower flushing rates allowing for accumulation of nutrients (Novick et al. 2015).

The dissolved oxygen (DO) timeseries on the lower Sacramento River and the Toe Drain display inherent differences between two channel reaches across seasonal and annual scales. Both the landward (Toe Drain) and seaward (Decker) time series exhibit diel and tidal variability. The daily mean DO time series can identify system-wide seasonal patterns inherent to changes with water temperature and community respiration. Of course, system-wide DO concentration trends vary across the water year due to several factors like water temperature, community respiration, precipitation events that increase surface runoff to the system, Yolo Bypass inundation, and agricultural activities

Patterns in DO concentrations are associated with several factors, but the steep declines of DO concentration observed in two distinct channels in 2021 and 2015 occurred following consecutive drought years in the short-term record. The greater distribution of high-frequency enhanced water quality measurements (e.g. dissolved oxygen, pH, algal fluorescence, dissolved organic matter fluorescence, and nitrate) at continuous monitoring stations that are co-located with flow measurements (Kraus et al. 2017) will perhaps offer an additional avenue for investigation of sub-regional constituent flux as it may relate to wet, neutral, and dry periods.

Chlorophyll-a

Long-term chlorophyll-a concentration varied with region, season, and water year type (Figure 56). Previous research for data collected between 1970 and 1993 also demonstrated the importance of these three factors in explaining the variation of chlorophyll-a concentration and phytoplankton carbon among phyla in the upper estuary (Lehman 1996). This finding indicates that these factors still describe patterns in chlorophyll-a concentration, despite the many changes the Delta has undergone in 50 years. However, the relatively low chlorophyll-a concentration measured since the 1980s suggests there has been a shift in the structure of the upper estuary (Glibert et al. 2011; Jassby et al. 2002; Kimmerer 2004; Lehman 1996). It is hypothesized that multiple impacts are responsible for this decrease in chlorophyll-a concentration, including climate change, clam and zooplankton grazing, water diversion, and toxic substances (Dugdale et al. 2007; Glibert et al. 2014b; Hammock et al. 2019; Jassby 2008; Kayfetz and Kimmerer 2017; Kimmerer and Thompson 2014). The loss of large diatoms

from reduced vertical mixing, increased clam grazing, salinity, and warm temperature due to climate change is also contributing to the loss of total biomass (Cloern 2018; Glibert et al. 2016; Lehman 2004; Lucas et al. 2016). Interestingly, the development of cyanobacteria blooms since 2000 has not significantly increased chlorophyll-*a* concentration, probably due to their small biomass and intermittent occurrence (Lehman et al. 2021). Alternatively, cyanobacterial chlorophyll-*a* may be underestimated by current monitoring methods which sample at 1 meter depth and do not effectively collect cyanobacteria at the surface.

The key finding that chlorophyll-*a* concentration is greater during intermediate flow years can be used by resource managers. Freshwater flow disperses organic matter from upstream regions across the upper estuary, with more chlorophyll-*a* occurring in the Delta during normal years and in Suisun Bay during wet years for the spring or summer (Jassby et al. 2002; Lehman 1996; Lehman 2000). As a result, the accumulation of chlorophyll-*a* upstream during dry and critical years can lead to low chlorophyll-*a* concentration throughout the upper estuary (Jassby 2008; Lehman 1996; Lehman 2000). Managers have used pulsed flow regimes to move chlorophyll-*a* biomass from upstream regions to downstream regions in the Delta near Rio Vista (Frantzich et al. 2018). Although flow is important for organic matter transport in Suisun Bay, the correlation between flow and chlorophyll-*a* concentration in Suisun Bay is often weak or non-existent (Kimmerer 2002a; Lehman 1992b). In Suisun Bay, chlorophyll-*a* concentration may also depend on the transfer of organic matter between the shoal and channel (Cloern et al. 1983). It is also likely that the low chlorophyll-*a* concentration measured during dry and critical years is controlled by biological factors. Dry and critical years are characterized by small flagellates such as cryptophytes which have low cell biomass compared with phyla such as diatoms which are more abundant (Cloern 2018; Cloern and Dufford 2005; Glibert et al. 2016; Lehman 1996; Lehman 2000; Lehman and Smith 1991). Benthic grazing rates by bivalves could also lower chlorophyll-*a* biomass in drier years (Brown et al. 2016a).

***Microcystis* index**

The recent drought in 2021 large cyanobacteria blooms occurred across much of the Delta. An in-depth analysis of the bloom in 2021 and the impact of the TUCP and Emergency Drought Barrier on the bloom can be found in the report: "Emergency Drought Barrer – Impact on Harmful Algal Blooms and Aquatic Weeds in the Delta" (Hartman et al. 2021). In brief, findings

suggested that drought and increased water temperatures were major factors leading to the development of HABs across the estuary, and that the 2021 TUCP and Emergency Drought Barrier are unlikely to have caused Delta-wide increases in *Microcystis* abundance. However, there was a localized cyanobacterial bloom during July and August 2021 in Franks Tract that was likely driven by increased water residence time caused by the Barrier. No major cyanobacteria blooms were detected in Franks Tract during installation of the drought barrier in 2015, but higher temperatures and growth of aquatic weeds may have exacerbated the problem in 2021.

On the Delta-wide level, *Microcystis* surface biomass index values were greater during drought and neutral years than wet years. This finding agrees with surface and sub-surface microscopy and genetic analysis which showed that *Microcystis* cell abundance and biomass was greater during drought years compared with wet years throughout the upper estuary since 2003 (Lehman et al. 2021; Lehman et al. 2017; Lehman et al. 2020). Because *Microcystis* abundance is greater at the surface and both surface and subsurface populations co-vary, the visual surface index was a reasonably good indicator of the magnitude of the bloom throughout the water column (Lehman et al. 2021). In addition, the *Microcystis* index values suggested that low *Microcystis* biomass and abundance were more common than high values, particularly at the Confluence and South-Central regions of the Delta. Microscopy indicated *Microcystis* abundance is highest in the southern Delta and increases seaward as the bloom season develops (Lehman et al. 2021). In addition, extremely high abundance was uncommon for most stations even in drought years (Lehman et al. 2021; Lehman et al. 2017). Bloom biomass is highly variable and is associated with highly variable toxin concentrations (Baxa et al. 2010). Toxin concentration can vary at 2-week intervals and is influenced by high frequency variation in local conditions, such as ammonium concentration or salinity (Baxa et al. 2010; Kurobe et al. 2018a; Kurobe et al. 2018b; Lehman et al. 2015). Importantly although cell biomass is not directly correlated with toxin concentration, toxin concentration generally increases with cell abundance, making biomass a good indicator of toxin concentration (Lehman et al. 2008).

Caution should be used when interpreting the surface *Microcystis* index as an indicator of overall cyanobacteria bloom magnitude and potential toxicity. The index does not provide information on other toxic species which now co-occur in the water column during *Microcystis* blooms, including *Dolichospermum*, *Aphanizomenon* and *Pseudanabaena* (Lehman et al. 2021; Otten et al. 2017). Recent research demonstrated that concentrations of the neurotoxins anatoxin-*a* and saxitoxin increased for the first time to above detection limits in 2016 (Lehman et al. 2021). Further, the index does not

provide information on the evolution of the bloom species and strains which have expanded since 2003 (Kurobe et al. 2018a; Lehman et al. 2021; Otten et al. 2017). Neither does it provide information on other potentially toxic phytoplankton species that regularly occur in the estuary and may increase during drought conditions including marine diatoms (e.g., *Pseudo-nitzschia*) and dinoflagellates (e.g., *Alexandrium*) (Peacock et al. 2018; Sutula et al. 2017).

Aquatic Vegetation

We did not observe higher coverage of aquatic vegetation during drier years, based on the remote sensing data set. However, it is difficult to draw strong conclusions. The 2021 data are not yet available, and sample sizes for each of the five water year types are limited to one to three data points. Also, the seasonal timing of the annual imagery collection has varied from June to November, which makes comparisons across years difficult. The spatial extent of aquatic vegetation coverage generally increases to a maximum in late summer or early fall. Surveys done earlier or later than this period may underestimate coverage. Also, imagery collected in October or November may underestimate SAV coverage because it is obscured by turbidity generated from rain events.

Variation in aquatic vegetation coverage due to water year type may be hard to isolate from the general expansion of aquatic vegetation over time due to the spread of non-native invasive species, particularly *Egeria densa* (SAV) (Durand et al. 2016). This expansion likely has been fueled, at least in part, by long term environmental changes in the Delta, such as reductions in turbidity, that are favorable for aquatic vegetation growth (Hestir et al. 2016). Many invasive aquatic plants are ecosystem engineers, which modify environmental conditions in ways that facilitate further spread (e.g., reducing flows and turbidity) (Hestir et al. 2016). In addition, management of aquatic vegetation may mute the signal of drought and drought related management actions, particularly for FAV which is easier to control with herbicides than is SAV. Discerning differences among water year types is also likely complicated by potential lags between changes in environmental conditions and changes in vegetation abundance.

Patterns of aquatic vegetation coverage in Franks Tract are qualitatively similar to those observed for the larger Delta region. This may suggest that landscape scale variation in environmental conditions plays a greater role in driving aquatic vegetation coverage than management actions, such as the 2015 Emergency Drought Barrier. Without the 2021 remote sensing data, it

is not possible to evaluate the effects of the most recent drought barrier. Preliminary analysis of the available SAV community composition data for 2021 suggests that relative abundances of some species changed, and it is possible that these changes were related to the 2021 drought barrier. Most notably, *Ceratophyllum demersum* (native SAV) declined substantially, while *Najas guadalupensis* (native SAV) increased to the highest abundances observed in the eight years of available data. For additional information, see the report about monitoring of harmful algal blooms and aquatic vegetation around the 2021 emergency drought barrier (Hartman et al. 2021).

Zooplankton

Total zooplankton biomass showed a slight increase during Drought years compared to Wet years, probably driven by increased residence time, decreased pelagic fish abundance, and localized increases in chlorophyll. Data from 2021 are not yet complete, so we cannot assess any impacts of the TUCP or barrier on zooplankton yet. Overall, the highest zooplankton concentrations were found in Neutral years, likely tied to the high abundances of chlorophyll also found in Neutral years. This trend interacted strongly with region of the Delta; in Drought year biomass increased substantially in the South-Central Delta and was decreased in Suisun Bay, while the relationship was reversed in Wet years. This could be due to the delivery of phytoplankton, nutrients, or zooplankton themselves to downstream regions during higher outflow years (Kimmerer et al. 2018a). Seasonal differences were also apparent, drought years having higher zooplankton abundances in the spring and fall, while wet years had the lowest abundances in spring, which could be due to high outflows pushing zooplankton, nutrients, and phytoplankton out of the sampling region.

Community composition, as shown by the NMDS, also differed between Droughts and Wet periods, with Neutral periods being somewhere in between. This shift is most likely due to water quality conditions. Salinity increases during droughts, so we see more brackish-tolerant species, like the calanoid copepod *Acartia spp.*, in downstream regions. Looking at the species-specific biomass graph, some freshwater taxa also show a strong increase with the low-flow conditions of droughts, particularly the cladocerans *Daphnia spp.* and *Diaphanisoma spp.*, which is driving the high biomass found in the South-Central Delta during Drought years. This may be due to high chlorophyll concentrations in upstream areas due to high residence times and a lack of export of phytoplankton downstream. It may

also be due to relatively low pelagic fish biomass found in the South Delta, which means lower top-down control on zooplankton populations.

Other taxa, particularly the calanoid copepod *Pseudodiaptomus forbesi* and the mysid *Neomysis mercedis* decrease with low-flow conditions in droughts, most likely due to a decrease in transport from freshwater into Suisun Bay (Kimmerer et al. 2018c). *Pseudodiaptomus forbesi* is one of the most common taxa in the Delta during the summer, so the decline in total biomass seen in summer of drought years may be driven largely by this copepod. Previous research on *P. forbesi* has seen similar positive flow-abundance relationships (Kimmerer 2002b; Kimmerer et al. 2018b; Kimmerer et al. 2018c).

The decrease in zooplankton biomass in Suisun during drought years may also be driven by the *P. forbesi*-outflow relationship. The presence of the invasive bivalve *Potamocorbula amurensis* (see clams section) in the Suisun region results in relatively low standing stock of chlorophyll, limiting food for in-situ production of zooplankton. Therefore, this region relies on transport of both phytoplankton and zooplankton from upstream for much of its zooplankton biomass (Kimmerer et al. 2014). In drought years, there is insufficient transport of productivity from upstream to counter-act the impact of the clams, as seen during studies of the 2015 salinity barrier as well (Kimmerer et al. 2019).

For some taxa showing increases with low outflow, such as *Acartia*, *Tortanus*, and *Limnoithona tetraspina*, shift in distribution may be the driving factor. These taxa are slightly more salt-tolerant than *P. forbesi* or *N. mercedis*, so the general upstream shift in distribution that occurs during droughts will put a greater percentage of their range within IEP's sampling frame. Other taxa, such as the Cladocerans *Diaphanosoma* and *Daphnia*, which are most abundant in the warm South Delta region, increases during droughts may be driven by increased temperature, residence time, and local increases in primary productivity, since Cladocera frequently have highest growth rates at high temperatures (Giebelhausen and Lampert 2001; Heugens et al. 2006).

Overall, the zooplankton community has a diverse response to drought conditions, based on region, season, and species. Several taxa that are key fish food, such as *P. forbesi* and mysids, see increases in abundance in the Suisun region during wet years, while others, such as the Cladocera, see increases in the South-Central Delta during drought years. This diversity of responses makes estuary wide predictions difficult.

Jellyfish

Our analysis of the jellyfish data is still ongoing; however, our preliminary results suggest highest abundances during wet years. This was contrary to our expectation because most jellyfish found in the region are brackish-water specialists. We therefore expected the overall abundance of jellyfish to be driven by salinity intrusion during droughts. Increases in abundance of jellyfish in the brackish regions of the estuary during wet periods may have been driven by the increases in zooplankton seen in Suisun during wet periods, but this is an area for further research.

Clams

The largest impact of drought on invasive clams is the shift in distribution of *Potamocorbula amurensis*. This brackish-water specialist moves upstream during drier years, increasing occupied habitat and overall abundance. Because *P. amurensis* has a much higher grazing rate than *Corbicula fluminea* (Crauder et al. 2016), benthic grazing rates in the estuary as a whole increase. We also observe higher grazing rates of *P. amurensis* during drier years. *P. amurensis* may continue to spawn during drought periods (Parchaso 1993) and is able to withstand some salinity variability (Werner et al. 2003). A similar pattern was seen during and after construction of the 2015 drought barrier (Kimmerer et al. 2019).

The increase in *P. amurensis* during droughts is likely part of the reason why zooplankton abundance in the Suisun region also decreases with drought. *P. amurensis*, with its high grazing rate and shifting biomass, has the capacity to compensate for decreasing *C. fluminea* populations where salinity is past its threshold, such as during drought years (Parchaso 1993). We likely see less of an impact from *C. fluminea* during droughts due to its low salinity tolerance.

The primary cause of drought's impact on benthic grazing is the shift in biomass however the increased temperature during droughts may also play a role. Grazing rates, are a function of species-specific pumping rates, temperature, biomass, and density (Thompson et al. 2008), so increased temperature during droughts, particularly during the summer when bivalve biomass is highest, will also increase grazing rates.

It was interesting that the observed shift in distribution was most apparent in the year after a dry year. Because clams are not mobile, unlike many of the other parameters analyzed in this report, impacts on distribution mostly occur through differential recruitment rather than shifts in adults moving with the salinity field, as was observed during the 2012-2016 drought (Kimmerer et al. 2019).

Fish

We found major changes to the fish community during drought years, probably driven in part by changes to salinity, temperature, and turbidity. In 2021, most pelagic fish continued their trends of low catch that has characterized much of the past 20 years. While some fish had slightly higher indexes of abundance in 2021 than 2020, the overall effect was a reduced pelagic fish biomass.

Fish community analysis

The principal tensor analysis found that both the catfish/shad and fresh/brackish cluster varied significantly with outflow, and both clusters had significantly different assemblages during droughts when compared to wet periods (Figure 88). It is notable that White Catfish and Threadfin Shad clustered together, since these two fish occupy very different habitats and ecological niches; catfish are benthic predators, whereas shad are pelagic planktivores (Moyle 2002). Neither species has been the subject of much study in the Delta. Both these species have relatively low salinity tolerances, but White Catfish is associated with relatively high freshwater flow (Feyrer and Healey 2003), whereas Threadfin Shad is associated with lower freshwater flow (Feyrer et al. 2009; Meng and Matern 2001). Since the White Catfish is demersal, the FMWT gear is not able to sample it as effectively as the pelagic Threadfin Shad, so the patterns in catfish catch may not be the best representation of population dynamics. More study is needed.

The fresh/brackish cluster, including Delta Smelt, Longfin Smelt, Splittail, and Chinook Salmon includes mostly anadromous or semi-anadromous species that have previously documented relationships with flow. This cluster had significant variation with Delta Outflow and had significantly different community composition between Droughts and Wet periods (Figure 88). Splittail are obligate floodplain spawners (Moyle et al. 2004), so young-of-year Splittail catch is highly correlated with periods of floodplain inundation seen during wet years. Longfin Smelt catch is also highly correlated with high outflow years, though the mechanism behind this relationship is poorly understood (Nobriga and Rosenfield 2016). Chinook Salmon juveniles also tend to have higher survival, faster migration through the Delta, and higher catches in high-outflow years (Michel et al. 2015; Singer et al. 2020). The relationships between outflow and abundance for the other species in the cluster – Delta Smelt, American Shad, and Yellowfin Goby – are less clear.

Species-Specific Analysis

Striped Bass

Striped Bass catch of age-0 fish in 2021 was one of the lowest on record, though catches have been low at least since 2002, and we found a significant relationship between droughts and low Striped Bass populations. Results indicating that population fluctuations are “non-random” are almost certainly a result of the prolonged period of low annual index levels. Despite the fact that Striped Bass are an introduced species, it is considered “naturalized” and often thought of as an indicator of overall estuarine health. Crashes in the Striped Bass population were noted in previous droughts (Mahardja et al. 2021), potentially due to food limitation or increasing contaminant concentration (Bennett et al. 1995; Nichols 1985).

While food limitation is often a hypothesized reason for Striped Bass declines during droughts, comparing fish abundance with zooplankton abundance makes it clear that there is more to the story. Zooplankton, the major prey for age-zero striped bass and other pelagic fish referred to here, frequently increased during droughts, especially in the South-Central Delta. Fall zooplankton abundance decreased in the Suisun region, probably due to decreased transport from freshwater (Kimmerer et al. 2019), and increased range of *Potamocorbula amurensis* (Figure 76), but many regions of the estuary have high zooplankton biomass during droughts due to increased chlorophyll and increased residence time. It is interesting that South-Central region, with the greatest increase of zooplankton during droughts typically has very low pelagic fish catch (CDFW Summer Townet data). It may be that lower predation pressure from fishes is part of the reason this regions sees such high zooplankton biomass.

American Shad

The American Shad index was higher in 2021 than 2020 and higher than in other recent drought years (2001-2006) but lower than in 2017 & 2019 (both neutral years). We also found that Wet periods had significantly higher American Shad catches in the FMWT than Drought years. Fluctuations in the American Shad index over the long-term (1970-2020) were indistinguishable from random (Table 23), unlike all other pelagic species reviewed in this work. American Shad, an anadromous species introduced from the Atlantic coast, have not been studied extensively in the Delta; previous analyses have found increasing abundance with increasing Delta Outflow (Contreras et al. 2012; Stevens and Miller 1983), but Stevens et al. (1987) were unable to find a robust correlation between year-class strength of adult shad and flow during their natal year. Stevens et al. (1987) report that YOY American

Shad rely on nursery habitat in the lower Feather River, Sacramento River, and the upper Delta, with most of these leaving by the early winter, and attribute declines since 1977 to habitat degradation. However, species-specific studies of American Shad in this system post POD, are lacking.

Longfin Smelt

Longfin Smelt had higher indices of abundance for all life stages in 2021 than 2020, Fall Midwater Trawl in particular (Figure 84), which is surprising since Delta Outflow was lower than 2020, and Longfin Smelt have previously been observed to increase in abundance with outflow (Nobriga and Rosenfield 2016; Stevens and Miller 1983). However, the indices for both 2020 and 2021 were much lower than recent wet years, and there is a highly significant trend is for low Longfin catch during droughts (Figure 85). The surveys used for this analysis (FMWT, STN, SKT, and 20mm survey) were not designed to sample Longfin Smelt, and therefore do not provide the best index of abundance for this species. In particular, Longfin Smelt spawning distribution tends to shift out into the San Francisco Bay during wet years, out of reach of the IEP surveys (Merz et al. 2013; Rosenfield and Baxter 2007).

Both the Bayesian model of Longfin Smelt catch and the linear model of log-transformed FMWT index found a strong decline in catch during drought years over the entire period of record (Table 24), Figure 91. The FMWT Longfin Smelt index over the period from 1970-2020 was convincingly non-random (Table 23), but this is best attributed to the prolonged period of near zero catches from 2017-2020. Longfin Smelt, like most pelagic fishes in the estuary, has experienced several step-declines in abundance (Thomson et al. 2010), making it difficult to extract the impact of the current drought from the long-term trend. However, the repeated droughts experienced in the estuary over the past twenty years may be part of the reason Longfin Smelt have continued to decline (Nobriga and Rosenfield 2016).

Delta Smelt

There was no catch of Delta Smelt in any of the CDFW surveys in 2021. Delta Smelt have declined more than other pelagic fish over the historic record, however their relationship with drought and Delta Outflow is less clear than that of Longfin Smelt. Our analyses found a trend toward higher Delta Smelt abundance during wet periods than droughts, however it was not statistically significant (Figure 85). Many studies have attempted to find

a relationship between Delta Outflow with Delta Smelt abundance, but fish populations do not always respond as expected. Some wet years, such as 2011, showed large increases in Delta Smelt abundance, whereas other wet years, such as 2017, showed only slight increases, or none at all. Polansky et al. (2021) found Delta Outflow in summer positively associated with survival between life stages, but other factors, including temperature and turbidity, were also important. A recent analysis of 2017 and similar wet years suggested that temperature may be a more controlling factor than Delta Outflow (FLOAT-MAST 2021). Droughts tend to be warmer than wet periods (Figure 23, Table 4), however some wet years, especially recently, are also hot. Our analyses also found drought years are also clearer than wet periods (Figure 22), and ideal Delta Smelt habitat is believed to be at moderate-high turbidities where they have optimal feeding and predation refuge (Hasenbein et al. 2016; Hasenbein et al. 2013; Sommer and Mejia 2013). The long-term declining population trend, which is believed to be driven by a variety of factors besides outflow (e.g. Thomson et al. 2010), may also be masking our ability to detect a drought response in Delta Smelt.

Threadfin Shad

Threadfin Shad have been scarce during the last 10 years, though the 2020 Fall Midwater Trawl index was comparatively high for this period and Threadfin do not appear to have declined as greatly as some of the other pelagic fishes in the Delta. Threadfin do decrease in abundance during drought years as identified by the Bayesian zero-inflated model of catch (Figure 90, Table 24), though the linear model of FMWT index was marginally significant ($p = 0.06$). Prior to 2010, trends in abundance suggested that density-dependent factors were relevant (Feyrer et al. 2009), but more recent data suggest that this species, too, has been impacted by the general decline in Delta pelagic fishes. Threadfin Shad are associated with comparatively deep, fresh, clear water (Kimmerer et al. 2013), so Threadfin Shad are likely to be affected when drought conditions reduce freshwater habitat, but will not be as impacted by decreases in turbidity as Delta Smelt.

Chinook Salmon

Chinook use of the Sacramento-San Joaquin River Delta is relatively brief in terms of their complete life cycle, and the environmental conditions in the Delta are likely less impactful than those higher in the watershed (i.e., in spawning and rearing habitat) or oceanic conditions where juveniles (mostly)

mature prior to their return to natal streams. Thus, linking Chinook population dynamics to Delta conditions is complicated and potentially muted by factors in other habitats. However, Delta conditions may reflect conditions upstream, and there is abundant evidence that juvenile survivorship during outmigration, including passage through the Delta, can be hugely impactful to the success or failure of a cohort.

In water year 2021, classified as Critically Dry, acoustic tag data reported on the CalFishTrack website show that through-Delta survival for hatchery produced SRWRC in 2021 was 35.7% for all study release groups combined (Table 22). This is higher than the previous year (2020, Dry) which had 23.9% through-delta survival, though not as high as 2019 (Wet), when through-Delta survival of hatchery produced SRWRC was 59% (Notch et al. 2021). These observations are consistent with an analysis of migration survival rates for late fall-run Chinook salmon, which found higher through-Delta survival in the observed Wet year (2011) compared to the observed drought years (2007-2010) (Michel et al. 2015; Notch et al. 2020). Likewise, a similar study of hatchery-produced SRWRC also found through-Delta survival to be highly correlated with flow where, despite poor overall survival conditions in droughts years (2014 & 2015), there were brief pulses of high flow coincident to relatively high (between 52% and 64%) through-Delta survival (Hance et al. 2022).

Also of note, the 2021 acoustic tag releases included a thiamine boost (and control group) where those fish that received a thiamine boost had better Delta survival (40%) compared to the thiamine control fish (22.2%) (Table 22). The third release group also had similarly high through Delta survival (37.8%) as the thiamine boost group. Thiamine deficiency in returning adults, potentially caused by a diet high in anchovies, was a major problem for juvenile egg-to-fry survival in brood year 2020 (NOAA Fisheries 2021), highlighting how interactions of conditions in multiple life stages can combine to influence salmon population status.

Using the GrandTab escapement data provided a consistently reliable long-term dataset to derive the annual CRR. When grouped by drought condition during juvenile migration (t-3) and normalized by run-specific age structure, we identify the relative influence of drought on juvenile migration success, including survival through the Delta. For age-3 SRWRC that migrated (t-3) during periods of drought, the average CRR is 0.9 (Figure 78). For those age-3 SRWRC that migrated (t-3) during wet and neutral periods, the average CRR is 1.6 and 1.9 respectively (Figure 78). Likewise, for age-3 CVSRC that migrated (t-3) during periods of drought, the average CRR is 0.8 but 1.5 and 2.4 for those age-3 CVSRC that migrated (t-3) during wet and neutral periods respectively (Figure 79). Lastly, the average CRR is 1.0 for

age-3 CVFRC that migrated (t-3) during periods of drought and 1.2 and 1.4 for those age-3 CVFRC that migrated (t-3) during wet and neutral periods respectively (Figure 80). These results conform with expectations of lower survival of outmigrants during dry years (Michel et al. 2015; Notch et al. 2020), as well as possible interactions with increased straying of adults that were trucked as juveniles (Sturrock et al. 2019).

Based on the DJFMP trawl data from 1988 – 2021, both winter-run and fall-run Chinook exhibit a bimodal timing distribution at Sherwood Harbor (Delta entry). Spring-run have a singular peak; however, this may be influenced by the considerable amount of overlap in length distributions between spring-run and fall-run and, therefore, large amount of mis-attribution to each run type by race-by-length criteria (Harvey et al. 2014). Apparent timing of spring-run Chinook salmon may be particularly affected by this mis-attribution once releases begin for the large hatchery production of fall-run Chinook salmon (approximately 75% of which are not marked). Winter-run Chinook may have somewhat earlier migration at Sherwood Harbor in drought years, compared to neutral or wet years (Figure 81), though this may have been due to late-migrants not surviving rather than a shift to early migration.

All three runs have a more singular peak at Chipps Island (the exit of the Delta), but winter-run are most variable and protracted in their timing at Chipps. Overall, drought years appear to have more of an impact on migration into the Delta (Sherwood Harbor) than migration out of the Delta (Chipps Island), consistent with del Rosario et al.'s (2013) observations of winter run from 1999-2007. Migration timing out of the Delta (at Chipps Island) is fairly consistent in each of the runs, whereas migration at Sherwood Harbor tends to vary more.

Regarding observed fish lengths in the Delta, there appears to be more variability at Sherwood Harbor than at Chipps Island (Figure 83), in a pattern similar to what is observed for migration timing. Size variability may coincide with migration timing: SRWRC migrating past Sherwood Harbor at different times do so across a range of sizes, whereas fish migrating past Chipps Island at a similar time have had a chance to equalize in growth and size. In drought periods, there are relatively more juvenile winter-run in the earlier, smaller-sized peak compared to neutral or wet periods. This may coincide with a slightly earlier migration in drought periods and/or smaller size due to less favorable growth conditions. It is also worth noting that, while length-at-date criteria for winter run are more accurate than spring-run or fall-run Chinook Salmon, they are still subject to error (Brandes et al. 2021), so some of these may be mis-identified.

Effect of Drought Management Actions

The summer 2021 TUCP and West False River Drought Barrier had a few obvious impacts on the Delta; however, the effects of the drought were so large that they masked the effects of these actions on the ecosystem-wide scale. To extract the impacts of these actions, we compared ecosystem components in 2021 to similar dry years, and, for the most part, levels were similar (Figure 101). The greatest differences between 2021 and similar dry years were:

1. Summer outflow and exports were unusually low.
2. Salinity was unusually high.
3. Secchi depth was high, continuing the general increasing trend.
4. Temperatures were unusually high.
5. Dissolved ammonia and nitrate+nitrite were low.
6. Harmful algal blooms were similar to 2020, but more intense than during the 2012-2016 drought. A large bloom in Franks Tract during July and August may have been exacerbated by the Barrier.
7. Pelagic fishes had some of the lowest abundances on record, lower than previous droughts, though Longfin Smelt experienced a surprising population increase.

TUCP and Barrier

The 2021 TUCP included a modification for reduced Delta outflow, and the Emergency Drought Barrier contributed to localized changes in flow and circulation. This aligns with modeling done prior to the TUCP which indicated an increase in X2 of approximately 2 KM (DWR 2021), and research done on the 2015 Emergency Drought Barrier which suggested possible increases to salinity in the Sacramento and North Delta regions (DWR 2019; Kimmerer et al. 2019). The previous TUCPs that were in place during 2014 and 2015 focused on outflow during the late winter and spring, whereas the 2021 TUCP focused on the summer, so drawing connections between TUCPs from these years was not attempted.

The other major impact the drought that may have been exacerbated by the Barrier was the cyanobacterial bloom observed in Franks Tract during July and August of 2021. While Delta-wide cyanobacterial blooms were driven more by the high temperatures and drought conditions than any management actions, the increase in residence time caused by the Barrier likely exacerbated the bloom seen in Franks Tract. For a full discussion of cyanobacteria in 2021, see (Hartman et al. 2021).

Managing HABs in the Delta is rapidly becoming a priority for State, federal, and local water agencies, and this condition will only increase in a warming climate. Mitigation methods for reducing residence time and controlling HABs locally near the Barrier are still under development. Many standard control methods may not be feasible at the scale required to affect the entirety of Franks Tract.

Other management actions

The Sacramento Valley Index and Delta Outflow were the primary metrics of hydrology used in this report, but flows within the Delta may also be important, particularly during droughts. Changing flows within the Delta through management actions like the operation of the Delta Cross Channel (DCC) alter transport time scales and subregional flow patterns across the system (Monsen et al. 2007). Changes to system-wide transport time scales alter hydrodynamic processes on the local and sub-regional scale that are important to migration of salmon and other native fishes (Perry et al. 2013; Smith 2019). Changes to transport time scales in turn affect water-quality gradients that have further implications to aquatic habitat quality (Monsen et al. 2007). Local investigations of the influence of hydrodynamics in the Sacramento River Deep Water Ship channel and how that may affect the pelagic community (Lenoch et al. 2021; Young et al. 2021) add to the breadth of research conducted over the last decades

The DCC operation has a strong effect on subregional flow patterns (Burau et al. 2016) particularly on Cache Slough in the examination of the short-term record. For example, the Cache Slough flow analysis suggested 2020 and 2021 were only statistically different from 2015 (Figure 16) - that is, in the recent record there were higher mean flows in Cache Slough that can be tied to intermittent operation of the DCC in the late summer and fall that otherwise diverts water to the Central Delta. In contrast, Dayflow outflow found 2020 and 2021 were similar to other drought years (Figure 15). These results suggest that Dayflow outflow may be too coarse a resolution to examine food web dynamics. Leveraging flow station data could tie regional flow metrics to regional patterns food web dynamics.

Upstream management actions can also have a large impact on the Delta, particularly for salmon and sturgeon. Analysis of these actions is out of the scope of this report; however, see "2021 Drought and Dry Year Actions Report" (Reclamation and DWR 2022) for more information. Several hatcheries increased production and/or infrastructure improvements to help overcome low survival during drought years. Other actions improved migration pathways through pulse flows or redistribution of flows, and several water supply actions also helped to conserve cold-water pools and

support temperature management below dams. The full benefits of these actions will not become clear until juveniles produced in 2021 out-migrate and successfully return to the Central Valley. If successful, these actions may result in cohort replacement rates higher than would have occurred absent these and other drought actions.

The Future

One of the difficulties in assessing impact of drought across all metrics assessed in this report is the conflation of drought impacts and long-term trends. The mid-20th century, when data used in this report began, was a particularly wet period in California's history (Ingram and Malamud–Roam 2013). In contrast, the past 20 years has included three major drought period and no extended wet periods (Figure 2). Other analyses have identified increasing frequency of droughts in California, and a delay in the onset of the rainy season (Diffenbaugh et al. 2015; Luković et al. 2021). Many water quality and ecological metrics have experienced declines over the past fifty years, due to a variety of factors including invasive species, changes to water management, changes to land use, and rising temperatures (Thomson et al. 2010). However, some of the long-term declines may have been exacerbated by the increase in drought frequency and severity. With multiple factors often at play in long-term species declines, it is difficult to extract the influence of repeated droughts from other factors.

Most climate models predict California's future will include more extreme droughts and more "weather whiplash" whereby extreme droughts are followed by extreme wet years (Dettinger 2011; Dettinger et al. 2016; Swain et al. 2018). Our analyses found multi-year droughts and multi-year wet periods often had a stronger impact on ecosystem components than single wet or dry years (for example, see Longfin Smelt analysis, above), highlighting the importance of recovery time for estuarine populations.

While predictions of climate change's precipitation timing and magnitude are often difficult, increases to temperatures are well-established. The past two droughts have been hot droughts, and the intervening wetter years have been hot as well. The link between anthropogenic warming and drought in California has also been well established, so this most recent drought should come as no surprise (Diffenbaugh et al. 2015). The historic record shows evidence of "megadroughts" lasting decades or hundreds of years (Williams et al. 2020); however, these previous droughts were not accompanied by increased temperatures (Mann and Gleick 2015). These new, hot droughts,

occurring at increased frequency, will provide greater sources of conflict for managing California's water resources.

There are many aspects to these ecosystem responses that are still poorly understood. We do not understand many of the mechanisms behind fishes' responses to drought. We have not uncovered many of the drivers behind the increase in aquatic vegetation or harmful algal blooms. While we found some changes to migration timing for salmon, we need further investigation to clarify the patterns. Many ecosystem components were not evaluated in this report, such as other migratory fishes (including sturgeon and lamprey), birds, mammals, upstream impacts, and many aspects of human responses to drought. All of these avenues may become important for future management of drought in the Delta.

Acknowledgements

We would like to thank all of the Interagency Ecological Program monitoring surveys for continuing to collect world-class environmental data in the face of all types of extreme hardships. Thanks also to the Center for Spatial Technology and Remote Sensing at UC-Davis for providing the 2004-2020 aquatic vegetation data set and for their ongoing efforts to expedite analysis of the 2021 vegetation data. Thank you to Brett Harvey, Steve Slater, Gonzalo Castillo, Brian Schreier, Shruti Khanna, and the IEP Flow Alteration Project Work Team for guidance and feedback on the analyses. Thank you to Ryan Reeves, Kurt Carpenter, Fred Feyrer, and Tripp Mizell for comments improving the manuscript.

Works Cited

- Acuña, S., D. Baxa, P. Lehman, F.-C. Teh, D.-F. Deng, and S. Teh. 2020. Determining the Exposure Pathway and Impacts of *Microcystis* on Threadfin Shad, *Dorosoma petenense*, in San Francisco Estuary. *Environmental Toxicology and Chemistry* 39(4):787-798. doi:<https://doi.org/10.1002/etc.4659>
- Acuna, S., D. Baxa, and S. Teh. 2012a. Sublethal dietary effects of microcystin producing *Microcystis* on threadfin shad, *Dorosoma petenense*. *Toxicon* 60:1191-1202.
- Acuna, S., D. F. Deng, P. Lehman, and S. Teh. 2012b. Sublethal dietary effects of *Microcystis* on Sacramento splittail, *Pogonichthys macrolepidotus*. *Aquatic Toxicology* 110-111:1-8.
- Ade, C., E. L. Hestir, and C. M. Lee. 2021. Assessing Fish Habitat and the Effects of an Emergency Drought Barrier on Estuarine Turbidity Using Satellite Remote Sensing. *Journal of the American Water Resources Association* 57(5):752-770. doi:<https://doi.org/10.1111/1752-1688.12925>
- Azat, J. 2021. GrandTab 2021.06.30 California Central Valley Chinook Population Database Report. California Department of Fish and Wildlife. <https://nrm.dfg.ca.gov/FileHandler.ashx?DocumentID=84381>
- Bashevkin, S. M. 2021. deltamapr: spatial data for the Bay-Delta. GitHub, <https://github.com/InteragencyEcologicalProgram/deltamapr>
- Bashevkin, S. M. 2022. Six decades (1959-2020) of water quality in the upper San Francisco Estuary: an integrated database of 11 discrete monitoring surveys in the Sacramento San Joaquin Delta, Suisun Bay, and Suisun Marsh ver 2. Environmental Data Initiative. <https://doi.org/10.6073/pasta/dc199c9fd9c452337f01bcd9f0a89f50>
- Bashevkin, S. M., and B. Mahardja. in press. Seasonally variable relationships between surface water temperature and inflow in the upper San Francisco Estuary. *Limnology and Oceanography* n/a(n/a). doi:<https://doi.org/10.1002/lno.12027>
- Bates, D., M. Maechler, B. Bolker, and S. Walker. 2020. lme4: Linear Mixed-Effects Models using 'Eigen' and S4. The Comprehensive R Archive Network (CRAN). <https://github.com/lme4/lme4/>
- Baxa, D. V., T. Kurobe, K. A. Ger, P. W. Lehman, and S. J. Teh. 2010. Estimating the abundance of toxic *Microcystis* in the San Francisco Estuary using quantitative real-time PCR. *Harmful Algae* 9:342-349.
- Beck, M. W., T. W. Jabusch, P. R. Trowbridge, and D. B. Senn. 2018. Four decades of water quality change in the upper San Francisco Estuary. *Estuarine, Coastal and Shelf Science* 212:11-22. doi:<https://doi.org/10.1016/j.ecss.2018.06.021>
- Begon, M., J. L. Harper, and C. R. Townsend. 1986. *Ecology. Individuals, populations and communities.* . Blackwell scientific publications.
- Bennett, W. A., D. J. Ostrach, and D. E. Hinton. 1995. Larval Striped Bass Condition in a Drought-Stricken Estuary: Evaluating Pelagic Food-Web Limitation. *Ecological Applications* 5(3):680-692. doi:<https://doi.org/10.2307/1941977>

- Bever, A. J., M. L. MacWilliams, and D. K. Fullerton. 2018. Influence of an Observed Decadal Decline in Wind Speed on Turbidity in the San Francisco Estuary. *Estuaries and Coasts* 41(7):1943-1967. doi:10.1007/s12237-018-0403-x
- Boyer, K., and M. Sutula. 2015. Factors controlling submersed and floating macrophytes in the Sacramento-San Joaquin Delta. Southern California Coastal Water Research Project. Technical Report 870, Costa Mesa, CA.,
- Brandes, P. L., B. Pyper, M. Banks, D. Jacobson, T. Garrison, and S. Cramer. 2021. Comparison of Length-at-Date Criteria and Genetic Run Assignments for Juvenile Chinook Salmon Caught at Sacramento and Chipps Island in the Sacramento–San Joaquin Delta of California. *San Francisco Estuary and Watershed Science* 19(3). doi:<https://doi.org/10.15447/sfews.2021v19iss3art2>
- Brown, L. R., W. Kimmerer, J. L. Conrad, S. Lesmeister, and A. Mueller–Solger. 2016a. Food webs of the Delta, Suisun Bay, and Suisun Marsh: an update on current understanding and possibilities for management. *San Francisco Estuary and Watershed Science* 14(3). doi:10.15447/sfews.2016v14iss3art4
- Brown, L. R., L. M. Komoroske, R. W. Wagner, T. Morgan-King, J. T. May, R. E. Connon, and N. A. Fanguie. 2016b. Coupled downscaled climate models and ecophysiological metrics forecast habitat compression for an endangered estuarine fish. *Plos ONE* 11(1):e0146724. doi:10.1371/journal.pone.0146724
- Burau, J. R., C. A. Ruhl, and P. A. Work. 2016. Innovation in Monitoring: The U.S. Geological Survey Sacramento-San Joaquin River Delta, California, Flow-Station Network: U.S. Geological Survey Fact Sheet 2015-3061. 6 p. doi:<http://dx.doi.org/10.3133/fs20153061>.
- Bürkner, P.-C. 2018. Advanced Bayesian Multilevel Modeling with the R Package brms. *The R Journal* 10:395-411.
- Bürkner, P.-C., and M. Vuorre. 2019. Ordinal Regression Models in Psychology: A Tutorial. *Advances in Methods and Practices in Psychological Science* 2(1):77-101. doi:<https://doi.org/10.1177/2515245918823199>
- California Department of Water Resources (DWR). 2020. California's Most Significant Droughts: Comparing Historical and Recent Conditions. California Department of Water Resources, Sacramento, CA.
- Caramujo, M.-J., H. T. S. Boschker, and W. Admiraal. 2008. Fatty acid profiles of algae mark the development and composition of harpacticoid copepods. *Freshwater Biology* 53(1):77-90. doi:<https://doi.org/10.1111/j.1365-2427.2007.01868.x>
- Cichocki, A., D. Mandic, L. De Lathauwer, G. Zhou, Q. Zhao, C. Caiafa, and H. A. Phan. 2015. Tensor decompositions for signal processing applications: From two-way to multiway component analysis. *IEEE signal processing magazine* 32(2):145-163.
- Clarke, K. R., and R. N. Gorley. 2015. PRIMER v7: User Manual/Tutorial. PRIMER-E, Plymouth.
- Cloern, J. E. 2018. Why large cells dominate estuarine phytoplankton. *Limnology and Oceanography* 63(S1):S392-S409. doi:10.1002/lno.10749

- Cloern, J. E. 2019. Patterns, pace, and processes of water-quality variability in a long-studied estuary. *Limnology and Oceanography* 64(S1):S192-S208.
doi:<https://doi.org/10.1002/lno.10958>
- Cloern, J. E., A. E. Alpine, B. E. Cole, R. L. J. Wong, J. F. Arthur, and M. D. Ball. 1983. River discharge controls phytoplankton dynamics in the northern San Francisco Bay estuary. *Estuarine, Coastal and Shelf Science* 16(4):415-429.
doi:[https://doi.org/10.1016/0272-7714\(83\)90103-8](https://doi.org/10.1016/0272-7714(83)90103-8)
- Cloern, J. E., and R. Dufford. 2005. Phytoplankton community ecology: principles applied in San Francisco Bay. *Marine Ecology Progress Series* 285:11-28.
doi:10.3354/meps285011
- Cloern, J. E., T. S. Schraga, E. Nejad, and C. Martin. 2020. Nutrient Status of San Francisco Bay and Its Management Implications. *Estuaries and Coasts*.
doi:10.1007/s12237-020-00737-w
- Comptroller General of the United States. 1977. California Drought of 1976 and 1977 - Extent, Damage, and Government Response, CED-77-137, Washington, DC. 108 pp.,
- Conrad, J. L., E. Wells, R. Baxter, A. Bever, L. R. Brown, G. Castillo, S. Culberson, M. P. Dekar, M. Eakin, G. Erickson, J. Hobbs, K. Jones, S. Lesmeister, M. MacWilliams, S. B. Slater, T. Sommer, and S. M. Tharratt. Unpublished Manuscript. Diagnosis of a drought syndrome in the San Francisco Estuary of California. Interagency Ecological Program for the Sacramento-San Joaquin Estuary.
- Contreras, D., K. Osborn, R. Baxter, and S. Slater. 2012. 2011 Status and Trends Report of Pelagic Fishes of the Upper San Francisco Estuary. *IEP Newsletter* 25(2):22-35.
- Corline, N. J., T. Sommer, C. A. Jeffres, and J. Katz. 2017. Zooplankton ecology and trophic resources for rearing native fish on an agricultural floodplain in the Yolo Bypass California, USA. *Wetlands Ecology and Management*:1-13.
doi:10.1007/s11273-017-9534-2
- Crauder, J. S., J. K. Thompson, F. Parchaso, R. I. Anduaga, S. A. Pearson, K. Gehrts, H. Fuller, and E. Wells. 2016. Bivalve effects on the food web supporting Delta Smelt—A long-term study of bivalve recruitment, biomass, and grazing rate patterns with varying freshwater outflow. Open-File Report 2016–1005, . Pages 216 p. *in*. U.S. Geological Survey, Reston, VA.<http://dx.doi.org/10.3133/ofr20161005>.
- CVRWQCB. 2009. Water quality control plan (Basin Plan) for the Sacramento River Basin and the San Joaquin River Basin. 4th ed. Revised October 2011. Central Valley Regional Water Quality Control Board.https://www.swrcb.ca.gov/centralvalley/water_issues/basin_plans/index.shtml
- Dahm, C. N., A. E. Parker, A. E. Adelson, M. A. Christman, and B. A. Bergamaschi. 2016. Nutrient Dynamics of the Delta: Effects on Primary Producers. *San Francisco Estuary and Watershed Science* 14(4).
<http://www.escholarship.org/uc/item/1789c0mz>

- DBW. 2020. Aquatic Invasive Plant Control Program 2019 Annual Monitoring Report, Sacramento, CA. https://dbw.parks.ca.gov/?page_id=29469
- De Cicco, L. A., R. M. Hirsch, D. Lorenz, and W. D. Watkins. 2018. dataRetrieval: R packages for discovering and retrieving water data available from Federal hydrologic web services. doi:10.5066/P9X4L3GE
- Del Rio, A. M., B. E. Davis, N. A. Fangué, and A. E. Todgham. 2019. Combined effects of warming and hypoxia on early life stage Chinook salmon physiology and development. *Conservation Physiology* 7(1):coy078.
- del Rosario, R. B., Y. J. Redler, K. Newman, P. L. Brandes, T. Sommer, K. Reece, and R. Vincik. 2013. Migration patterns of juvenile winter-run-sized Chinook Salmon (*Oncorhynchus tshawytscha*) through the Sacramento–San Joaquin Delta. *San Francisco Estuary and Watershed Science* 11(1). <http://www.escholarship.org/uc/item/36d88128>
- Dettinger, M. 2011. Climate change, atmospheric rivers, and floods in California—a multimodel analysis of storm frequency and magnitude changes. *Journal of the American Water Resources Association* 47(3):514-523. doi: <https://doi.org/10.1111/j.1752-1688.2011.00546.x>
- Dettinger, M., J. Anderson, M. Anderson, L. Brown, D. Cayan, and E. Maurer. 2016. Climate change and the Delta. *San Francisco Estuary and Watershed Science* 14(3). doi:<http://dx.doi.org/10.15447/sfews.2016v14iss3art5>
- Diffenbaugh, N. S., D. L. Swain, and D. Touma. 2015. Anthropogenic warming has increased drought risk in California. *Proceedings of the National Academy of Sciences* 112(13):3931-3936. doi:10.1073/pnas.1422385112
- Dugdale, R. C., F. P. Wilkerson, V. E. Hogue, and A. Marchi. 2007. The role of ammonium and nitrate in spring bloom development in San Francisco Bay. *Estuarine Coastal and Shelf Science* 73(1-2):17-29. doi:<https://doi.org/10.1016/j.ecss.2006.12.008>
- Durand, J., W. Fleenor, R. McElreath, M. J. Santos, and P. Moyle. 2016. Physical controls on the distribution of the submersed aquatic weed *Egeria densa* in the Sacramento–San Joaquin Delta and implications for habitat restoration. *San Francisco Estuary and Watershed Science* 14(1). <http://www.escholarship.org/uc/item/85c9h479>
- Durand, J. R. 2015. A conceptual model of the aquatic food web of the upper San Francisco Estuary. *San Francisco Estuary and Watershed Science* 13(3). doi:<http://escholarship.org/uc/item/0gw2884c>
- Durand, J. R., F. Bombardelli, W. E. Fleenor, Y. Henneberry, J. Herman, C. Jeffres, M. Leinfelder–Miles, J. R. Lund, R. Lusardi, A. D. Manfree, J. Medellín-Azuara, B. Milligan, and P. B. Moyle. 2020. Drought and the Sacramento-San Joaquin Delta, 2012–2016: Environmental Review and Lessons. *San Francisco Estuary and Watershed Science* 18(2). doi:10.15447/sfews.2020v18iss2art2
- DWR. 2002. Dayflow: and estimate of daily average Delta Outflow. Dayflow documentation 1997 through present., California Natural Resources Agency Open Data. 25. <https://data.cnra.ca.gov/dataset/dayflow/resource/776b90ca-673e-4b56-8cf3-ec26792708c3>

- DWR. 2019. Efficacy Report - 2015 Emergency Drought Barrier Project. State of California California Natural Resources Agency. Department of Water Resources, Bay-Delta Office, West Sacramento, CA. 106 pp.
- DWR. 2021. Attachment 1. Supplement to 2021 Temporary Urgency Change to Certain DWR and Reclamation Permit Terms as Provided in D-1641. California Department of Water Resources, Sacramento, CA.
- DWR and USBR. 2015. Temporary Urgency Change Petition to Certain DWR and Reclamation Permit Terms as Provided in D-1641. State Water Resources Control Board, (SWRCB), Sacramento, CA,
- Farrell, A. P. 2009. Environment, antecedents and climate change: lessons from the study of temperature physiology and river migration of salmonids. *Journal of Experimental Biology* 212(23):3771-3780. doi:10.1242/jeb.023671
- Feyrer, F., and M. P. Healey. 2003. Fish community structure and environmental correlates in the highly altered southern Sacramento-San Joaquin Delta. *Environmental Biology of Fishes* 66:123-132.
- Feyrer, F., T. Sommer, and S. B. Slater. 2009. Old school vs new school: status of threadfin shad (*Dorosoma petenense*) five decades after its introduction to the Sacramento-SanJoaquin Delta. *San Francisco Estuary and Watershed Science* 7(1). doi:<https://doi.org/10.15447/sfews.2009v7iss1art3>
- FLOAT-MAST (Flow Alteration - Management Analysis and Synthesis Team). 2021. Synthesis of data and studies relating to Delta Smelt biology in the San Francisco Estuary, emphasizing water year 2017. Interagency Ecological Program, Sacramento, CA.
<https://cadwr.app.box.com/v/InteragencyEcologicalProgram/file/838721643382>
- Fox, J., S. Weisberg, and B. Price. 2021. Package 'car': Companion to Applied Regression. Version 3.0-11. Comprehensive R Archive Network (CRAN),
<https://CRAN.R-project.org/package=car>
- Frantzych, J., T. Sommer, and B. Schreier. 2018. Physical and biological responses to flow in a tidal freshwater slough complex. *San Francisco Estuary and Watershed Science* 16(1). doi:<https://doi.org/10.15447/sfews.2018v16iss1/art3>
- Ger, K. A., P. Arneson, C. R. Goldman, and S. J. Teh. 2010a. Species specific differences in the ingestion of *Microcystis* cells by the calanoid copepods *Eurytemora affinis* and *Pseudodiaptomus forbesi*. *Journal of Plankton Research* 32(10):1479-1484. doi:10.1093/plankt/fbq071
- Ger, K. A., S. J. Teh, D. V. Baxa, S. Lesmeister, and C. R. Goldman. 2010b. The effects of dietary *Microcystis aeruginosa* and microcystin on the copepods of the upper San Francisco Estuary. *Freshwater Biology* 55:1548-1559.
- Ger, K. A., S. J. Teh, and C. R. Goldman. 2009. Microcystin-LR toxicity on dominant copepods *Eurytemora affinis* and *Pseudodiaptomus forbesi* of the upper San Francisco Estuary. *Science of the Total Environment* 407:4852-4857.
- Giebelhausen, B., and W. Lampert. 2001. Temperature reaction norms of *Daphnia magna*: the effect of food concentration. *Freshwater Biology* 46(3):281-289. doi:<https://doi.org/10.1046/j.1365-2427.2001.00630.x>

- Glibert, P. M., R. Dugdale, F. P. Wilkerson, A. E. Parker, J. Alexander, E. Antell, S. Blaser, A. Johnson, J. Lee, T. Lee, S. Murasko, and S. Strong. 2014a. Major—but rare—spring blooms in 2014 in San Francisco Bay Delta, California, a result of the long-term drought, increased residence time, and altered nutrient loads and forms. *Journal of Experimental Marine Biology and Ecology* 460:8-18.
- Glibert, P. M., D. Fullerton, J. M. Burkholder, J. C. Cornwell, and T. M. Kana. 2011. Ecological Stoichiometry, Biogeochemical Cycling, Invasive Species, and Aquatic Food Webs: San Francisco Estuary and Comparative Systems. *Reviews in Fisheries Science* 19(4):358-417. doi:10.1080/10641262.2011.611916
- Glibert, P. M., F. P. Wilkerson, R. C. Dugdale, A. E. Parker, J. Alexander, S. Blaser, and S. Murasko. 2014b. Phytoplankton communities from San Francisco Bay Delta respond differently to oxidized and reduced nitrogen substrates - even under conditions that would otherwise suggest nitrogen sufficiency. *Frontiers in Marine Science* 1:17. doi:10.3389/fmars.2014.00017
- Glibert, P. M., F. P. Wilkerson, R. C. Dugdale, J. A. Raven, C. L. Dupont, P. R. Leavitt, A. E. Parker, J. M. Burkholder, and T. M. Kana. 2016. Pluses and minuses of ammonium and nitrate uptake and assimilation by phytoplankton and implications for productivity and community composition, with emphasis on nitrogen-enriched conditions. *Limnology and Oceanography* 61(1):165-197. doi:10.1002/lno.10203
- Grimaldo, L., F. Feyrer, J. Burns, and D. Maniscalco. 2017. Sampling Uncharted Waters: Examining Rearing Habitat of Larval Longfin Smelt (*Spirinchus thaleichthys*) in the Upper San Francisco Estuary. *Estuaries and Coasts* 40:1771-1748.
- Grosholz, E., and E. Gallo. 2006. The influence of flood cycle and fish predation on invertebrate production on a restored California floodplain. *Hydrobiologia* 568(1):91-109.
- Hammock, B. G., S. P. Moose, S. S. Solis, E. Goharian, and S. J. Teh. 2019. Hydrodynamic Modeling Coupled with Long-term Field Data Provide Evidence for Suppression of Phytoplankton by Invasive Clams and Freshwater Exports in the San Francisco Estuary. *Environmental Management*. doi:10.1007/s00267-019-01159-6
- Hance, D. J., R. W. Perry, A. C. Pope, A. J. Ammann, J. L. Hassrick, and G. Hansen. 2022. From drought to deluge: spatiotemporal variation in migration routing, survival, travel time and floodplain use of an endangered migratory fish. *Canadian Journal of Fisheries and Aquatic Sciences* 0(0):1-19. doi:10.1139/cjfas-2021-0042
- Hartman, R., E. Ateljavich, M. Berg, K. Bouma-Gregson, D. Bosworth, N. Rasmussen, T. Flynn, and T. Pennington. 2021. Report on the Impact of the Emergency Drought Barrier on Harmful Algal Blooms and Aquatic Weeds in the Delta, Sacramento: California Department of Water Resources. 86p.,
- Harvey, B. N., D. P. Jacobson, and M. A. Banks. 2014. Quantifying the Uncertainty of a Juvenile Chinook Salmon Race Identification Method for a Mixed-Race Stock. *North American Journal of Fisheries Management* 34(6):1177-1186.

- Hasenbein, M., N. A. Fangué, J. Geist, L. M. Komoroske, J. Truong, R. McPherson, and R. E. Connon. 2016. Assessments at multiple levels of biological organization allow for an integrative determination of physiological tolerances to turbidity in an endangered fish species. *Conservation Physiology* 4(1):cow004. doi:10.1093/conphys/cow004
- Hasenbein, M., L. M. Komoroske, R. Connon, J. Geist, and N. A. Fangué. 2013. Turbidity and Salinity Affect Feeding Performance and Physiological Stress in the Endangered Delta Smelt. *Integrative and Comparative Biology* 53(4):620-634. doi:10.1093/icb/ict082
- Hassrick, J. L., M. J. Henderson, D. D. Huff, W. J. Sydeman, M. C. Sabal, J. A. Harding, A. J. Ammann, E. D. Crandall, E. P. Bjorkstedt, J. C. Garza, and S. A. Hayes. 2016. Early ocean distribution of juvenile Chinook salmon in an upwelling ecosystem. *Fisheries Oceanography* 25(2):133-146. doi:<https://doi.org/10.1111/fog.12141>
- Hecht, B. C., A. P. Matala, J. E. Hess, and S. R. Narum. 2015. Environmental adaptation in Chinook salmon (*Oncorhynchus tshawytscha*) throughout their North American range. *Molecular Ecology* 24(22):5573-5595. doi:<https://doi.org/10.1111/mec.13409>
- Henderson, M. J., I. S. Iglesias, C. J. Michel, A. J. Ammann, and D. D. Huff. 2019. Estimating spatial-temporal differences in Chinook salmon outmigration survival with habitat- and predation-related covariates. *Canadian Journal of Fisheries and Aquatic Sciences* 76(9):1549-1561. doi:10.1139/cjfas-2018-0212
- Hestir, E. L., D. H. Schoellhamer, J. Greenberg, T. Morgan-King, and S. L. Ustin. 2016. The effect of submerged aquatic vegetation expansion on a declining turbidity trend in the Sacramento-San Joaquin River Delta. *Estuaries and Coasts* 39(4):1100-1112. doi:10.1007/s12237-015-0055-z
- Hestir, E. L., D. H. Schoellhamer, T. Morgan-King, and S. L. Ustin. 2013. A step decrease in sediment concentration in a highly modified tidal river delta following the 1983 El Niño floods. *Marine Geology* 345:304-313. doi:<https://doi.org/10.1016/j.margeo.2013.05.008>
- Heugens, E. H. W., L. T. B. Tokkie, M. H. S. Kraak, A. J. Hendriks, N. M. van Straalen, and W. Admiraal. 2006. Population growth of *Daphnia magna* under multiple stress conditions: Joint effects of temperature, food, and cadmium. *Environmental Toxicology and Chemistry* 25(5):1399-1407. doi:<https://doi.org/10.1897/05-294R.1>
- Hobbs, J. A., C. Denney, L. Lewis, and M. Willmes. 2019. The effect of drought on Delta Smelt vital rates. Prepared for California Department of Fish and Wildlife Contract # P1696005 00, Sacramento, CA.
- Hutton, P. H., J. S. Rath, and S. B. Roy. 2017. Freshwater flow to the San Francisco Bay-Delta estuary over nine decades (Part 1): Trend evaluation. *Hydrological Processes* 31(14):2500-2515. doi:10.1002/hyp.11201
- IEP Long-term Survey Review Team. 2021. Interagency Ecological Program Long-term Monitoring Element Review: Pilot approach and methods development (2020). IEP Technical Report 96.

- Ingram, B., and F. Malamud–Roam. 2013. The west without water—what past floods, droughts, and other climatic clues tell us about tomorrow. University of California Press, Berkeley (CA).
- Jabusch, T., Phil Trowbridge, A. Wong, and M. Heberger. 2018. Assessment of Nutrient Status and Trends in the Delta in 2001–2016: Effects of drought on ambient concentrations and trends. Delta Regional Monitoring Program.
- Jassby, A. 2008. Phytoplankton in the upper San Francisco Estuary: recent biomass trends, their causes and their trophic significance. *San Francisco Estuary and Watershed Science* 6(1):24 pages.
- Jassby, A., and J. Cloern. 2000. Organic matter sources and rehabilitation of the Sacramento - San Joaquin Delta (California, USA). *Aquatic Conservation: Marine and Freshwater Ecosystems* 10(5):323-352.
- Jassby, A. D., J. E. Cloern, and B. E. Cole. 2002. Annual primary production: Patterns and mechanisms of change in a nutrient-rich tidal ecosystem. *Limnology and Oceanography* 47(3):698-712. doi:<https://doi.org/10.4319/lo.2002.47.3.0698>
- Jeffres, C. A., E. J. Holmes, T. R. Sommer, and J. V. E. Katz. 2020. Detrital food web contributes to aquatic ecosystem productivity and rapid salmon growth in a managed floodplain. *Plos ONE* 15(9):e0216019. doi:10.1371/journal.pone.0216019
- Jeffries, K. M., R. E. Connon, B. E. Davis, L. M. Komoroske, M. T. Britton, T. Sommer, A. E. Todgham, and N. A. Fanguie. 2016. Effects of high temperatures on threatened estuarine fishes during periods of extreme drought. *The Journal of Experimental Biology* 219(11):1705-1716. doi:10.1242/jeb.134528
- Jungbluth, M., C. Lee, C. Patel, T. Ignoffo, B. Bergamaschi, and W. Kimmerer. 2021. Production of the Copepod *Pseudodiaptomus forbesi* Is Not Enhanced by Ingestion of the Diatom *Aulacoseira granulata* During a Bloom. *Estuaries and Coasts* 44:1083-1099. doi:10.1007/s12237-020-00843-9
- Kayfetz, K., and W. Kimmerer. 2017. Abiotic and biotic controls on the copepod *Pseudodiaptomus forbesi* in the upper San Francisco Estuary. *Marine Ecology Progress Series* 581:85-101. doi:<https://doi.org/10.3354/meps12294>
- Kimmerer, W. 2002a. Physical, biological, and management responses to variable freshwater flow into the San Francisco Estuary. *Estuaries* 25(6B):1275-1290. doi:<https://doi.org/10.1007/BF02692224>
- Kimmerer, W. 2004. Open water processes of the San Francisco Bay Estuary: from physical forcing to biological responses. *San Francisco Estuary and Watershed Science* 2(1). <http://escholarship.org/uc/item/9bp499mv>
- Kimmerer, W., T. R. Ignoffo, B. Bemowski, J. Modéran, A. Holmes, and B. Bergamaschi. 2018a. Zooplankton Dynamics in the Cache Slough Complex of the Upper San Francisco Estuary. *San Francisco Estuary and Watershed Science* 16(3). doi: <https://doi.org/10.15447/sfews.2018v16iss3art4>
- Kimmerer, W., F. Wilkerson, B. Downing, R. Dugdale, E. S. Gross, K. Kayfetz, S. Khanna, A. E. Parker, and J. K. Thompson. 2019. Effects of Drought and the Emergency Drought Barrier on the Ecosystem of the California Delta. *San*

- Francisco Estuary and Watershed Science 17(3).
doi:<https://doi.org/10.15447/sfews.2019v17iss3art2>
- Kimmerer, W. J. 2002b. Effects of freshwater flow on abundance of estuarine organisms: physical effects or trophic linkages? Marine Ecology Progress Series 243:39-55. doi:<https://doi.org/10.3354/meps243039>
- Kimmerer, W. J., E. S. Gross, and M. L. MacWilliams. 2014. Tidal migration and retention of estuarine zooplankton investigated using a particle-tracking model. Limnol. Oceanogr. 59(3):901-916. doi:<https://doi.org/10.4319/lo.2014.59.3.0901>
- Kimmerer, W. J., E. S. Gross, A. M. Slaughter, and J. R. Durand. 2018b. Spatial Subsidies and Mortality of an Estuarine Copepod Revealed Using a Box Model. Estuaries and Coasts. doi:10.1007/s12237-018-0436-1
- Kimmerer, W. J., T. R. Ignoffo, K. R. Kayfetz, and A. M. Slaughter. 2018c. Effects of freshwater flow and phytoplankton biomass on growth, reproduction, and spatial subsidies of the estuarine copepod *Pseudodiaptomus forbesi*. Hydrobiologia 807(1):113-130. doi: <https://doi.org/10.1007/s10750-017-3385-y>
- Kimmerer, W. J., M. L. MacWilliams, and E. S. Gross. 2013. Variation of fish habitat and extent of the low-salinity zone with freshwater flow in the San Francisco Estuary. San Francisco Estuary and Watershed Science 11(4):16.
<https://escholarship.org/uc/item/3pz7x1x8>
- Kimmerer, W. J., and J. K. Thompson. 2014. Phytoplankton growth balanced by clam and zooplankton grazing and net transport into the low-salinity zone of the San Francisco Estuary. Estuaries and Coasts:1-17.
- Kraus, T. E. C., B. A. Bergamaschi, and B. D. Downing. 2017. An Introduction to High-Frequency Nutrient and Biogeochemical Monitoring for the Sacramento–San Joaquin Delta, Northern California. U.S. Geological Survey.
- Kurobe, T., P. W. Lehman, B. G. Hammock, M. B. Bolotaolo, S. Lesmeister, and S. J. Teh. 2018a. Biodiversity of cyanobacteria and other aquatic microorganisms across a freshwater to brackish water gradient determined by shotgun metagenomic sequencing analysis in the San Francisco Estuary, USA. Plos ONE 13(9):e0203953. doi:10.1371/journal.pone.0203953
- Kurobe, T., P. W. Lehman, M. E. Haque, T. Sedda, S. Lesmeister, and S. Teh. 2018b. Evaluation of water quality during successive severe drought years within Microcystis blooms using fish embryo toxicity tests for the San Francisco Estuary, California. Science of the Total Environment 610-611:1029-1037. doi:<https://doi.org/10.1016/j.scitotenv.2017.07.267>
- Kuznetsova, A., P. B. Brockhoff, and R. H. Christensen. 2017. lmerTest package: Tests in linear mixed effects models. Journal of Statistical Software 82(13):1-26. doi:<https://doi.org/10.18637/jss.v082.i13>
- Lehman, B. M., M. P. Gary, N. Demetras, and C. J. Michel. 2019. Where Predators and Prey Meet: Anthropogenic Contact Points Between Fishes in a Freshwater Estuary. San Francisco Estuary and Watershed Science 17(4). doi:10.15447/sfews.2019v17iss4art3

- Lehman, P. 2004. The influence of climate on mechanistic pathways that affect lower food web production in northern San Francisco Bay Estuary. *Estuaries* 27(2):311-324.
- Lehman, P. W. 1992a. Environmental factors associated with long-term changes in chlorophyll concentration in the Sacramento-San Joaquin Delta and Suisun Bay, California. *Estuaries* 15(3):335-348.
- Lehman, P. W. 1992b. Influence of climate on environmental factors associated with long-term changes in chlorophyll production for the Sacramento-San Joaquin delta and Suisun Bay, California. Proceedings of the Eighth Annual Pacific Climate (PACLIM) California Department of Water Resources, Asilomar, California,
- Lehman, P. W. 1996. Changes in chlorophyll *a* concentration and phytoplankton community composition with water-year type in the upper San Francisco Estuary. Pages 351-374 in J. T. Hollibaugh, editor. *San Francisco Bay the Ecosystem*. Pacific Division of the American Association for the Advancement of Science, San Francisco, California.
- Lehman, P. W. 2000. The influence of climate on phytoplankton community biomass in San Francisco Bay Estuary. *Limnology Oceanography* 45(3):580-590.
- Lehman, P. W., G. Boyer, C. Hall, S. Waller, and K. Gehrts. 2005. Distribution and toxicity of a new colonial *Microcystis aeruginosa* bloom in the San Francisco Estuary, California. *Hydrobiologia* 541:87-99.
- Lehman, P. W., G. Boyer, M. Satchwell, and S. Waller. 2008. The influence of environmental conditions on the seasonal variation of *Microcystis* cell density and microcystins concentration in San Francisco Estuary. *Hydrobiologia* 600(1):187-204. doi:10.1007/s10750-007-9231-x
- Lehman, P. W., C. Kendall, M. A. Guerin, M. B. Young, S. R. Silva, G. L. Boyer, and S. J. Teh. 2015. Characterization of the *Microcystis* bloom and its nitrogen supply in San Francisco Estuary using stable isotopes. *Estuaries and Coasts* 38(1):165-178. <http://www.scopus.com/inward/record.url?eid=2-s2.0-84901737218&partnerID=40&md5=7d05579e670818e8a5d23f30315b94e1>
- Lehman, P. W., T. Kurobe, K. Huynh, S. Lesmeister, and S. J. Teh. 2021. Covariance of Phytoplankton, Bacteria, and Zooplankton Communities Within *Microcystis* Blooms in San Francisco Estuary. *Frontiers in Microbiology* 12(1184). doi:10.3389/fmicb.2021.632264
- Lehman, P. W., T. Kurobe, S. Lesmeister, D. Baxa, A. Tung, and S. J. Teh. 2017. Impacts of the 2014 severe drought on the *Microcystis* bloom in San Francisco Estuary. *Harmful Algae* 63(Supplement C):94-108. doi:<https://doi.org/10.1016/j.hal.2017.01.011>
- Lehman, P. W., T. Kurobe, S. Lesmeister, C. Lam, A. Tung, M. Xiong, and S. J. Teh. 2018. Strong differences characterize *Microcystis* blooms between successive severe drought years in the San Francisco Estuary, California, USA. *Aquatic Microbial Ecology* 81(3):293-299. <https://www.int-res.com/abstracts/ame/v81/n3/p293-299/>

- Lehman, P. W., T. Kurobe, and S. J. Teh. 2020. Impact of extreme wet and dry years on the persistence of *Microcystis* harmful algal blooms in San Francisco Estuary. *Quaternary International*. doi:<https://doi.org/10.1016/j.quaint.2019.12.003>
- Lehman, P. W., and R. W. Smith. 1991. Environmental factors associated with phytoplankton succession for the Sacramento-San Joaquin Delta and Suisun Bay estuary, California. *Estuarine, Coastal and Shelf Science* 32:105-128.
- Leibovici, D. G. 2010. Spatio-Temporal Multiway Data Decomposition Using Principal Tensor Analysis on k-Modes: The R Package PTAK. *Journal of Statistical Software* 34(10):1 - 34. doi:10.18637/jss.v034.i10
- Lenoch, L. K., P. R. Stumpner, J. R. Burau, L. C. Loken, and S. Sadro. 2021. Dispersion and Stratification Dynamics in the Upper Sacramento River Deep Water Ship Channel. *San Francisco Estuary and Watershed Science* 19(4). doi:<https://doi.org/10.15447/sfews.2021v19iss4art5>
- Lenth, R. V., P. Buerkner, M. Herve, J. Love, H. Riebl, and H. Singmann. 2021. Package 'emmeans': Estimated Marginal Means, aka Least-Squares Means. Version 1.6.2. Comprehensive R Archive Network, CRAN, <https://cran.r-project.org/web/packages/emmeans/index.html>
- Lucas, L. V., J. E. Cloern, J. K. Thompson, M. T. Stacey, and J. R. Koseff. 2016. Bivalve grazing can shape phytoplankton communities. *Frontiers in Marine Science* 3:14. doi:10.3389/fmars.2016.00014
- Luković, J., J. C. H. Chiang, D. Blagojević, and A. Sekulić. 2021. A Later Onset of the Rainy Season in California. *Geophysical Research Letters* 48(4):e2020GL090350. doi:<https://doi.org/10.1029/2020GL090350>
- Mac Nally, R., J. R. Thomson, W. J. Kimmerer, F. Feyrer, K. B. Newman, A. Sih, W. A. Bennett, L. Brown, E. Fleishman, S. D. Culberson, and G. Castillo. 2010. Analysis of pelagic species decline in the upper San Francisco Estuary using multivariate autoregressive modeling (MAR). *Ecological Applications* 20(5):1417-1430. doi:<https://doi.org/10.1890/09-1724.1>
- Magnusson, A., H. Skaug, A. Nielsen, C. Berg, K. Kristensen, M. Maechler, K. v. Bentham, N. Sadat, B. Bolker, and M. Brooks. 2019. Package 'glmmTMB': Generalized Linear Mixed Models using Template Model Builder. The Comprehensive R Archive Network. <https://github.com/glmmTMB>
- Mahardja, B., J. L. Conrad, L. Lusher, and B. Schreier. 2016. Abundance Trends, Distribution, and Habitat Associations of the Invasive Mississippi Silverside (*Menidia audens*) in the Sacramento–San Joaquin Delta, California, USA. *San Francisco Estuary and Watershed Science* 14(1). <http://www.escholarship.org/uc/item/55f0s462>
- Mahardja, B., V. Tobias, S. Khanna, L. Mitchell, P. Lehman, T. Sommer, L. Brown, S. Culberson, and J. L. Conrad. 2021. Resistance and resilience of pelagic and littoral fishes to drought in the San Francisco Estuary. *Ecological Applications* 31(2):e02243, 16 p. doi:<https://dx.doi.org/10.1002%2Feap.2243>
- Mann, M. E., and P. H. Gleick. 2015. Climate change and California drought in the 21st century. *Proceedings of the National Academy of Sciences* 112(13):3858-3859. doi:10.1073/pnas.1503667112

- Marine, K. R., and J. J. Cech Jr. 2004. Effects of High Water Temperature on Growth, Smoltification, and Predator Avoidance in Juvenile Sacramento River Chinook Salmon. *North American Journal of Fisheries Management* 24(1):198-210.
- McKenzie, R. 2020. 2019 Delta Juvenile Fish Monitoring Program- Salmonid Annual Report. US Fish and Wildlife Service, Lodi, CA. 14 p., https://www.fws.gov/loidi/juvenile_fish_monitoring_program/djfm/annual_reports/Salmonids/DJFMP%20FY%202019%20Salmonid%20Report.pdf
- Melnychuk, M. C., D. W. Welch, and C. J. Walters. 2010. Spatio-Temporal Migration Patterns of Pacific Salmon Smolts in Rivers and Coastal Marine Waters. *Plos ONE* 5(9):e12916. doi:10.1371/journal.pone.0012916
- Meng, L., and S. A. Matern. 2001. Native and introduced larval fishes of Suisun Marsh, California: the effects of freshwater outflow. *Transactions American Fisheries Society* 130:750-765.
- Merz, J. E., P. S. Bergman, J. F. Melgo, and S. Hamilton. 2013. Longfin smelt: spatial dynamics and ontogeny in the San Francisco Estuary, California. *California Fish & Game* 99(3):122-148.
- Michel, C. J., A. J. Ammann, S. T. Lindley, P. T. Sandstrom, E. D. Chapman, M. J. Thomas, G. P. Singer, A. P. Klimley, and R. B. MacFarlane. 2015. Chinook salmon outmigration survival in wet and dry years in California's Sacramento River. *Canadian Journal of Fisheries and Aquatic Sciences* 72(11):1749-1759. doi:10.1139/cjfas-2014-0528
- Miller, J. A., A. Gray, and J. Merz. 2010. Quantifying the contribution of juvenile migratory phenotypes in a population of Chinook salmon *Oncorhynchus tshawytscha*. *Marine Ecology Progress Series* 408:227-240. doi:10.3354/meps08613.
- Monismith, S. G. 2016. A note on Delta outflow. *San Francisco Estuary and Watershed Science* 14(3). doi:<https://doi.org/10.15447/sfews.2016v14iss3art3>
- Monsen, N. E., J. E. Cloern, and J. R. Burau. 2007. Effects of Flow Diversions on Water and Habitat Quality: Examples from California's Highly Manipulated Sacramento-San Joaquin Delta. *San Francisco Estuary and Watershed Science*, <http://escholarship.org/uc/item/04822861>
- Morita, K. 2019. Earlier migration timing of salmonids: an adaptation to climate change or maladaptation to the fishery? *Canadian Journal of Fisheries and Aquatic Sciences* 76(3):475-479. doi:10.1139/cjfas-2018-0078
- Moyle, P. 2002. *Inland fishes of California*. University of California Press, Berkeley, CA.
- Moyle, P., W. Bennett, J. Durand, W. Fleenor, B. Gray, E. Hanak, J. Lund, and J. Mount. 2012. *Where the Wild Things Aren't: Making the Delta a Better Place for Native Species*. Public Policy Institute of California, San Francisco, CA. <https://www.pplic.org/publication/where-the-wild-things-arent-making-the-delta-a-better-place-for-native-species/>
- Moyle, P. B., R. D. Baxter, T. Sommer, T. C. Foin, and S. A. Matern. 2004. Biology and population dynamics of the Sacramento splittail (*Pogonichthys macrolepidotus*) in the San Francisco Estuary: a review. *San Francisco Estuary and Watershed Science* 2(2):1-47. doi:<https://doi.org/10.15447/sfews.2004v2iss2art3>

- Moyle, P. B., J. A. Israel, and S. E. Purdy. 2008. Salmon, Steelhead, and Trout in California: status of an emblematic fauna. UC Davis Center for Watershed Sciences. 316.
- Moyle, P. B., J. R. Lund, W. A. Bennett, and W. E. Fleenor. 2010. Habitat variability and complexity in the Upper San Francisco Estuary. *San Francisco Estuary and Watershed Science* 8(3). doi:10.15447/sfews.2010v8iss3art1
- Munsch, S. H., C. M. Greene, R. C. Johnson, W. H. Satterthwaite, H. Imaki, and P. L. Brandes. 2019. Warm, dry winters truncate timing and size distribution of seaward-migrating salmon across a large, regulated watershed. *Ecological Applications* 29(4):e01880. doi: <https://doi.org/10.1002/eap.1880>
- Newsom, G. 2021. Proclamation of a State of Emergency. Pages 5 p. *in*. Executive Department, State of California, <https://www.gov.ca.gov/wp-content/uploads/2021/05/5.10.2021-Drought-Proclamation.pdf>
- Nichols, F. H. 1985. Increased benthic grazing: An alternative explanation for low phytoplankton biomass in northern San Francisco Bay during the 1976–1977 drought. *Estuarine, Coastal and Shelf Science* 21(3):379-388. doi:[https://doi.org/10.1016/0272-7714\(85\)90018-6](https://doi.org/10.1016/0272-7714(85)90018-6)
- NOAA Fisheries. 2021. Monitoring Thiamine Deficiency in California Salmon. National Oceanic and Atmospheric Administration Southwest Fisheries Science Center, <https://www.fisheries.noaa.gov/west-coast/science-data/monitoring-thiamine-deficiency-california-salmon>
- Nobriga, M., F. Feyrer, R. Baxter, and M. Chotkowski. 2005. Fish community ecology in an altered river delta: Spatial patterns in species composition, life history strategies, and biomass. *Estuaries* 28(5):776-785.
- Nobriga, M. L., C. J. Michel, R. C. Johnson, and J. D. Wikert. 2021. Coldwater fish in a warm water world: Implications for predation of salmon smolts during estuary transit. *Ecology and Evolution* 11(15):10381-10395. doi:<https://doi.org/10.1002/ece3.7840>
- Nobriga, M. L., and J. A. Rosenfield. 2016. Population Dynamics of an Estuarine Forage Fish: Disaggregating Forces Driving Long-Term Decline of Longfin Smelt in California's San Francisco Estuary. *Transactions of the American Fisheries Society* 145(2):44-58.
- Notch, J., R. Robinson, T. Pham, R. Logston, A. McHuron, A. Ammann, and C. Michel. 2021. Enhanced Acoustic Tagging, Analysis, and Real-Time Monitoring of Wild and Hatchery Salmonids in the Sacramento River Valley – 2018 – 2020 Final Report. Report prepared by University of California – Santa Cruz for the U.S. Bureau of Reclamation, prepared under contract USDI/BOR# R18AC00039.
- Notch, J. J., A. S. McHuron, C. J. Michel, F. Cordoleani, M. Johnson, M. J. Henderson, and A. J. Ammann. 2020. Outmigration survival of wild Chinook salmon smolts through the Sacramento River during historic drought and high water conditions. *Environmental Biology of Fishes*. doi:10.1007/s10641-020-00952-1
- Novick, E., R. Holleman, T. Jabusch, J. Sun, P. Trowbridge, D. Senn, M. Guerin, C. Kendall, M. Young, and S. Peek. 2015. Characterizing and quantifying nutrient sources, sinks and transformations in the Delta: synthesis, modeling, and

- recommendations for monitoring. San Francisco Estuary Institute, San Francisco, CA.
http://www.sfei.org/sites/default/files/biblio_files/785%20Delta%20synthesis%20modeling.pdf
- Otten, T. G., H. W. Paerl, T. W. Dreher, W. J. Kimmerer, and A. E. Parker. 2017. The molecular ecology of *Microcystis* sp. blooms in the San Francisco Estuary. *Environmental Microbiology* 19(9):3619-3637. doi:<https://doi.org/10.1111/1462-2920.13860>
- Parchaso, F. 1993. Seasonal reproduction of *Potamocorbula amurensis* in San Francisco Bay, California. M.S. Thesis, California State University, San Francisco, CA.
- Parker, C., J. Hobbs, M. Bisson, and A. Barros. 2017. Do Longfin Smelt Spawn in San Francisco Bay Tributaries? *IEP Newsletter* 30(1):29-36.
- Peacock, M. B., C. M. Gobble, D. B. Senn, J. E. Cloern, and R. M. Kudela. 2018. Blurred lines: Multiple freshwater and marine algal toxins at the land-sea interface of San Francisco Bay, California. *Harmful Algae* 73:138-147.
doi:<https://doi.org/10.1016/j.hal.2018.02.005>
- Perry, R. W., P. L. Brandes, J. R. Burau, A. P. Klimley, B. MacFarlane, C. Michel, and J. R. Skalski. 2013. Sensitivity of survival to migration routes used by juvenile Chinook salmon to negotiate the Sacramento-San Joaquin River Delta. *Environmental Biology of Fishes* 96(2):381-392.
- Perry, R. W., A. C. Pope, J. G. Romine, P. L. Brandes, J. R. Burau, A. R. Blake, A. J. Ammann, and C. J. Michel. 2018. Flow-mediated effects on travel time, routing, and survival of juvenile Chinook salmon in a spatially complex, tidally forced river delta. *Canadian Journal of Fisheries and Aquatic Sciences*:1-16.
doi:10.1139/cjfas-2017-0310
- Polansky, L., K. B. Newman, and L. Mitchell. 2021. Improving inference for nonlinear state-space models of animal population dynamics given biased sequential life stage data. *Biometrics* 77(1):352-361. doi:<https://doi.org/10.1111/biom.13267>
- Pope, A. C., R. W. Perry, B. N. Harvey, D. J. Hance, and H. C. Hansel. 2021. Juvenile Chinook Salmon Survival, Travel Time, and Floodplain Use Relative to Riverine Channels in the Sacramento–San Joaquin River Delta. *Transactions American Fisheries Society*. doi:10.1002/tafs.10271
- Rath, J. S., P. H. Hutton, E. S. Ateljevich, and S. B. Roy. 2021. A Survey of X2 Isohaline Empirical Models for the San Francisco Estuary. *San Francisco Estuary and Watershed Science* 19(4). doi:<https://doi.org/10.15447/sfews.2021v19iss4art3>
- RegionalSan. 2021. Progress Report Method of Compliance Work Plan and Schedule for Ammonia Effluent Limitations and Title 22 or Equivalent Disinfection Requirements. Sacramento Regional County Sanitation District, Sacramento, CA.
- Reis, G. J., J. K. Howard, and J. A. Rosenfield. 2019. Clarifying effects of environmental protections on freshwater flows to and water exports from the San Francisco Bay Estuary. *San Francisco Estuary and Watershed Science* 17(1).
doi:<https://doi.org/10.15447/sfews.2019v17iss1art1>

- Romine, J. G., R. W. Perry, P. R. Stumpner, A. R. Blake, and J. R. Burau. 2021. Effects of Tidally Varying River Flow on Entrainment of Juvenile Salmon into Sutter and Steamboat Sloughs. *San Francisco Estuary and Watershed Science* 19(2). doi:<https://doi.org/10.15447/sfews.2021v19iss2art4>
- Rosenfield, J. A., and R. D. Baxter. 2007. Population dynamics and distribution patterns of longfin smelt in the San Francisco Estuary. *Transactions American Fisheries Society* 136:1577-1592.
- Sabal, M., S. Hayes, J. Merz, and J. Setka. 2016. Habitat alterations and a nonnative predator, the Striped Bass, increase native Chinook Salmon mortality in the Central Valley, California. *North American Journal of Fisheries Management* 36(2):309-320. doi:<https://doi.org/10.1080/02755947.2015.1121938>
- Saleh, D., and J. Domagalski. 2015. SPARROW Modeling of Nitrogen Sources and Transport in Rivers and Streams of California and Adjacent States, U.S. *JAWRA Journal of the American Water Resources Association* 51(6):1487-1507. doi:<https://doi.org/10.1111/1752-1688.12325>
- Saleh, D., and J. Domagalski. 2021. Concentrations, Loads, and Associated Trends of Nutrients Entering the Sacramento–San Joaquin Delta, California. *San Francisco Estuary and Watershed Science* 19(4). doi:<https://doi.org/10.15447/sfews.2021v19iss4art6>
- Satterthwaite, W. H., S. M. Carlson, and A. Criss. 2017. Ocean Size and Corresponding Life History Diversity among the Four Run Timings of California Central Valley Chinook Salmon. *Transactions of the American Fisheries Society* 146(4):594-610. doi:10.1080/00028487.2017.1293562
- Schultz, A. A., L. Grimaldo, J. Hassrick, A. Kalmbach, A. Smith, O. T. Burgess, D. Barnard, and J. Brandon. 2019. Effect of Isohaline (X2) and Region on Delta Smelt Habitat, Prey and Distribution During the Summer and Fall: Insights into Managed Flow Actions in a Highly Modified Estuary. Pages 237-286 *in* A. A. Schultz, editor. *Directed Outflow Project: Technical Report 1*. U.S. Bureau of Reclamation, Bay-Delta Office, Mid-Pacific Region, Sacramento, CA.
- Shafira, S. A., and D. Lestari. 2020. Bayesian Zero Inflated Negative Binomial Regression Model for The Parkinson Data. *ICSA 2019: Proceedings of the 1st International Conference on Statistics and Analytics, ICSA 2019, 2-3 August 2019, , Bogor, Indonesia,*
- Singer, G. P., E. D. Chapman, A. J. Ammann, A. P. Klimley, A. L. Rypel, and N. A. Fangué. 2020. Historic drought influences outmigration dynamics of juvenile fall and spring-run Chinook Salmon. *Environmental Biology of Fishes* 103(5):543-559. doi:10.1007/s10641-020-00975-8
- Smith, W. E. 2019. Integration of Transport, Survival, and Sampling Efficiency in a Model of South Delta Entrainment. *San Francisco Estuary and Watershed Science* 17(4). doi:10.15447/sfews.2019v17iss4art4
- Smith, W. E., L. Polansky, and M. L. Nobriga. 2021. Disentangling risks to an endangered fish: using a state-space life cycle model to separate natural mortality from anthropogenic losses. *Canadian Journal of Fisheries and Aquatic Sciences* 78(8):1008-1029. doi:10.1139/cjfas-2020-0251

- Sommer, T., C. Armor, R. Baxter, R. Breuer, L. Brown, M. Chotkowski, S. Culberson, F. Feyrer, M. Gingras, B. Herbold, W. Kimmerer, A. Mueller-Solger, M. Nobriga, and K. Souza. 2007. The collapse of pelagic fishes in the upper San Francisco Estuary. *Fisheries* 32(6):270-277. doi:[https://doi.org/10.1577/1548-8446\(2007\)32\[270:TCOPFI\]2.0.CO;2](https://doi.org/10.1577/1548-8446(2007)32[270:TCOPFI]2.0.CO;2)
- Sommer, T., and F. Mejia. 2013. A place to call home: a synthesis of Delta Smelt habitat in the upper San Francisco Estuary. *San Francisco Estuary and Watershed Science* 11(2):25 pages. doi:10.15447/sfews.2013v11iss2art4
- Sommer, T. R., M. L. Nobriga, W. C. Harrell, W. Batham, and W. J. Kimmerer. 2001. Floodplain rearing of juvenile chinook salmon: Evidence of enhanced growth and survival. *Canadian Journal of Fisheries and Aquatic Sciences* 58(2):325-333. doi:<https://doi.org/10.1139/f00-245>
- Stevens, Chadwick, and Painter. 1987. American Shad and Striped Bass in California's Sacramento-San Joaquin River System. Pages 66-78 *in* American Fisheries Society Symposium,
- Stevens, D. E., and L. W. Miller. 1983. Effects of river flow on abundance of young chinook salmon, American shad, longfin smelt, and delta smelt in the Sacramento-San Joaquin River System. *North American Journal of Fisheries Management* 3(4):425-437.
- Stine, S. 1994. Extreme and persistent drought in California and Patagonia during mediaeval time. *Nature* 369(6481):546-549. doi:10.1038/369546a0
- Stumpner, E. B., B. A. Bergamaschi, T. E. C. Kraus, A. E. Parker, F. P. Wilkerson, B. D. Downing, R. C. Dugdale, M. C. Murrell, K. D. Carpenter, J. L. Orlando, and C. Kendall. 2020. Spatial variability of phytoplankton in a shallow tidal freshwater system reveals complex controls on abundance and community structure. *Science of the Total Environment* 700:134392. doi:<https://doi.org/10.1016/j.scitotenv.2019.134392>
- Sturrock, A. M., W. H. Satterthwaite, K. M. Cervantes-Yoshida, E. R. Huber, H. J. W. Sturrock, S. Nusslé, and S. M. Carlson. 2019. Eight decades of hatchery salmon releases in the California Central Valley: Factors influencing straying and resilience. *Fisheries* 44(9):433-444.
- Sutula, M., R. Kudela, J. D. Hagy, L. W. Harding, D. Senn, J. E. Cloern, S. Bricker, G. M. Berg, and M. Beck. 2017. Novel analyses of long-term data provide a scientific basis for chlorophyll-a thresholds in San Francisco Bay. *Estuarine, Coastal and Shelf Science* 197:107-118. doi:<https://doi.org/10.1016/j.ecss.2017.07.009>
- Swain, D. L., B. Langenbrunner, J. D. Neelin, and A. Hall. 2018. Increasing precipitation volatility in twenty-first-century California. *Nature Climate Change* 8(5):427-433. doi:10.1038/s41558-018-0140-y
- SWRCB. 2000. Revised Water Right Decision 1641. In the Matter of Implementation of Water Quality Objectives for the San Francisco Bay/Sacramento-San Joaquin Delta Estuary; A Petition to Change Points of Diversion of the Central Valley Project and the State Water Project in the Southern Delta, and A Petition to Change Places of Use and Purposes of Use of the Central Valley Project. State

- Water Resources Control Board, California Environmental Protection Agency, Sacramento, CA,
- SWRCB. 2018. Water Quality Control Plan for the San Francisco Bay/Sacramento-San Joaquin Delta Estuary. Resolution no. 2018-0059. State Water Resources Control Board, Sacramento, CA. 76 p.,
- SWRCB. 2021. Order conditionally approving a petition for temporary agency changes to license and permit terms and conditions requiring compliance with Delta water quality objectives in response to drought conditions. State of California, California Environmental Protection Agency, State Water Resources Control Board, Sacramento, CA,
https://www.waterboards.ca.gov/waterrights/water_issues/programs/drought/docs/tucp/2015/tucp_order070315.pdf
- Taylor, M. 2016. The 2016-2017 Budget: The State's Drought Response. Pages 32 p. *in*. Legislative Analysts's Office, <https://lao.ca.gov/publications/report/3343>
- Thompson, J. K., J. R. Koseff, S. G. Monismith, and L. V. Lucas. 2008. Shallow water processes govern system-wide phytoplankton bloom dynamics: A field study. *Journal of Marine Systems* 74(1–2):153-166.
doi:<http://dx.doi.org/10.1016/j.jmarsys.2007.12.006>
- Thomson, J. R., W. J. Kimmerer, L. R. Brown, K. B. Newman, R. Mac Nally, W. A. Bennett, F. Feyrer, and E. Fleishman. 2010. Bayesian change point analysis of abundance trends for pelagic fishes in the upper San Francisco Estuary. *Ecological Applications* 20(5):1431-1448. doi:<https://doi.org/10.1890/09-0998.1>
- Tobias, V. D., J. L. Conrad, B. Mahardja, and S. Khanna. 2019. Impacts of water hyacinth treatment on water quality in a tidal estuarine environment. *Biological Invasions* 21(12):3479-3490. doi:10.1007/s10530-019-02061-2
- Twardochleb, L., A. Maguire, L. Dixit, M. Bedwell, J. Orlando, M. MacWilliams, A. Bever, and B. Davis. 2021. North Delta Food Subsidies Study: Monitoring Food Web Responses to the North Delta Flow Action, 2019 Report. Department of Water Resources, Division of Environmental Services, West Sacramento, CA.
- USFWS et al. 2013. Suisun Marsh Habitat Management, Preservation, and Restoration Plan. California Department of Fish and Game, US Fish and Wildlife Service, and US Bureau of Reclamation Sacramento, CA,
- USGS. 2016. National Water Information System data available on the World Wide Web (USGS Water Data for the Nation). US Geological Survey,
<http://waterdata.usgs.gov/nwis/>
- Wankel, S. D., C. Kendall, C. A. Francis, and A. Paytan. 2006. Nitrogen sources and cycling in the San Francisco Bay Estuary: A nitrate dual isotopic composition approach. *Limnology and Oceanography* 51(4):1654-1664.
doi:10.4319/lo.2006.51.4.1654
- Werner, I., S. Clark, and D. Hinton. 2003. Biomarkers aid understanding of aquatic organism responses to environmental stressors. *California Agriculture* 57(4):110-115.
- Williams, A. P., E. R. Cook, J. E. Smerdon, B. I. Cook, J. T. Abatzoglou, K. Bolles, S. H. Baek, A. M. Badger, and B. Livneh. 2020. Large contribution from anthropogenic

- warming to an emerging North American megadrought. *Science* 368(6488):314-318. doi:10.1126/science.aaz9600
- Wilson, C. M. 2013. *Gates and Barriers in the Delta*. State Water Resources Control Board, Sacramento, CA.
- Windell, S., P. L. Brandes, J. L. Conrad, John W. Ferguson, P. A. L. Goertler, B. N. Harvey, J. Heublein, Joshua A. Israel, D. W. Kratville, J. E. Kirsch, R. W. Perry, Joseph Pisciotto, W. R. Poytress, K. Reece, B. G. Swart, and R. C. Johnson. 2017. Scientific framework for assessing factors influencing endangered Sacramento River Winter-Run Chinook Salmon (*Oncorhynchus tshawytscha*) across the life cycle. U.S. Department of Commerce, National Oceanic and Atmospheric Administration, National Marine Fisheries Service, NOAA-TM-NMFS-SWFSC-586. doi:<http://doi.org/10.7289/V5/TM-SWFSC-586>
- Workie, M. S., and A. G. Azene. 2021. Bayesian zero-inflated regression model with application to under-five child mortality. *Journal of Big Data* 8(1):4. doi:10.1186/s40537-020-00389-4
- Wright, S. A., and D. H. Schoellhamer. 2004. Trends in the sediment yield of the Sacramento River, California, 1957-2001. *San Francisco Estuary and Watershed Science* 2(2). doi:<https://doi.org/10.15447/sfews.2004v2iss2art2>
- Young, M. J., F. Feyrer, P. R. Stumpner, V. Larwood, O. Patton, and L. R. Brown. 2021. Hydrodynamics drive pelagic communities and food web structure in a tidal environment. *International Review of Hydrobiology* 106(2):69-85. doi:<https://doi.org/10.1002/iroh.202002063>